THE HYDRAULIC TRANSPORT OF HIGH CONCENTRATION STABILIZED FLOW FULL PLANT MINERAL TAILINGS

by

Angus John Cawood Paterson

BSc (Eng) in Civil Engineering, MSc (Eng)

A thesis submitted in fulfilment of the requirements for the degree of Doctor of Philosophy.

Department of Civil Engineering
University of Cape Town

January 1991

DECLARATION

I, Angus John Cawood Paterson, declare that this thesis is essentially my own work and has not been submitted for a degree at another university.

Signed by candidate

A J C PATERSON

January 1991

ACKNOWLEDGEMENTS

Firstly, I would like to thank my thesis supervisor, Professor J H Lazarus, of the Department of Civil Engineering, University of Cape Town, for all the help, guidance and encouragement throughout the research project, and especially for first introducing me to the fascinating field of Hydrotransport.

My thanks also to Professor F A Kilner, Head of the Civil Engineering Department, for his support and advice at all times.

Dr Anthony Sive for computer programming advice and motivation during the initial stages of the Research Project.

Cheryl, for the typing, corrections and retyping of numerous reports and thesis drafts.

The technical and laboratory staff for their persistent humour and unfailing work when it was most needed.

My colleagues in Hydrotransport Research for inspiration and encouragement throughout the duration of the research project.

To my family and friends for their support.

For financial support :

- The University of Cape Town
- Hydrotransport Research, University of Cape Town
- The Council for Scientific and Industrial Research
- The Chamber of Mines of South Africa.

ABSTRACT

THE HYDRAULIC TRANSPORT OF HIGH CONCENTRATION STABILIZED FLOW FULL PLANT MINERAL TAILINGS

ANGUS JOHN CAWOOD PATERSON

Department of Civil Engineering, University of Cape Town,
Private Bag, Rondebosch, 7700, South Africa

February 1991

This thesis involves an analytical and experimental investigation of the flow behaviour of high concentration stabilized mineral tailings used as backfill material. At high solids concentrations "anomalous" behaviour occurs and is indicated by diameter dependancy on rheogram curves. These curves are not coincident in the laminar flow region. The anomalous behaviour is examined by postulating the following mechanisms :

1. Slip velocity at the pipe wall
2. Wall effects due to particle interaction
3. Boundary layer effects
4. Plug flow at high concentrations
5. Particle migration away from the wall leaving a sheared annular zone
6. Lateral dispersive stress acting between particle and pipe wall.

The mechanism responsible for "anomalous" behaviour is found to be due to the presence of a dispersive stress acting on the pipe wall due to particle-particle and pipe wall contact. This only occurs above a critical solids concentration ratio which is defined in terms of the critical void ratio or freely settled particle concentration. The total wall shear stress is a combination of both the viscous shear stress and the solid shear stress due to the lateral dispersive stress.

Measured data was obtained from several test facilities in pipe diameters ranging from 13,48 mm to 101,5 mm and for solids volumetric concentrations from 25% to 55%. Measurements included mean mixture velocity, pressure gradient, *in situ* and delivered volumetric concentration, temperature and the solids particle size distribution. Vertical down pipeline pressure gradients were obtained for a 40 mm NB pipeline which was constructed for the research. A tube viscometer was used to obtain rheological parameters.

The measured data was compared with several analytical models using the log standard error. Existing models were found to be unsuitable for these slurries.

The "anomalous" behaviour of the high concentration stabilized slurries is explained. The flow behaviour of these slurries is analysed in detail. The output is in the form of a user friendly interactive pipeline design computer program.

THESIS LAYOUT

CONTENTS

LIST OF FIGURES

LIST OF TABLES

NOMENCLATURE

		Units
a	area	m^2
A	internal area of pipe	m^2
C	mean concentration of solids by volume	-
C_{bfree}	minimum concentration with solid particles in contact (freely settled concentration)	-
C_{bmax}	maximum attainable concentration	-
C_D	drag coefficient	-
d	particle diameter	m
d_{10}	particle diameter such that 10% by mass of solids are less than d_{10}	m
d_{50}	particle diameter such that 50% by mass of solids are less than d_{50}	m
d_{90}	particle diameter such that 90% by mass of solids are less than d_{90}	m
D	internal diameter of pipe	m
E	energy	N.m
f	friction factor	-
g	gravitational acceleration	m/s^2
G	shear rate	s^{-1}
G_d	grading coefficient	-
He	Hedstrom number	-
ΔH	head loss in metres of water	m
i	hydraulic gradient in metres of water	m
k	pipe roughness	m
K	fluid consistency index	$Pa.s^n$
K'	apparent fluid consistency index	$Pa.s^n$
$K_{1,2}$	constants	-
K_r	dispersive stress coefficient	-
L	length along pipe	m
m	mass	kg
M^*	mass flow ratio	-
n	average number of particle contacts	-
n	flow behaviour index	-
n'	apparent flow behaviour index	-
p	fluid pressure	Pa
ΔP	pressure change	Pa
Q	volumetric flow rate	m^3/s
r	pipe radius (local)	m
R	pipe radius	m
R_c	core radius ratio	-
Re	Reynolds number	-
R_v	velocity ratio	-

S	relative density	-
S_f	particle settling shape factor	-
S^*	mixture relative density ratio	-
t	time	s
T	temperature	^oC
u^*	shear velocity	m/s
u_c	core velocity	m/s
u_s	slip velocity	m/s
V	mean velocity	m/s
V'	hindered particle settling velocity	m/s
α_a	shear stress ratio	-
α	area ratio	-
β	slip velocity coefficient	-
$\dot{\gamma}$	shear rate	s^{-1}
δ	boundary layer thickness	m
ϵ	rheogram slope	-
η	viscosity	$N.s/m^2$
η_a	apparent plastic viscosity	$N.s/m^2$
η_p	plastic viscosity	$N.s/m^2$
η^*	viscosity ratio	-
λ	linear concentration	m^{-1}
μ	dynamic coefficient of viscosity	$N.s/m^2$
μ_d	dynamic coefficient of sliding friction	-
μ_s	coefficient of incipient sliding friction	-
ν	kinematic coefficient of viscosity	m^2/s
ξ	shear stress ratio	-
ρ	bulk density	kg/m^3
σ_d	dispersive stress	Pa
τ	shear stress	Pa
τ_y	yield shear stress	Pa
ϕ	angle defining pipe slope	rad.
ϕ	freely settled particle porosity	-
ϕ	rheogram shape factor	-

Subscripts

a	apparent
A	axial
b	particle packing
BP	Bingham plastic
c	critical
ca	carrier
core	unsheared core
C	coarse fraction
d	dispersive
f	friction
F	fine fraction
FP	floc volume
g	generalized

h	hydrostatic
HIGH	high solids concentration
i	intercept
LOW	low solids concentration
m	solid-liquid mixture
max	maximum
min	minimum
n	Newtonian
nn	non-Newtonian
o	at the pipe wall
p	pseudo
p	particle
s	solid phase
sep	separation
vt	in situ volumetric
vd	delivered volumetric
w	water
w	weight
∞	infinity

CHAPTER 1

INTRODUCTION

The hydraulic transport of high solids concentration mineral tailings has become a major industry. The South African Gold Mines are transporting increasing tonnages of backfill to underground mining areas using sophisticated pipeline reticulation systems. The design of these pipeline systems requires input from a variety of scientific, engineering and technical disciplines. These involve aspects of :

1. Hydraulic transportation of material
2. Material properties and performance
3. Preparation of material
4. Placement of the material
5. System management.

The transportation of the material is of major importance and problems encountered at present are due to :

1. Poor system design
2. Pumping
3. Blockages of pipelines
4. Wear of pipelines.

These problems can largely be overcome by sound engineering management and system design principles. The most important aspect of any slurry pipeline system design is an accurate assessment of the flow behaviour of the slurry, and especially a knowledge of the energy required to transport the slurry over long distances.

The reasons for studying the high concentration stabilized flow of backfill slurries on South African Gold Mines are :

1. To satisfy requirements relating to the support characteristics of the fill when placed underground.

2. To balance the friction head loss with the available gravity head to avoid free fall of slurry in vertical pipelines. Free fall backfill systems have yielded problems due to slurry impact at the interface and high wear rates.

3. Current analytical models are found to be unsuitable for design of backfill pipeline systems.

1.1 The problem and its setting

In this research project an analytical model for the hydrotransport of high concentration stabilized full plant tailings is identified and evaluated. Full plant tailings have a wide particle size distribution and are one of the primary backfill material types used.

Previous researchers have shown that these materials cannot be modelled using traditional methods. At high concentrations "anomalous" behaviour occurs. This is indicated by a pipe diameter dependancy as shown on a pseudo shear diagram. The laminar flow curves are not co-incident for varying pipe diameters.

This anomalous behaviour is evaluated using several techniques and a method is presented which accounts for the anomalous behaviour. The method involves the separation of the measured wall shear stress into two components, a viscous component and a solid component. The viscous component can be determined from the rheogram using the yield pseudoplastic rheological model. The solid component is due to particle-particle interaction at the pipe wall and is explained by the presence of a dispersive stress which exists at high concentrations. The dispersive stress is related to the solid wall shear stress by a dispersive stress coefficient. The total wall shear stress is the summation of both the viscous shear stress and the solid shear stress.

The model is applicable at high solids concentrations for typical full plant tailings. The range of data over which the model is evaluated is presented in Table 1.1.

The definition of high solids concentration flow regime presented is based on analysis of experimental results. This definition defines the range over which the model is evaluated.

Parameter		Range		
Diameter	(m)	0,01348	to	0,1015
C_{vd}	(%)	25	to	52
S_s		2,72	to	2,74
d_{50}	(μm)	20	to	40
V_m	(m/s)	0,1	to	5

Table 1.1 : Range of parameters of the data base evaluated using existing and proposed mathematical models

1.2 Research methodology

The research is divided into five parts :

1. Review of basic theory
2. Experimental investigation
3. Analysis of experimental results
4. Computer aided analysis of current model compared with previous models
5. Conclusions.

PART 1 :

In the review of basic theory, high concentration stabilized flow of slurries is discussed. Non-Newtonian fundamentals are presented and current models for predicting the non-Newtonian flow of slurries are reviewed.

PART 2 :

The experimental investigation is discussed. A pipeline test facility was specifically built for this research and is explained in detail. Other sources of experimental data obtained from existing test facilities are explained. The experimental procedure is presented and the associated experimental errors in the observations are analysed.

The materials tested are detailed and characterized by the particle size distribution and solids concentration. The measured data from the test facilities is presented and discussed.

PART 3 :
Part 3 details the analysis of the experimental data. This involves the analysis of the "anomalous" behaviour of the slurry at high concentrations. The model is formulated on the basis of the analysis of the results.

PART 4 :
Part 4 describes the computer program written specifically to evaluate the available analytical models and proposed analytical model by comparison with the measured data. The computer program is a sophisticated design tool and can be used for a variety of purposes. Models included within the program can be used to predict the flow behaviour of mixed regime slurries as well as non-Newtonian slurries. The models used by the mining industry at present are evaluated using the computer program. It is shown that these models are not suitable for design use and under-predict the required energy gradients. The current model is evaluated against the measured data and is shown to be applicable to pumped high concentration full plant tailings.

PART 5 :
Part five contains the conclusions of the research program.

The Appendices contain the following additional information :

A. Tube flow derivations.

B. The determination of parameters for yield stress, fluid consistency index and flow behaviour index from a pseudo shear diagram.

C. The computer program users manual.

D. Data base containing the experimental data.

1.3 Summary

In summation, the main objectives of this research program are :

1. To explain the "anomalous" behaviour of high concentration full plant tailings.

2. To develop a mathematical model for the high concentration flow of full plant tailings.

3. To obtain a set of measured data over a range of pipe diameters and solids concentration.

4. To produce a user-friendly computer program containing all the relevant available analytical models and the current model.

5. To use the computer program to compare each of the mathematical models with the measured data and to provide limitations on the applicability of the models when used to predict the flow behaviour of high concentration full plant tailings.

This research fulfils these objectives and in addition makes a direct contribution to the mining industry in the form of the computer program. The computer program is entirely user-friendly and requires a minimum amount of training to use. It is a powerful design tool and can greatly assist in the optimization of the design of a backfill reticulation system.

The research program entailed a detailed investigation of high concentration stabilized flow. Many important parameters and distinguishing criterion were identified and will serve to facilitate the design of backfill slurry pipeline systems.

PART ONE

REVIEW OF BASIC THEORY

CHAPTER 2

HIGH CONCENTRATION HYDRAULIC TRANSPORT OF SOLIDS IN PIPELINES

2.1 Historical development

In order to present the relevant literature and research on high concentration backfill pipeline transport, it is necessary to define the limits of the work reviewed and to place the current review in the correct context.

Hydrotransport is a well established technology and numerous successful slurry pipelines around the world bear testament to its economic, environmental, commercial and industrial advantages over conventional bulk solids handling methods. Traditionally the majority of slurry pumping applications involve the transportation of relatively fine material in what is termed either heterogeneous or pseudo-homogeneous flow regimes at dilute solids concentrations. The transport velocities of the solids is generally high, greater than the settling velocity of the individual solids, in order to prevent solids deposition on the pipe invert which could lead to pipeline blockages. Recent developments in the coal mining industry and mineral waste disposal industries have identified that it is feasible and economically advantageous to transport solids at much higher concentrations and lower velocities than previously thought possible. The same technology has been utilised with varying degrees of success for the transport of high concentration mineral slurries at various mines worldwide. This work was first pioneered by Elliott and Gliddon (1970), who identified the stabilized flow concept, as applicable to hydrotransport, whereby the larger solid particles are supported by the yield stress of the high-concentration fines carrier or vehicle portion of the slurry. Bantin and Streat (1970) developed the dense-phase conveying of solids, whereby predominantly large particles are supported by particle-particle interaction, the weight being transferred to the pipe invert. Work by Calvert and Miller (1958) showed that it is possible to transport solids at volumetric solids concentrations approaching the freely settled bed-packing concentration (C_b) , where :

$$C_b = 1 - \phi \qquad (2.1)$$

ϕ = freely settled packed bed porosity.

The work of Calvert and Miller (1958) was later confirmed by Cloete, Miller and Streat (1967), who showed that dense phase flow is feasible at relatively high velocities (up to 3.05 m/s). Bantin and Streat (1970) showed that dense-phase transport of solid-water mixtures is possible in both vertical and horizontal pipes and that reasonably high flow rates with corresponding low pressure drops can be achieved. Further work by the same authors in 1972 concluded that dense-phase flow is possible at all flow rates for *in situ* concentrations (C_{vt}) equal to the freely settled bed-packing concentration (Equation 2.1). This implies that there is no solids settling occurring, which would increase the concentration to greater than the freely settled packed bed condition. Measurements of the velocity profiles at various concentrations and velocity ranges showed that at the high solids concentrations, the horizontal flow is dominated by gravity effects for low velocities, resulting in non-uniform velocity and concentration gradient profiles. At high velocities the particles were found to be supported by the carrier fluid at an *in situ* solids concentration, C_{vt}, approximating the freely settled bed packing concentration, C_b. The calculated slip-velocities indicated that the delivered volumetric solids concentration, C_{vd}, and the *in situ* solids concentration, C_{vt}, are similar, a distinguishing criterion for high concentration solids transport (for heterogeneous or mixed-regime flow, the *in situ* volumetric solid concentration, C_{vt}, is generally greater than the delivered volumetric concentration, C_{vd}).

Tests performed on sand/water mixtures and gravel/water mixtures by Streat *et al* (1976) confirmed the feasibility of dense phase transport for solids of varying particle size distributions and ranges. Televantos *et al* (1979) examined the flow of high concentration gravel and coal shale slurries and used a modified two layer model of Wilson to predict the pressure gradient. Considerable input is required for the coefficients of sliding friction, and the concentrations of solids

in the lower and upper layers of the model have to be determined from experimental test work observations. The dense phase conveying of solids, as opposed to dilute or low concentration solid water mixtures, was compared by Streat (1987). Results indicated that dense phase flow can reduce frictional energy gradients at high mass throughput, and states that there are many applications for dense phase transport in the commercial and industrial fields.

There are two major types of flow regimes that exist at high concentrations, viz., dense phase and stabilized flow.

Dense phase flow

The term 'dense phase' refers to a particular type of slurry containing a relatively small portion of fine material and a high percentage of coarser particles. Dense phase flow regimes are classified by the following features:, illustrated schematically in Figure 2.1.

1. Few fine particles in a predominantly coarse material matrix. The particles are supported by particle-particle interaction and the weight is transferred directly to the pipe invert.

2. High solids concentrations. The *in situ* volumetric solids concentration must be at least equal to or greater than the freely settled packed bed solids concentration
i.e. $C_b \geq C_{vt}$.

3. Uniform concentration and velocity profiles.

4. Relatively narrow particle size distribution.

5. Particles assemble and move as a single packed sliding bed with little or no slip at the pipe wall.

Stabilized flow

An alternative high concentration flow regime exists and has been termed stabilized flow. The predominant features of stabilized flow, represented in Figure 2.1, are as follows:

1. Large particles are suspended by the viscosity and yield stress of the fine particle/water mixture. There is a predominantly high percentage of fine particles in the slurry.

2. High solids concentration, as for dense phase flow. The *in situ* solids concentration, C_{vt} , must be greater than the freely settled bed packing concentration, C_b .

3. Uniform concentration and velocity profiles.

4. Uniform, well graded particle size distribution.

5. Generally non-Newtonian and homogeneous.

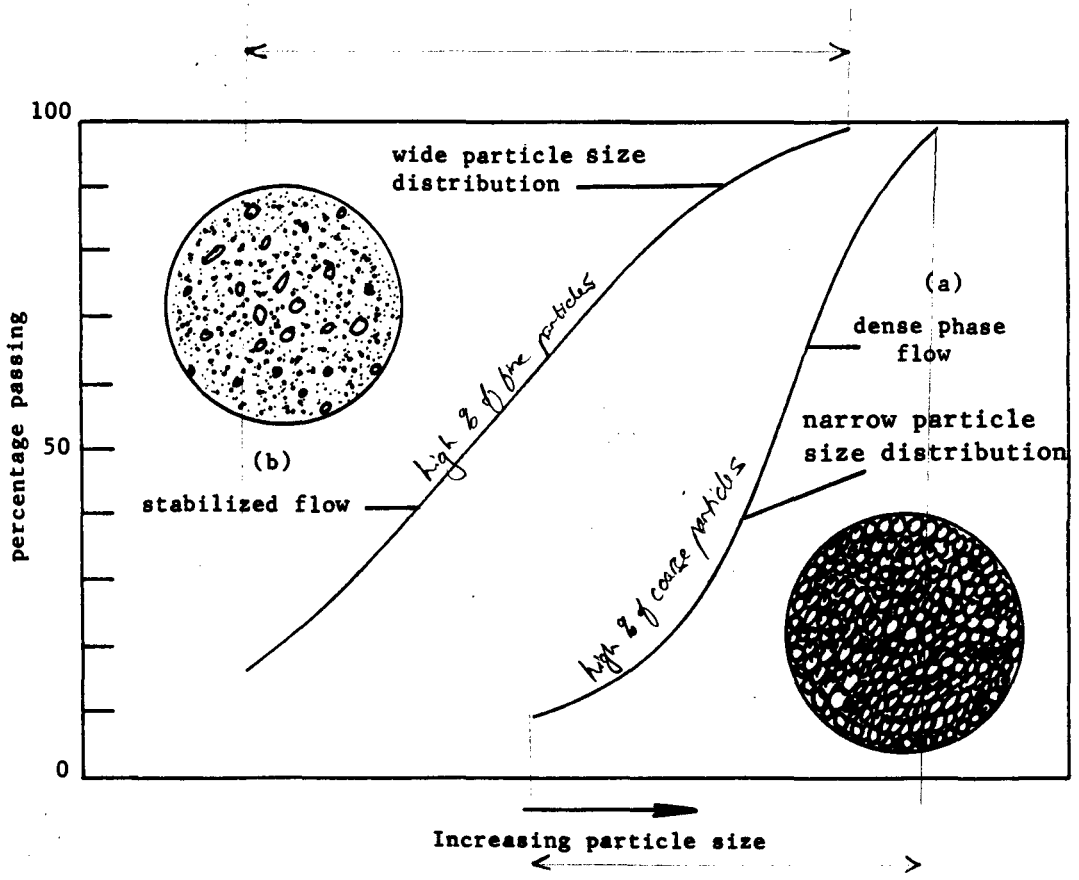

Figure 2.1 : Typical dense phase and stabilized flow particle size distribution curves

Stabilized flow is largely concerned with the high concentration transport of coal-water mixtures. The term "stab-flo" was first used by Lawler *et al* (1978) to describe these particular coal-water slurries. Viscometer tests indicated a Bingham plastic fluid at solids concentrations of 72% by weight. These tests indicated the feasibility of transporting coal slurries at the so-called "stab-flo" condition. An economic evaluation comparing conventional coal slurry transport (i.e. heterogeneous low concentration) to "stab-flo" indicated the considerable advantages of high concentration pumping technology. Brookes and Dodwell (1984) reviewed the status of current coal transport systems and reported that the stabflow approach yields the most potential in terms of economic viability and as a new alternative to the standardized or conventionally accepted methods of coal transport. Duckworth *et al* (1983) performed a series of tests on the transport of coarse coal at high concentrations ($53\% < C_w < 67\%$) and concluded that the stabflow condition is possible if the vehicle or fluid carrier is non-Newtonian and has a yield stress large enough to support the top size particle (the internal yield stress, τ_y, must be greater than the submerged weight of the largest particle in the slurry). Brookes and Snoek (1987) described test work on "stab-flo" mixtures and verified that for pipeline distances 2.5 km or longer, it is possible to transport these mixtures. Other authors, including Lagana *et al* (1984), Navrade and Klose (1984) and Verkerk (1986) have reported on the success and feasibility of transporting coal-water mixtures in the stabilized or "stab-flo" regime. Table 2.1 shows the concentrations and pipe diameters used by several authors when transporting stabilized flow slurries.

Authors		Maximum C_w(%)	Pipe Diameter
Lawler *et al*	(1978)	72.0	102mm
Duckworth *et al*	(1983)	65.6	152mm, 203mm, 254mm
Duckworth *et al*	(1986)	67.3	152mm
Brookes and Snoek	(1987)	79.0	300mm

Table 2.1 : Pumping of stabilized coal-water mixtures.
A selection of published data.

The development of the "stab-flo" work for coal-water mixtures has led to the application of this technology to other mineral slurry types, particularly in the mining industry. The mineral processing and mining industries are now using both the dense phase and stabilized flow solid transport technologies in a variety of applications. A major development is the use of 'backfilling' on the South African deep level gold mines. Backfilling refers to the hydraulic placement of particulate material in mined out stopes to be used as an underground support medium for the exposed hanging rock wall. The material originates from the mineral processing or metallurgical extraction plant and consists of the ground or crushed mined ore from which the precious minerals have been extracted. This waste material is transported from the metallurgical plant to the underground stopes by means of a pipeline reticulation system. A schematic representation of a typical system from surface plant to underground mining haulages via the mine shaft is shown in Figure 2.2. Backfill as a means of providing underground fill has been successfully used for many years in both Germany (Lerche and Renetzeder (1984)) and Australia at Alcoa mine and is a proven technique for these particular fill types used on these mines.

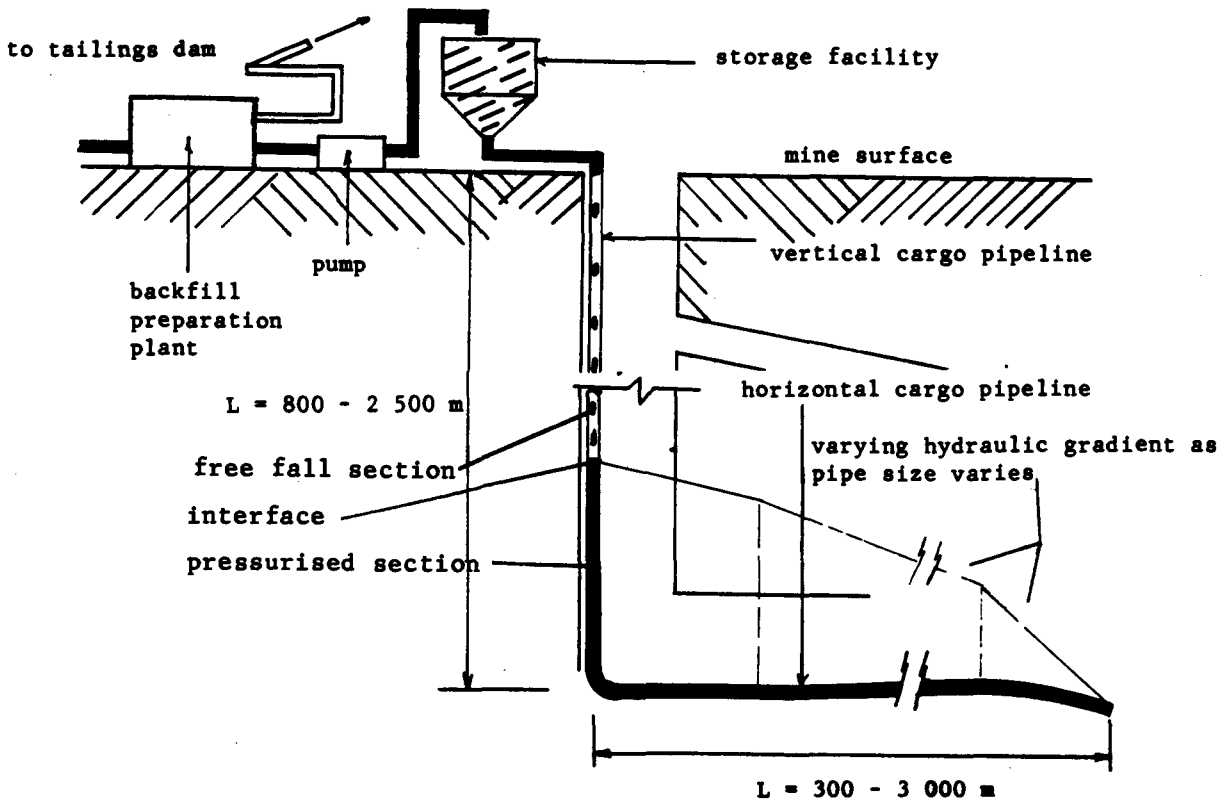

Figure 2.2 : Schematic representation of a typical backfill reticulation system

South African gold mines began backfilling in the early twentieth century (circa 1925) using sand fills, but this did not last as problems were encountered at increasing depths. Increasing costs of traditional underground support mediums led to the re-introduction of backfilling on South African gold mines. The placement of backfill has been predicted to increase from 0.2 million tons per month in 1988 to 2 million tons per month in 1995 (Piper (1988)). Because of the sudden and rapid growth of backfill pipeline reticulation systems, the available methodology for determining the design criteria for these slurries is inadequate and has led to major problems and pipeline failures in the mining industry. Despite these problems, the inherent and numerous advantages (Sive (1988)) has led to renewed research and development in this field.

Several different types of backfill material exist, the differences resulting from the mineral extraction process, and these are generally divided into two broad groups, full plant tailings and classified tailings. These two tailings are derived from the same materials and exhibit similar material properties. Full plant tailings is the total waste product from the extraction process, containing a broad range of particles. The classified tailings is merely the result of hydrocycloning the full plant tailings and removing the majority of the fine particles below 38 μm. This process results in two materials, inherently identical, but with vastly differing hydraulic transportation characteristics. Table 2.2 shows the general types of backfill slurries and an indication of their differing particle size distributions. The complete particle size distribution envelopes for full plant and classified tailings is shown in Figure 2.3. Comparing this figure with Figure 2.1, the distinction and comparisons between these two materials and the criterion for dense phase and stabilized flow regimes can be seen. The classified tailings behave as a dense phase slurry, and the full plant tailings behave as a homogeneous stabilized slurry.

Backfill Type	Typical Relative Density (S_m)	d_{10} (μm)	d_{50} (μm)	d_{90} (μm)
Classified Tailings	1.50 to 1.75	10 to 20	120 to 180	250 to 350
Full Plant Tailings	1.50 to 1.90	4 to 8	20 to 50	100 to 150

The top size of both these materials is < 550 μm

Table 2.2 : The two primary types of backfill material used on the South African Gold Mines at present (1990) - full plant tailings and classified tailings

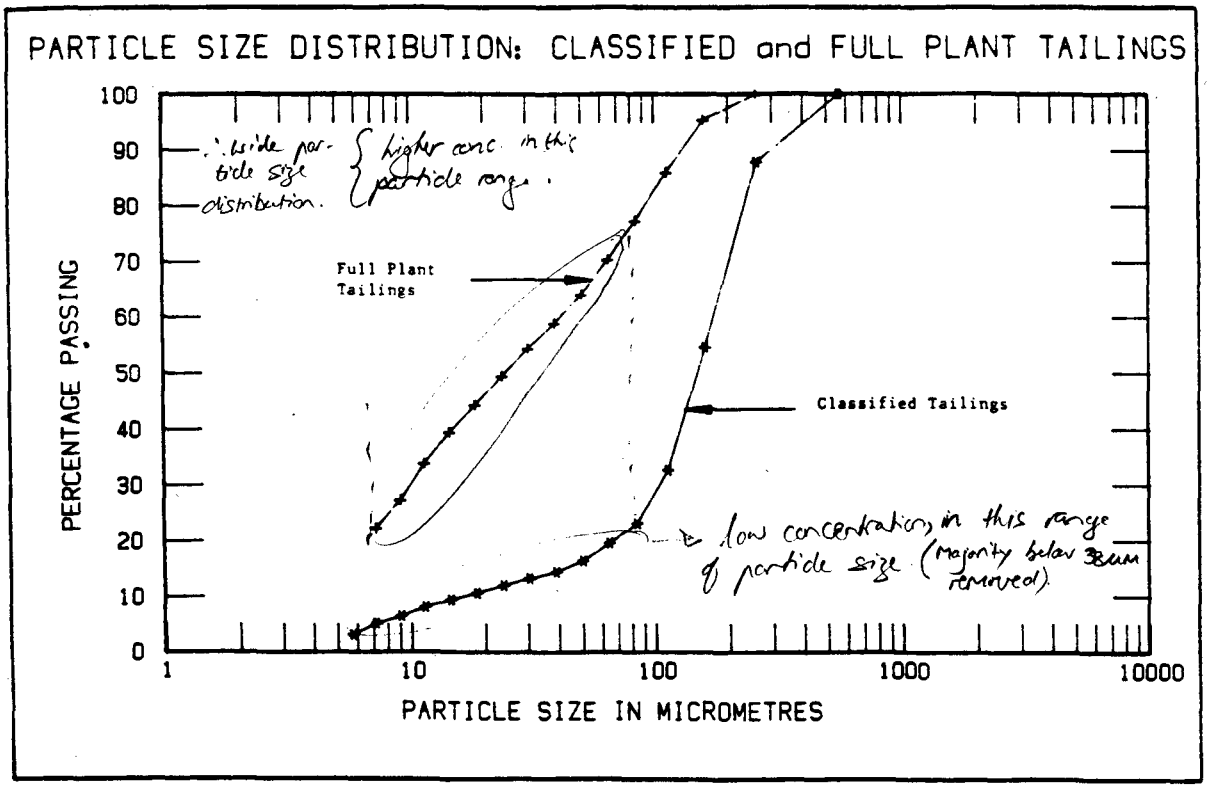

Figure 2.3 : Particle size distribution curves for full plant and classified tailings

This investigation is primarily concerned with the development of an analytical model to predict the flow behaviour of full plant tailings at high concentrations. This is only one aspect of the total backfill placement industry, but fulfills the need to enable engineers and designers to design optimum backfill pipeline systems. The unique flow behaviour of full plant tailings is different from that of classified tailings and is therefore a separate study. There is not a great deal of literature or past research data on this specific aspect, and reference is made to general stabilized flow concepts, developed in both the coal industry, waste processing industry and gold mining industry.

2.2 Review of analysis of the high concentration stabilized flow regime

Stabilized flow slurries, by definition, have been found to exhibit non-Newtonian rheological characteristics by numerous researchers, including Elliot and Gliddon (1972), Thomas (1979), Duckworth *et al* (1983), Duckworth (1986), Brookes and Snoek (1986) and Streat (1986). This non-Newtonian behaviour is attributed to the high percentage of fine particles and the high solids concentration. For mineral backfill full plant slurries several authors, Verkerk (1988), Lazarus and Slatter (1988), Horsley (1982), Neill (1988) and Paterson (1988) have found strong non-Newtonian characteristics. Non-Newtonian behaviour is associated with homogeneous laminar flow conditions, and several empirical rheological correlations exist to model the fluid behaviour. These fluids can be either time-independent or time dependent. Figure 2.4 is a schematic representation of a rheogram, indicating the shear stress versus shear rate curves for a range of common constitutive fluid models. It is important to note that these proposed models are not governing laws of fluid behaviour, but are merely empirical descriptions of the mathematical behaviour of the homogeneous fluid in pipe flow. Bowen (1961) and Hanks (1982) stressed that these generalized correlations failed to correlate data accurately, except in the range over which they were tested, and that design procedures are only applicable to certain fluid types.

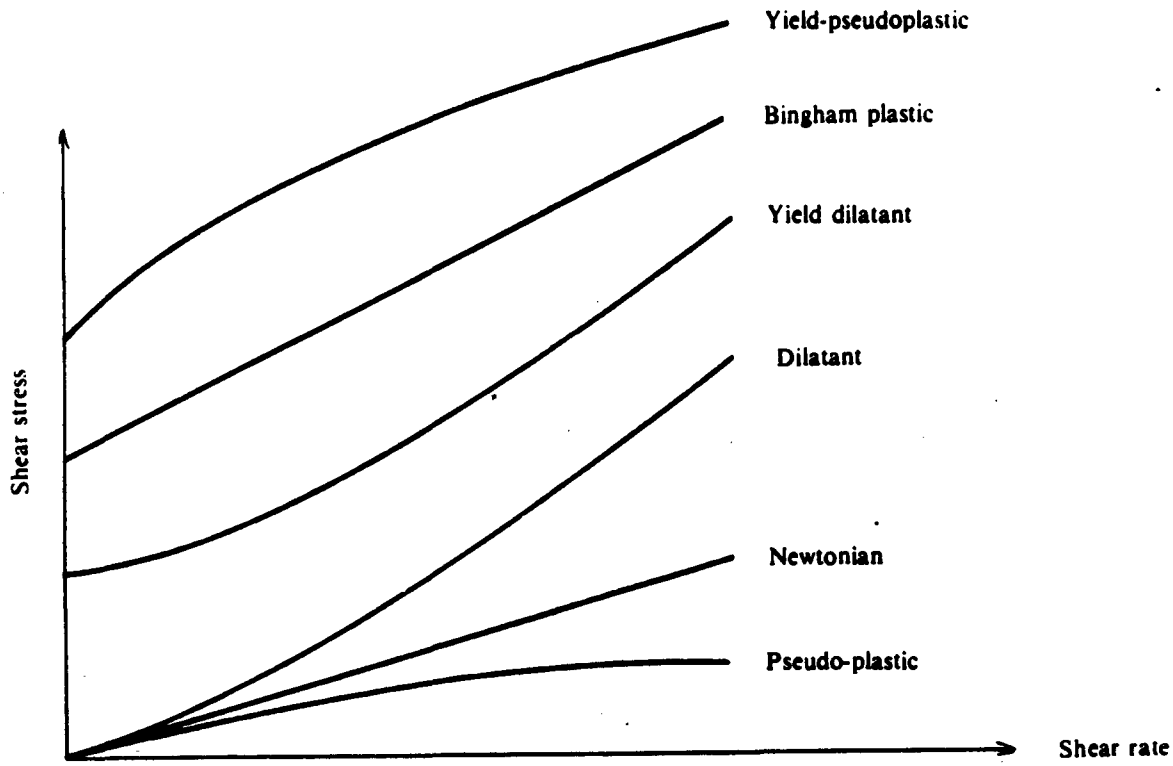

Figure 2.4 : Rheogram illustrating the flow behaviour of time independent non-Newtonian fluids

2.2.1 Laminar flow of Newtonian fluids

Idealized laminar flow in a pipe requires no transverse velocity components to the direction of flow. Variation in both viscosity and temperature of the fluid may give rise to small transverse velocity components, but these are generally of negligible magnitude.

Poiseuille's law for laminar pipe flow is given by :

$$Q = \frac{k R^4 \Delta P}{L} \qquad (2.2)$$

where $k = \frac{\pi}{8\mu}$

Defining the well known Fanning friction factor, f , as :

$$\frac{-dP}{dL} = \frac{2 f \rho V^2}{D} \qquad (2.3)$$

where $f = \frac{2 \tau_y}{\rho V^2}$

For laminar flow, the value of f must be such that Equations 2.2 and 2.3 yield the same pressure gradient $\Delta P/L$, resulting in Equation 2.4.

$$f = \frac{16}{Re_n} \qquad (2.4)$$

where Re_n = Newtonian or non-Newtonian Reynolds Number of the fluid.

2.2.2 Stress-strain relationship of Newtonian fluid

The linear response curve on the rheogram in Figure 2.4 is governed by Equation 2.5 for tube flow. The coefficient, μ , is a property of the fluid and depends to a large extent on temperature. It is a measure of the 'viscosity' of the fluid and Equation 2.5, often referred to as Newton's law of friction, serves to define fluid viscosity.

$$\tau = \mu \left(-\frac{du}{dr}\right) \qquad (2.5)$$

where τ = shear stress

μ = coefficient of dynamic viscosity

$\frac{du}{dr}$ = rate of increase of velocity

Whenever frictional and inertial forces interact, the ratio of viscosity, μ , to fluid density, ρ , is denoted by the kinematic viscosity, ν ;

$$\nu = \frac{\mu}{\rho} \qquad (2.6)$$

Referring to the rheogram in Figure 2.4, the viscosity can be referred to as an *apparent viscosity* at any point on the curve. From Equation 2.5, μ is clearly the slope of the rheogram, and for a Newtonian fluid , the viscosity is the slope of the straight line and is thus consistent for all rates of shear. Whenever the slope of the rheogram changes direction, the viscosity changes, indicating a specific value of viscosity at a particular state of fluid stress. In these instances, the fluid is non-Newtonian, and further parameters are needed to define the fluid behaviour.

2.2.3 Non-Newtonian rheological models

There are two main non-Newtonian fluid types :

1. Time-independent viscous fluids,
2. Time-dependent viscous fluids.

Both coal and backfill material stabilized slurries have been reported to be time-independent non-Newtonian fluids and these fluid types will be discussed below.

2.2.3.1 Pseudoplastic fluids

Shear thinning fluids which have no yield stress are referred to as pseudoplastic materials, and are often described by the power law correlation. The power law model replaces the basic Newtonian model by the inclusion of the flow behaviour index, n . The form of the equation is as follows :

$$\tau = K \left(-\frac{du}{dr}\right)^n \qquad (2.7)$$

where K = fluid consistency index.

The power law model is a simplified empirical observation made by Ostwald (Hanks (1982)), and is valid for a limited range of shear rates as highlighted in Figure 2.5. The viscosity varies for a range of shear rates, and for $n < 1$, it can be seen that the apparent viscosity vanishes at high rates of shear. For limited shear rates, a log-log plot will indicate the linearity of the viscosity, however at

higher shear rates the rheogram will assume the curve shown in Figure 2.5. Assuming the validity of the power law model over a working range of shear rates, several fluid types can be approximated.

Newtonian fluid	$n = 1$
Pseudo-plastic fluid	$n < 1$
Dilatant fluid	$n > 1$

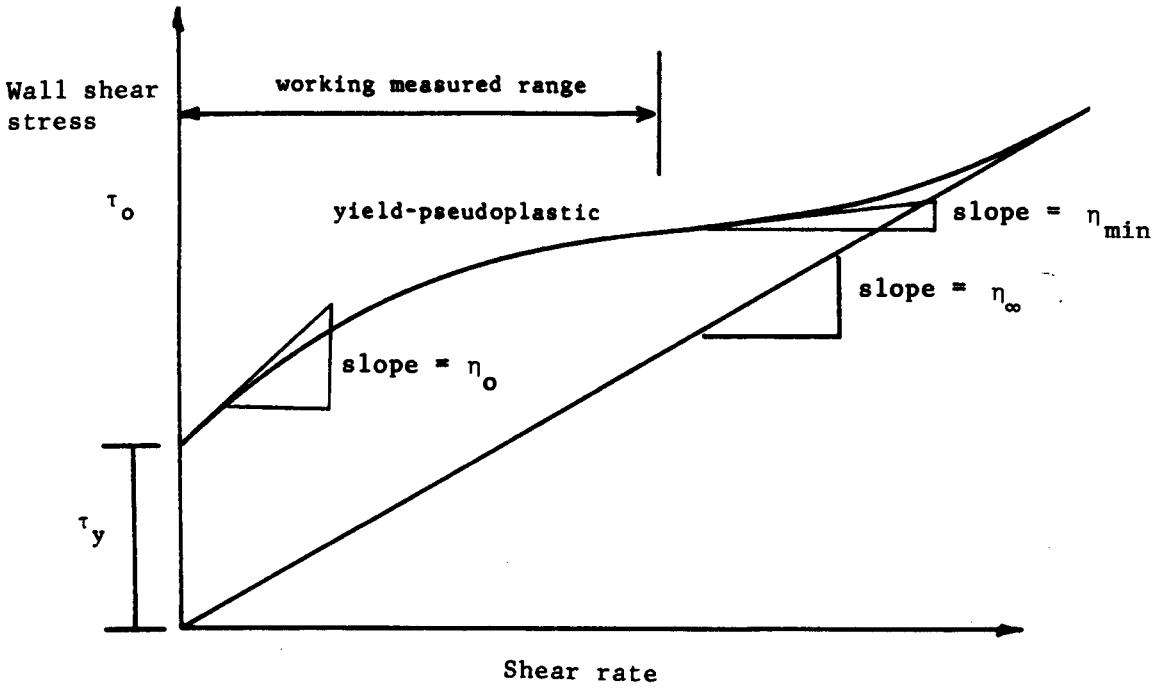

Figure 2.5 : Rheogram indicating variation of viscosity with increasing shear rate

2.2.3.2 **Plastic fluids**

Plastic fluids do not have a finite viscosity at low shear rates, but possess a yield stress, τ_y , at zero shear rate. There are several models which describe this type of behaviour.

2.2.3.2.1 Bingham Plastic Model

This is a simplification of the actual rheogram curve, where the curve is approximated by a straight line and is represented by Equation 2.8.

$$\tau = \tau_y + \eta_p \left(-\frac{du}{dr}\right) \qquad (2.8)$$

where η_p = plastic viscosity, or coefficient of rigidity.

The Bingham plastic model is a two parameter rheological model which accurately describes a large number of suspension bearing fluids. Coal-water slurries as well as mineral stabilized slurries have been described using a Bingham plastic model. As in the power law model, and since the flow behaviour index is unity, the model is only valid for a limited range of shear rates.

2.2.3.2.2 Yield Power Law Model

By the addition of a yield stress term, τ_y, to the power law model, the Herschel-Bulkley correlation is as follows :

$$\tau = \tau_y + K \left(-\frac{du}{dr}\right)^n \qquad (2.9)$$

where K = fluid consistency index
n = flow behaviour index.

The yield power law model essentially represents the interpolation from the simple power law model ($\tau_y = 0$), to a Bingham plastic type fluid ($n = 1$, $\tau_y > 0$). This is often referred to as a generalized model, but this is not a valid generalization as no account of varying flow behaviour over an extended range of shear rates is included. Appendix A contains the full derivation from tube flow theory of the solution to Equation 2.9. Other approximations to various fluid type may be made using the power law model, as shown below :

		n	τ_y
i.	Newtonian	1	0
ii.	Bingham Plastic	1	>0
iii.	Pseudo-Plastic	<1	0
iv.	Yield Pseudo-Plastic	<1	>0
v.	Dilatant	>1	0
vi.	Yield Dilatant	>1	>0

2.2.3.2.3 Metzner and Reed generalized approach

For fluids whose laminar flow behaviour does not relate to any standardized rheological equation, a generalized approach exists, developed by Metzner and Reed (1953), using the expressions 2.10 and 2.11.

$$\tau_o = K' \left(\frac{8\ V}{D}\right)^{n'} \qquad (2.10)$$

$$\tau_o = \frac{D\ \Delta P}{4L} \qquad (2.11)$$

where $\Delta P/L$ = pipeline pressure gradient
D = pipeline internal diameter
K' = apparent fluid consistency index
n' = apparent flow behaviour index.

Equation 2.10 represents the tangent to the log-log plot of $D\Delta P/4L$, (τ_o) versus $8V/D$ at any particular bulk shear rate. n' is determined by the slope of the curve.

The Fanning friction factor, f, is given by Equation 2.12.

$$f = \frac{D\ \Delta P}{2\ \rho\ V^2\ L} = \frac{\tau_o}{\frac{1}{2}\ \rho\ V^2} \qquad (2.12)$$

The generalized Reynolds Number (Re_{nn}) can be defined for laminar flow, from Equation 2.4, as :

$$f = \frac{16}{Re_{nn}} \tag{2.13}$$

The Reynolds number, Re_{nn}, given by Equation 2.14, is derived by substituting Equation 2.10 and Equation 2.13 into 2.12.

$$Re_{nn} = \frac{8 \rho V^2}{K' (8V/D)^{n'}} \tag{2.14}$$

The Metzner and Reed approach has been successfully used for coal-water slurries with concentrations in excess of 60% by weight (Streat (1986)), but has not been used for high concentration mineral tailings.

2.2.4 Turbulent flow

Laminar flow is characterized by no velocity components normal to the direction of flow, whereas turbulent flow is characterized by varying or rapidly fluctuating velocity components in all directions (these chaotic vortex motions are called eddies). For all types of non-Newtonian fluids, laminar flow will become turbulent flow as the Reynolds number increases. The transition point is termed the critical Reynolds number and several definitions of the transition point exist, illustrated below in Table 2.3. Transition occurs at different values of Reynolds number for different fluid types.

Bingham Plastic Fluids

Hanks (1963) $$Re_c = \frac{He}{8\,x_c}\left(1 - \frac{4}{3}x_c + \frac{1}{3}x_c^4\right) \qquad (2.15a)$$

where x_c is defined by :

$$\frac{x_c}{(1 - x_c)^3} = \frac{He}{16\,800} \qquad (2.15b)$$

where He = Hedström Number

Pseudoplastic (power law) fluid

$$f_c = \frac{1}{404}\,\frac{(1 + 3n)^2}{n}\,\left(\frac{1}{2 + n}\right)^{(2+n)/(1+n)} \qquad (2.16a)$$

which can be expressed in terms of the power law Reynolds number as :

$$Re_c = \frac{6\,464\,n}{(1 + 3n)^2\,(1/(2+n))^{(2+n)/(1+n)}} \qquad (2.16b)$$

Generalised non-Newtonian laminar-turbulent transition (Hanks (1974))

$$Re_c = \frac{6\,464\,n}{(1 + 3n)^2}\,\frac{(2 + n)^{(2+n)/(1+n)}\;\sigma_c^{(2/n)}}{(1 - \xi_c)^{(1+2/n)}} \qquad (2.17a)$$

where $$\xi_c = \frac{\tau_y}{\tau_{oc}} \qquad (2.17b)$$

$$\sigma_c = (1 - \xi_c)^{1+n}\left[(1 - \xi_c)^2 + 2\,\xi_c\,(1 - \xi_c)\left(\frac{1+3n}{1+2n}\right) + \xi_c^2\left(\frac{1+3n}{1+n}\right)\right]^n \qquad (2.17c)$$

ξ_c is solved from Equations (2.17d) and (2.17e), where He_g is the generalised Hedström number

$$He_g = \frac{D^2\,\rho}{\tau_y}\left(\frac{\tau_y}{K}\right)^{2/n} \qquad (2.18)$$

$$\frac{\xi_c^{(2/n-1)}}{(1 - \xi_c)^{(2/n+1)}} = \frac{n\,He_g}{3\,232}\left[\frac{1}{2 + n}\right]^{\frac{2+n}{1+n}} \qquad (2.19)$$

Table 2.3 : Formulae for determining the critical Reynolds number for the transition from laminar to turbulent non-Newtonian flow

Duckworth *et al* (1986) confirmed the use of Equation 2.15(a) in the generalized form of Hanks (1962) for Bingham plastic stabilized flow analysis to predict successfully the onset of turbulent flow. The critical shear stress ratio, α_{ac}, referred to in Equation 2.20 below is defined by τ_{ya}/τ_o, where τ_{ya} is the apparent yield stress of the coarse fraction slurry and τ_o is the wall shear stress.

$$\rho_w S_m \tau_{ya} D^2 / \eta_a^2 = \frac{16\ 800\ \alpha_{ac}}{(1 - \alpha_{ac})^3} \qquad (2.20)$$

The pressure gradient for the turbulent flow for non-Newtonian fluids can be expressed in several forms, depending on the rheological model. The friction factor for a yield-pseudoplastic can be expressed by the generalized Torrance equation below (Torrance (1963)).

$$\sqrt{(2/f)} = [\ (3,8/n) - 4,17\ ] + [\ (2.78/n) \ell n\ \{1-(\tau_y/\tau_o)\}\ ]$$

$$+ [\ (2,78/n)\ \ell n\ (Re_{nn} \sqrt{f^{2-n}})\ ] \qquad (2.21(a))$$

$$+ (0,965/n)(5n-8)$$

$$\text{where } Re_{nn} = \frac{8\ \rho_m\ V^2}{K\ (8V/D)^n} \qquad (2.21(b))$$

Using Equation 2.21(a) and setting $\tau_y > 0$ and $n = 1$, the relationship for a Bingham plastic fluid can be found and is expressed in Equation 2.22 below.

$$1/\sqrt{f} = 4,53\ [\log\ (1 - (\tau_y/\tau_o)\ ) + \log\ (Re_{BP} \sqrt{f})\ ] - 2,3 \qquad (2.22)$$

where Re_{BP} = Bingham plastic Reynolds Number.

Note : Equation 2.21 can be used for simple power law fluid by setting $\tau_y = 0$, and for a Newtonian fluid by setting $\tau_y = 0$, $n = 1$ and $Re_{nn} = Re$.

A generalized method based on the Metzner and Reed analysis for laminar flow can be extended to Equation 2.23 using K' and n' evaluated at the appropriate shear rate corresponding to the wall shear stress, τ_o .

$$\frac{1}{\sqrt{f}} = \frac{4,0}{n'^{0,75}} \log \left[Re'_{nn} f (1 - n'/2) \right] - \frac{0,40}{n'^{0,5}} \qquad (2.23)$$

2.2.5 Discussion - Wilson, K.C. (1986) "Modelling the effects of non-Newtonian and time dependant slurry behaviour", 10th International Conference on the Hydraulic Transport of Solids in Pipes, Innsbruck, Austria, 1986, pp. 283-289

The problems associated with the yield pseudo-plastic rheological constitutive equation limits the validity and use of the equation to a small range of shear rates. The abovementioned paper discusses the shortcomings of this equation and provides a more generalized form of the equation for a broader range of non-Newtonian fluid types. The paper highlights the possibilities of drag reduction in turbulent pipe flow which is shown to be attributed to the formation of dissipitative eddies, termed micro-eddies, resulting in the thickening of the viscous sub-layer. Wilson and Thomas (1985), stated that for turbulent flow, the rate of energy dissipation is determined by the area beneath the non-Newtonian rheogram.

For a Newtonian rheogram, the area is a triangle ($\tau_o = 0$ and viscosity is constant) and is equivalent to $0.5\ \tau\ (du/dy)$. Figure 2.6 represents both the Newtonian and non-Newtonian rheogram. The ratio of the areas under the two rheograms for the same values of shear stress and shear rate is denoted by α , the area ratio constant. α is larger than unity, and is found to be between 1.0 and 2.0. The increased area under the non-Newtonian rheogram is attributed to the increased viscosity and not a greater rate of energy dissipation. The non-Newtonian fluid is said to behave as a Newtonian fluid with an increased viscosity proportional to the increased area under the rheogram or $\mu_{nn} = \alpha \mu_n$.

At high shear rates, the mathematical function for τ should approach a straight line for a limiting viscosity, μ_∞, and is given by :

$$\tau = \tau_i + \eta \frac{du}{dy} \qquad (2.24)$$

The terms τ_i and τ_y are defined in Figure 2.7. The mid range of the rheogram is incorporated into Equation 2.24 by an exponentially decreasing function, yielding the general form of the Wilson equation in Equation 2.25.

$$\tau = \tau_i + \eta \frac{du}{dy} - (\tau_o - \tau_y)\exp^{(-\phi\,(du/dy))} \qquad (2.25)$$

Equation 2.25 needs four terms to be evaluated :

(i) ϕ, the rheogram shape factor,

(ii) τ_i, the shear stress intercept,

(iii) τ_y, the actual yield stress,

(iv) η, the slope of the rheogram at high shear rates.

The above parameters need to be solved by analysis of the actual rheogram, reducing the method to a series of successive interpolations. It is doubtful whether shear rates sufficiently high enough to calculate η will be obtained using conventional viscometric measurement methods, a problem discussed by Hanks (1982). The shape factor, ϕ, is not given in terms of the area ratio, and needs to be found using least squares regression analysis techniques.

Using this method, it was however found suitable for the scaling of non-Newtonian data for a range of pipe sizes, using Equations 2.26, 2.27 and 2.28. This is based on the premise that u^*, the shear velocity, is the same in both pipe diameters.

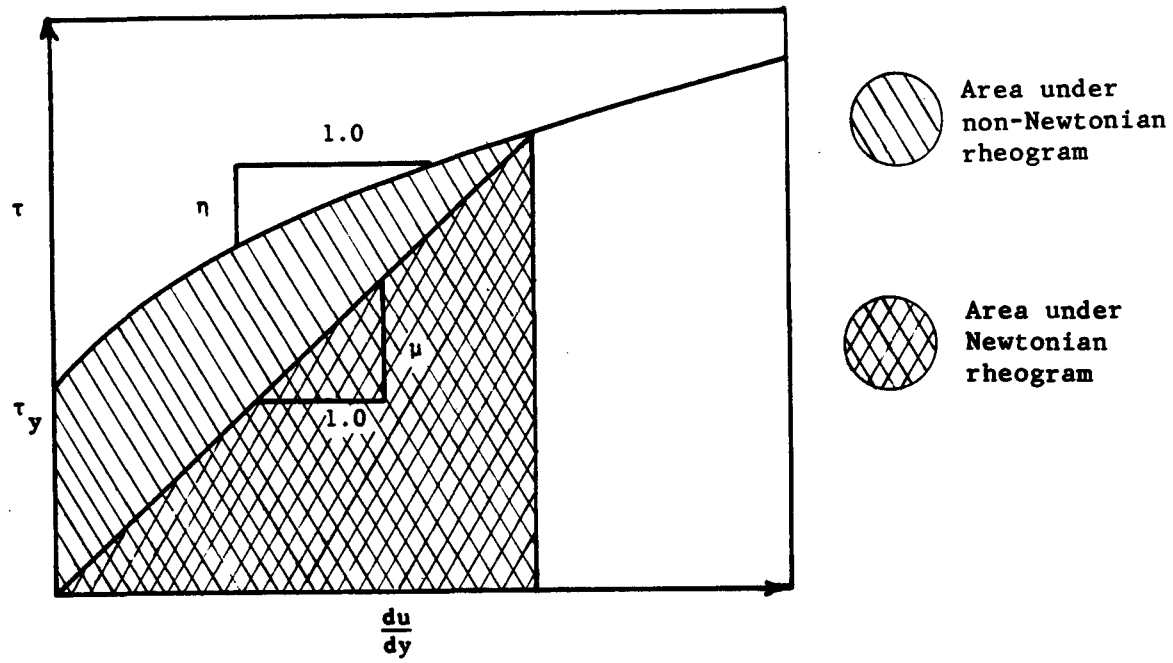

Figure 2.6 : Newtonian and non-Newtonian schematic rheograms indicating the differences between the relative areas below the rheogram curves

$$u^* = \sqrt{(\tau_o/\rho_m)} \qquad (2.26)$$

$$V_2 = V_1 + 2.5\, u^* \ln (D_2/D_1) \qquad (2.27)$$

$$\frac{\Delta P_2}{\Delta x_2} = \frac{\Delta P_1}{\Delta x_1}\,\frac{D_1}{D_2} \qquad (2.28)$$

where $\Delta P/\Delta x$ = pressure gradient.

The general Equation 2.25 can be used for the power law fluid, provided that the logarithmic plot of the data is represented by a straight line for appropriate selected parameter values and the yield stress, τ_y, equals zero. This seems to be a drawback of the model, as parameters need to be determined from the rheogram. Normally, the rheogram will provide a means to determine the primary parameters of yield stress and viscosity of the fluid and not secondary parameters such as curve shape. The generalized approach of Metzner and Reed seems sufficient to provide for varying parameters with increasing shear rate. By

adjusting the parameters in Equation 2.25, several fluid types can be approximated. To represent typical dilatant behaviour, the parameter, τ_y , the actual yield stress, can be set to be greater than the yield stress intercept, τ_i . This will alter the rheogram and in effect will increase the flow behaviour index, n , to greater than unity.

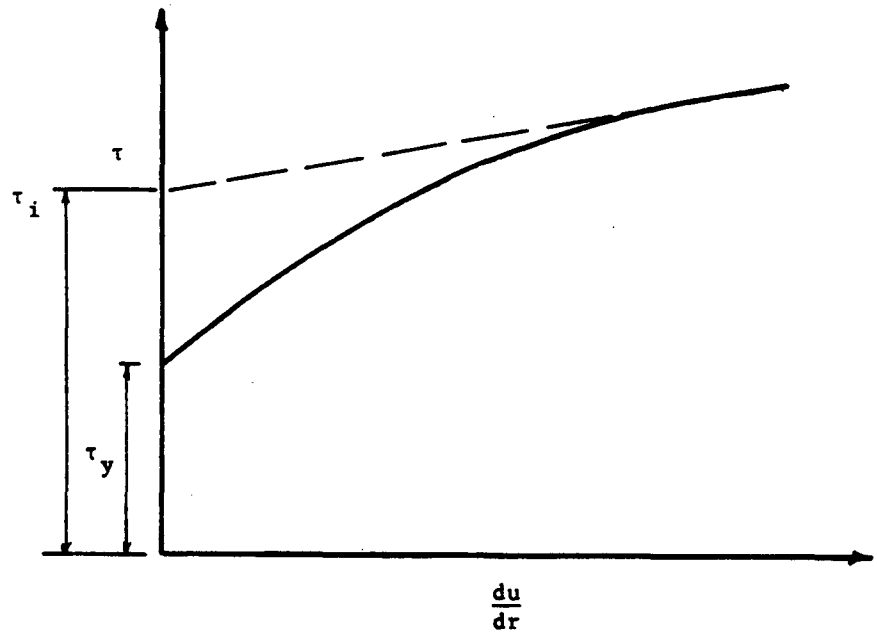

Figure 2.7 : Graphical representation of the terms (τ_i and τ_y) used in Equation 2.25 to describe the variation in apparent viscosity

2.2.6 Discussion - Duckworth, R.A.; Pullum, L.; Addie, G.R.; Lockyear, C.F. (1986) "The pipeline transport of coarse materials in a non-Newtonian carrier fluid", 10th International Conference on the Hydraulic Transport of Solids in Pipes, Innsbruck, Austria, 1986, pp.69-87

The analysis of stabilized coal slurries, carrying coarse coal particles with a top size of 20 to 25 mm, and for mine waste disposal is discussed. The equations presented are for a typical Bingham plastic fluid type, and the paper demonstrates the 'stab-flo' concept of Lawler *et al* (1978) to be generally applicable.

Previous work by Duckworth and Pullum (1981) demonstrated that considerations other than particle packing density are important when considering stabilized flow. The rheological properties of the minus 500 μm fraction are the dominant criterion. For laminar flow conditions, the vehicle portion (carrier) should have a sufficient yield stress to support the coarser particles. This stable equilibrium equation is given below :

$$\tau_y >= 0.1\ \rho_w\ g\ d'\ (S_s - S_{mca}) \qquad (2.29)$$

where d' = size of largest particle to be supported or d_{50} for the mineral slurry tested.

S_{mca} = Relative density of carrier portion.

The use of the top size particle to be suspended by the carrier portion of the slurry is obviously over-conservative. The d_{50} , the geometric mean diameter, is chosen by the authors as being representative of the supported size particle, as the premise is that the coarse particles of $d < d_{50}$ will provide additional support for those of $d > d_{50}$.

The addition of the coarser materials to the carrier fluid affects the rheological properties, the yield stress (τ_y) and the viscosity (η), referred to as the modified yield stress, τ_{ya} , and the modified apparent viscosity, η_a . The generalized forms of the equations to predict these modified parameters are shown below in Equations 2.30 and 2.31.

$$(\tau^*-1) = \phi_1\ [(S^*-1),\ M^*,\ dy/d',\ d_{50}/d',\ d'/D,\ \mu_s,\ S_s] \qquad (2.30)$$

$$(\tau^*-1) = \phi_2\ [(S^*-1),\ M^*,\ dy/d',\ d_{50}/d',\ d'/D,\ \mu_s,\ S_s] \qquad (2.31)$$

where $\tau^* = (\tau_{ya}/\tau_y)$

$\eta^* = (\eta_a/\eta)$

$S^* = (S_m - 1)/(S_{mca} - 1)$

$M^* =$ mass flow ratio $= M_C/M_F$

$dy = 10\ T_y/\rho_{wg}\ (S_s - S_{mca})$

Analysis of measured data determines the functional relationships ϕ_1 and ϕ_2. For mineral waste tailings, the Equations 2.30 and 2.31 reduce to the following semi-empirical correlations.

$$(\tau^* - 1) = 18\ (S_s - 1)\ (S^* - 1)^{1.5} \qquad (2.32)$$

$$(\eta^* - 1) = 2.33\ (S^* - 1)^3\ /\ (S_s - 1)^{2.58}\ M^{*2} \qquad (2.33)$$

Combining the standard Buckingham equation, Equation 2.34, with the criterion for the onset of turbulent flow by Hanks (1962), Equation 2.35, the rheogram relating wall shear stress to the pseudo shear rate can be calculated.

<u>Buckingham equation for Bingham plastic pipe flow</u>

$$\frac{8}{N_{ya}} = \left[\ 1 - \frac{4\ \alpha_a}{3} + \frac{\alpha_a^4}{3}\ \right] / \alpha_a \qquad (2.34)$$

where N_{ya} = yield number $= \tau_{ya}\ D\ /\ \eta_a\ V_m$

$\alpha_a = \tau_{ya}\ /\ \tau_o$

Hanks (1962) laminar - turbulent transition

$$\rho_w S_m \tau_{ya} D^2 / \eta_a^2 = 16\,800\, \alpha_{ac} / (1 - \alpha_{ac})^3 \qquad (2.35)$$

where α_{ac} = critical shear stress ratio.

For critical shear values greater than the critical Reynolds number, the turbulent flow analysis can be done using the Jain (1976) form of the Colebrook-White equation as follows :

$$1/f^{1/3} = 1.14 - 2 \log [e/D + 21.25\, Re_{BP} - 0.9] \qquad (2.36)$$

where f = friction factor = $\tau_o / \rho_m V_m^2 / 8$

$Re_{BP} = \rho_m V_m D / \eta_a$

e/D = roughness ratio.

The pressure gradient can be calculated from Equation 2.37, to transform the shear stress versus shear rate rheogram to the standard pressure gradient versus mean mixture velocity diagram ($\Delta P/L$ versus V_m).

$$\frac{\Delta P}{L} = \frac{4\, \tau_o}{D} \qquad (2.37)$$

Experimental results are needed for the determination of S* , the ratio of the mixture specific density to carrier fluid specific density, and the mass flow ratio, M* , the ratio of the mass flow of coarse material, M_c , to the mass flow rate of the fine portion, M_f . In principle, values of M* and S* are necessary for all values of velocity as they are essentially dependant on the differences between *in situ* and delivered volumetric concentrations. For a homogeneous stabilized slurry, these differences are inherently small, implying a small modification of the apparent yield stress and viscosity in Equations 2.32 and 2.34. Values of M* and S* are presented for a range of corresponding yield stresses. These values are summarized in

Table 2.4 below. By definition, S* is larger than unity, and M* is less than unity. Both these parameters are evaluated according to the coarse to fine particle definitive split size, and it is not clearly indicated whether it is the d_{50} size or 500 μm.

The modified apparent viscosity and yield stress were shown to be valid, but several constants need to be defined more explicitly. The correlation of measured data to predicted values was good, but the constants for the functional relationships were derived from the same data, therefore assuring good results.

Dimensionless parameters			
τ^*	η^*	S*	M*
3.40	1.10	1.21	0.31
to	to	to	to
14.63	2.0	1.67	0.89

Table 2.4 : Range of dimensionless parameters used in the analysis of coefficients for Equations 2.24 and 2.25 (from Duckworth *et al* (1986))

The scale up of results based on equivalent shear strain rate in pipes of varying diameter indicated that the equations provided a reasonable estimation to predict the transport properties of Bingham Plastic fluid types. The main area of concern is the division between fine and coarse particles, and this will determine the ratios M* and S* . Analysis of the Equations 2.32 and 2.33 indicates the importance of these constants. Assuming that the *in situ* and delivered concentration is the same, then the relative density ratio should approach unity and then reduce the righthand side of Equation 2.32 to zero, i.e. $(\tau^* - 1) = 0$ or $\tau_{ya} = \tau_y$, resulting in no change to the actual yield stress of the homogeneous slurry. A similar result will occur if the mass flow rate of the coarse material is zero, either all the particles are below 500 μm or the d_{50} is small, and M* will then approach zero, implying no change in the viscosity due to the coarse particles. The analysis then reduces to the standard Bingham plastic equation. This highlights the importance of correctly defining the

coarse/fine split of particles. Generally definitions are made based on the particle size distribution, those particles of below a certain diameter will constitute the vehicle, the remainder the coarse fraction. Durand (1953) was the first to recognize this split for heterogeneous mixtures and decided upon a value of 25 μm to 50 μm as being the limit between the homogeneous and heterogeneous suspension, but this was only for a limited concentration range. Neill (1988) did not find a portion corresponding to the vehicle, but this could be due to the choice of successive size fractions analyzed. Hanks (1982) suggested an experimental method to determine the vehicle portion by testing succeedingly increasing size fractions. The size fraction is then the particle diameter above which no further changes in the rheology of the mixture occurs.

The method proposed by Faddick (1982) and used by Sive (1988) and Lazarus (1986) is based on the particle Reynolds number = 1. The maximum particle size, d_{max}, of the suspended load portion is calculated using Equation 2.38 (Faddick (1982)).

$$d_{max} = \left[\frac{18\ \nu^2\ S_w}{g\ (S_s - S_w)} \right]^{1/3} \qquad (2.38)$$

The choice of $Re_p = 1$ is arbitrary but is determined by Stokes settling. For full plant tailings this would account for approximately 85% of the material and could be considered a reasonable estimate, although no definitive work has been done on the split ratio.

2.2.7 Physico-chemical effects

The effects of chemical additives on the transport characteristics of slurries are well documented. The addition of chemical compounds to a backfill material may either decrease or increase the pressure gradients considerably. Verkerk and Marcus (1988) found that the addition of chemical additives and neutralizers to mineral tailings had a marked effect on the yield stress, but did not significantly change the absolute viscosity of the slurry. The slope of the rheogram did not alter, but the increase in the initial yield stress correspondingly

increased the pressure losses. This has important significance in the determination of the yield stress and demonstrates that the nature of the yield stress is inherently linked to the chemical particle interactions. Horsley and Reizes (1982) attributed the changes in head loss to the variations in the 'zeta-potential' of the particles. Zeta-potential is the measure of the particle surface charge and is directly proportional to the associated floc structure of the slurry.

For slurries containing a high percentage of colloidal size particles, agglomeration of these particles into larger groups of particles or flocs can occur. This results in an increase in the effective diameter of the particles and can therefore significantly alter the rheological characteristics. Hoffert and Poling (1985) indicated that the addition of lime to mill tailings changed the particle surface charge, decreasing the zeta-potential which resulted in increased settling rates of the slurry.

Horsley and Reizes (1982) used sodium hexametaphosphate to reduce the zeta potential to decrease pressure gradients of gold slime tailings by effectively destroying the floc formation. There was no effect on the pressure gradients at low concentrations or in turbulent flow, but only in high concentration laminar flow conditions. This indicates that floc formation and zeta potential are relevant at concentrations high enough to force the particles together, or in conditions of reduced particle mobility. At high velocities, the turbulent flow appears to break down the initial floc formations and could lead to an equilibrium floc size condition.

Hoffert and Poling (1985) also used variations in pH to control the zeta potential and found definitive changes in viscosity in variations with acidity. Duckworth *et al* (1983) found that the pH had marked effects on the slurry yield stress for fine coal materials of $d_{50} < 20\ \mu m$. This is a similar result to Verkerk and Marcus (1988) and could be attributed to the pH changing the zeta potential as does the addition of a chemical additive. For coarser coal, Elliot and Gliddon (1972), showed differing behaviour for two different coal types. One material was insensitive to variations in pH and showed little

variation in viscosity or initial yield stress, while the other was extremely sensitive and showed excessive variations in both yield stress and viscosity with changes in pH. This highlights the difficulties associated with floc formation and zeta potential and indicates the specific nature of physico-chemical effect to independent slurries.

Verkerk (1988) did not indicate pH values, but the effect of chemical additives on full plant tailings is clear. The zeta potential, floc formation and pH of the slurry are interlinked and cannot readily be separated. It is suggested that for a given set of steady state equilibrium flow conditions, the pH and chemical nature of the slurry will remain stable and will not additionally affect the pressure losses with time (this does not include the expected variation of pressure gradient due to particle degradation which will inherently change the transport characteristics).

2.3 Independent rheological parameters

The previous sections dealt with the classical rheological characterization of slurries using established data measured in traditional rotational or tube viscometers, the nature of which are beyond the scope of this review. If the material can be classified according to one of the constitutive equations, then the pressure gradients can be readily calculated.

It is the aim of this research, however, to analyze the stabilized flow regime from a mechanistic mathematical viewpoint and not on an entirely rheological basis. Neill (1988) demonstrated that these specific slurries cannot be analyzed in the classical sense of rheology. For this the mechanistic approach of mathematical modelling has been adopted and several of the rheological parameters have to be calculated from established mathematical correlations. The primary variables used in the analysis are given in Table 2.5, and it is from these variables that the relevant secondary flow parameters need to be calculated or experimentally determined. It is desirable to have the minimum amount of secondary variables, but several parameters are of utmost necessity. These include the particle size distribution, the relative viscosity and yield stress, the solids concentrations and the pipeline parameters.

PRIMARY VARIABLES	SECONDARY VARIABLES
Pipe variables • I.D. (mm) • Length (m) • Pipe roughness (μm)	
Solid variables • Solid relative density (S_g)	• Loose particle packing concentration • Maximum particle packing concentration • Solids sliding friction coefficient
Particle variables • Particle size distribution	• Shape factor
Slurry Variables • Solids concentration • Temperature	• Yield stress • Viscosity • Flow behaviour index

Table 2.5 : Primary and secondary pipeline slurry parameters

Standard methods exist for the determination of the primary variables, but the secondary variables need to be determined, and these will be presented in the following sections.

2.3.1 Solid particle packing

Elliot and Gliddon (1972) recognized the importance of achieving an optimum particle packing density for the dense phase pumping of slurries. The idealized solid mixture will contain a high proportion of fine material interspersed with a larger amount of coarser particles. The importance of particle characteristics is highlighted as solids concentrations increase and the flow regime changes from a heterogeneous or mixed regime flow to a single-phase fluid with definitive non-Newtonian characteristics. Non-Newtonian behaviour is

expected as particles approach their loose-packing or freely-settled density, defined in Equation 2.1. The particle size distribution, porosity, chemical effects and the shape of the particles obviously have a great effect on the packing density. For spherical mono-dispersed systems the values of porosity attained according to arrangement of the sphere are shown in Table 2.6 representing the preliminary analysis of Elliott and Gliddon (1972). This is an idealized solution and does not consider any particle interactions.

Random parametric evaluation of the porosity is possible. Yu and Standish (1987 and 1988) developed an analytical method to determine porosity of binary size mixtures using a linear analytical model. This can be extended to multi-component mixtures if the results from the binary mixtures are known. Other mathematical models exist that predict porosities of particular mixtures using a random packing configuration of the particles. Unfortunately, all these models involve the use of experimental constraints and do not eliminate the need for laboratory measurements.

RHOMBOHEDRAL ARRANGEMENT						
	Primary	Secondary	Tertiary	Quaternary	Quinary	Filler
Radius of sphere	R	0.414R	0.225R	0.177R	0.116R	Very Small
Relative No. of spheres	1	1	2	8	8	Volume added $0{,}622r^3$
Voidage of packing	25.95	20.7	19.0	15.8	14.9	3.9
%Weight of spheres in mixture	77.1	5.5	1.7	3.3	0.97	11.4

Table 2.6 : Properties of densest possible packing of spheres (from Elliott and Gliddon (1972))

Note : packing concentration, C_b = 100 - voidage.

Two different types of bed packing arrangements exist, the loosely-packed concentration and the maximum achievable packing concentration. These two extremes are important parameters of the solid particle size distribution and are independent of pipeline parameters. Figure 2.8 illustrates the difference between the loose and maximum measured densities with increasing particle size. The importance of particle size is clearly seen, particularly in the range up to 600 μm (the range of full plant backfill tailings). A graphic illustration of the two packing concentrations is shown in Figure 2.9. This constitutes a simple bench top test and will provide both concentrations. As all analytical techniques use laboratory determined constants, it is expedient to obtain the actual measured values for the particular particle size distribution.

Several techniques are available using either centrifuge or settling tests. Tests done at the University of Cape Town indicate the usefulness of the settling methods. Vibration of the freely settled porosity will attain the maximum packing density.

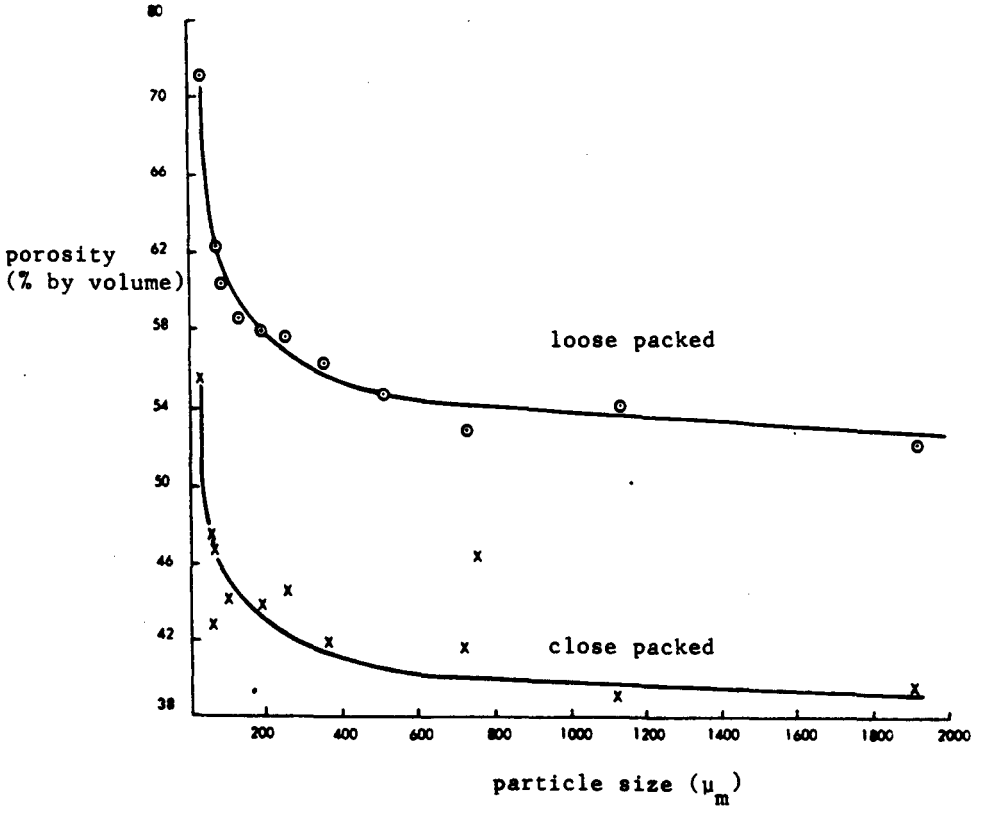

Figure 2.8 : Variation of particle packing concentration with increasing particle size (Elliott and Gliddon (1972))

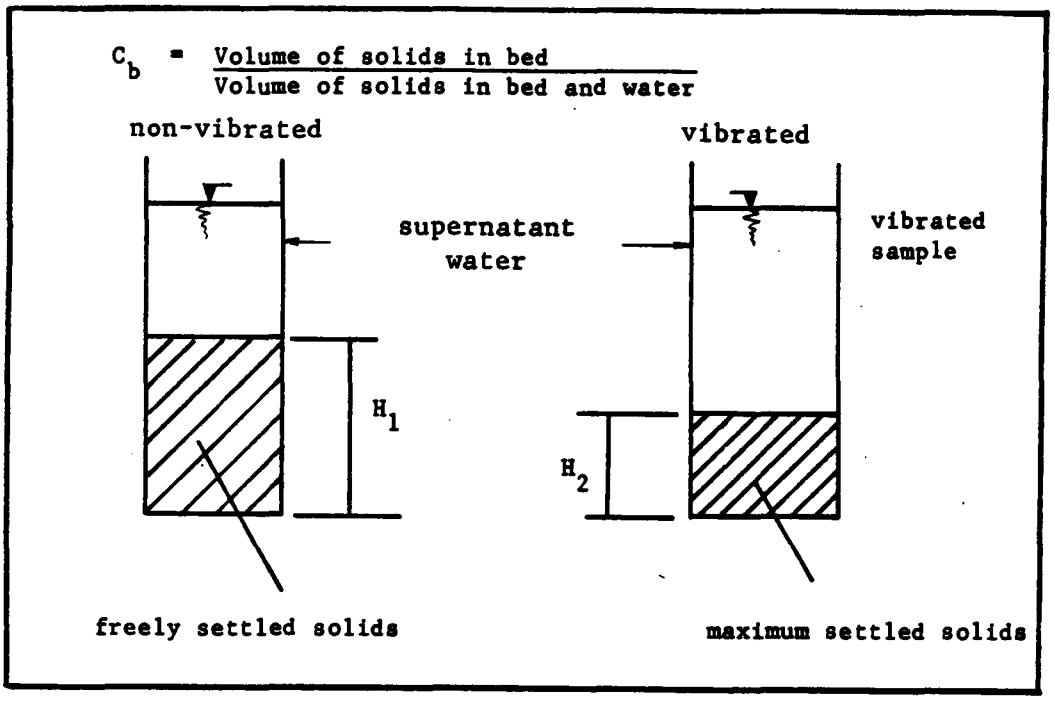

Figure 2.9 : Freely settled and maximum particle packing concentration determined using sedimentation and vibration bench top laboratory tests

2.3.2 Relative viscosity

Newtonian relative viscosities for dispersed systems can be analyzed using several equations. Einstein's original correlation, shown in Equation 2.39 is valid only for dilute concentrations of $C_v < 0,01$. Hanks (1982) recommended the use of the empirical relation of Thomas (1963) in Equation 2.40. This is a simplified correlation dependent upon the volumetric concentration only. Lazarus (1985) and Sive (1988) used the Landel *et al* (1963) correlation represented in Equation 2.46. This accounts for the particle size distribution in the form of the maximum possible solids packing concentration. Comparison of Equations 2.40 and 2.41 is shown in Figure 2.10 and the importance of the correct packing density is highlighted. Several other correlations of a similar form exist and are generally derivations of the expansion in Equation 2.42.

Einstein's equation

$$\eta_r = 1 + 2.5\ C_v \qquad (2.39)$$

Thomas (1963)

$$\eta_r = 1 + 2.5C_v + 10.05C_v^2 + 0.00273 \exp(16.6\ C_v) \qquad (2.40)$$

Landel et al (1963)

$$\eta_r = [\ 1 - (C_v\ /\ C_{bmax})\ ]^{-2.5} \qquad (2.41)$$

General form of expansion

$$\eta_r = \sum_{n-1}^{\infty} k_n\ C_v n \qquad (2.42)$$

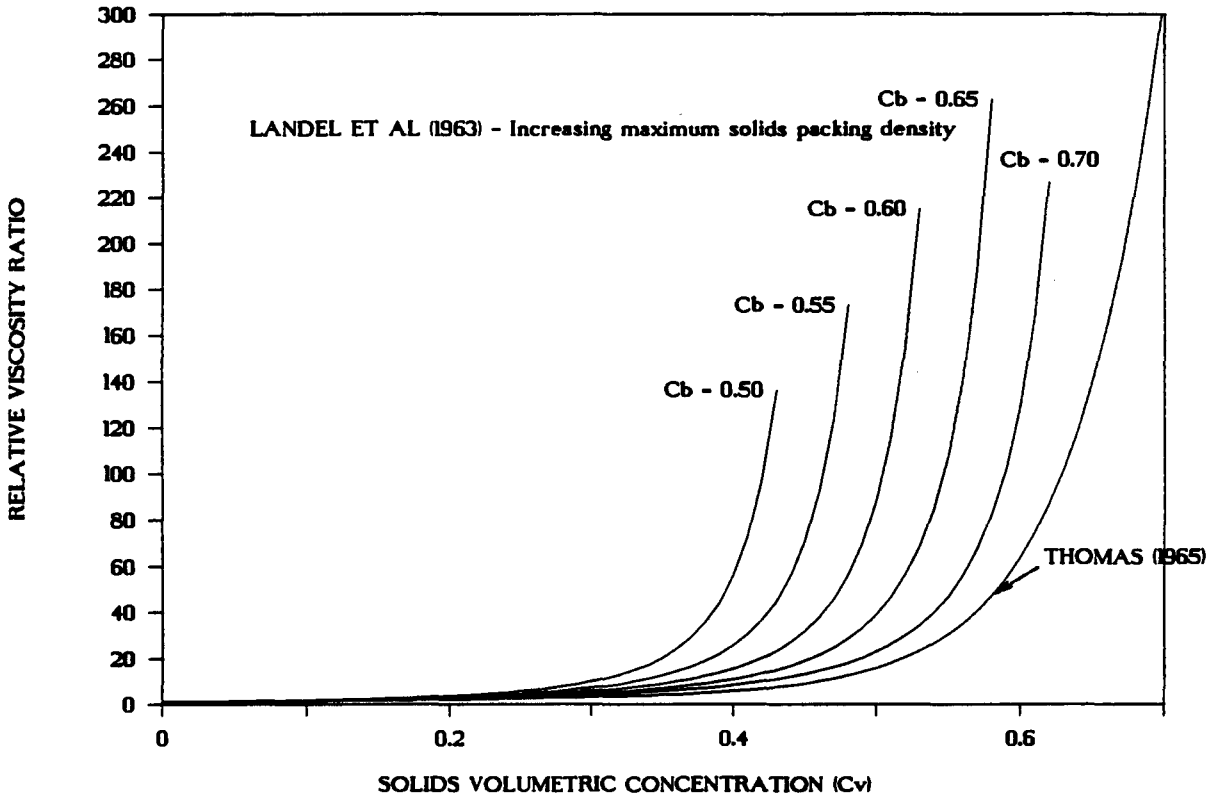

Figure 2.10 : Variations in calculated relative viscosities using Equations 2.40 and 2.41, highlighting the effect of solids packing concentration and asymptotic behaviour as C_{vt} approaches C_{bmax}

The importance of the maximum packing parameter cannot be underestimated. The relative value of the solids concentration to maximum particle concentration gives a physical interpretation of the mobility of the solids particles. A mobility parameter defined by Dabak and Yucel (1986) as C_v / (C_{bmax} - C_v) , successfully demonstrates the importance of maximum attainable bed packing with viscosity. Dabak and Yucel (1986) presented a correlation to determine both the relative viscosity and maximum packing densities for a variety of Newtonian suspensions. The study confirmed that maximum packing and relative viscosity are two of the most crucial parameters associated with the rheological behaviour of high concentration dense phase suspensions.

However, for non-Newtonian suspension, the calculation of viscosity based purely on particle characteristics is not possible. Hanks (1982), states "*At the present state of development of the field of rheology there are no theories that permit the a-priori prediction of non-Newtonian rheological properties from fundamental physical property data.*" This means that experimental results for the viscosity of the suspension should be used and necessitates the use of a viscometer. Work has been done on flocculated suspensions based on the floc characteristics. This relies on the evaluation of the ratio of the floc volume to the particle volume at varying rates of shear (C_{FP}). Alessandrini *et al* (1983) used this formulation approach for coal water slurries and proposed the following correlation, Equation 2.43, in steady state.

$$\eta_r = \text{fn}\ (C_{vfloc}) = \text{fn}\ (C_v\ ,\ C_{FP}) \qquad (2.43)$$

where $C_{FP} = \text{fn}\ (\frac{du}{dr})$

Several expansions of this functional form exist, but all rely on the correct determination of C_{FP}.

For non-Newtonian viscosity, both the floc characteristics and particle characteristics are important, but there exists no correlation to determine accurately the relative viscosity based on both these parameters. The viscosity behaviour of full plant tailings needs to be determined from experimental results and dimensional analysis.

2.3.3 Yield stress

As discussed in Section 2.2.7.4, the variation of the zeta potential and floc size has a marked effect on the initial slurry yield stress, as reported by Verkerk and Marcus (1988). Hence yield stress is closely linked to the degree of flocculation of the slurry. Sive (1988) suggested that there exists no reliable equations for the prediction of yield stress, and experimental measurements should be used. If no data is available, then the yield stress should be assumed to be equal to zero. This, however, is not practical for full plant tailings, as the yield stress is of utmost importance in determining the flow behaviour.

Tadros (1985) formulated the following expression incorporating an energy component, E_{sep}. E_{sep} is defined as the energy required to separate the flocs or agglomerated particles into single units.

$$\tau_y = \frac{3\, C_{vt}^{n}}{8\, \pi\, r^3} \cdot E_{sep} \qquad (2.44)$$

where r = radius of particle

n = average number of contacts per particle.

Equation 2.44 highlights the dependence of yield stress on flocculation. The evaluation of E_{sep} is, at best, only an estimate and generally results in high yield stress approximations.

Dabak and Yucel (1986) investigated the modelling of highly concentrated suspensions. The characterization of the suspension should be represented by a shear dependent maximum packing concentration $C_{bmax}(\tau)$, and an intrinsic relative viscosity parameter. Of fundamental importance in the analysis of these slurries is the ratio of C_v / C_{bmax} in determining the viscosity and yield stress. The developed formulation consists of four basic parameters, the yield stress, a flow resistance parameter, and the shear viscosity behaviour at low and high concentrations.

Equation 2.45 is defined in Figure 2.11 for a yield pseudoplastic slurry.

$$\tau - \tau_y = \eta_\infty(G) + (\eta_o - \eta_\infty)G \,/\, (1 + (\eta_o - \eta_\infty)G/B \,) \qquad (2.45)$$

where η_o = initial viscosity at low shear stress

η_∞ = infinite viscosity at high shear rates

$G = -\frac{du}{dr}$

The rheogram is divided into the low, intermediate and high shear rate regions and the major parameters to be determined are τ_y , μ_o , μ_∞ and B , where B = fn (τ).

The yield stress, τ_y , is evaluated from Equation 2.46, and parameter B can be found using Equation 2.47. To calculate the initial and final relative viscosities, Equation 2.48 is used, and the rheogram can be approximated. The constants K_1 and K_2 are related to a specific mixture type, and once determined, are applicable over a range of varying concentrations. This approach does not elliminate the need for experimental results, but provides a means for determining from experimental data, a specific correlation for τ_y .

Results indicated that diameter dependence was predicted by high concentrations and Equation 2.46 indicates $\tau_y = fn\ (D, C_v)$.

$$\tau_y = K_1 \left[(\rho_s - \rho)\ g\ D\ C_v \right] \frac{C_v}{(C_{bmax} - C_v)} \frac{S_a\ D_s\ C_v}{S_f} \qquad (2.46)$$

where S_a = specific surface area
D_s = mean particle size = d_{50}
S_f = mean particle shape factor

$$B = \tau_\infty - \tau_y = K_2\ \tau_y\ C_v \frac{C_v}{(C_{bmax} - C_v)} \frac{1}{Re_p} \qquad (2.47)$$

where Rep = particle Reynolds number

$$\eta r_{o,\infty} = \left[1 + \frac{\eta\ C_v\ C_{bmax}}{n\ (C_{bmax} - C_v)} \right]^n \qquad (2.48)$$

where n_∞ = 2 for $\eta = \eta_\infty$
η_o calculated at low shear rate.

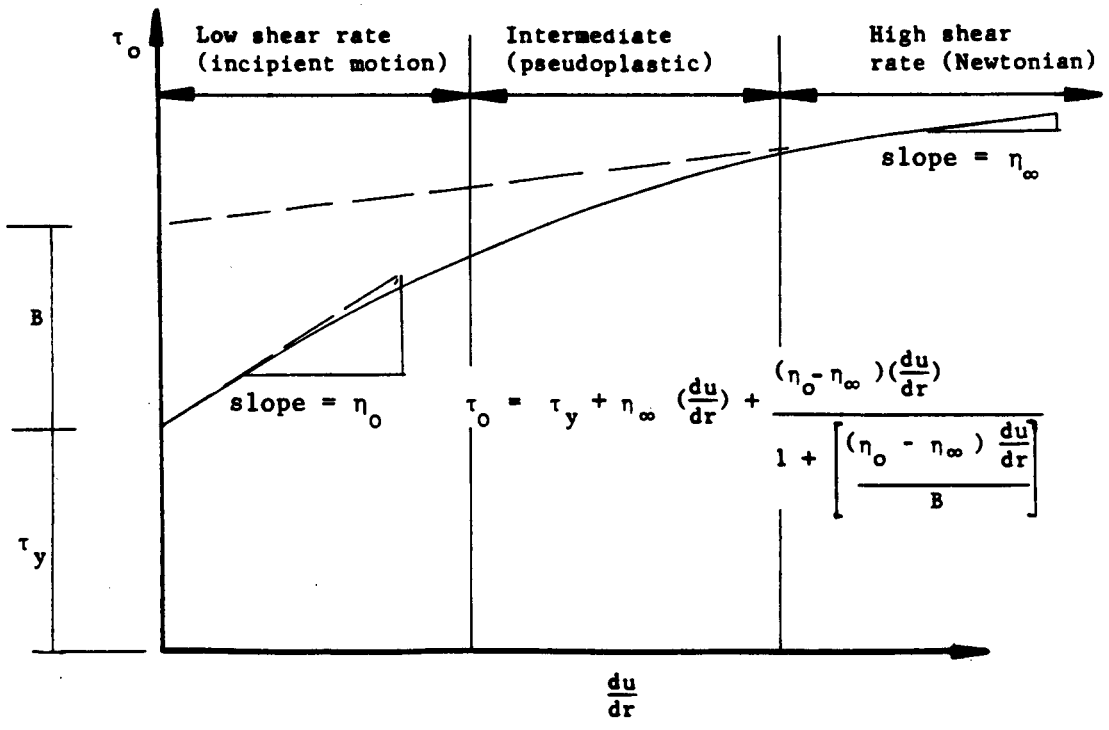

Figure 2.11 : The formulation of Dabak and Yucel (1987) for low, intermediate and high shear rates

2.3.4 Flow behaviour index, n

The flow behaviour index, n , has been discussed in Section 2.2.3 for non-Newtonian fluids and is determined from a rheogram. The flow behaviour index, n , can vary with concentration as shown by Lazarus and Slatter (1988), and Slatter (1986) in Figure 2.12. Neill (1988) found a slight variation in n at low concentrations for full plant tailings. It is important to note that the parameters τ_y , K and n are specific to a given set of slurry conditions and cannot be separated from one another.

2.3.5 Particle shape factor, S_f

An estimation of the relative shape of the particles contained within the size bands of the particle size distribution is needed. Dabak and Yucel (1987) defined a shape factor as the ratio of the surface area of a sphere of equivalent volume to the surface area of the actual non-spherical particle. This is a difficult parameter to define, and a more conveniently measured shape factor can be defined in terms of relative settling velocities, in Equation 2.49

$$S_f = \frac{\text{measured particle settling velocity}}{\text{sphere settling velocity}} \qquad (2.49)$$

The sphere settling velocity is calculated using either Stokes, Allens or Newton's law for the terminal settling of an equivalent diameter sphere (a sphere with the same mass as the particle) in water. This definition is the most common and is used in this review. The particle shape has an important influence on the fluid consistency index, spherical particles having the least effect as opposed to rod-like particles which will increase the relative viscosity due to their irregular rotation.

Interesting results at high concentrations, however, report that the addition of up to 3% (C_v) of fibre like (low shape factor) particles to coarse high concentration slurries, will dramatically reduce the pressure gradient, (Verkerk (1988)). This drag reduction phenomena is closely associated with the zeta-potential and decrease of floc formulation due to the presence of the fibre particles.

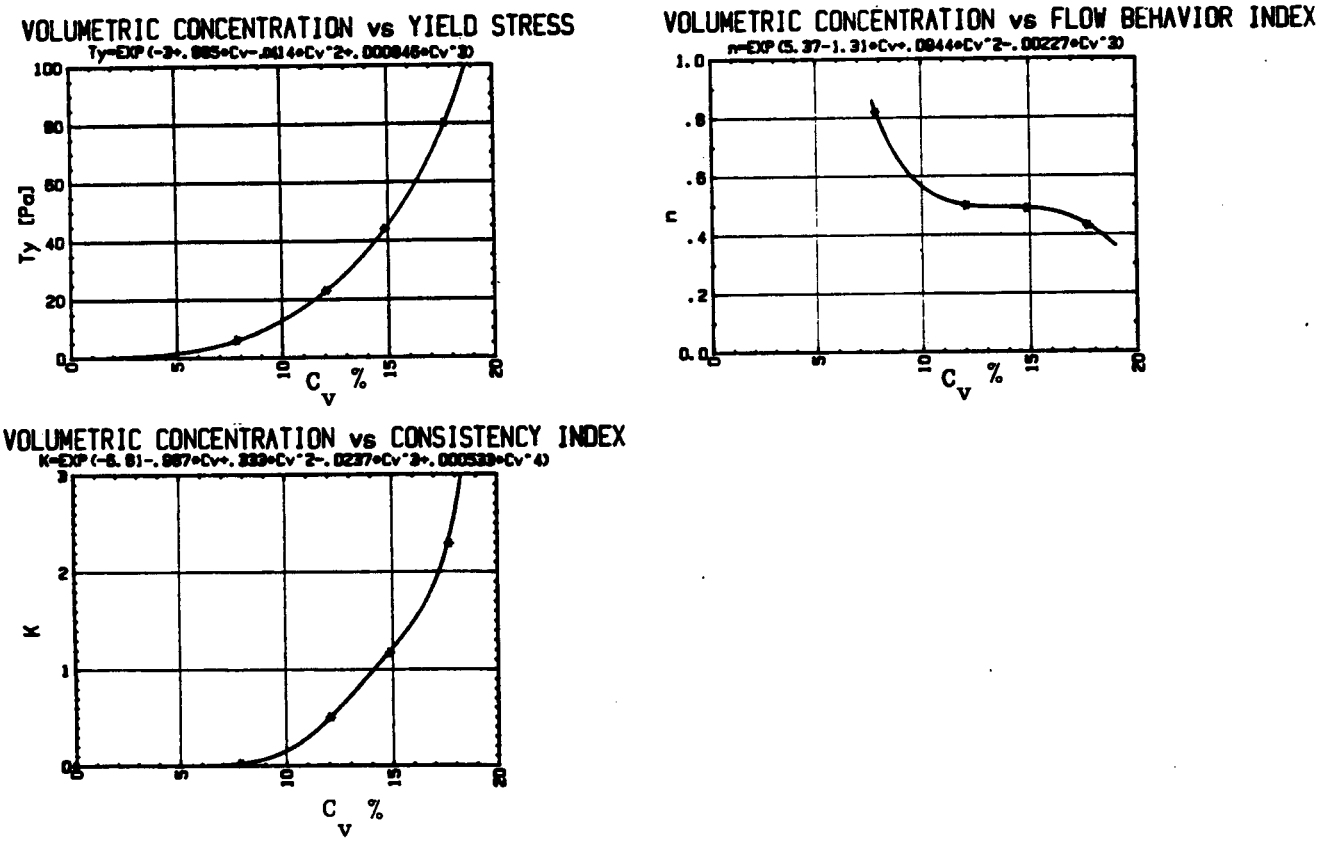

Figure 2.12 : Variation of rheological parameters with increasing volumetric solids concentration (extracted from Slatter (1986))

2.3.6 Coefficient of sliding friction, μ_s

The coefficient of sliding friction between the bed load and pipe wall is a measure of the friction between the pipe solids and the pipe invert. For dense phase flow, this is an extremely important parameter and needs to be determined accurately. In a stabilized flow regime, the coefficient of sliding friction is relevant only to those coarse particles not contained within the vehicle portion and in contact with the pipe wall. Cooke (1989) investigated the importance of μ_s for dense phase flow and concluded that a detailed experimental analysis program is needed to quantify accurately sliding friction.

Sliding friction is dependent upon the solids concentration and pipeline material (roughness) and cannot be evaluated analytically.

Generally it is measured by the "tilting-tube" apparatus (Wilson (1972)), which effectively determines the static coefficient of friction. Under normal velocity flow, the dynamic coefficient is less than the static coefficient and needs to be determined. The dynamic coefficient of sliding friction was measured by Briscoe *et al* (1983) using a rotating horizontal cylinder and was found to be a function of velocity, decreasing from 0.65 to 0.22 over a narrow velocity range of 0.47 to 1.07 m/s.

2.4 Conclusions

1. The distinction between stabilized flow and dense phase flow is important when considering the analysis of backfill materials. Stabilized transport is a well established concept for coal/water transport and high concentrations can be achieved.

2. Conventional stabilized slurries can be characterized by the standard rheological equations for time independent behaviour. In certain instances a modified Bingham plastic fluid can be used if the top size of the particles can be supported by the internal yield stress of the mixture.

3. Generalized correlations such as Metzner and Reed (1953) can be used for stabilized flow (Streat (1986)), or that of Wilson (1986) can be used, provided the shape parameter of the rheogram can be determined.

4. The viscosity and yield stress of a non-Newtonian suspension cannot be predicted by existing correlations, but a specific correlation for full plant tailings could be developed using dimensional analysis.

5. The physico-chemical effects on pressure gradient are important, but for a given steady state flow condition, these can be ignored provided the yield stress and viscosity is known for the condition.

6. The particle packing concentration can be approximated using a random parametric theory of packing. Two packing states occur, the first settled bed packing and the maximum possible packing density. Both these values need to be known and are crucial in determining the relative viscosity. It is suggested that a simple bench top test be used for the measurement of these two parameters.

7. The separation of stabilized slurries into a vehicle and coarse portion for mathematical analysis needs further investigation. The assumption of a particle Reynolds number of unity for Stokes settling could be perhaps used initially which would mean that 85% of the material is the vehicle, but the actual limiting particle size is probably smaller.

8. The analytical model to be developed would need to take into account the above factors, with particular emphasis on the rheological behaviour of the slurry. Relationships will have to be developed to describe adequately the yield stress and relative viscosity. For a generalized case, a yield power law model can be assumed, thus allowing for the variation of the yield stress (τ_y) flow consistency index (K) and flow behaviour index (n).

PART TWO

EXPERIMENTAL INVESTIGATION

CHAPTER 3

RESEARCH APPARATUS

This chapter describes the experimental investigation on the flow behaviour and slurry properties for full plant backfill tailings. Pressure gradient measurements were taken from 3 different test facilities over a range of pipe internal diameters from 13 mm NB to 100 mm NB at slurry relative densities between $S_m = 1,5$ and $S_m = 1,9$. The test facilities at the University of Cape Town will be briefly discussed and the ancillary slurry test procedures are presented.

3.1 The vertical test facility at the University of Cape Town

There is a paucity of measured data available on the vertical transport of solids in pipelines. Since the vertical downward transport of backfill slurries is a common feature of the mine backfilling operations, it was decided to construct a pipeline test loop in which both the vertical and horizontal pressure gradients could be measured. Current mine backfilling procedures utilise the free fall or gravity feed transport systems. For this reason, a continuous gravity feed vertical pipeline was specifically designed and constructed for this investigation. The schematic layout of the test facility is presented in Figure 3.1, and the operation and primary components are discussed below.

The slurry is transported from the main hopper on the basement level to a constant head tank 15 m above. The overflow from the head tank returns via a 75 mm NB pipeline back to the main hopper. The slurry flows through the head tank down the vertical test pipeline and around the horizontal test section before returning back to the main hopper. The flow through the test section is regulated using a remote controlled pneumatic pinch valve at the outlet of the horizontal section.

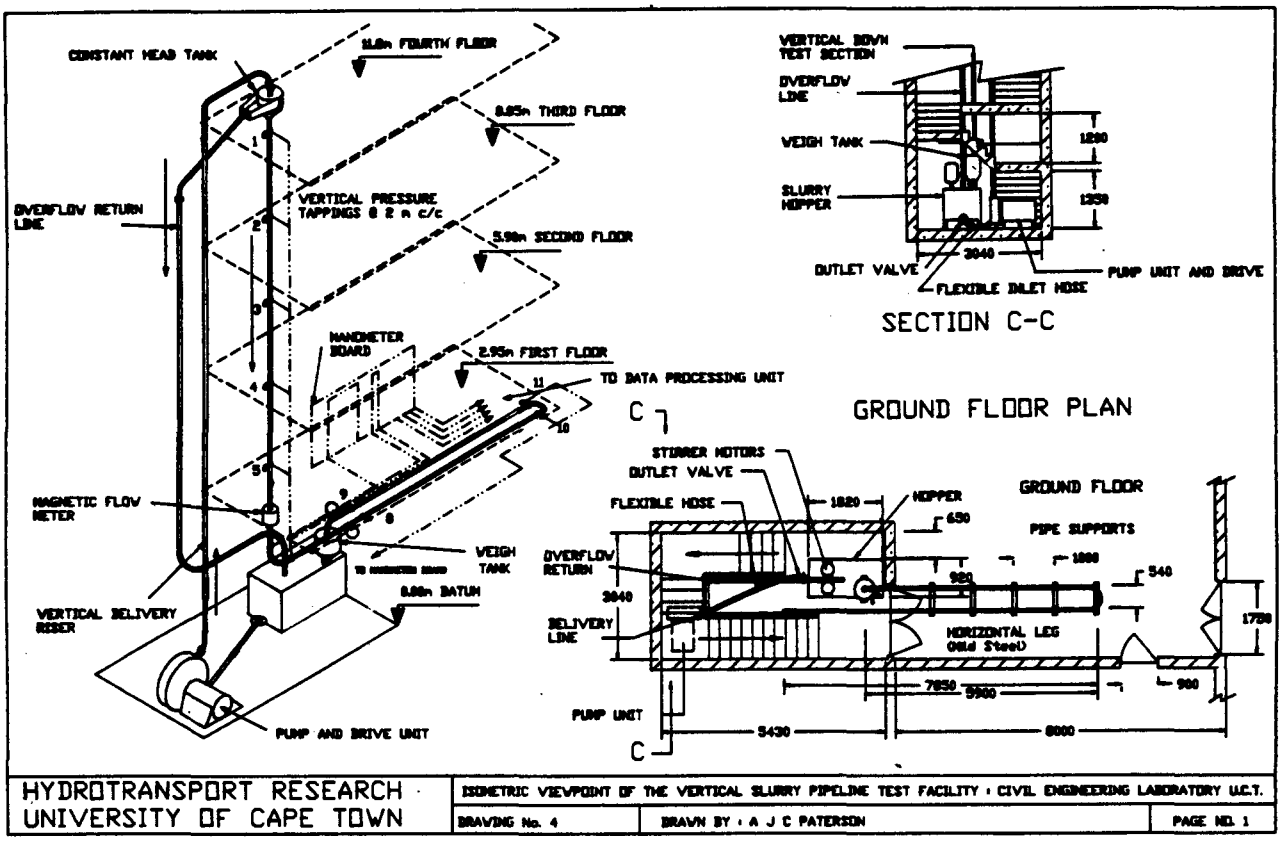

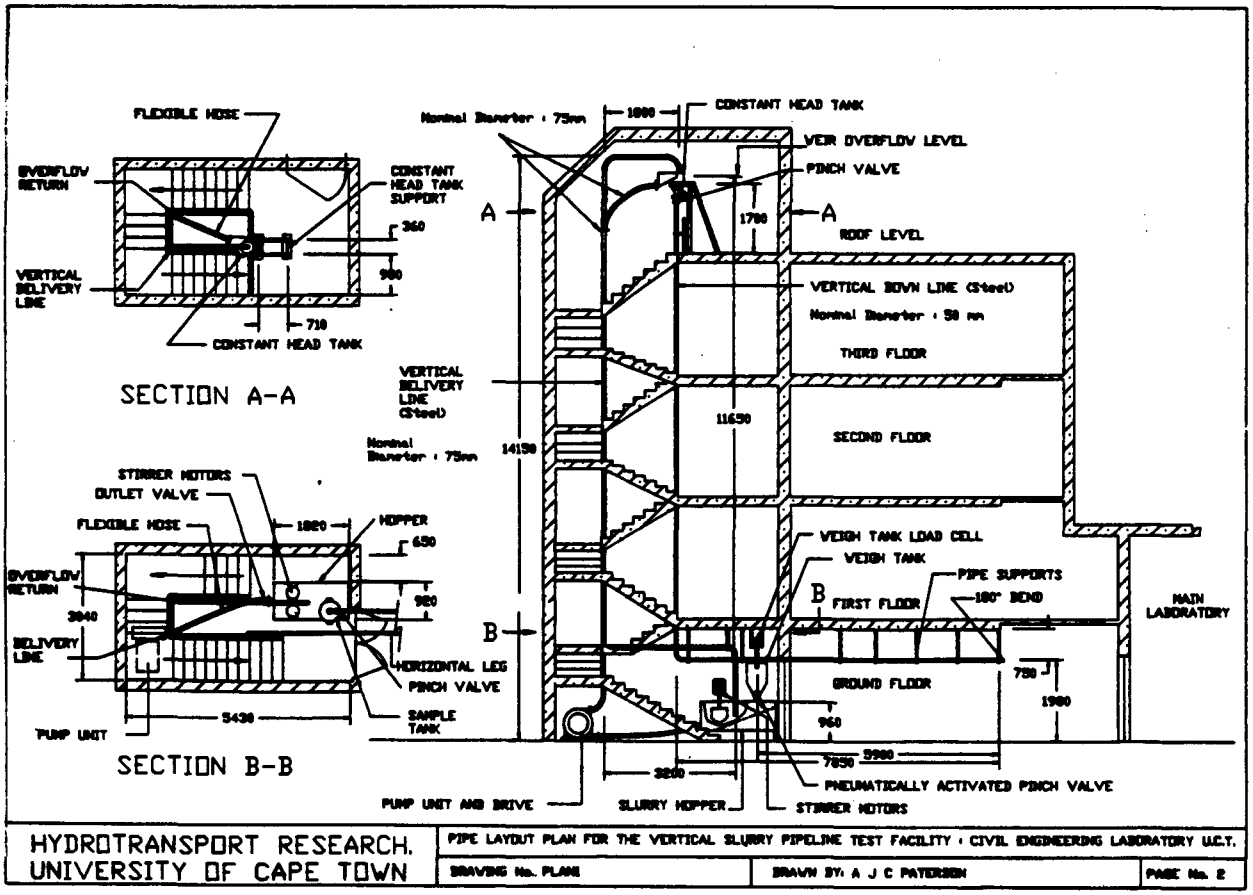

Figure 3.1 : Vertical pipeline test facility at the University of Cape Town

System components

1. Peristaltic pump

The high solids concentration stabilized slurry is pumped to the constant head tank using an 11 kW peristaltic positive displacement pump (hose pump).

2. Pipeline

The test section is constructed using 40 mm NB seamless steel piping. Viewing sections, using clear PVC piping, are provided in both the horizontal and the vertical limbs of the pipeline, the internal diameter of these being both 45,90 mm. Later additions to the system included 75 mm NB PVC test sections.

3. Pressure tappings

Pressure measurements along the line are made using static pressure tappings located in the pipeline wall. These are 4 tappings in the vertical section, 1,5 m apart, inserted at 90° to the pipe wall, and 2 pairs of tappings in the horizontal sections, situated at 2 m and 1 m apart, at 45° to the vertical. Each tapping is provided with a solids trap to ensure that the slurry being tested is isolated from the water manometers.

4. Manometer board

Each pair of pressure tappings is linked to an independent set of manometers, enabling visual readings of the differential pressure losses. The range of the manometers is 1 500 mm. Each manometer set is linked to a differential pressure transducer on the rear of the manometer board. Flushing water is provided by the water mains (400 kPa) and air pressure (800 kPa) is supplied by a central compressor.

5. Pressure transducer

Four pressure transducers are used for differential pressure measurement. The range of differential pressure is -1 500 mm to 1 500 mm water.

6. Magnetic flow meter

A Kent VCA magnetic flow meter, consisting of a detection head and signal processor, provides a current output which is linearly proportional to the mean mixture flow velocity (V_m).

7. Gamma ray densitometer

In order to monitor the slurry density continuously, a Krohne gamma ray densitometer is used. The isotope radioactivity is monitored using the detection head and transferred to the signal processor, producing a linear output voltage with increasing slurry density (S_m). This corresponds to the measurement of the *in situ* concentration (C_{vt}) in the downcoming vertical pipeline. The position of the densitometer in the vertical test section relative to the vertical pressure tappings is given in Figure 3.2.

8. Weigh test equipment

The delivered concentration (C_{vd}) is determined using a sample weigh tank. The slurry flow is diverted into the sampling tank using a two way diverter valve. The mass of the sample added is measured using a 300 kg suspended scale and the volume is determined from the height of slurry in the tank, viewed through a calibrated clear perspex window.

9. Data logging equipment

The data acquisition system for the pipeline test loop consists of a Hewlett-Packard 86 microcomputer interfaced with a dot matrix printer, single floppy disk drive, Hewlett-Packard pen plotter, analogue to digital data acquisition unit and a constant voltage power supply.

For pipeline tests the data logger collects three sets of voltages from each instrument and averages them, and a further three sets are taken several seconds later, averaged, and compared with the initial set. When the two consecutive values are within a pre-selected tolerance then the next stage is begun and time averaged readings for a period of from 18 to 180 seconds are taken. After the required number of loops have been completed the average value is compared with the variation with time. If this value is within a further selected tolerance, then the value is recorded.

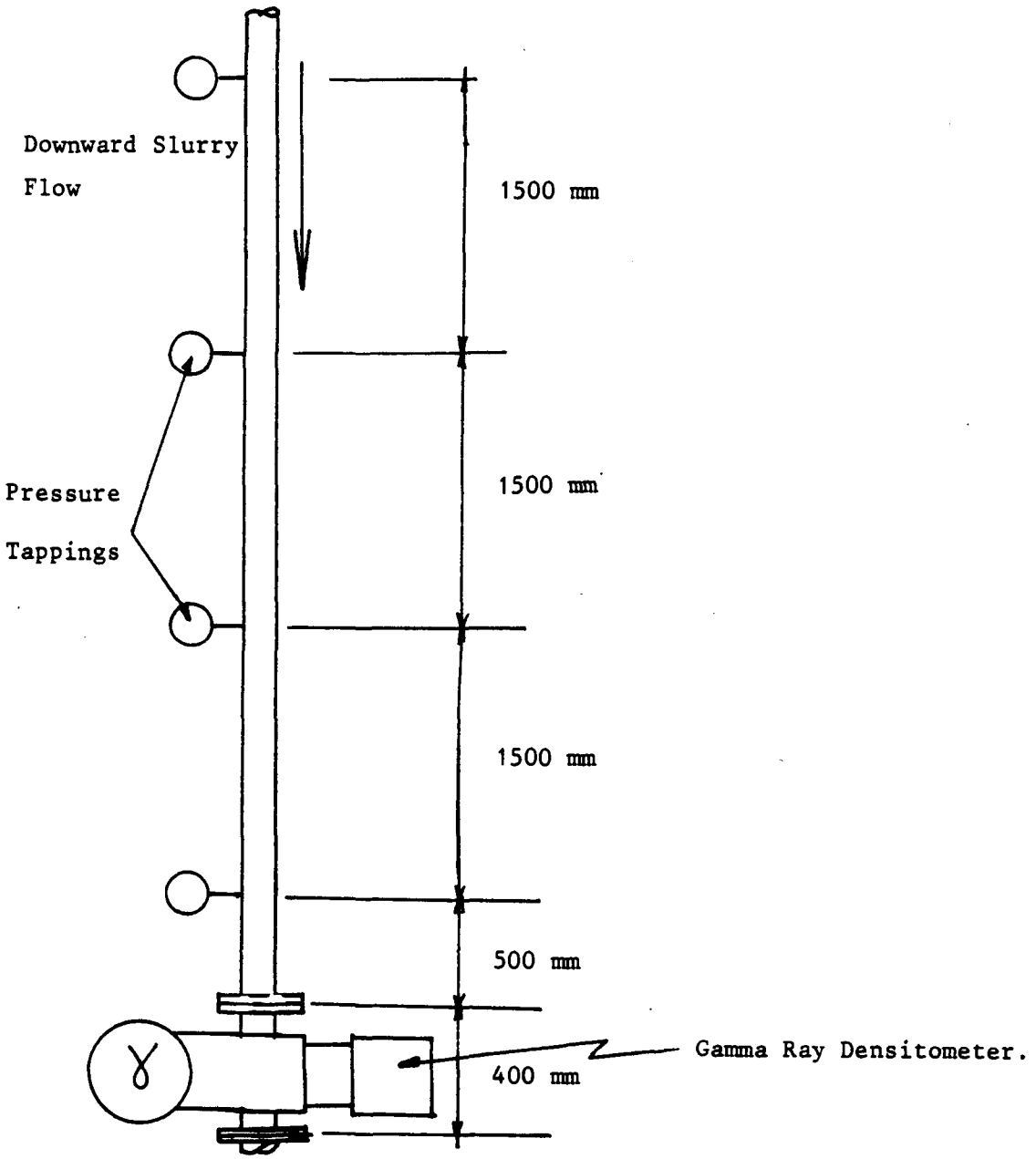

Figure 3.2 : Relative positions of the vertical pressure tappings and Gamma ray densitometer

3.1.1 Calibration of the apparatus

All instrumentation is calibrated *in situ*. The differential pressure transducers are re-calibrated at the beginning of each new set of tests. A set of typical linear regression analysis curves for the instruments are shown in Figure 3.3.

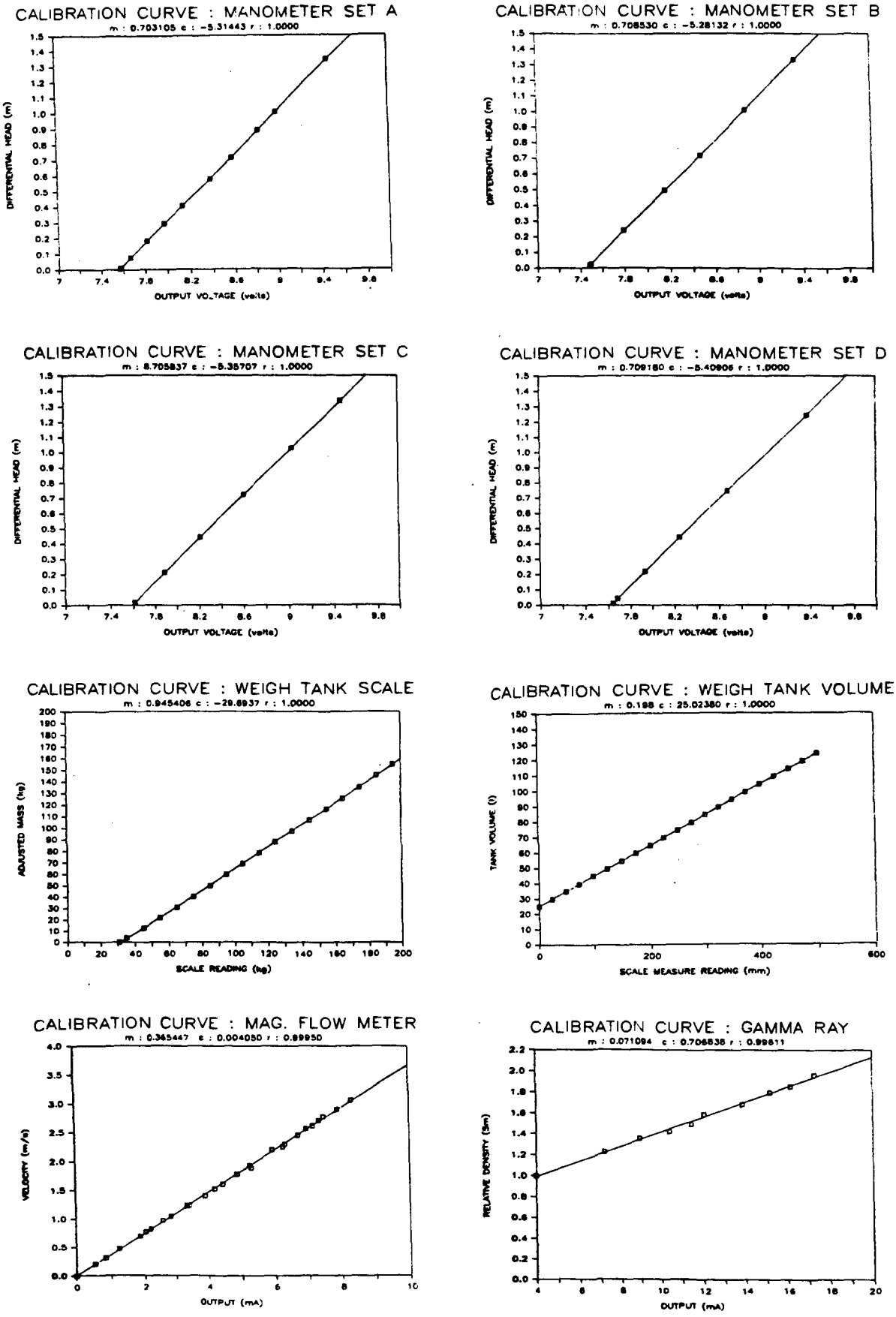

Figure 3.3 : Typical calibration curves for instruments in the vertical test facility (r = correlation coefficient, m = slope of correlation, c = intercept)

3.1.2 Measurement of parameters

3.1.2.1 Analogue to digital data acquisition

In order to ensure reliable readings of experimental parameters, a sophisticated method of data collection and reduction was developed by Sive (1988) at the University of Cape Town. The measurement of the time averaged values of the following parameters is considered :

(i) Vertical downward flowing energy gradient (2 transducers)

(ii) Horizontal energy gradient (2 transducers)

(iii) *in situ* solids concentration using a gamma ray densitometer

(iv) Slurry flow rate using a magnetic flow meter.

A descriptive flow chart of the data acquisition procedure is given in Figure 3.4.

3.1.2.2 Temperature measurement

The temperature of the slurry is not monitored using a thermometer probe. A graduated thermometer is used at each reading during the test to measure the slurry temperature at the outlet of the horizontal test section.

3.1.2.3 Delivered concentration

The delivered concentration is measured for each accepted data point using the weigh scale and weigh tank at the outlet of the horizontal section.

3.2 The Balanced Beam Tube Viscometer

Additional data on full plant tailings backfill material was obtained by Neill (1988) using the novel Balanced Beam Tube Viscometer developed at the University of Cape Town. Extensive test work was done on the rheological characterization of full plant tailings using this instrument. Data from Neill (1988) is used as an additional source of reference in the analysis of full plant tailings.

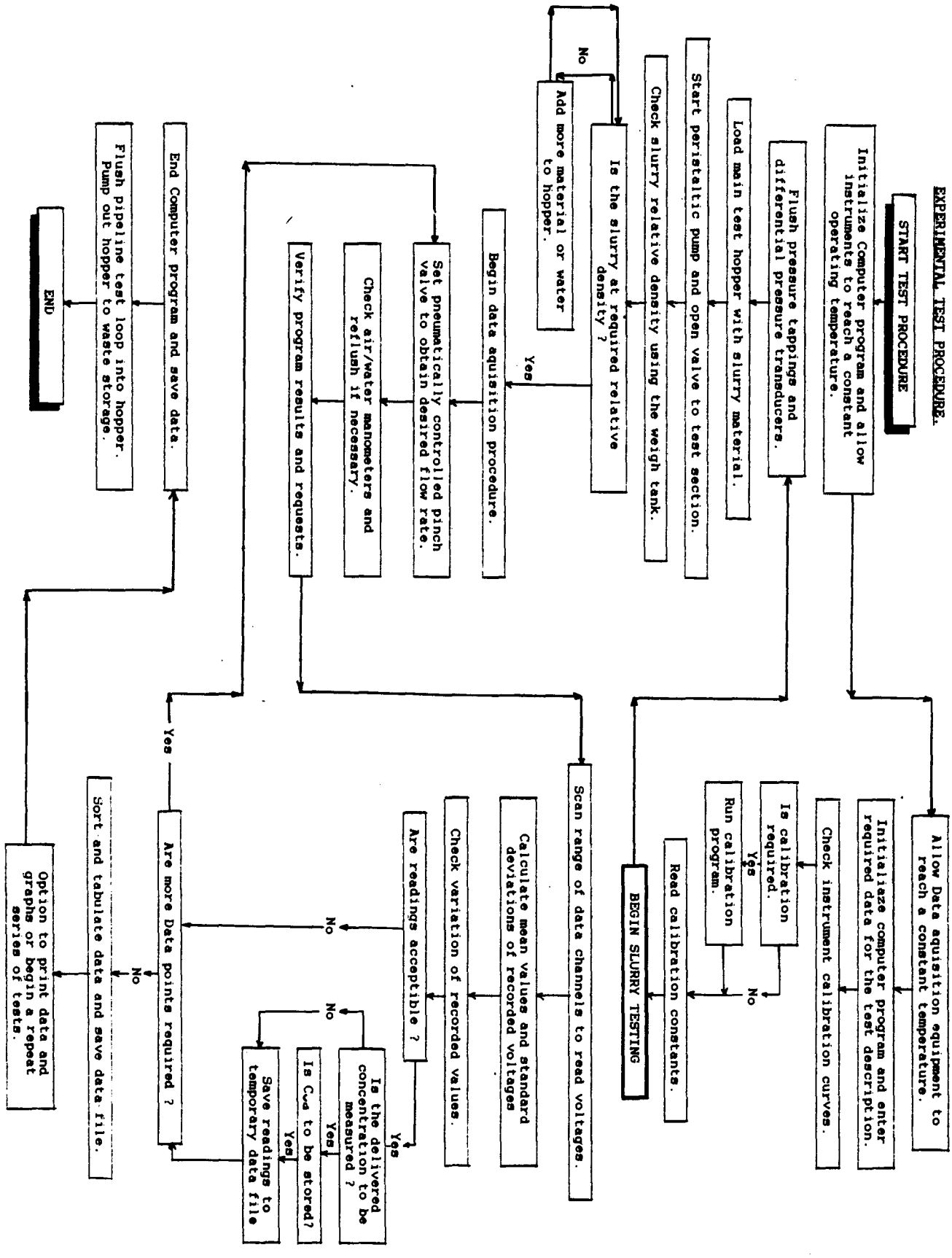

Figure 3.4 : Descriptive flow chart of test procedure when operating vertical pipeline

Figure 3.5 shows the BBTV components. The BBTV consists of two pressure vessels mounted at either end of a rigid steel beam which is supported at the centre on a knife edge pivot and at one other end by a load cell unit. The BBTV has 3 pipeline diameters of 4 mm NB, 13 mm NB and 28 mm NB. Each of the pipelines has a ball valve at either end to isolate an individual diameter for testing. 700 kPa air pressure is supplied to either one of the pressure vessels via a regulator and three-way valve. The air pressure is used to drive the slurry from one vessel to another during a test sequence.

A series of pressure tappings on each of the pipe tubes allows for pressure gradient measurement. The flow measurement is determined from the mass flow rate of the slurry from one pressure vessel to the other.

A data acquisition unit is used to measure the flow measurement via the load cell, and the pressure gradient via a differential pressure transducer.

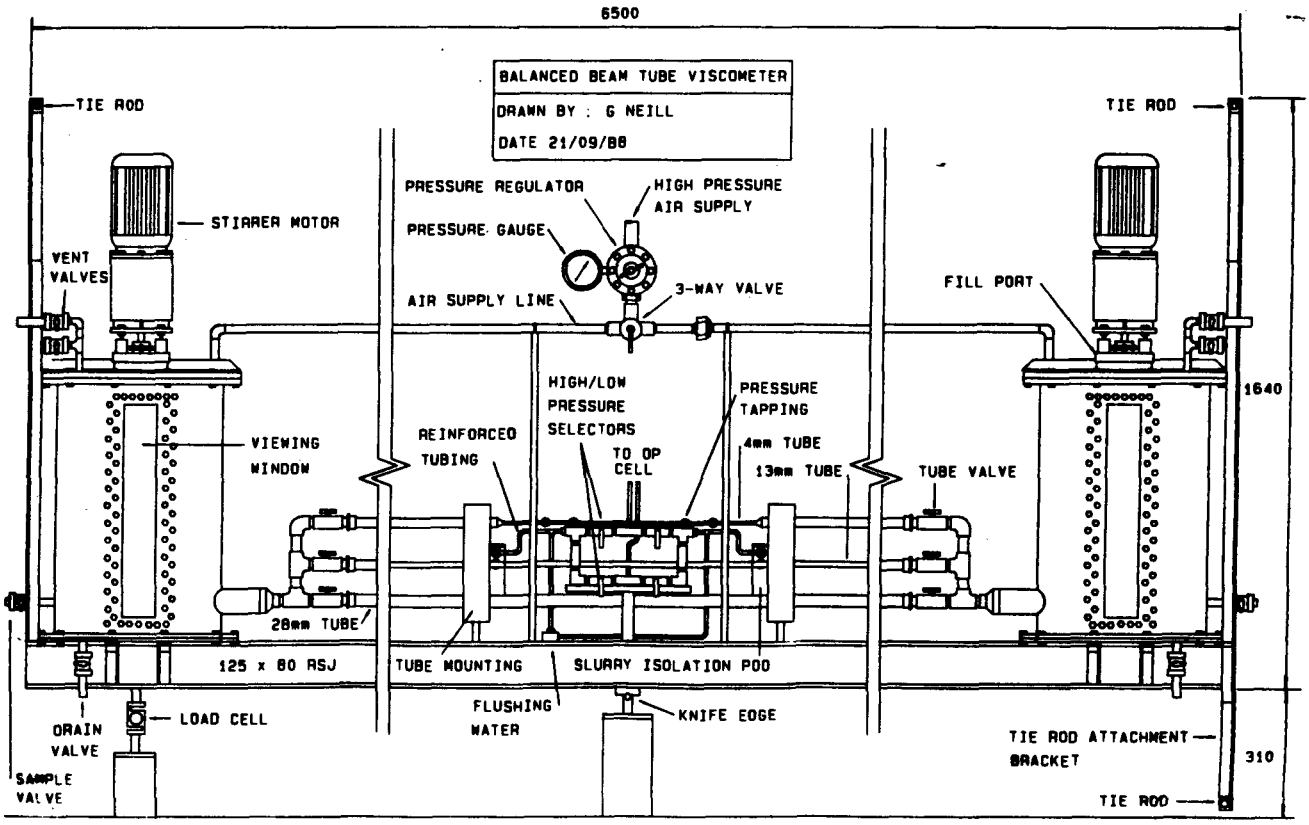

Figure 3.5 : The Balanced Beam Tube Viscometer (BBTV), University of Cape Town

3.3 Experimental error analysis

In all experimental observations, experimental error exists. It is important to quantify these errors for each of the measured parameters. This can be done using a statistical analysis. For each of the parameters measured the functional relationship is known, therefore the maximum possible error associated with the parameter can be determined.

The measured parameter, X, is a function of several variables represented in Equation 3.1 :

$$X = f_n (a, b, c, ...) \tag{3.1}$$

The error in X due to experimental measurement is found by Equation 3.2.

$$\frac{(\Delta X)^n}{X} = \left(\frac{\partial X}{\partial n} \cdot \frac{\Delta n}{n} \right) \tag{3.2}$$

$$\frac{(\Delta X)^n}{X} = \frac{\partial X}{\partial n} \cdot \frac{n}{X} \cdot \frac{\Delta n}{n} \tag{3.3}$$

The greatest possible error in X is the summation of the errors associated with each of the n measured quantities.

$$\text{i.e.} \quad \left[\frac{\Delta X^n}{X} \right]_{max} = \Sigma \sqrt{\left(\frac{\partial X}{\partial n} \cdot \frac{n}{X} \cdot \frac{\Delta n}{n} \right)^2} \tag{3.4}$$

where X = overall result
ΔX = error in the result
n = measured parameter
Δn = error in quantity measured.

For example, the determination of error associated with the measurement of pipe internal diameter (I.D.) is given as follows :

1. The I.D. is determined by the measurement of the mass of water, m_w, that fills a section of tube of length L, using Equation 3.5.

$$ID = \sqrt{\frac{4\, m_w}{\rho_w\, \pi\, L}} \tag{3.5}$$

2. The maximum error given by Equation 3.4 is calculated from Equation 3.6.

$$\left(\frac{\Delta D}{D}\right) = \sqrt{\left(\tfrac{1}{2}\sqrt{\frac{4}{\rho_w\, m_w\, \pi\, L}} \cdot \frac{m_w}{D} \cdot \frac{\Delta m_w}{m_w}\right)^2} + \sqrt{\left(-\tfrac{1}{2}\sqrt{\frac{4\, m_w}{\rho_w\, \pi\, L^3}} \cdot \frac{L}{D} \cdot \frac{\Delta L}{L}\right)^2} \tag{3.6}$$

Using this analysis the associated errors for all the parameters were determined and are summarised in Table 3.1 for both the vertical test facility and the BBTV.

Diameter (mm)	Diameter % error	Velocity % error	Shear Stress % error	Solid Concentration % error
* 4,2	0,0815	1,62	0,882	(C_{vt}) 0,092
* 13,37	0,0034	1,47	0,803	(C_{vt}) 0,092
* 28,38	0,0026	1,46	0,803	(C_{vt}) 0,092
* 32,63	0,0026	1,46	0,803	(C_{vt}) 0,092
▽ 41,22	0,286	1,73	0,250	(C_{vd}) 1,310
▽ 75,88	0,090	1,90	0,250	(C_{vd}) 1,270

* BBTV
▽ vertical test facility

Table 3.1 : Summary of expected highest errors associated with the measurement of pipe diameter, slurry velocity, pressure gradient and solids concentration

3.4 Conclusions

1. A specific pipeline test facility was constructed for this research and has been described in detail.

2. Additional sources of experimental data were briefly explained.

3. The experimental errors associated with the measurement of the slurry parameters were presented.

CHAPTER 4

MATERIAL DESCRIPTION

The use of mineral tailings as an underground support medium has been discussed in Part 1. A primary consideration when using tailings to provide underground support is the design or choice of an optimum solids particle size distribution. This particle size distribution is primarily chosen to provide maximum support once it has been placed in the underground stope. The required particle size distribution for optimal support is not, however, the optimum particle size distribution for hydraulic transport conditions. Full plant backfill tailings comprise essentially finely crushed ore that is left after the extraction of the precious minerals. Cementitious binders are often added to provide extra strength and support to the slurry. Slurries tested in this thesis do not contain binders.

4.1 The particle size distribution

Various methods can be used to measure the particle size distribution of the slurry. These typically include dry and wet sieving, use of an hydrometer or laser particle size analysers. Figure 4.1 demonstrates a set of data obtained by measuring the particle size distribution in several ways. It is clearly seen that for a specific sample there is a considerable difference in the results obtained. In order to compare relative particle size distributions it is necessary to ensure that the same instrument is used. All particle size distributions were measured using a Malvern 2500/3600 particle sizer VF.6. This instrument is calibrated using Coulter calibration standard particles over a range of different lenses of varying focal length.

Full plant tailings contain a broad range of well distributed particle sizes, from less than 10 μm to approximately 550 μm. It is not sufficient to merely use a representative mean diameter, d_{50}, to describe the characteristic particle size distribution. Figure 4.2 represents the particle size distribution envelope of full plant tailings that were evaluated. Three different full plant tailings were tested - denoted materials 1, 2 and 3. The outer limits of this envelope are presented in Table 4.1. The d_{50} range varies between 20 μm to 40 μm, indicating a high degree of fine material.

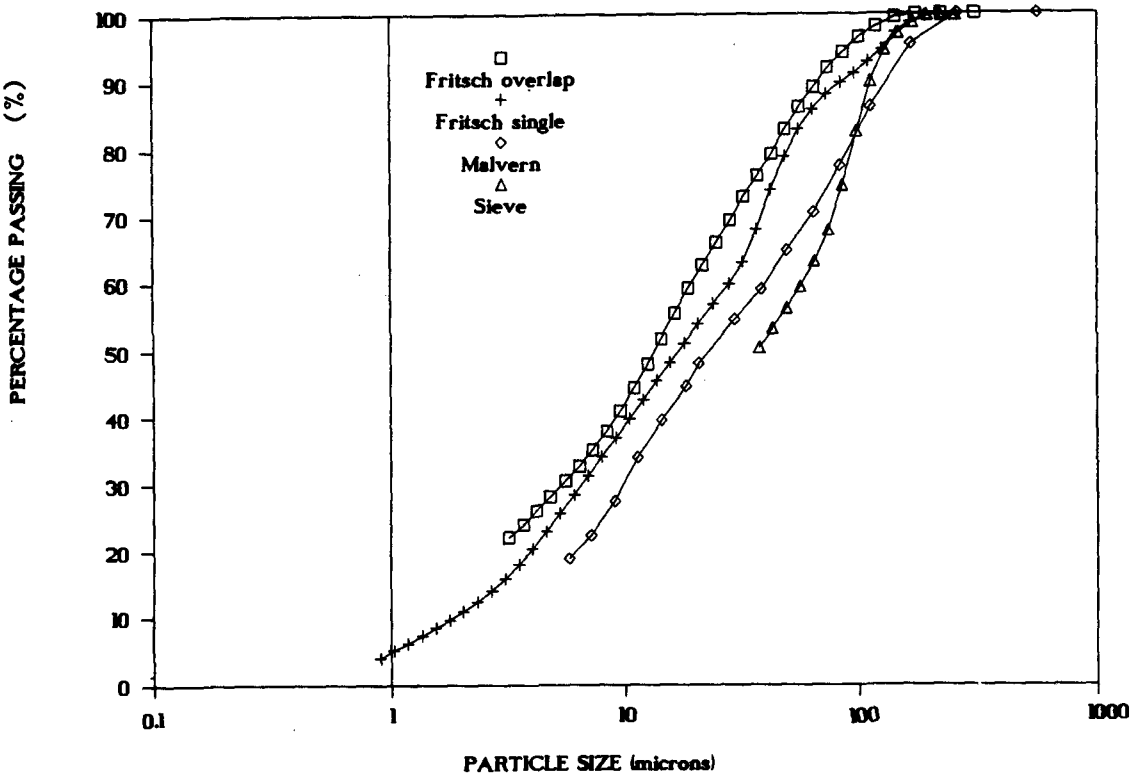

Figure 4.1 : Comparative analysis of the measurement of the particle size distribution curve using various techniques

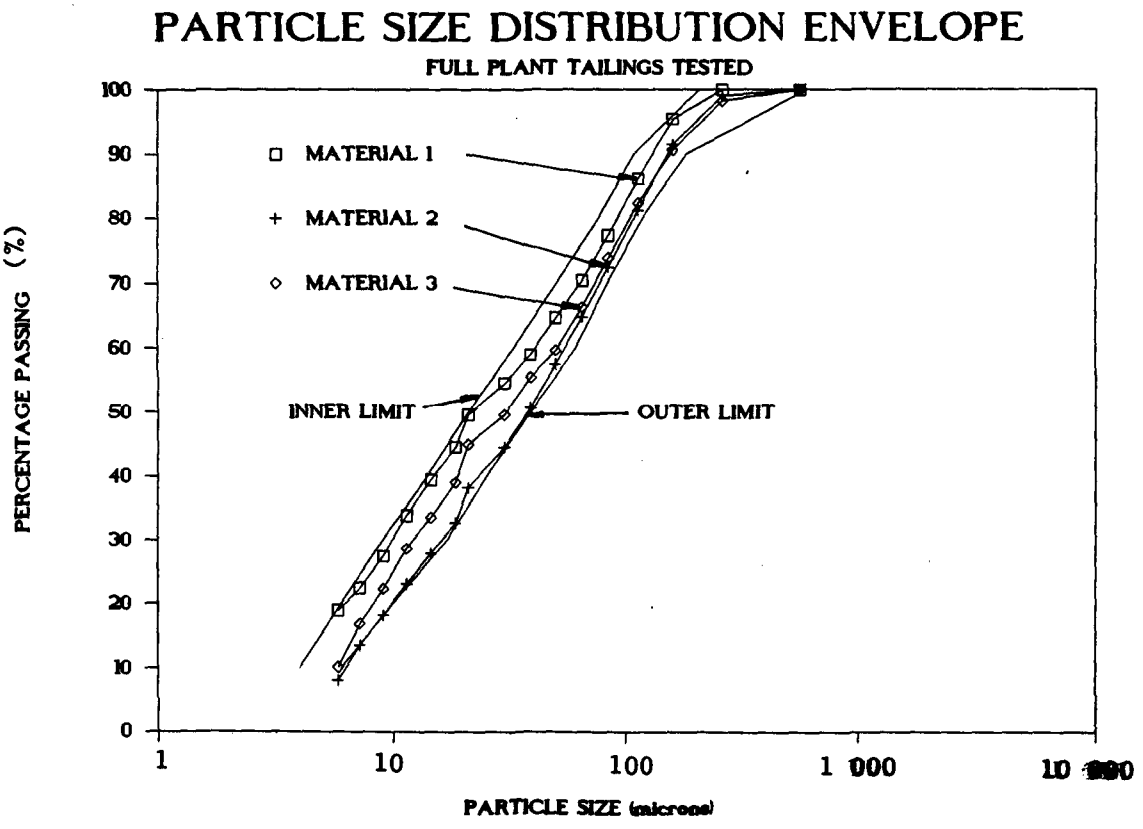

Figure 4.2 : Particle size distribution and particle size envelope of full plant tailings tested

Size Fraction	Inner Limit (μm)	Outer Limit (μm)
d_{10}	4	8
d_{20}	6	10
d_{30}	9	17
d_{40}	14	28
d_{50}	20	40
d_{60}	33	61
d_{70}	50	83
d_{80}	76	118
d_{90}	108	183
d_{100}	200	600
$G_d = \frac{d_{90}}{d_{10}}$	27,00	30,50

Table 4.1 : Particle size distribution envelope describing full plant tailings (using a Malvern particle size analyser)

4.2 Solid and slurry relative density

The relative density of the solids and of the slurry mixture was sampled for each test. The material solids relative density, S_s , was obtained using the method specified in BS 1377, Methods of test for soils for Civil Engineering purposes, Test 6(B): Determination of the specific gravity of fine grained soils.

Typical results are presented in Table 4.2.

Materials	Solids Relative Density S_s
1	2,743 to 2,720
2	2,800
3	2,680

Table 4.2 : Solids relative density of materials tested

The variation of relative density for various materials is due to the changes of primary ore-body from which the ore was originally extracted. The three different materials are each from different locations and ore-bodies.

4.3 pH determination

Values of pH were determined using a radiometer model pHM 80 pH meter and a GK 2401C glass electrode using radiometer buffer of pH = 7,2 (± 0,001) at 20°C, calibrated at the measuring temperature. Variations in pH were slight throughout the tests. The average pH for the slurries tested was 7,43.

4.4 Particle characteristics

The angular nature of the particles can clearly be seen in the Electron Micrographs shown in Figures 4.3 and 4.4. The particles are all extremely irregular in shape as a result of the ore crushing process.

4.5 Settling of coarse particles in the slurry

The full plant tailings tested exhibited slow or non-settling characteristics and can be considered stabilized slurries. Stabilized slurries generally exhibit a definite yield stress, and this has a marked effect on the settling of the particles. If a large particle is suspended within the vehicle and does not settle, it does not contribute to the vehicle friction loss. Its only contribution would be the additional submerged weight of the particle when transporting the slurry in an inclined pipeline. The coarse particles referred to

above are supported by the vehicle yield stress. For the largest size particles, a minimum yield stress is required to support the particle mass. Dedegil (1986) calculated the drag coefficient and settling velocity of particles in non-Newtonian suspension and presented Equation 4.1 for the critical particle size to differentiate between settling and non-settling of the particle for $\tau_y \neq 0$.

$$\hat{d} = \frac{3\pi}{2} \frac{\tau_y}{(\rho_s - \rho_{mf})g} \tag{4.1}$$

Duckworth *et al* (1986) proposed that for a stabilized fluid, the carrier must exhibit a yield stress and be either a Bingham plastic or yield pseudoplastic fluid. The condition of static equilibrium for a stabilized slurry is given by Equation 4.2, and rearranging in terms of particle size, yields Equation 4.3, of the same form as Dedegil (1986). The only difference between Equations 4.1 and 4.3 is the magnitude of the constant, which can be termed the yield stress constant. Dedegil (1986) derives a constant $\frac{3\pi}{2}$ which is less than half of that of Duckworth *et al* (1986) who use a constant of 10.

$$\tau_y \geq 0.1\, \rho_w\, g\, \hat{d}\, (S_s - S_{mf}) \tag{4.2}$$

$$\hat{d} \leq 10 \frac{\tau_y}{(S_s - S_{mf})\, \rho_w\, g} \tag{4.3}$$

where $\hat{d}$ = top size particle in suspension.

The particle size $\hat{d}$ was replaced by d_{50}, based on the assumption that the particles of $\hat{d} < d_{50}$ provide additional support for these larger particles of $\hat{d} > d_{50}$.

The results of Equations 4.1 and 4.2, calculated for a minimum required yield stress to support the top size particle of 550 μm in a typical full plant tailings slurry, indicate a required yield stress of only 1,50 Pa for a vehicle concentration of S_{mf} = 1,4, are illustrated in Figure 4.5.

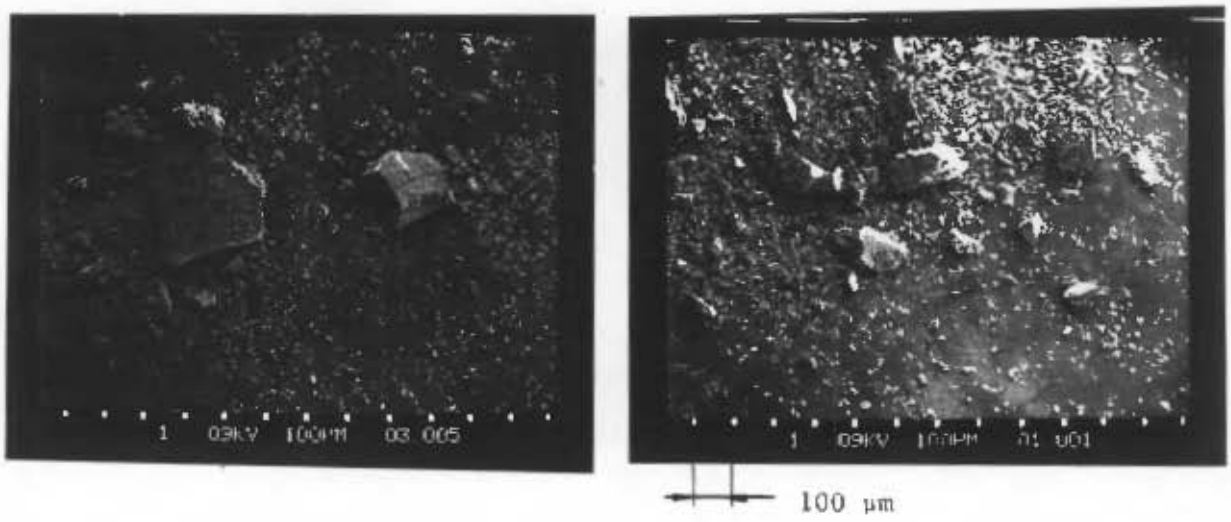

Figure 4.3 : Micrograph of typical full plant tailings :
Scale interval = 100 µm

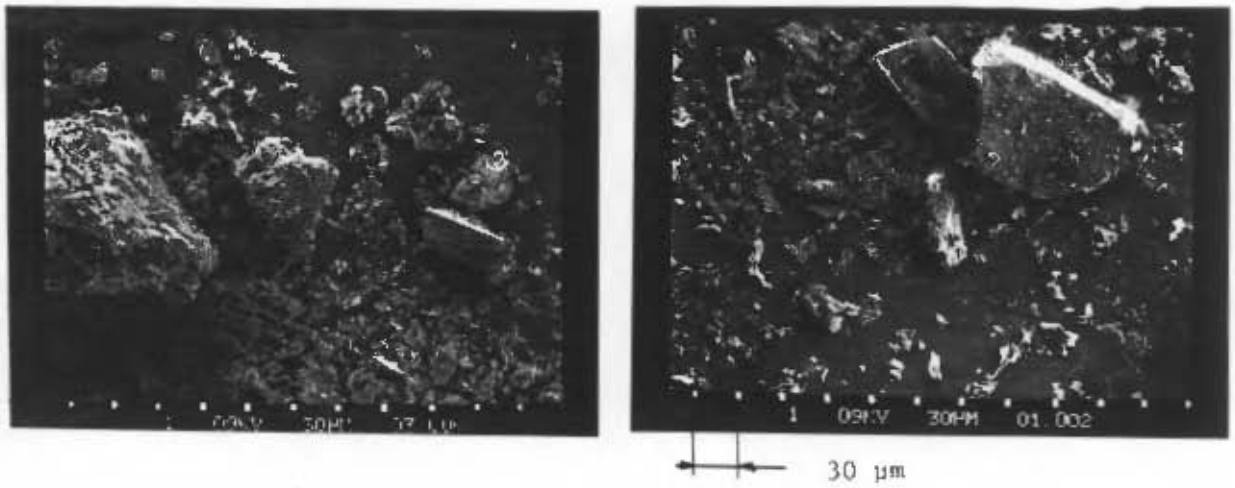

Figure 4.4 : Micrograph of full plant tailings tested :
Scale interval = 30 µm

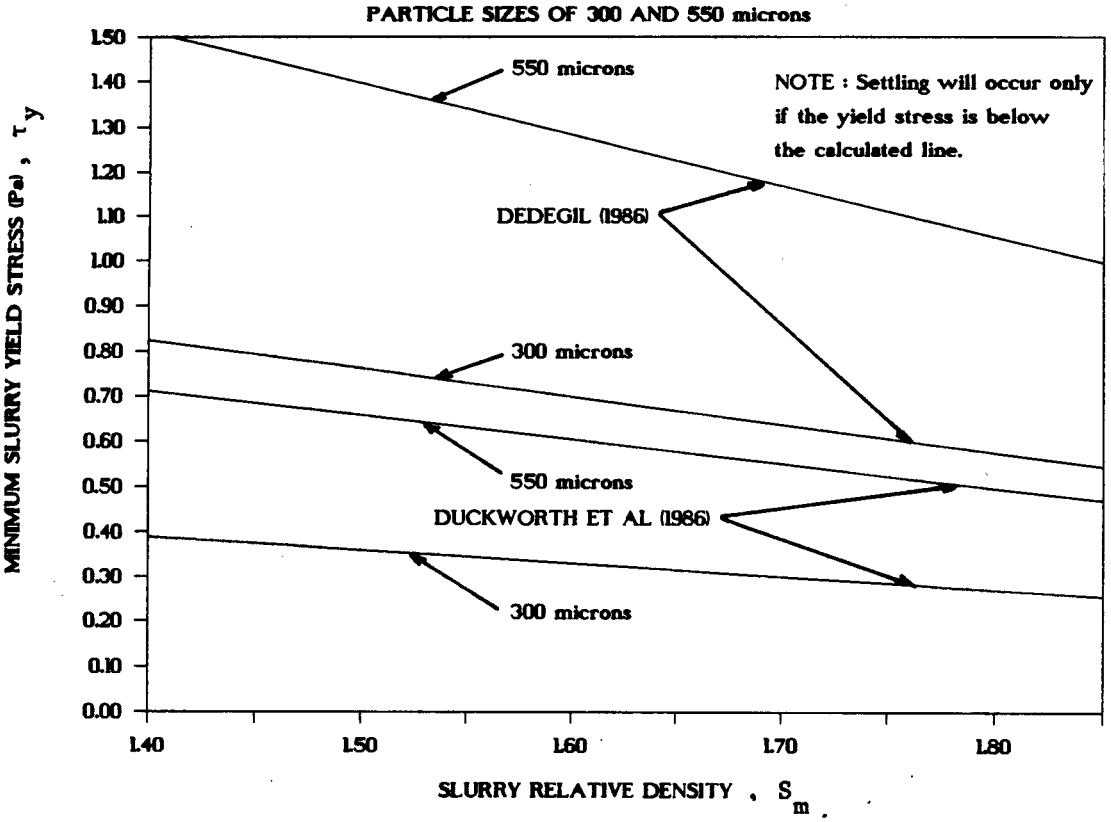

Figure 4.5 : Minimum yield stress required to support top size particle in the slurry

4.5.1 **Drag coefficient of particles settling in a non-Newtonian fluid**

Several methods for calculating the drag coefficient of particles settling in non-Newtonian slurries can be used. For particles settling in a Bingham type carrier fluid, Hanks (1982) suggests using an iterative solution based on the Hedström number. The particle Hedström number is defined as

$$He_p = \frac{\hat{d}_p^2 \, \tau_y \, \rho_f}{\eta_f^2} \qquad (4.4)$$

where ρ_f, η_f are the density and viscosity of vehicle.

The drag coefficient C_D, is calculated from Equation 4.5, based on a correlation developed by Ansley and Smith (1967).

$$C_D = 0{,}40 \left(1 + 6.423 \times 10^{5} \, P_D^{-2{,}856}\right) \tag{4.5}$$

where $P_D = f_n \, (C_D, Y, He)$

$$P_D = \frac{Y}{\left(\frac{Y}{C_D}\right)^{1/2} + \frac{7 \pi He_p}{24}} \tag{4.6}$$

$$Y = \frac{4 \, g \, (\rho_s - \rho_{mf}) \, \rho_{mf} \, \hat{d}_p^3}{3 \, \eta_{mf}^2} \tag{4.7}$$

Equations 4.5 and 4.6 are solved iteratively for C_D . The method of Hanks (1982) yields extremely high drag coefficients. For a slurry at S_m = 1,650 and using typical data the drag coefficient, C_D versus Hedstrom number and particle diameter is presented in Figure 4.6.

The shaded region represents the zone in which the full plant tailings particle size distribution fall. This zone clearly indicates that no settling of the top size particles will occur.

A more generalized solution is presented by Dedegil (1986), based on a force balance of the forces acting on a particle settling in a non-Newtonian fluid.

The particle Reynolds number is given by

$$R_{ep} = \frac{(V_t') \, \rho_f}{\tau} \tag{4.8}$$

where V_t' = hindered settling velocity

τ = fn $\left(\frac{du}{dr}\right)$

The hindered settling velocity, V_t' , can be calculated from Equation 4.9, where C_D is found from the analysis of R_{ep} for the following conditions :

$$R_{ep} \leq 8 \quad : \quad C_D = 24/R_{ep}$$

$$8 \leq R_{ep} \leq 150 \quad : \quad C_D = \frac{22}{R_{ep}} + 0{,}25$$

$$R_{ep} > 150 \quad : \quad C_D = 0.4.$$

$$V_t' = \left[\frac{2}{C_D} \left[\frac{2}{3} \left(S_s - S_{mf} \right) gd - \frac{\pi \tau_y}{\rho_f} \right] \right]^{1/2} \qquad (4.9)$$

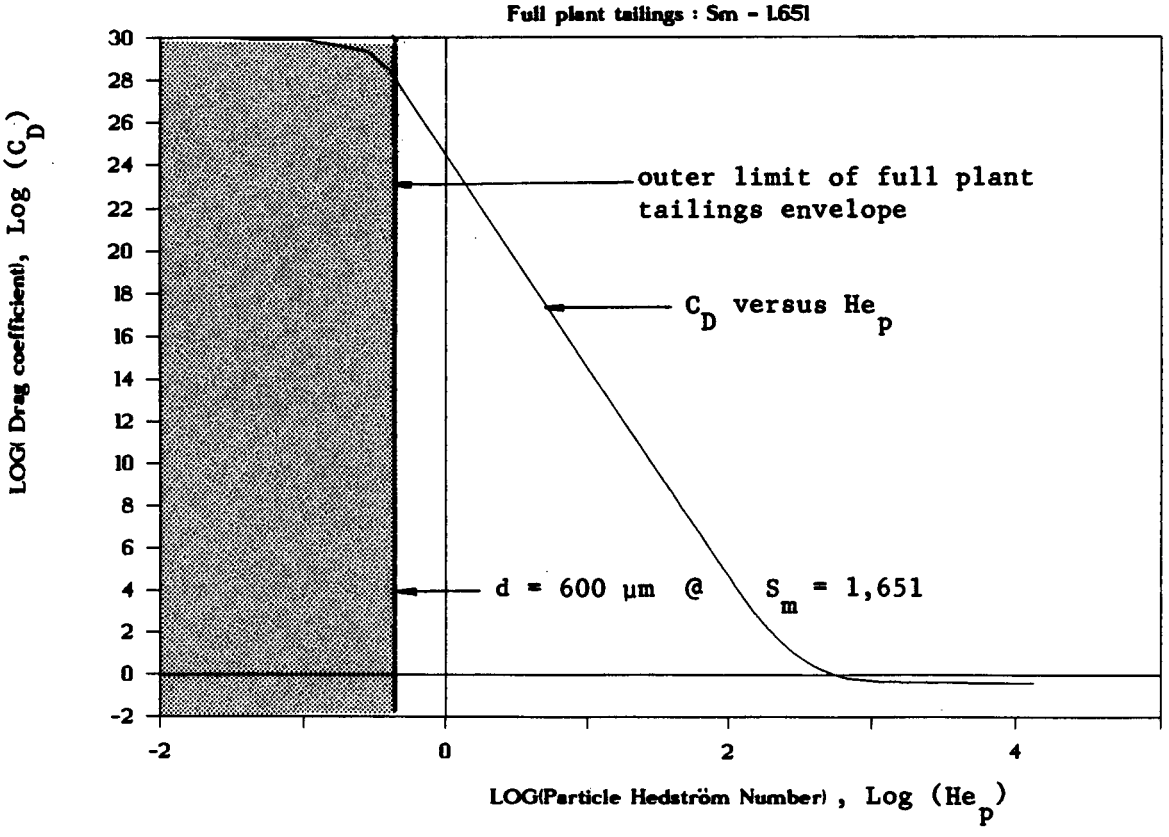

Figure 4.6 : Calculated drag coefficient for particle settling in full plant tailings at S_m = 1,651

4.6 Freely settled bed packing concentration

The particle packing of the slurries tested was measured using a bench top test to determine the freely settled concentration. The results of these tests for the different slurries is shown in Figure 4.7. A known mass and volume of oven dry solids is placed in a calibrated measuring cylinder and mixed with water to form a dilute solid-water mixture. The settling of the particles is measured by the height of the interface of slurry and supernatant water. This test allows for the determination of the particle packing density that would result in the volumetric concentration that distinguishes between low, heterogeneous flow regimes and high concentration stabilized flow regimes, a concept fully discussed in Part 4. Once the freely-settled bed packing concentration has been determined, the sample can be further mechanically vibrated on a Sweco concrete vibrator to allow for further particle packing. This gives an indication of the maximum possible particle packing arrangement that could be achieved.

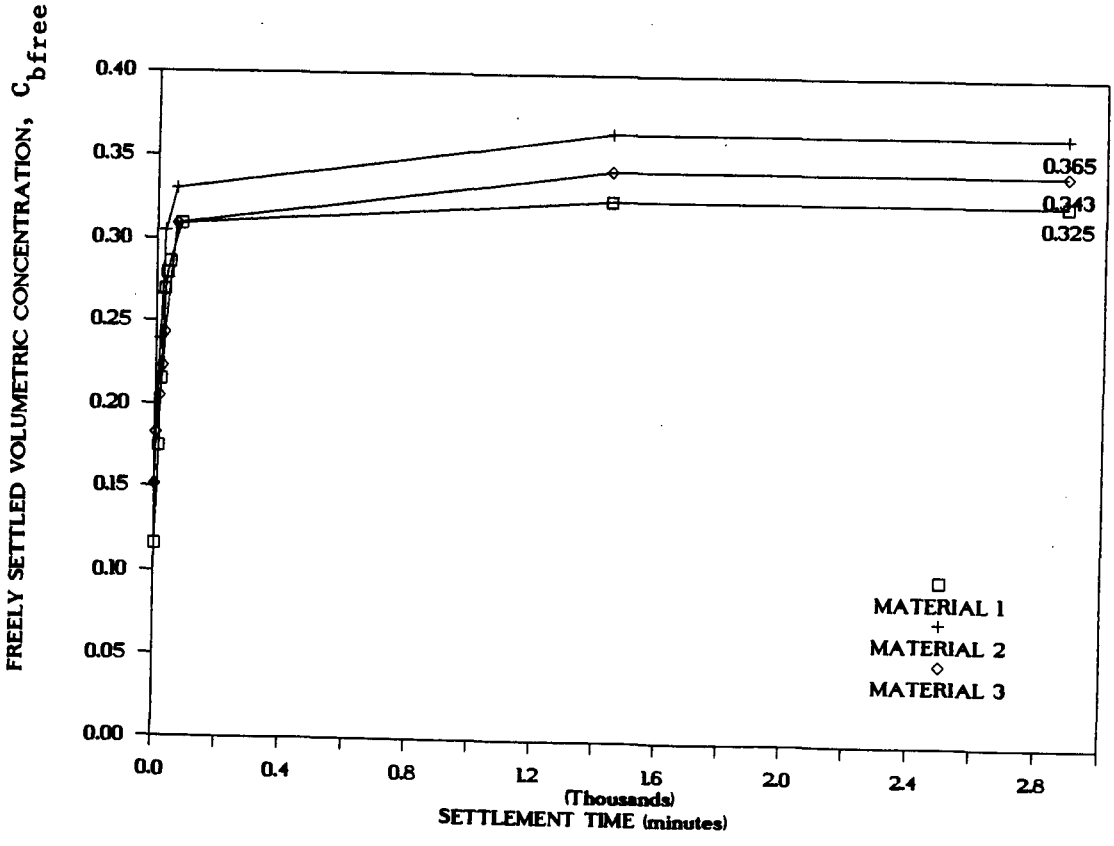

Figure 4.7 : Measurement of the freely settled bed packing concentration - variation with time

4.7 Conclusions

1. The particle size distribution of all the materials tested was measured using a Malvern particle size analyser, model VF.6 to enable comparison of the PSD to be made on a common basis.

2. The largest size particles occurring in the slurry will not settle and are supported by the slurry yield stress.

3. The slurry is a non-settling stabilized slurry.

CHAPTER 5

EXPERIMENTAL RESULTS

5.1 Range of measured data

The three test facilities provided a range of pipe diameters from 4 mm NB to 100 mm NB. Limitations on each facility varied and maximum concentrations achieved differ. Table 5.1 illustrates the range of pipe diameters and concentrations measured. The Balanced Beam Tube Viscometer (BBTV) and Chamber of Mines test facilities do not have pipe test sections in the vertical and measurements are only for horizontal test sections in these instances.

Facility	Pipe Diameters	Slurry Relative Density Range	Material Tested
BBTV	13,48 mm	1,651 to 1,902	1
	32,63 mm	1,651 to 1,902	
Vertical test facility	41,22 mm	1,530 to 1,850	1,2,3
	75,88 mm	1,430 to 1,740	1
Chamber of Mines	101,5 mm	1,500 to 1,740	1

Table 5.1 : Range of experimentally measured data

5.2 Data obtained from the Balanced Beam Tube Viscometer

The data from Neill (1988) obtained in the BBTV contains measured results from various sieved particle size fractions of full plant tailings for material 1. These results are presented in the form of a pseudo-shear diagram from which the rheological parameters of τ_y , K and n can be determined at the low concentrations. The size fractions analysed are :

(i) -550 μm fraction, containing the complete particle range of full plant tailings.

(ii) -106 μm fraction, containing approximately 90% of the particle size distribution curve.

(iii) -62 μm fraction, comprising 70% of the particle size distribution curve.

(iv) -42 μm fraction, containing approximately 50% of the particle size distribution curve.

A set of typical pseudo-shear diagrams is presented in Figure 5.1. The anomalous behaviour of the material is clearly seen in the form of diameter dependence. This is dealt with in detail in Part 3. Figure 5.2 represents the complete set of laminar flow curves for the -500 μm micron fraction of the full plant tailings from slurry relative density S_m = 1,651 to S_m = 1,902 and for pipe internal diameters of 13,48 and 32,63 mm.

5.3 Data obtained from the vertical test facility

Data from the vertical test facility for materials 1 to 3 is represented by Figures 5.3 to Figures 5.5 for horizontally measured pressure gradients. Vertically measured total pressure gradients are represented in Figures 5.6 to 5.8.

The horizontal and vertical pressure gradients in these tests were measured at the same velocities. Figure 5.9 is a typical set of raw data measured during a test. Referring to Figure 5.10, the total head difference read on the water manometers is ΔH. This is a measure of both the submerged weight of the slurry and the friction head loss. The friction head loss is determined from Equations 5.1 and 5.2 for low and high flow rates respectively :

(LOW FLOW)

$$\Delta H_f = (S_m - S_w)\, L - \Delta H_{TOTAL} \qquad (5.1)$$

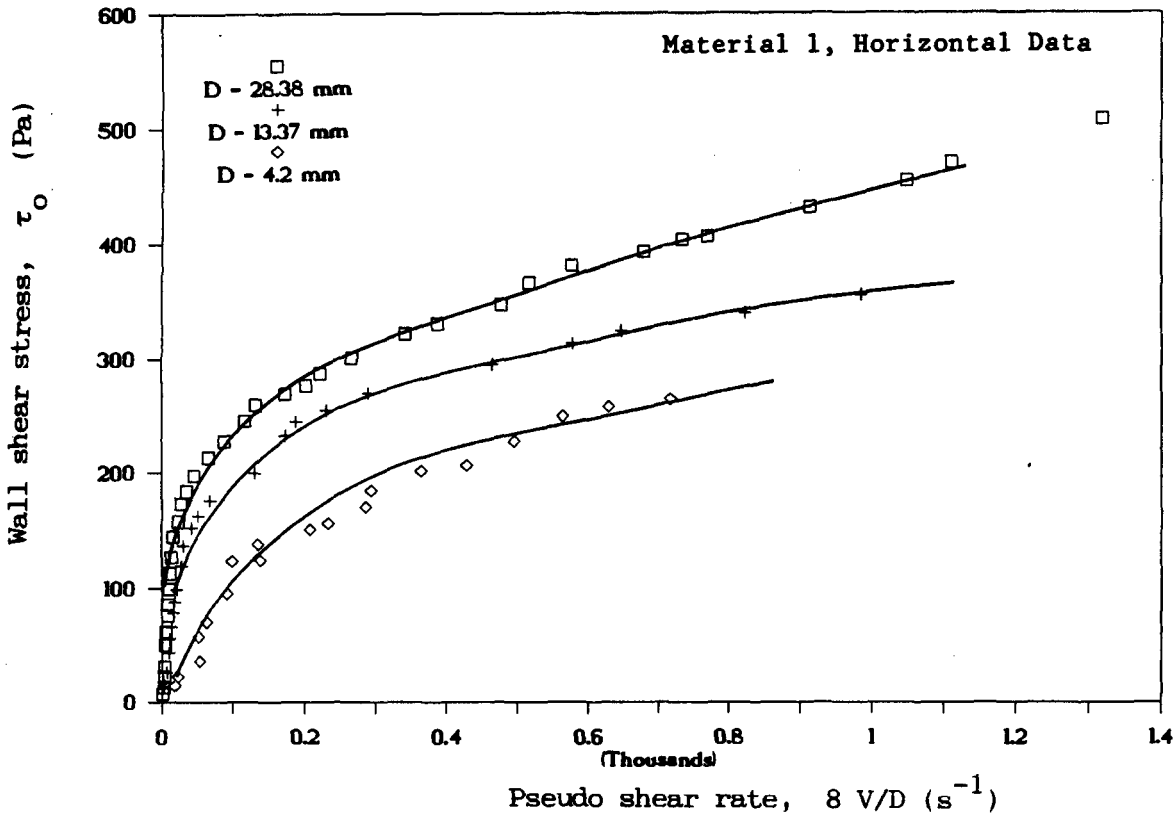

Figure 5.1 : Typical pseudo-shear diagram of results taken from BBTV, S_m = 1,74 (Neill (1988))

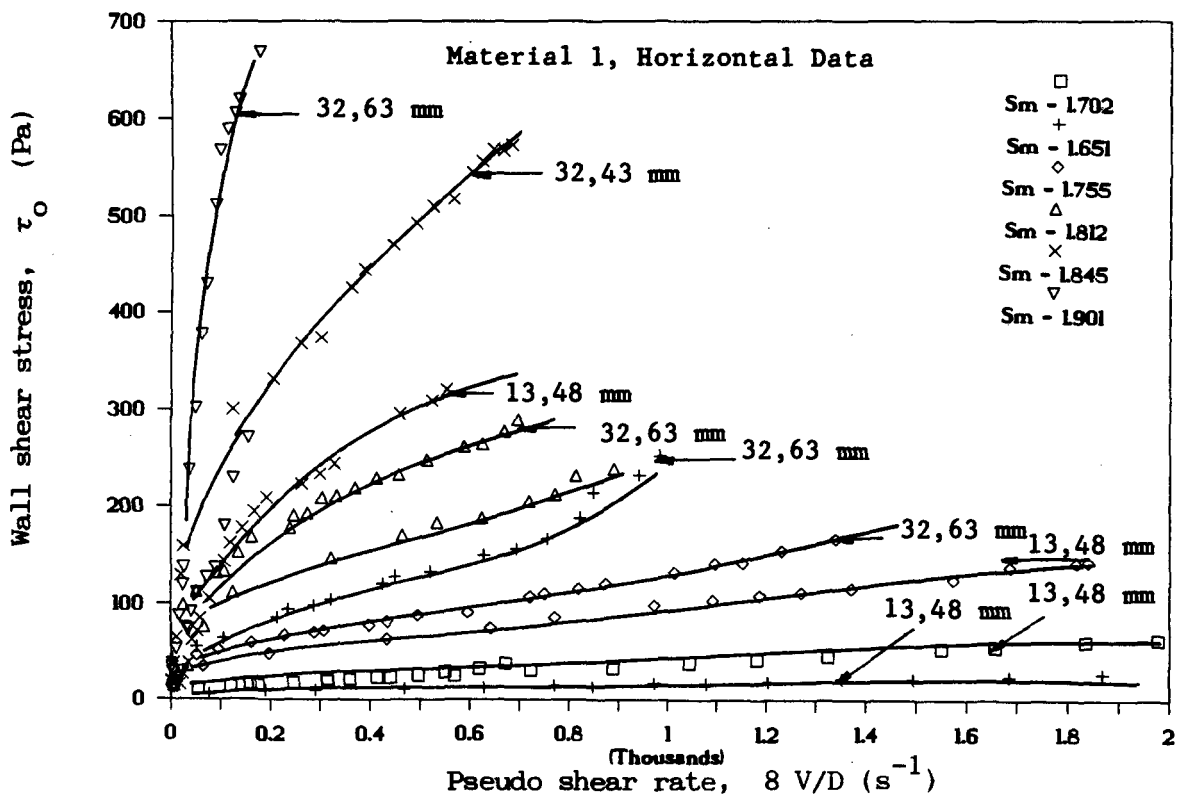

Figure 5.2 : Laminar flow curves of BBTV test data (Neill (1988))

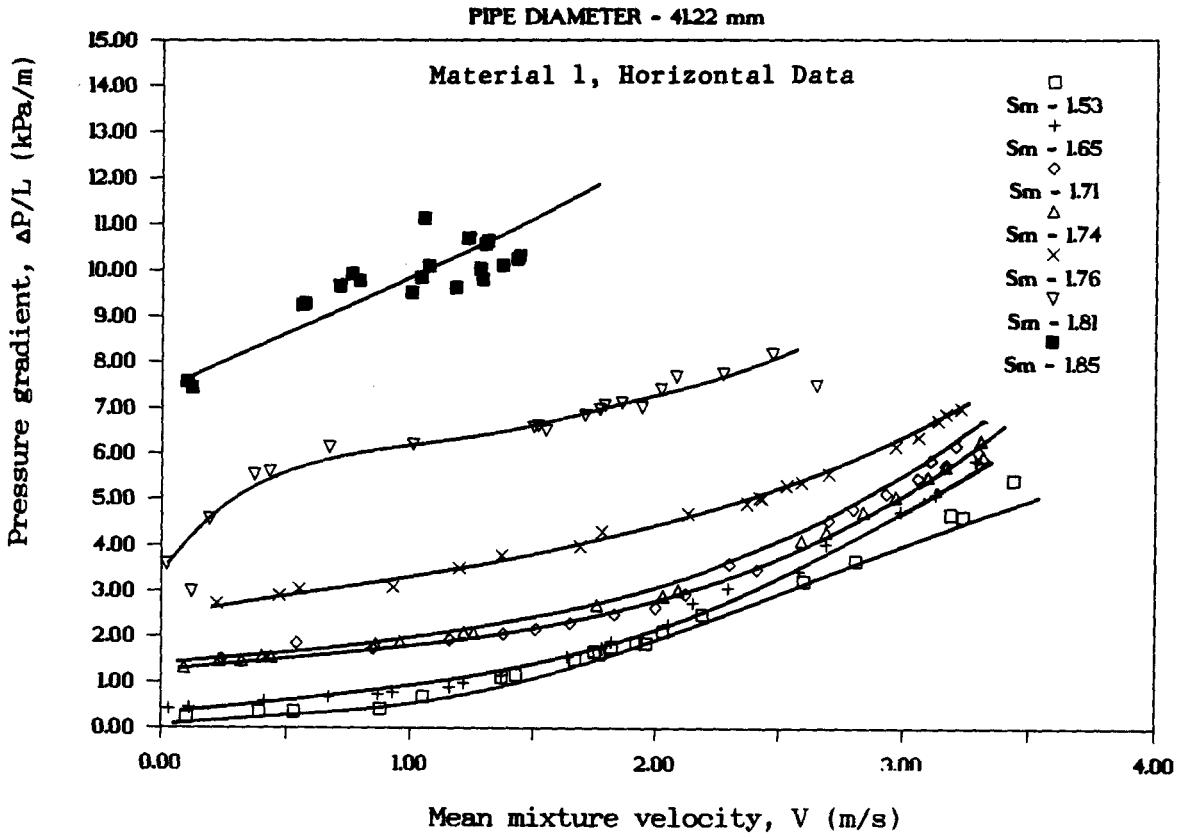

Figure 5.3 : Horizontally measured pressure gradients for material 1 - vertical test facility

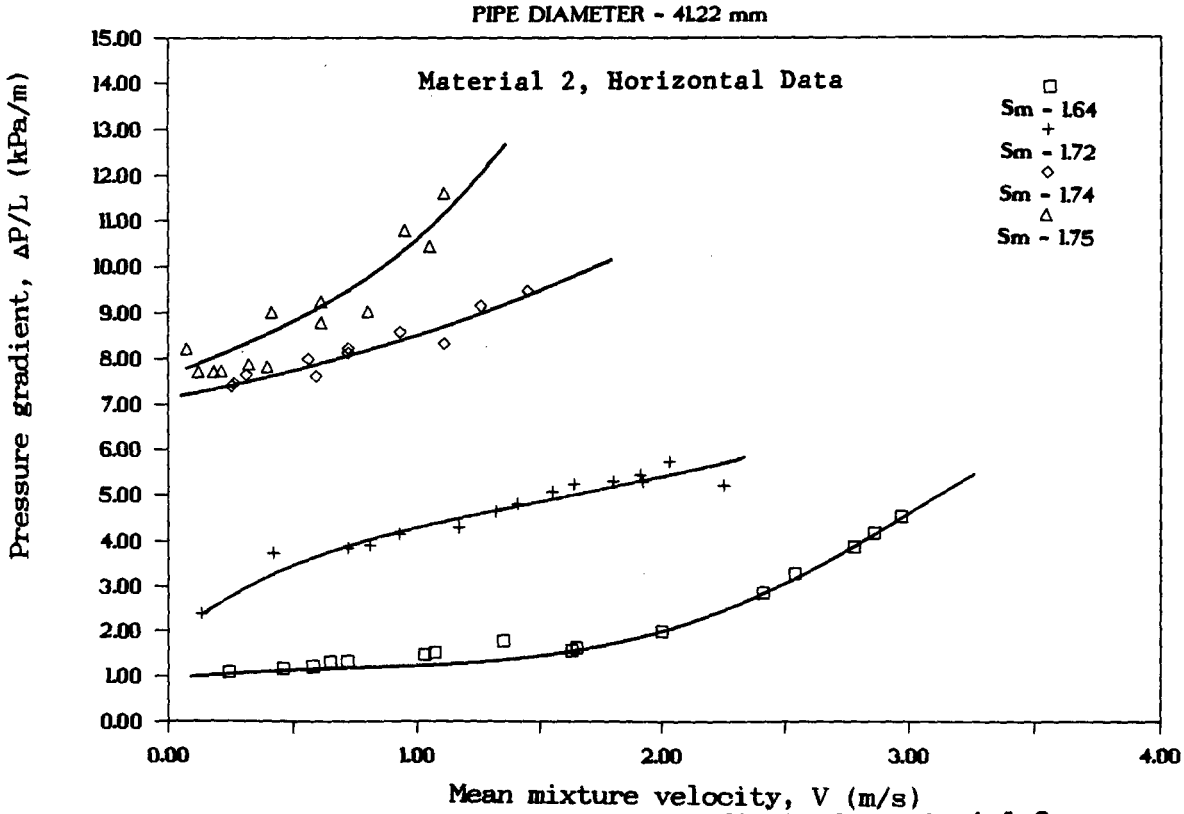

Figure 5.4 : Horizontally measured pressure gradients for material 2 - vertical test facility

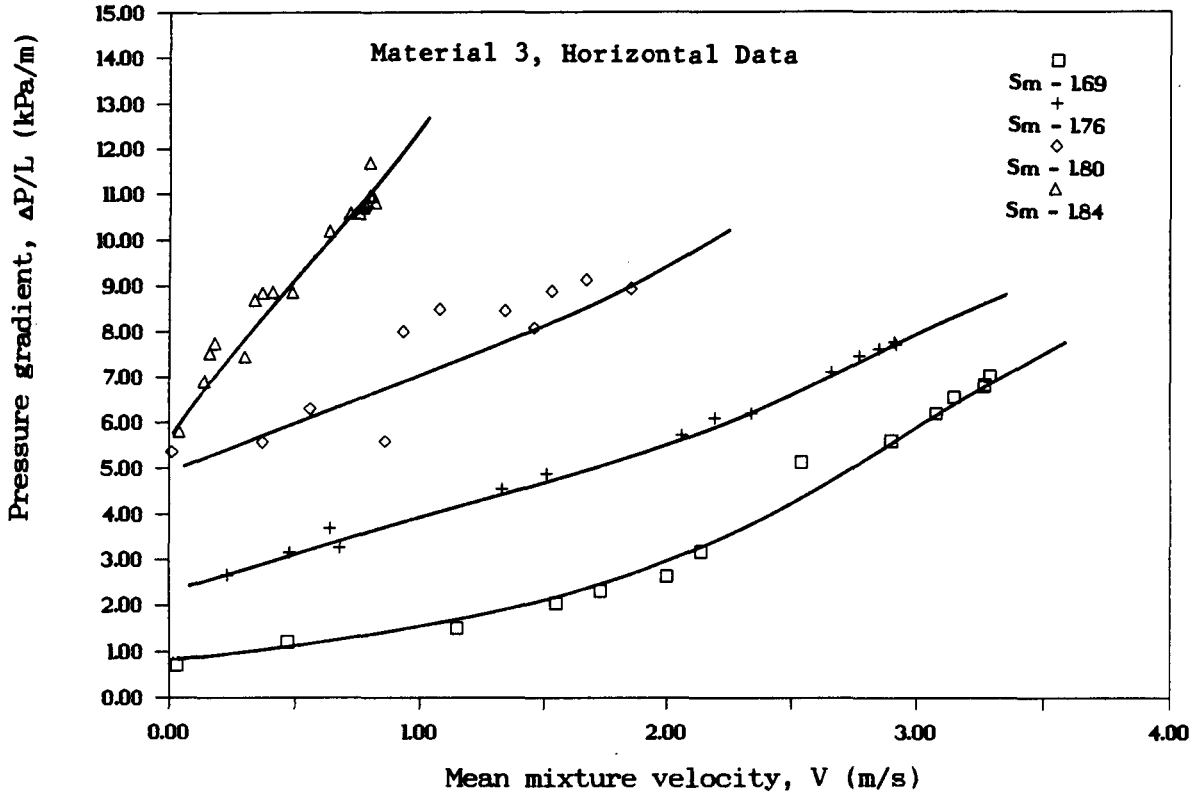

Figure 5.5 : Horizontally measured pressure gradients for material 3 - vertical test facility

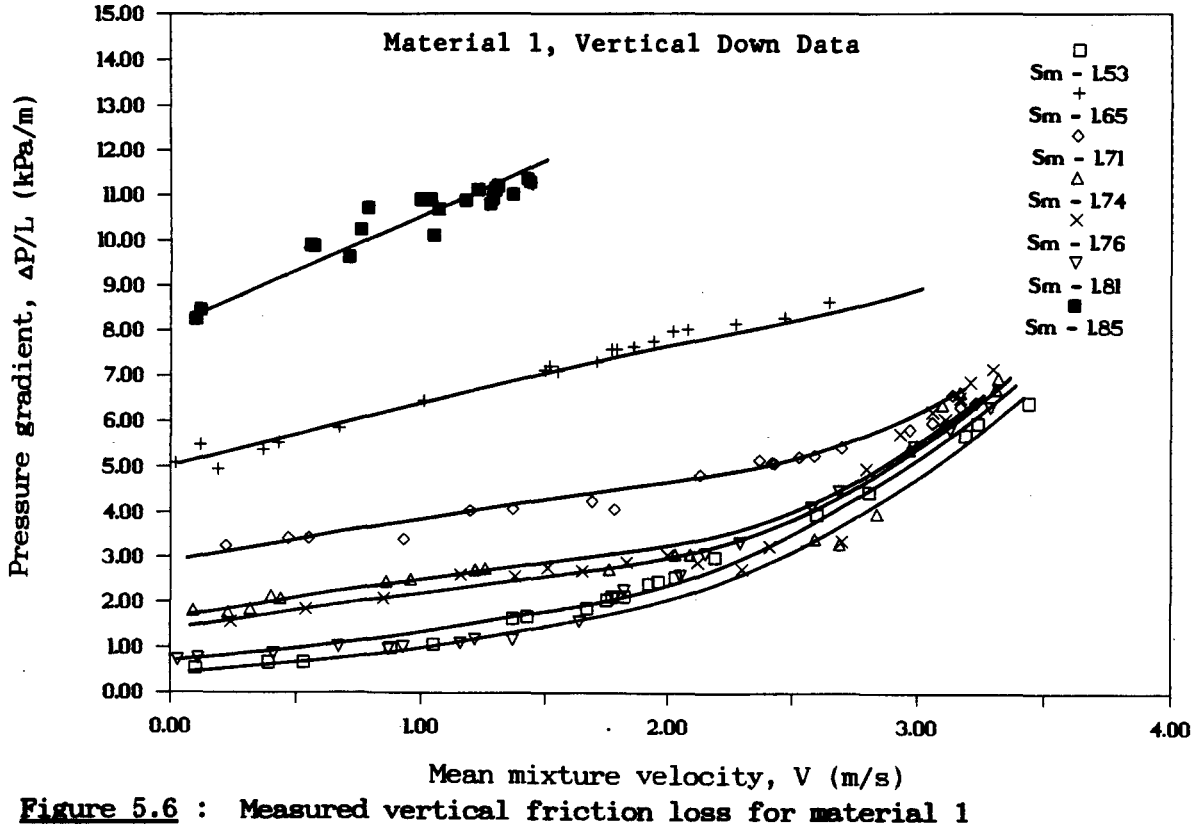

Figure 5.6 : Measured vertical friction loss for material 1

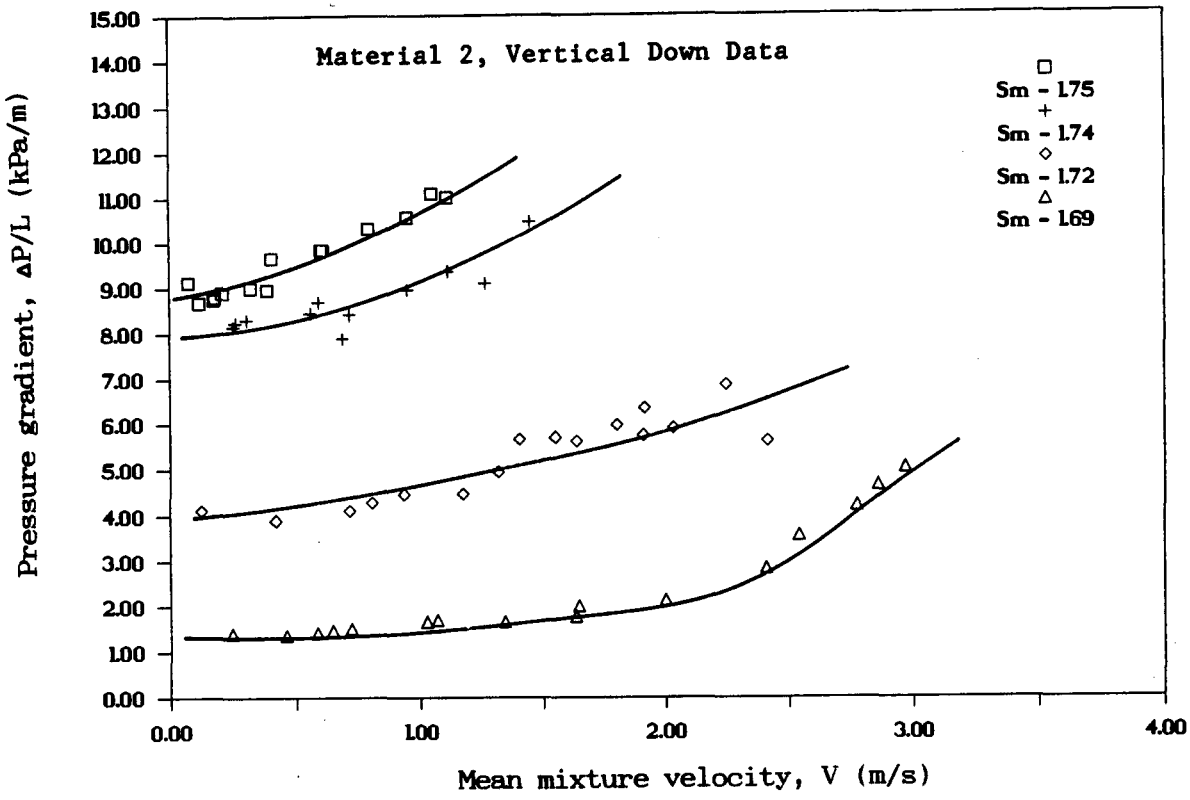

Figure 5.7 : **Measured vertical friction loss for material 2**

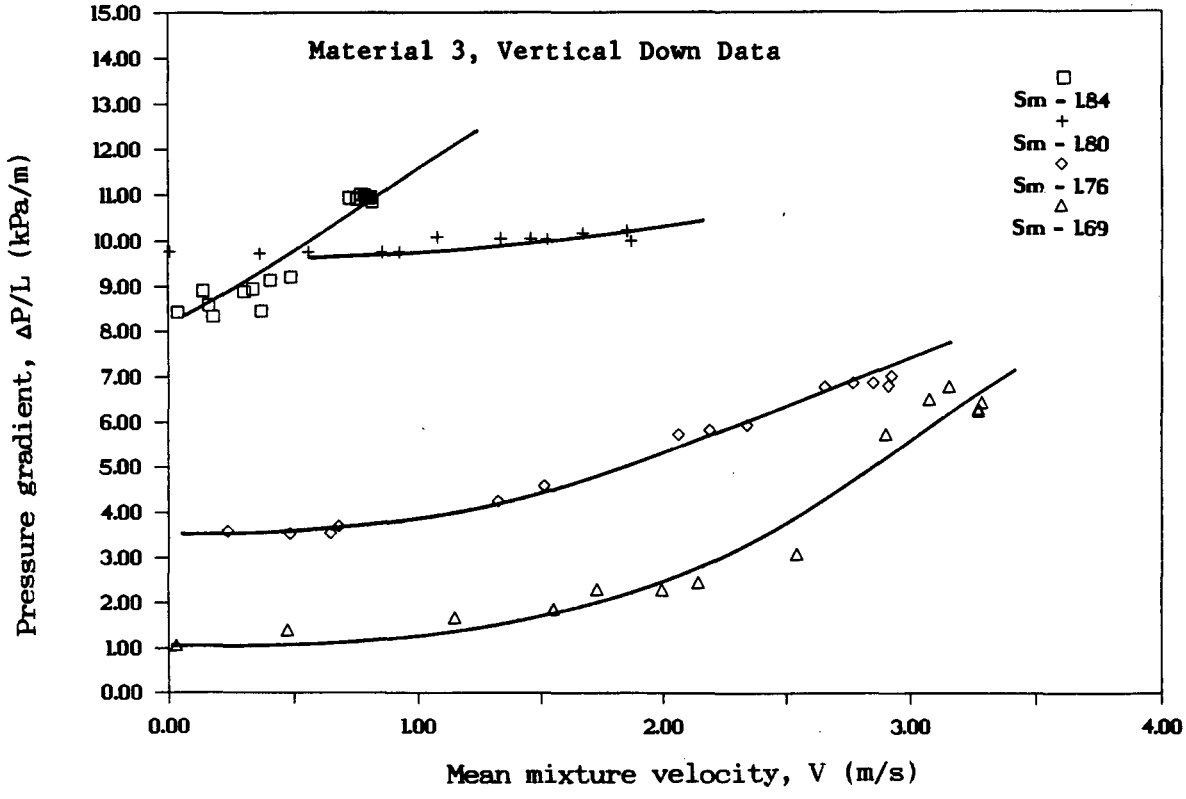

Figure 5.8 : **Measured vertical friction loss for material 3**

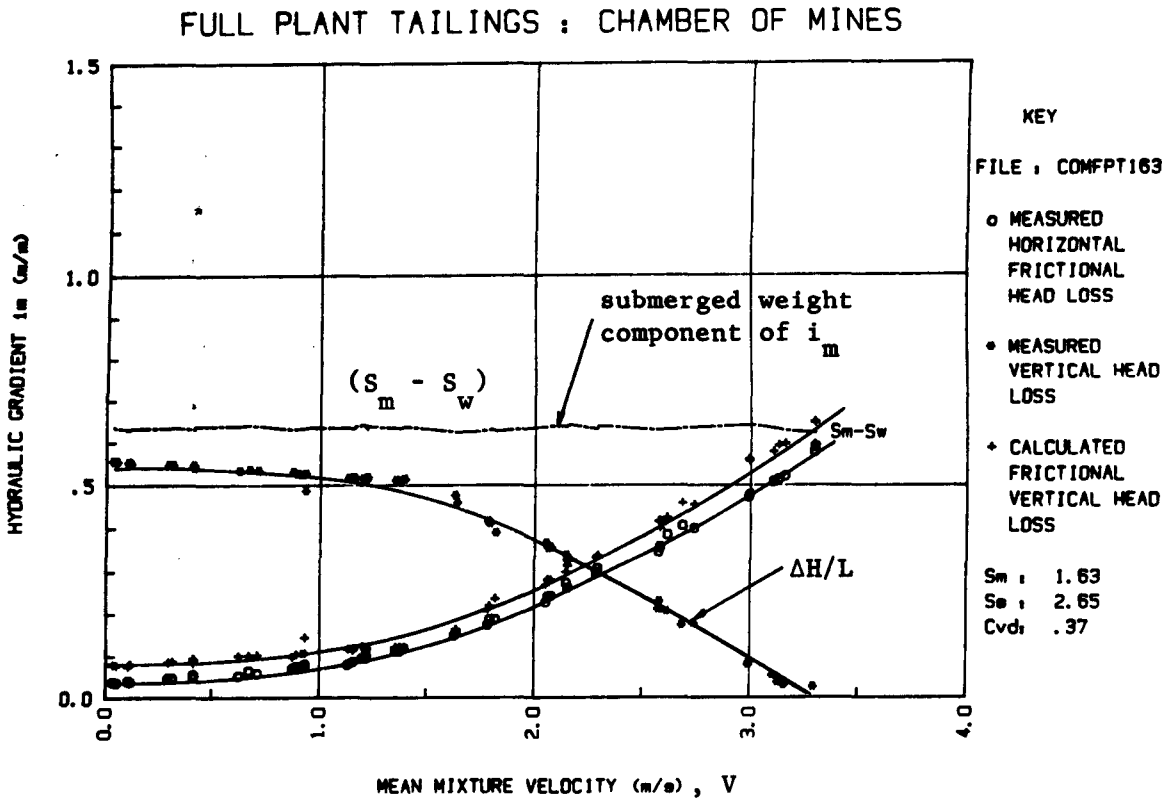

Figure 5.9 : Typical set of raw data measured during a test run at the vertical test facility

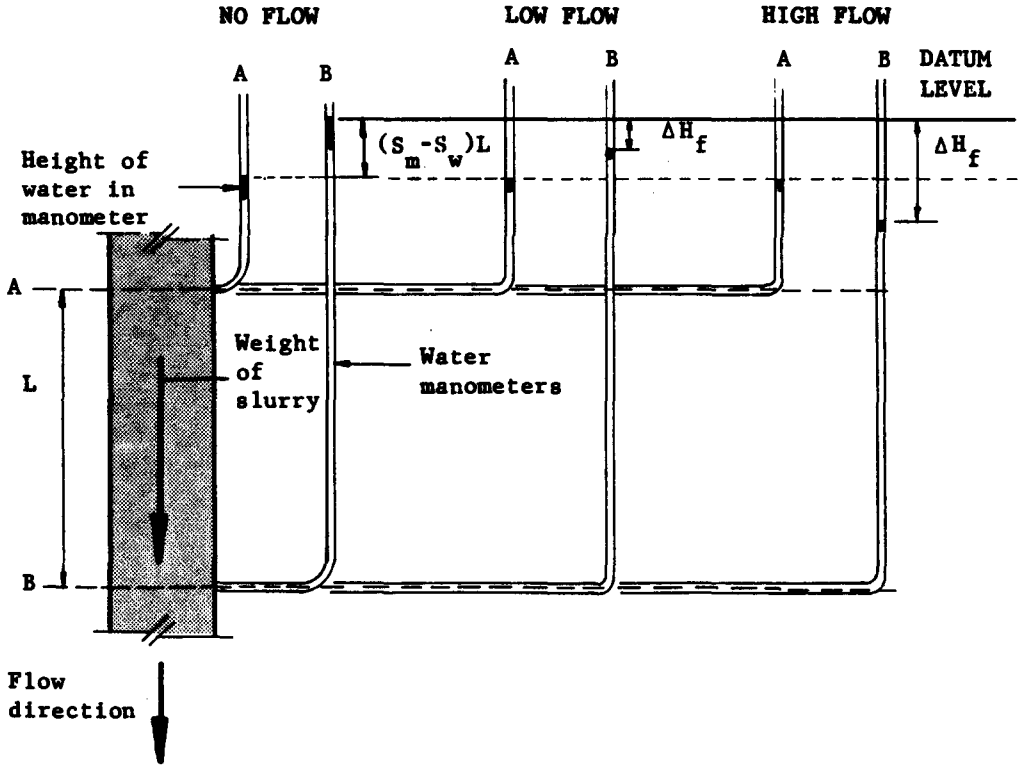

Figure 5.10 : Measurement of vertical head losses

(HIGH FLOW)

$$\Delta H_f = (S_m - S_w)\, L + \Delta H_{TOTAL} \qquad (5.2)$$

The graph in Figure 5.9 represents both the measured data as well as the calculated vertical losses (Equations 5.1 and 5.2). It is important to know the submerged weight if vertical measurements are to be taken, and the gamma ray densitometer is used for this purpose. The submerged weight is plotted on the graph by the curve denoted $(S_m - S_w)\, L$.

The vertical friction losses shown in Figure 5.8 were calculated using Equation 5.2. Differences between vertical downward and horizontal friction losses can be attributed to either pipe roughness variations or variations of *in situ* concentration. The measured pipe roughness using the standard Colebrook-White analysis for the horizontal and vertical pipelines is 103 μm and 207 μm respectively, the vertical pipe being twice as rough as the horizontal test section. For small pipe diameters, the effect of roughness is large and decreases as pipe diameter increases, as per the friction factor Reynolds number diagram. A sensitivity analysis of the effect of pipe roughness on the vertical facility indicated that the observed differences between the calculated vertical friction loss and the measured horizontal friction loss is of the same order of magnitude as for differences obtained for the clear water tests. A typical comparison between vertical and horizontal friction losses is shown in Figure 5.11, combined with the results of pipe roughness effects for water using the measured values of roughness. At high velocities the order of magnitude of variation between vertical and horizontal friction losses is comparable to the curves obtained from the Colebrook-White analysis.

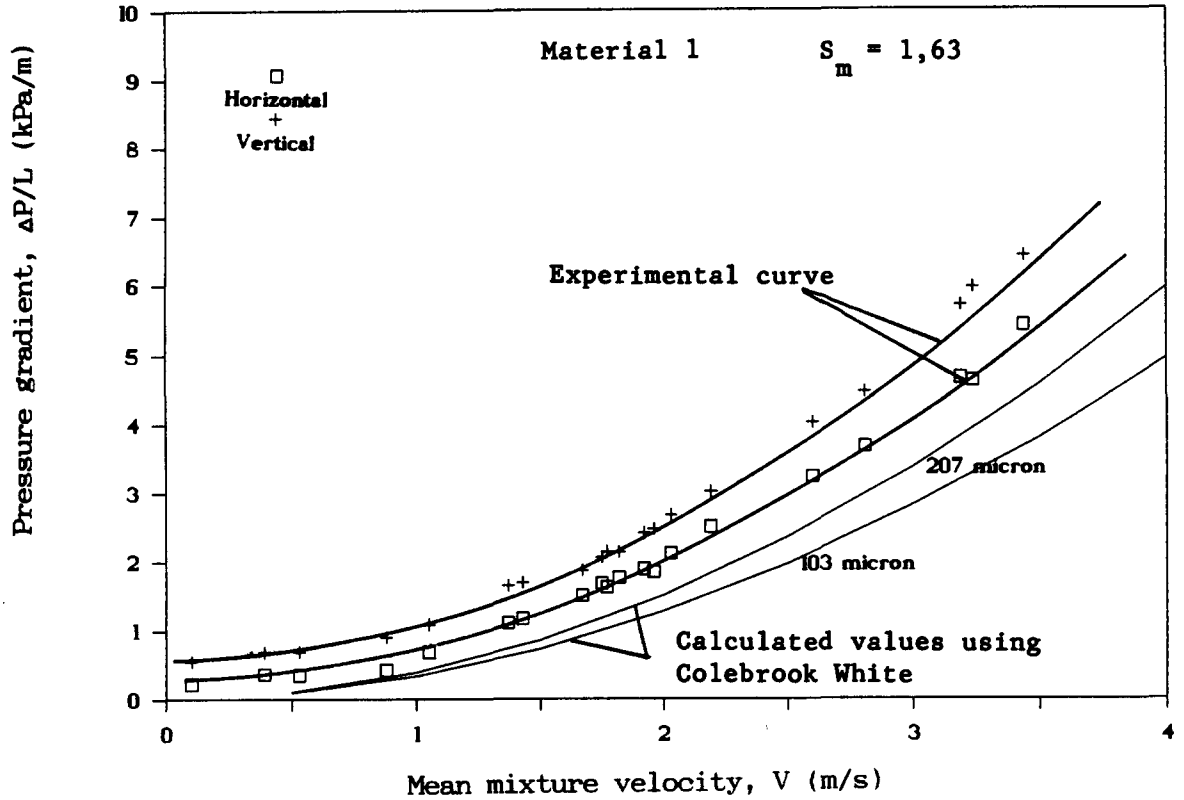

Figure 5.11 : Comparative effect of pipe roughness on measured friction losses in horizontal and vertical test sections

Because the vertical friction pressure loss is a calculated value, small variations in measured *in situ* volumetric concentration have a marked effect on the calculated difference. When observing the measured data points and density for each of the tests, the fluctuation of submerged weight is clearly seen. The measured density values for each reading are used to determine the vertical friction pressure loss from the corresponding measured total head loss. As the measured total vertical head decreases, so the percentage error of calculated vertical friction loss increases for small variations of *in situ* concentration.

The observed scatter of measured data for both horizontal and vertical pressure losses is not significant and is only noticeable at the higher concentrations tested in Figures 5.3 to 5.8, but there is nonetheless a definitive trend. Particularly noticeable is the rapid increase in pressure gradient with increasing slurry relative density. This is best illustrated in Figures 5.12 to 5.14 where pressure gradient is compared to slurry solids concentration for contours of equal velocity.

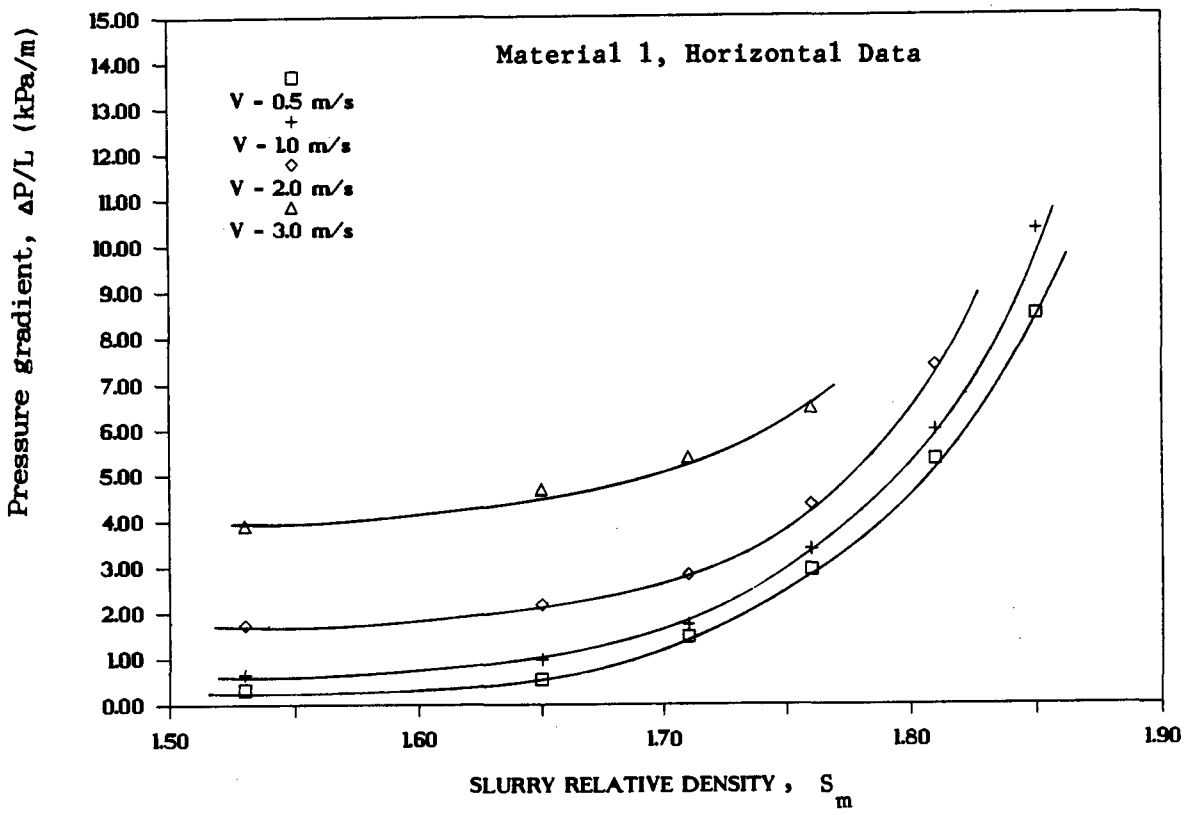

Figure 5.12 : Pressure gradient versus slurry relative density for contours of equal velocity - material 1, vertical test facility (I.D. = 41,22 mm)

For these slurries, it can be seen that there is a rapid increase in pressure gradient for a small increase of solids concentration at the higher relative densities. This is an important feature of high concentration flow and gives an indication as to the maximum pumpable solids concentration. The sudden increase in pressure gradient is largely due to the sudden increase in relative viscosity as the solids particle mobility decreases and the solids volumetric concentration approaches the maximum possible solids packing concentration.

Data obtained using the 75,88 mm pipeline using material 1 in both horizontal and inclined pipelines is represented in Figures 5.15 to 5.16. The increase of pressure gradient with slurry relative density at higher concentrations is clearly seen in Figure 5.17. Vertical measurements were not obtained for slurry relative density values greater than S_m = 1,70 for this series of tests.

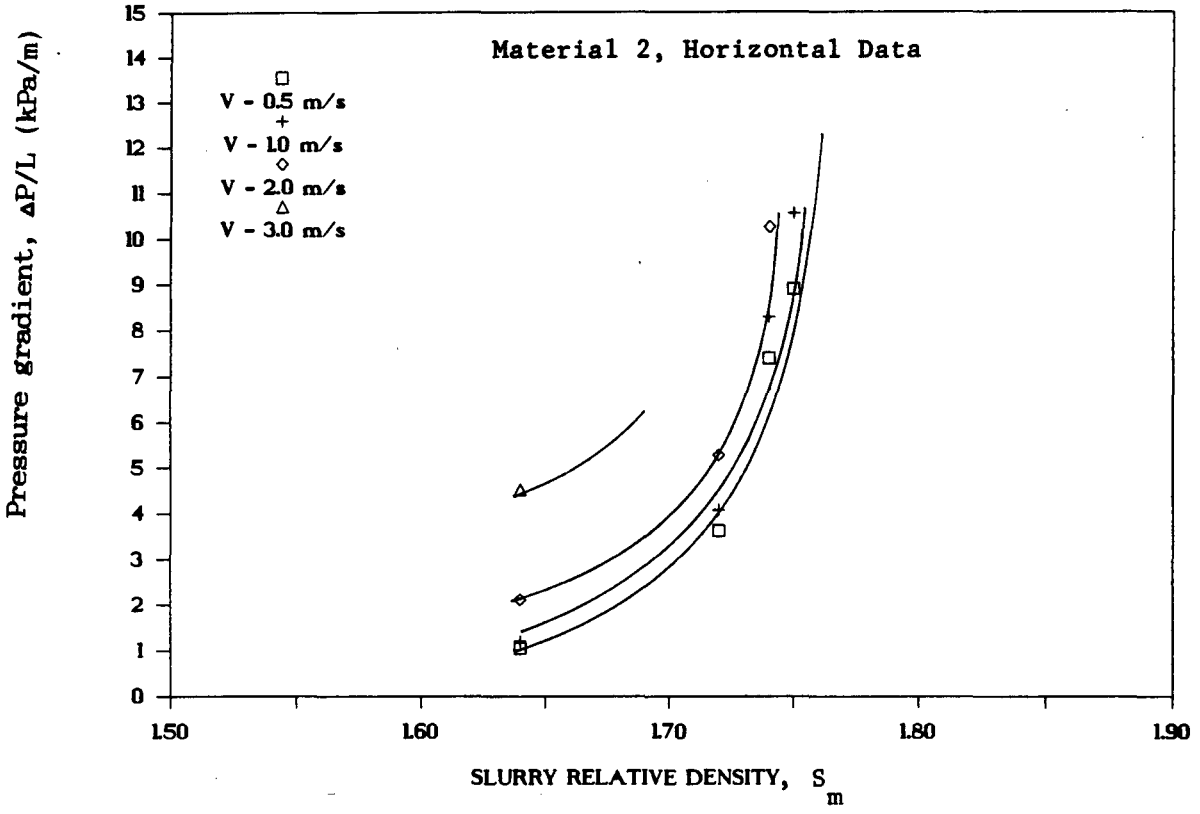

Figure 5.13 : Pressure gradient versus slurry relative density for contours of equal velocity - material 2, vertical test facility (I.D. = 41,22 mm)

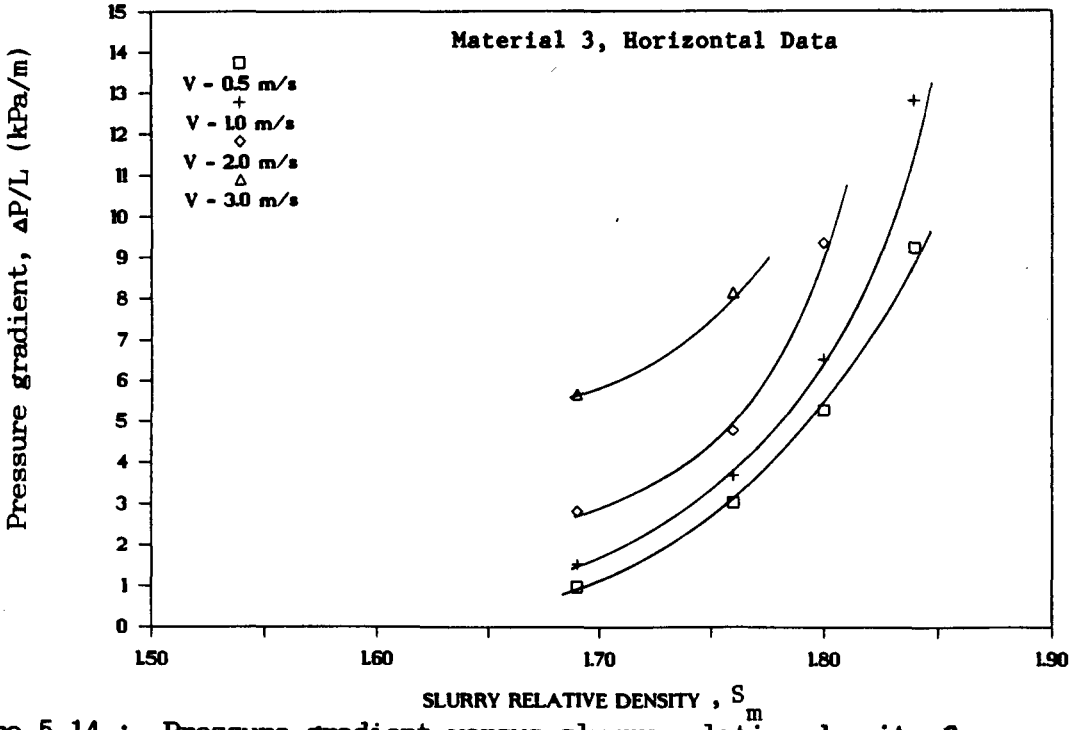

Figure 5.14 : Pressure gradient versus slurry relative density for contours of equal velocity - material 3, vertical test facility (I.D. = 41,22 mm)

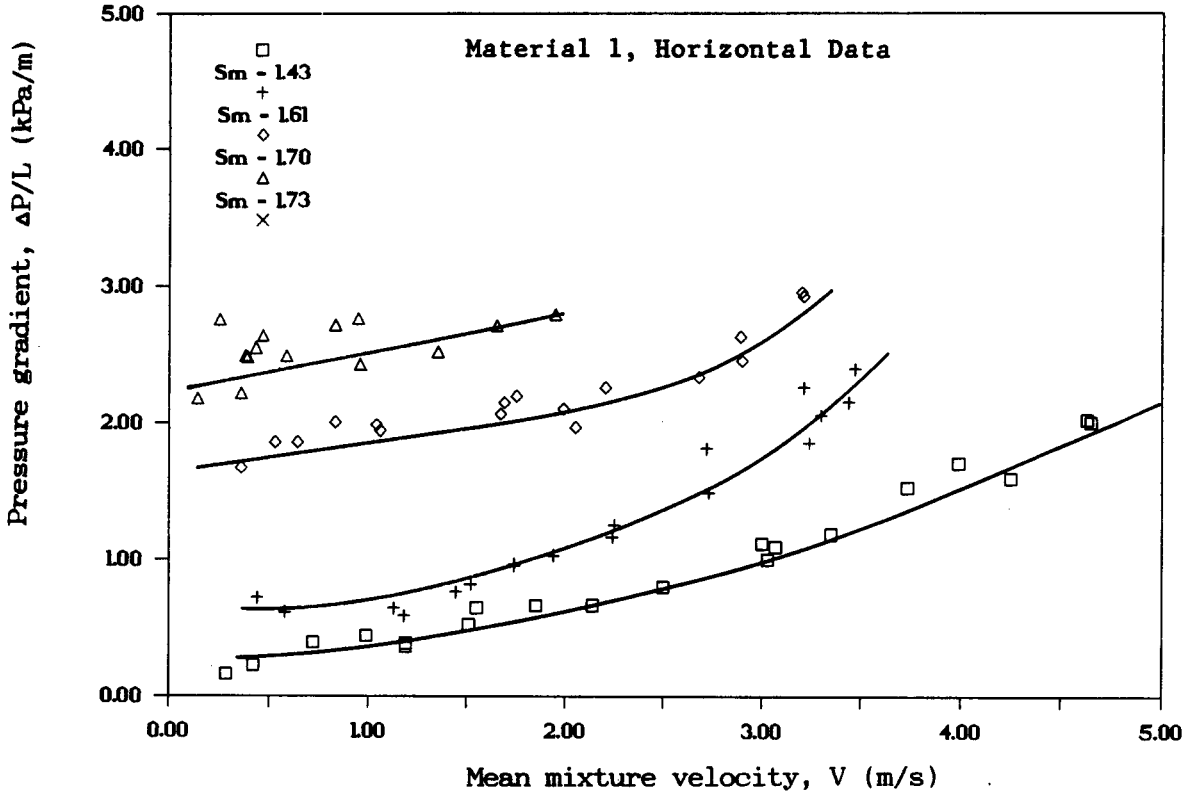

Figure 5.15 : Measured horizontal pressure gradients for material 1, I.D. = 75,88 mm

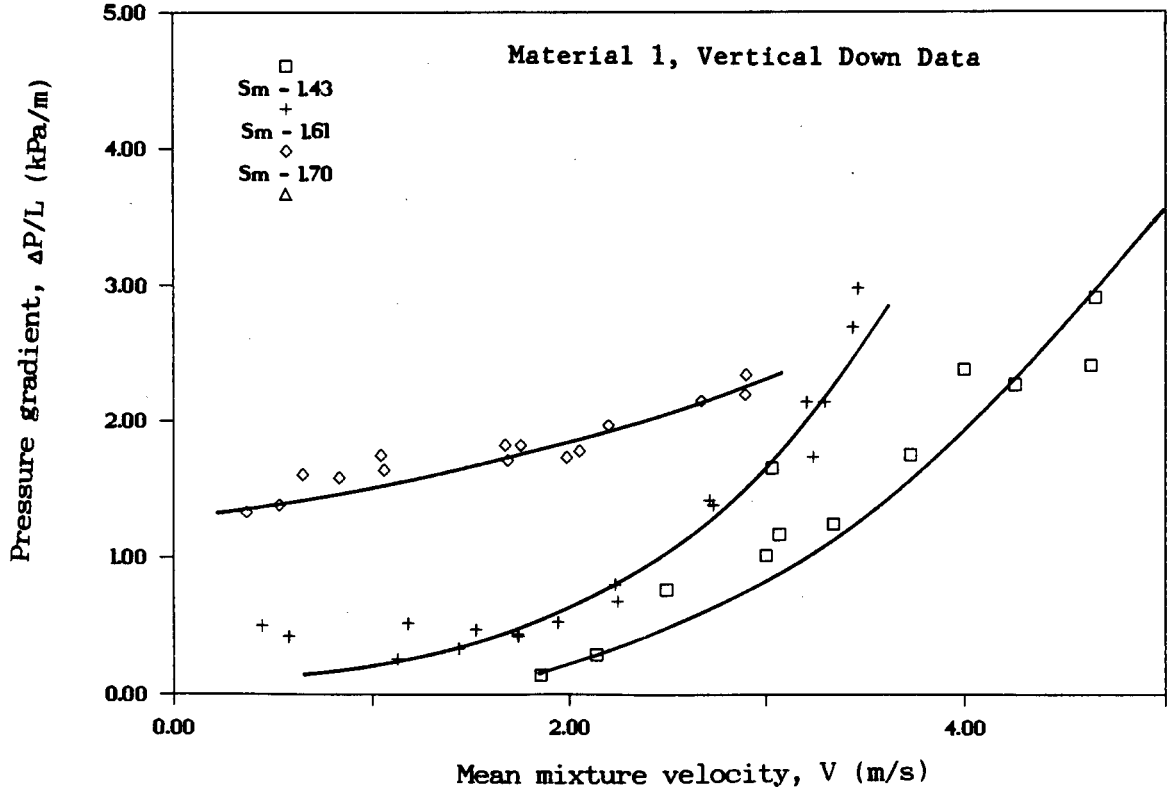

Figure 5.16 : Measured vertical friction loss for material 1, I.D. = 75,88 mm

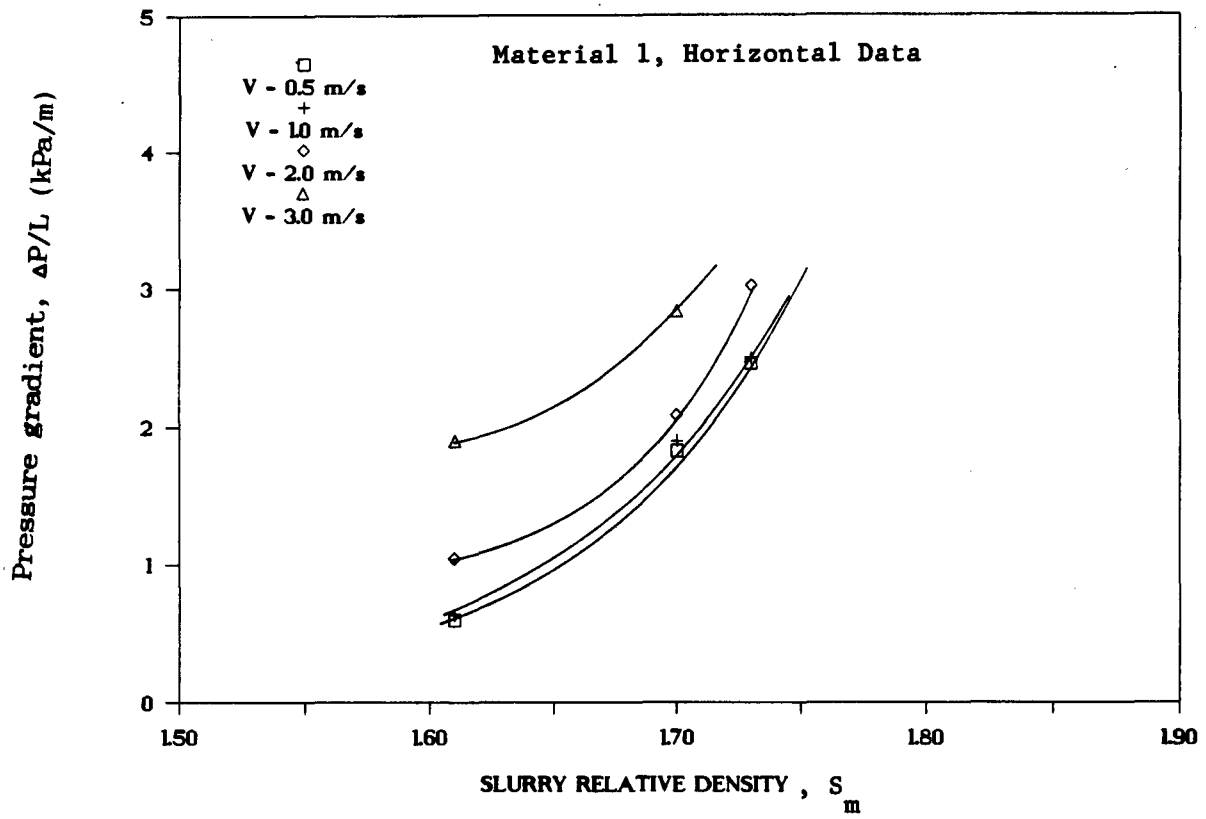

Figure 5.17 : Pressure gradient versus slurry relative density for contours of equal velocity - material 1, I.D. = 75,88 mm

The results from the vertical test facility indicated that for full plant stabilized slurries, the frictional pressure losses are of the same order of magnitude in both vertical down and horizontally inclined pipelines. This is an indication of the stabilized nature of the slurry and has a significant effect on the proposed modelling of the flow behaviour. These results indicate that for this slurry type, pressure gradients in inclined pipelines can be calculated on the assumption that the frictional losses are independant of inclination. To determine total pressure losses in inclined pipelines for this slurry type, equations of the form of Equation 5.1 can be used, provided ΔH_f is calculated.

5.4 Data from The Chamber of Mines test facility

Measured data for material 1 in a 101,5 mm I.D. horizontal pipeline is presented in Figure 5.18 for slurry relative densities ranging from 1,50 to 1,74. This data indicates a similar trend when comparing slurry relative density to pressure gradient, shown in Figure 5.19, as found for other pipe diameters. No vertically measured pressure gradients are available from this test facility.

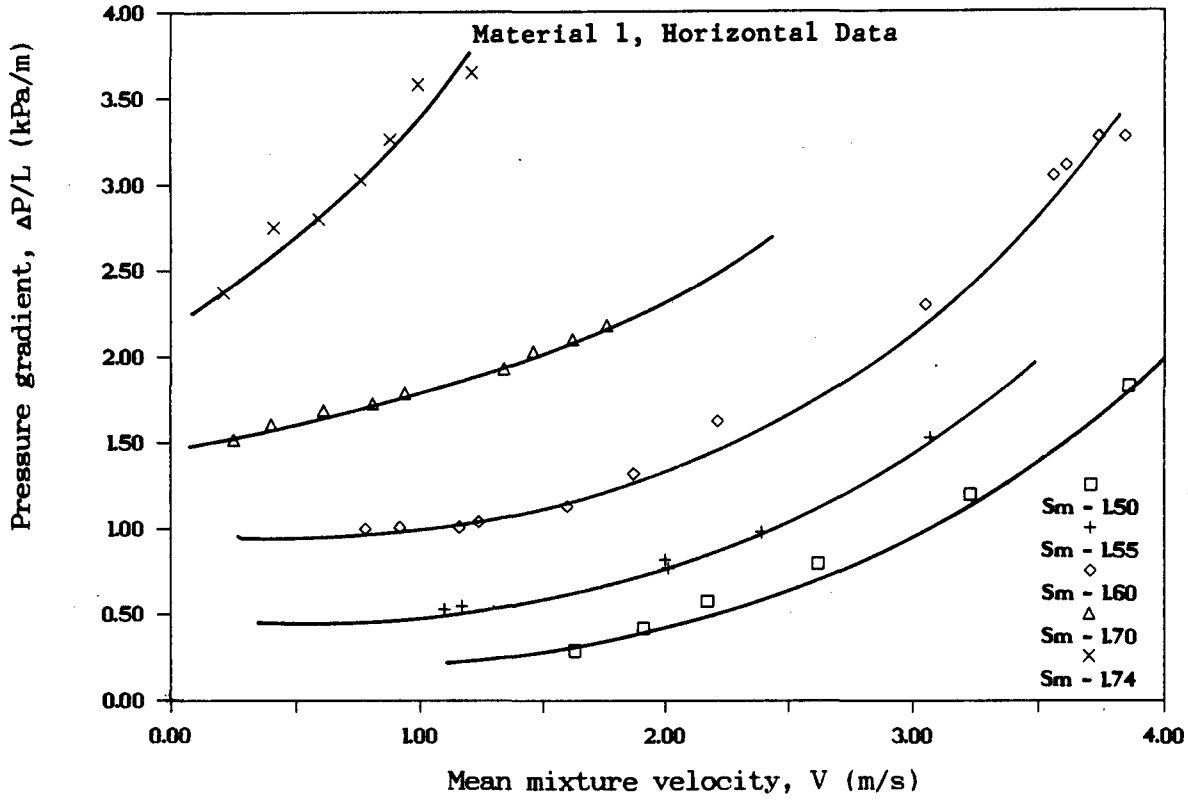

Figure 5.18 : Measured horizontal pressure gradients for material 1, I.D. = 101,5 mm - Chamber of Mines test facility

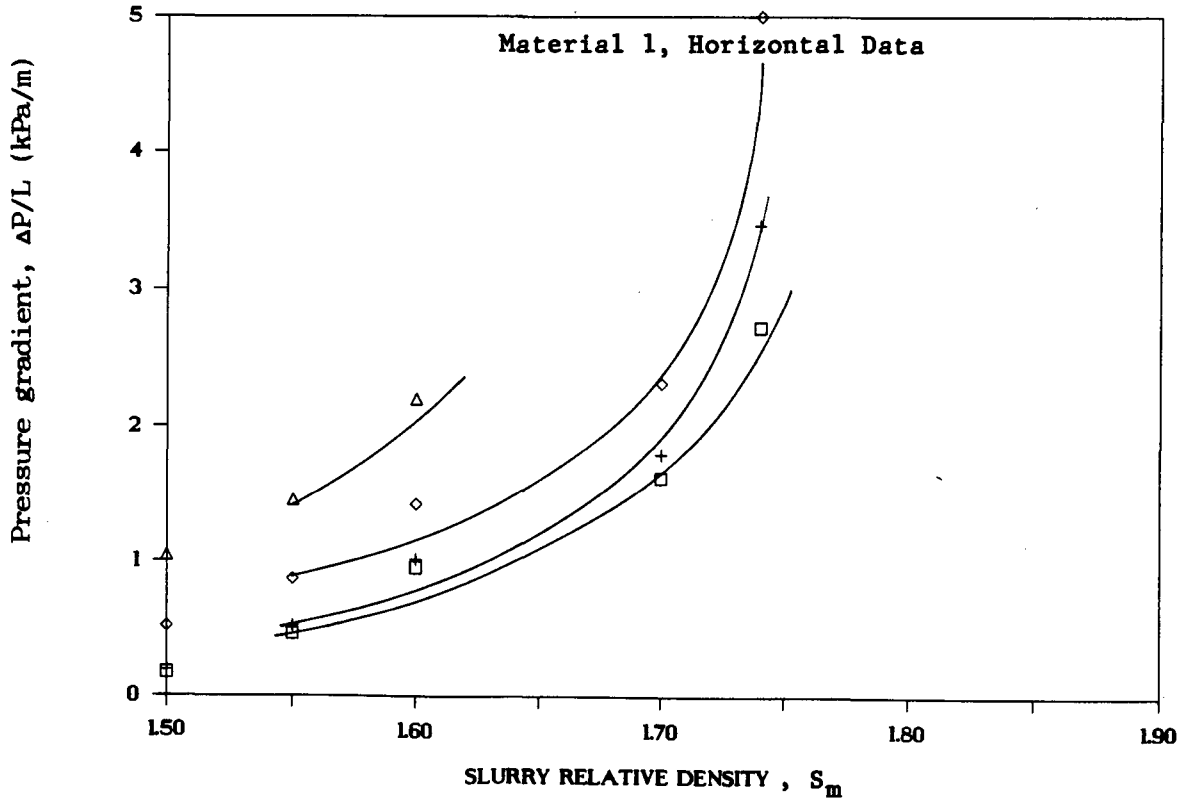

Figure 5.19 : Pressure gradient versus slurry relative density for contours of equal velocity, material 1, Chamber of Mines test facility

5.5 Comparison of measured data

Table 5.2 indicates the measured slurry relative densities for the range of data obtained in each pipeline. Data for material 1 is available for all pipe ranges analysed, whereas materials 2 and 3 were only measured in the 41,22 mm vertical pipeline test facility. Comparison of the effect of pipe diameter on pressure gradient for material 1 is shown in Figures 5.20 to 5.24, at slurry relative densities of 1,65, 1,70, 1,75, 1,81 and 1,85 respectively. Analysis of Figures 5.20 to 5.24 indicates the effect of pipe diameter and concentration on pressure gradient.

13,84	32,63	41,22	75,88	101,5
-	-	-	1,43	-
-	-	-	-	1,50
-	-	1,52	-	-
-	-	-	-	1,55
-	-	-	-	1,60
-	-	-	1,61	-
-	-	1,63	-	-
1,65	1,65	-	-	-
1,70	1,70	1,71	1,70	1,70
-	-	-	1,73	-
1,75	1,75	1,75	-	1,74
1,81	1,81	1,80	-	-
1,85	1,85	1,84	-	-
1,90	1,90	-	-	-

Table 5.2 : Measured data for material 1 at range of slurry relative densities for various pipe diameters

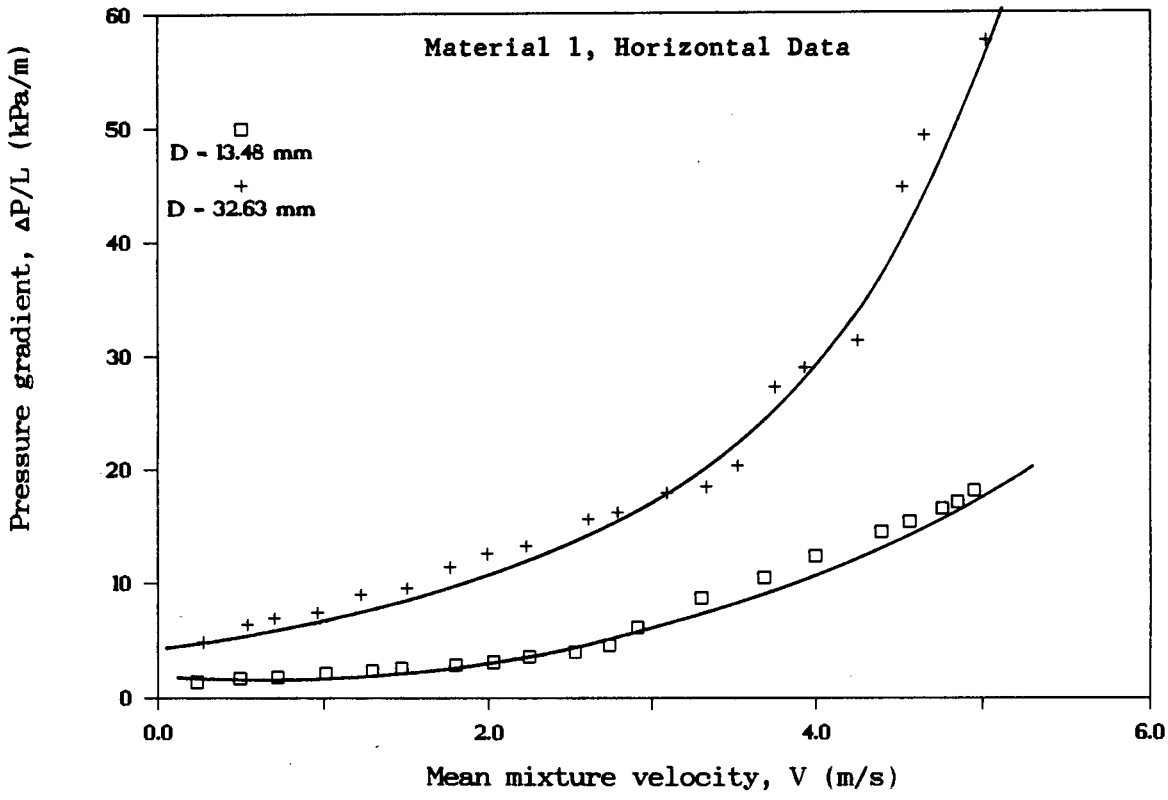

Figure 5.20 : Variation of pressure gradient with increasing pipe internal diameter, S_m = 1,65

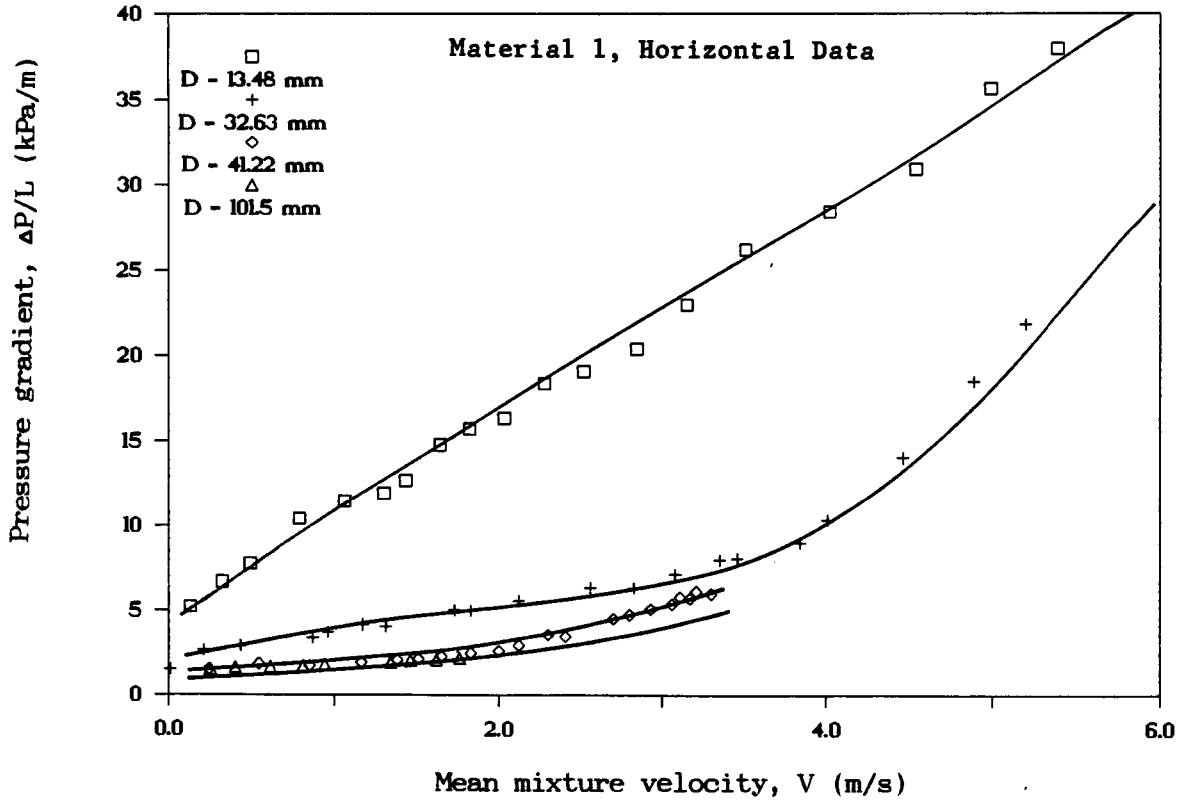

Figure 5.21 : Variation of pressure gradient with increasing pipe internal diameter, S_m = 1,70

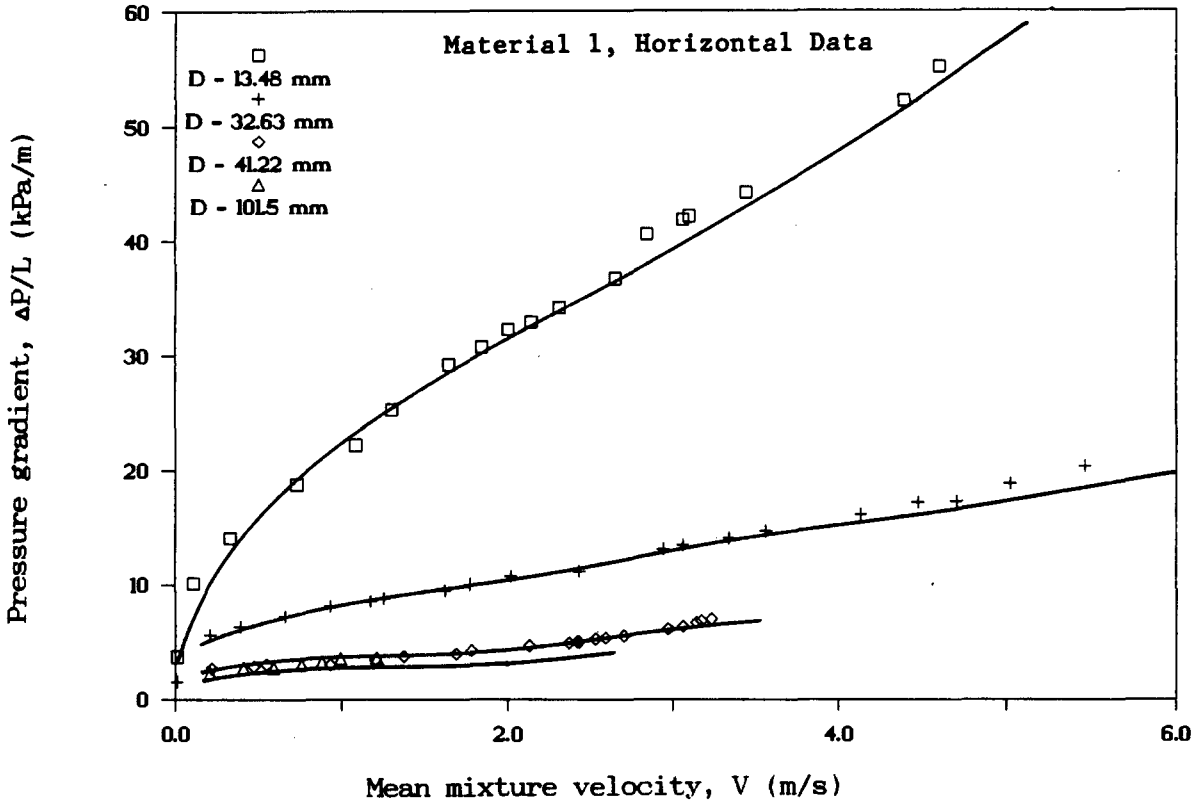

Figure 5.22 : Variation of pressure gradient with increasing pipe internal diameter, S_m = 1,75

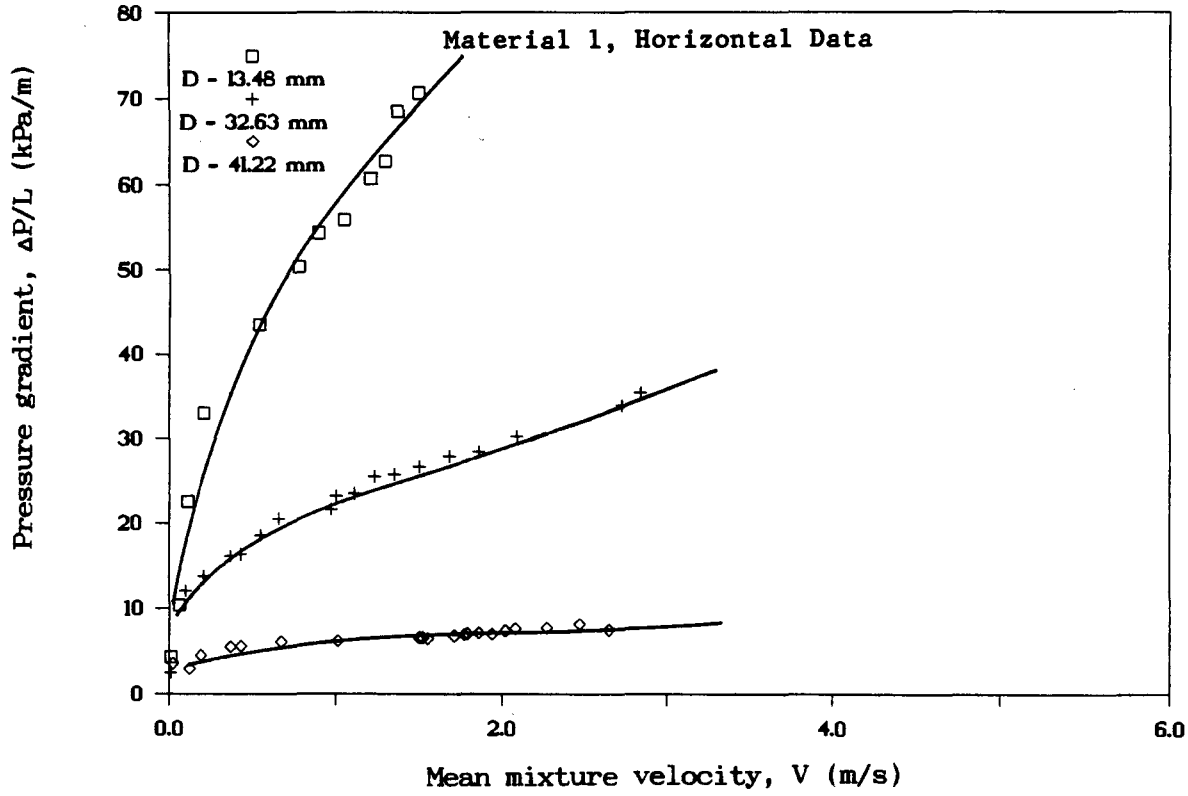

Figure 5.23 : Variation of pressure gradient with increasing pipe internal diameter, S_m = 1,81

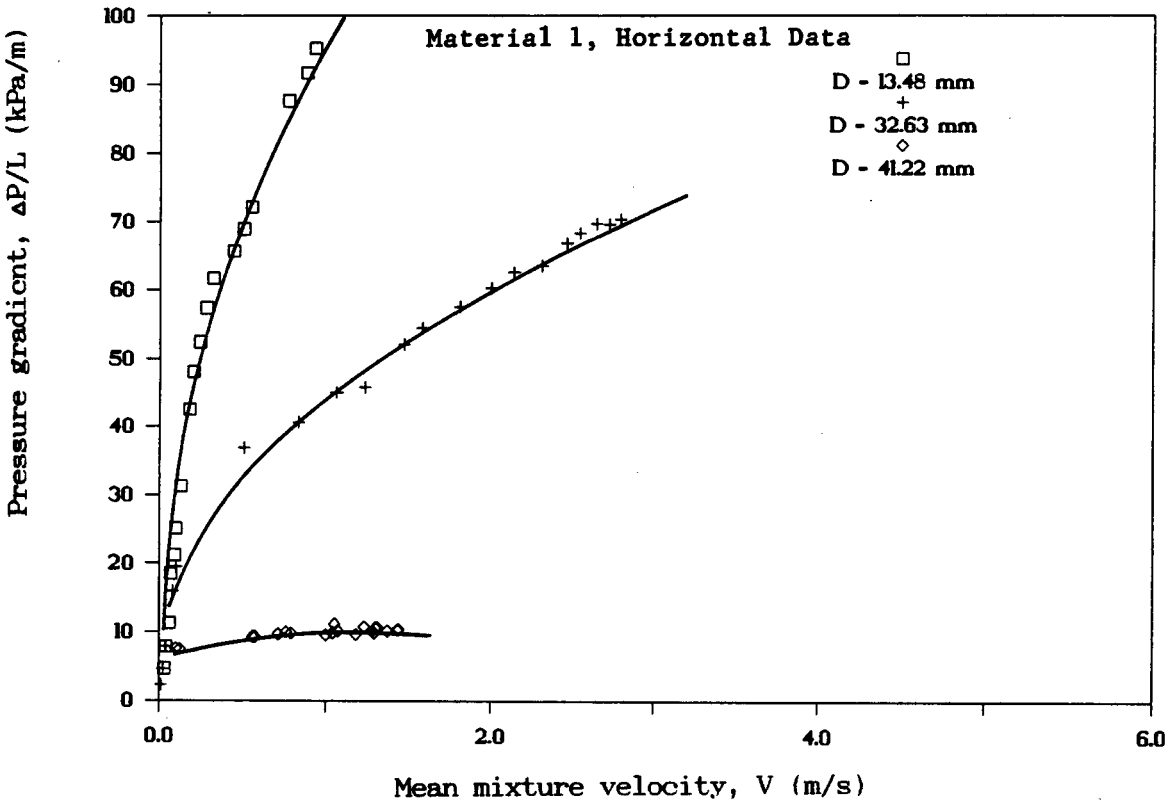

Figure 5.24 : Variation of pressure gradient with increasing pipe internal diameter, S_m = 1,85

5.6 Conclusions

1. Measurements of horizontal pressure gradients were recorded over a wide range of pipe diameters and solids volumetric concentrations for material 1.

2. Analysis of results measured in the vertical test facility indicated a difference between horizontal and vertical friction losses. This difference can be attributed to the variation in pipe roughness between the vertical and horizontal test sections. On the basis of pipe roughness variation, the measured gradients can be considered similar, indicating fully stabilized flow conditions exist for the full plant tailings tested at high concentrations. The friction head loss in both horizontal and vertical pipes is the same when transporting stabilized full plant tailings.

3. Since materials 2 and 3 have only been tested in one pipe diameter, it is not possible to use these results for detailed analysis. These material types can be anlysed on a comparative basis only.

4. The data base for material 1 is sufficient to allow for a detailed analysis of the results to be used as input to the formulation of a mathematical model.

PART THREE

ANALYSIS OF THE FLOW BEHAVIOUR OF FULL PLANT TAILINGS

CHAPTER 6

THEORETICAL ANALYSIS OF THE FLOW BEHAVIOUR OF FULL PLANT TAILINGS

Foreword

This chapter describes the analysis of the anomalous behaviour of the high concentration full plant tailings. The data presented in Chapter 5 is used for this analysis.

The chapter is divided into two parts. Part A examines various existing theories to describe anomalous behaviour at high concentrations. Part B presents the analysis used to solve the anomalous behaviour and analytical model used to describe the flow behaviour of high concentration full plant tailings.

PART A :

Several existing theories to explain anomalous behaviour are presented and evaluated for the data. These include :

(1) The traditional Rabinowitsch-Mooney transformation to transform the pseudo-shear diagram to a rheogram

(2) The investigation of the presence of a slip velocity at the pipe wall

(3) The effect of pipe diameter versus particle size

(4) The presence of a boundary layer at the pipe wall.

None of these methods successfully explained the anomalous behaviour of full plant tailings.

PART B :

A new analysis is presented which is based on the premise that at high solids concentration the nature of the slurry changes. At low solids concentration the total wall shear stress is due to the viscous wall shear stress only. At high solids concentration the total wall shear stress is due to both the viscous wall shear stress and the wall shear stress due to particle-particle interaction. This contribution to the total wall shear stress is termed the solid shear stress. The viscous portion is characterized using the yield pseudoplastic constitutive equation.

The solid shear stress is evaluated using the following methods :

(1) The presence of a coarse plug and sheared annulus

(2) The presence of a coarse plug, sheared annulus and a slip velocity component

(3) The effect of particle-particle interaction.

The solid shear stress component can best be analysed using particle-particle interaction effects which occur when the solids concentration is greater than the freely settled solids concentration ($C_{vt} > C_{bfree}$).

PART A

6.1 Rheological behaviour

The rheological behaviour of dilute solid-liquid suspensions is well documented and the flow behaviour of these slurry types can readily be approximated. For a given set of conditions, the rheological characterization of a particular slurry is governed by the yield pseudoplastic equation which involves the parameters of the slurry yield stress, the fluid consistency index and the flow behaviour index (τ_y , K and n) and the basic scaling laws apply. A set of typical rheogram curves, illustrating the effect of pipeline internal diameter is shown in Figure 6.1, and represented by the solid set of curves. For a given solids volumetric concentration, the shear stress versus shear rate is consistent over the range of different pipe diameters and the laminar flow curves are co-incident. For these conditions, flow behaviour can be modelled by the appropriate choice of the time-independant rheological model, discussed in Chapter 2.

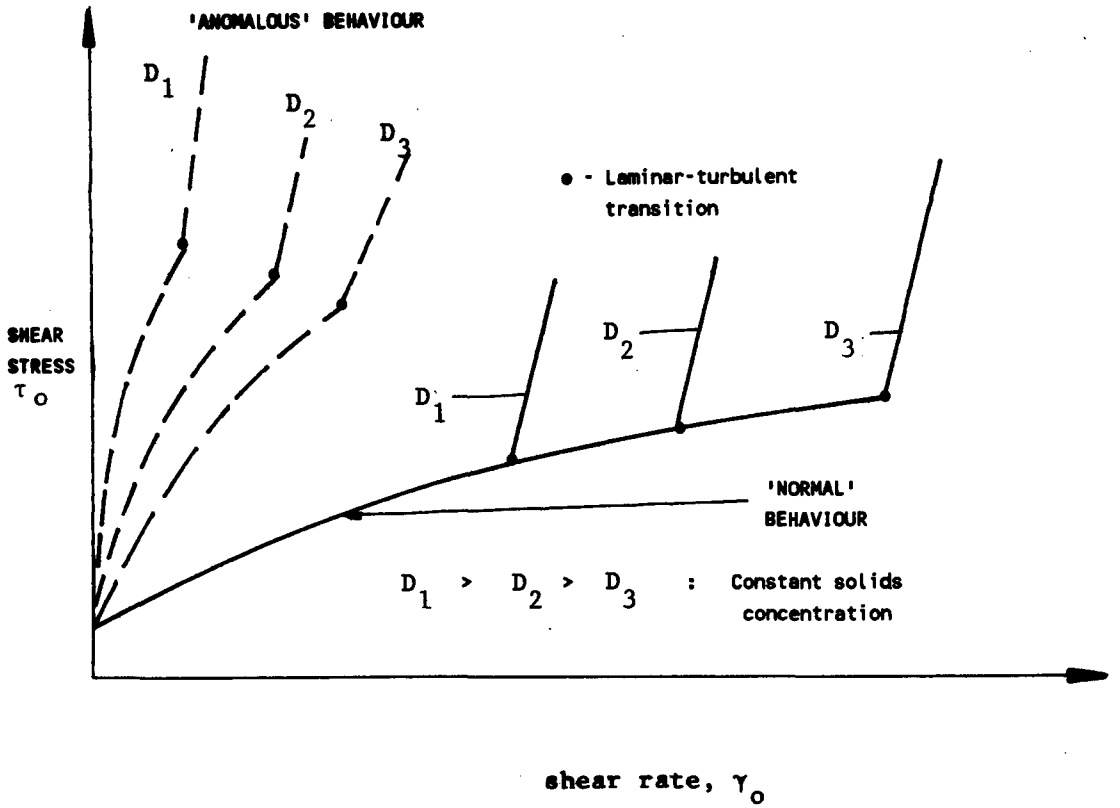

Figure 6.1 : Typical non-Newtonian fluid rheogram for several different pipe diameters, showing both normal and anomalous behaviour

6.2 Anomalous behaviour

Certain slurry types do not behave in this manner and, at high solids concentrations they exhibit the behaviour represented by the dashed lines in Figure 6.1. This effect is often represented by a strong pipe diameter dependency and increases with increasing solids concentration. This behaviour is termed "anomalous behaviour" i.e. a deviation from a general rule. Anomalous behaviour is generally any inconsistent result and need not necessarily be due to diameter effects. Hanks (1982) refers to this effect and states "there are no anomalous results: you just don't understand the problem well enough". These results are often due to the over-simplification of the initial formulation of the rheological models, and as fluids become more complex in nature, approximations that were valid for simpler fluids are no longer applicable for complex flow fields. A typical example of such an approximation is the traditional 'no-slip' boundary condition at the pipe wall, which at higher solids concentrations may not be valid.

Anomalous behaviour has been reported for several non-Newtonian suspensions at high concentrations (Frith *et al* (1987), Baker *et al* (1979), Cheng (1975), Thomas (1963)) and is attributed to several factors, which will be described below. Frith *et al* (1987) states 'near the maximum packing density, even the basic laws start to fail' and draws an analogy between the anomalous flow behaviour and dense phase powder flow as being similar.

As shown in Chapter 5, the full plant tailings exhibit anomalous behaviour at high concentrations. Neill (1988) conducted a thorough series of tests to attempt to rheologically characterise full plant tailings. An extensive range of tests at varying concentrations and tube diameters was done for each of a series of sieved particle size fractions. Results of these tests indicated strong diameter dependency at high solids concentrations. It is important to note that for each of the particle size fractions analysed, the anomalous behaviour occurred at different solids concentrations. Several analytical models were evaluated to account for this behaviour, but no satisfactory theory was found.

6.3 Definition of high concentration stabilized full plant tailings

The distinction between slurry types is dependant upon a large number of parameters. At "low" concentrations several flow regimes exist, and at "high" concentrations we refer to flow being either dense phase or stabilized in nature. No attempt has yet been made to distinguish between low and high concentrations and varying definitions exist. Sive (1988) correlated a series of analytical models for mixed regime slurries up to 54,6% solids volumetric concentration. Lazarus and Paterson (1989) compared these models when analysing full plant tailings and concluded that there is a critical slurry relative density, S_{mc} above which there is a marked decrease in the accuracy of the correlations. Below this relative density, the full plant tailings behaved as a mixed regime slurry, and the correlations predicted reasonable results. The need for an accurate explanation of this critical relative density was highlighted.

The relevance and importance of the particle packing density in determining viscosity has been discussed in Chapter 2. Neill (1988) found a distinct discontinuity in his results and a marked increase in pressure gradient with a slight increase in relative density above a certain critical value. This was also found by Cooke (1989) and Paterson (1989) when testing backfill materials. Analysis of the various size fractions of full plant tailings indicated that the onset of anomalous behaviour varied according to the size fraction. Measurement of the freely settled solids concentration (C_{bfree}) for these size fractions indicated a close relationship between the measured concentrations and the solids concentration at which the anomalous behaviour was first noticeable.

6.4 Critical concentration value for determining the onset of anomalous behaviour

It is proposed that for mineral backfill tailings, including both classified and full plant tailings, that this critical solids concentration can be determined from the measurement of the submerged freely settled bed packing concentration. Figure 6.2 illustrates the results of Neill (1988) compared to the measured freely settled solids

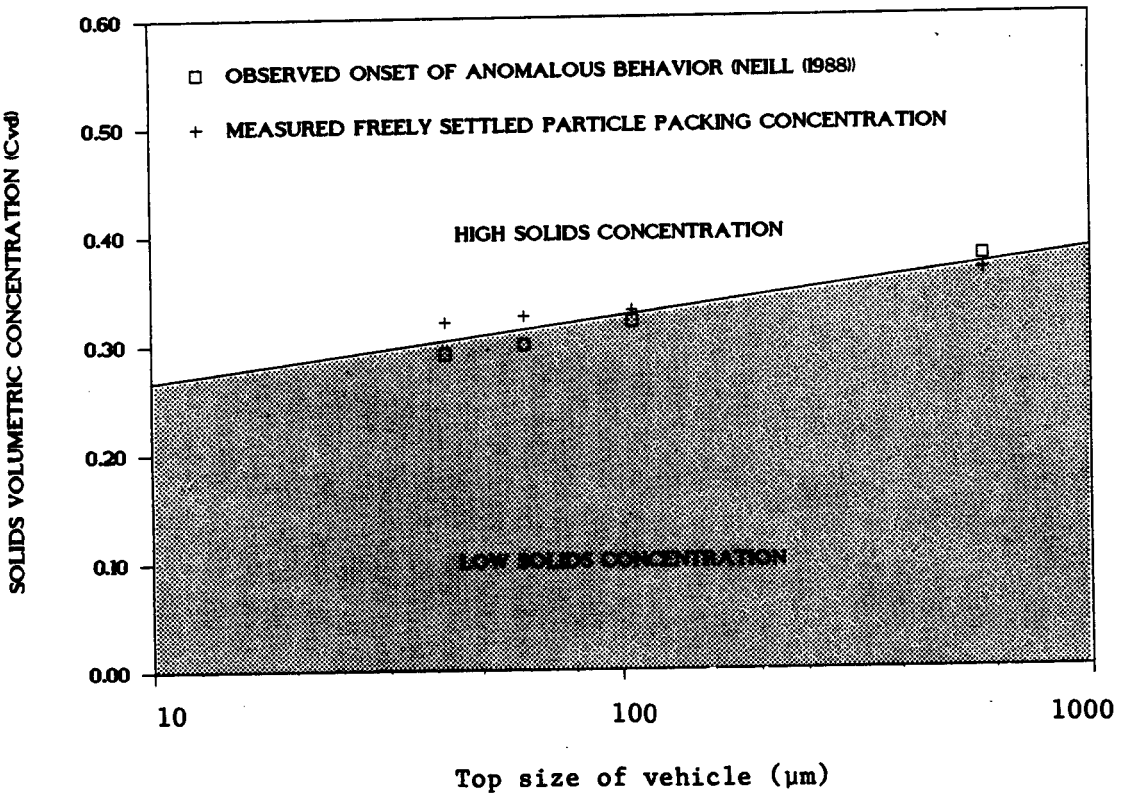

Figure 6.2 : Comparison of measured freely settled volumetric solids concentration compared to the solids concentration at which anomalous behaviour first occurred

concentration (C_{vd}) for the size fractions analysed. The results are in close agreement and clearly indicate the zones of low and high solids concentrations.

For a particular maximum packing density, the increase in pressure gradient with concentration becomes asymptotic to C_{bmax} as C_v approaches C_{bmax}. Note the correlation between this behaviour and that of the sudden increase of pressure gradient versus relative density for backfill materials as illustrated in Chapter 5, Figures 5.12 and 5.17.

Normal behaviour occurs at low solids volumetric concentrations (C_{vLOW}) and the pseudo-shear diagrams, for varying pipe diameters, are co-incident in the laminar flow region. When the solids volumetric concentration exceeds the freely settled solid packing volumetric concentration (C_{bfree}), anomalous behaviour indicated by different pseudo shear diagrams for different pipe diameters becomes a feature of the pseudo-shear diagrams. High concentration flow exists in the region of solids volumetric concentration above C_{bfree} and up to and including the maximum possible particle packing solids concentration

The dispersive stress coefficient, K_r , is a function of both solids volumetric concentration and pipe diameter. It is determined from the tube viscometer data for two pipeline sizes and increases linearly with pipe diameter. The relationship of K_r with diameter and slurry relative density for full plant tailings is given in Equation 6.41.

The solid wall shear stress is calculated from Equation 6.44 :

$$\tau_s = \frac{4 \mu_s K_r \tau_v}{(D - 4 \mu_s K_r)} \qquad (6.44)$$

6.9.3 The total wall shear stress, τ_o

The total wall shear stress is the sum of both the viscous shear stress and the solid shear stress, i.e.

$$\tau_o = \tau_{ov} + \tau_{os} \qquad (6.45)$$

$$\frac{D \Delta P}{4L} = \tau_o \qquad (6.46)$$

The pipeline pressure gradient, ΔP , is calculated from the relationship between wall shear stress, τ_o , and pressure gradient, $\Delta P/L$, expressed by Equation 6.46.

6.10 Conclusions

1. A definition of high concentration flow for full plant tailings based on the freely settled volumetric solids concentration, C_{bfree} , is presented.

2. High concentration full plant tailings pipe flow is characterized by "anomalous" behaviour when a rheogram shows pipe diameter dependence.

3. Several techniques to account for the "anomalous" behaviour of full plant tailings were presented. None of these successfully corrected the measured data except for the method of dividing the total wall shear stress into a viscous and a solid shear stress component.

4. A new data analysis method is presented to account for the "anomalous" behaviour. The total wall shear stress, τ_o , is considered to be the sum of the viscous wall shear stress, τ_{ov} , and the solid wall shear stress τ_{os} .

5. The viscous and solid contributions to the total wall shear stress can be separated using the proposed data transformation technique which involves the "subtraction" of the solid wall shear stress from the "total" wall shear stress leaving the "viscous" wall shear stress.

6. The viscous shear stress component, τ_{ov} , can be determined using the yield pseudoplastic rheological equation.

7. The solid wall shear stress component is due to a dispersive stress which causes particle-particle contact with the pipe wall.

9. The proposed technique can be used for a range of pipe diameters from 13 mm NB to 100 mm NB.

10. The laminar to turbulent transition can be determined using the method of Hanks (1974).

11. Turbulent viscous flow can be analysed using the method of Torrance (1963).

$C_{b_{max}}$. This relationship between low and high solids concentration is expressed by Equation 6.1 and serves to define high concentration for this research.

$$C_{v_{LOW}} \leq C_{b_{free}} < C_{v_{HIGH}} \leq C_{b_{max}} \qquad (6.1)$$

6.5 Transformation of measured data from a pseudo-shear diagram to a rheogram

Data measured using the balanced beam tube viscometer, the vertical test facility and the Chamber of Mines test facility has to be compared and analysed on a common basis. Full plant tailings clearly exhibit time-independant non-Newtonian flow characteristics. For such a material, the flow behaviour can generally be expressed using the Herschel-Bulkey or yield pseudoplastic rheological model. This involves the evaluation of the rheological parameters for a particular solids concentration from the rheogram of measured data.

Using a pipeline as a viscometer, one obtains a set of data which can be represented on a pseudo-shear diagram, where the wall shear stress and pseudo-shear rate are given by Equations 6.2 and 6.3 respectively.

$$\tau_o = \frac{D\ \Delta P}{4L} \qquad (6.2)$$

$$\dot{\gamma}_p = \frac{8V}{D} \qquad (6.3)$$

For Newtonian fluids the variables τ_o and $\dot{\gamma}_p$ are normally related to one another by the fluid viscosity, μ . The pseudo-shear rate, $\dot{\gamma}_p$ is equivalent to the true wall shear rate, $\dot{\gamma}_o$ and the pseudo-shear diagram is thus a true rheogram.

For non-Newtonian fluids, however, this is not the case, since the values of n', the apparent flow behaviour index, and K', the apparent fluid consistency index, are not constant as shear rate increases. In these instances, the data has to be transformed and the pseudo-shear rate, $\dot{\gamma}_p$, has to be transformed to the true shear rate $\dot{\gamma}_o$. The general relationship, known commonly as the Rabinowitsch-Mooney relationship is traditionally used to reduce experimental data.

6.5.1 The Rabinowitsch-Mooney transformation

It is recommended in the literature to use the Rabinowitsch-Mooney relation to reduce capillary tube viscometer measurements to a set of measurements comprising the measured wall shear stress and the corrected true shear rate. This procedure does not require any prior knowledge of the fluid rheology. A detailed derivation (Skelland (1967)) of the method is not presented here, but it will be illustrated by example.

The rate of shear at the viscometer wall is determined from Equation 6.4, the general Raboniwitsch-Mooney relationship.

$$\dot{\gamma}_o = \left(\frac{3n' + 1}{4n'}\right) \dot{\gamma}_p \qquad (6.4)$$

where $\dot{\gamma}_o = \left(\frac{du}{dr}\right)_o$

$$\dot{\gamma}_p = \frac{8V}{D}$$

$$n' = \frac{d\left(\ell n \frac{D\,\Delta P}{4L}\right)}{d\left(\ell n \frac{8V}{D}\right)} = \frac{d(\ln \tau_o)}{d\left(\ln \frac{8V}{D}\right)}$$

= slope of the double logarithmic plot of $\frac{D\,\Delta P}{4L}$ versus $\frac{8V}{D}$.

The complete Rabinowitsch-Mooney transformation procedure is as follows :

1. Obtain the raw measured data from the viscometer and calculate τ_o and $\frac{8V}{D}$, to obtain the pseudo-shear diagram, illustrated in Figure 6.3(a).

2. Convert the normal pseudo-shear diagram to a logarithmic plot of τ_o versus $\frac{8V}{D}$ and determine n' as a function of $\frac{8V}{D}$, illustrated in Figures 6.3(b) and 6.3(c), using the linear approximation for the 32,63 mm pipe in Figure 6.3(b) to calculate Figure 6.3(c).

3. Using the calculated values of n' and Equation 6.4, $\dot{\gamma}_o$ can be calculated.

4. Plot the measured wall shear stress τ_o amd the corrected true shear rate $\dot{\gamma}_o$ as in Figure 6.3(d) and choose the appropriate rheological constitutive equations to model the fluid behaviour.

since the flow curves are not co-incident.

For these high concentration full plant tailings it can be seen from Figure 6.3(d) that the correction for wall shear rate does not account for the anomalous behaviour. This was confirmed for the remaining measured data for material 1 described in Chapter 5 and presented in Table 5.1.

The Rabinowitsch Mooney transformation does not explain why anomalous behaviour exists for the high concentration slurries.

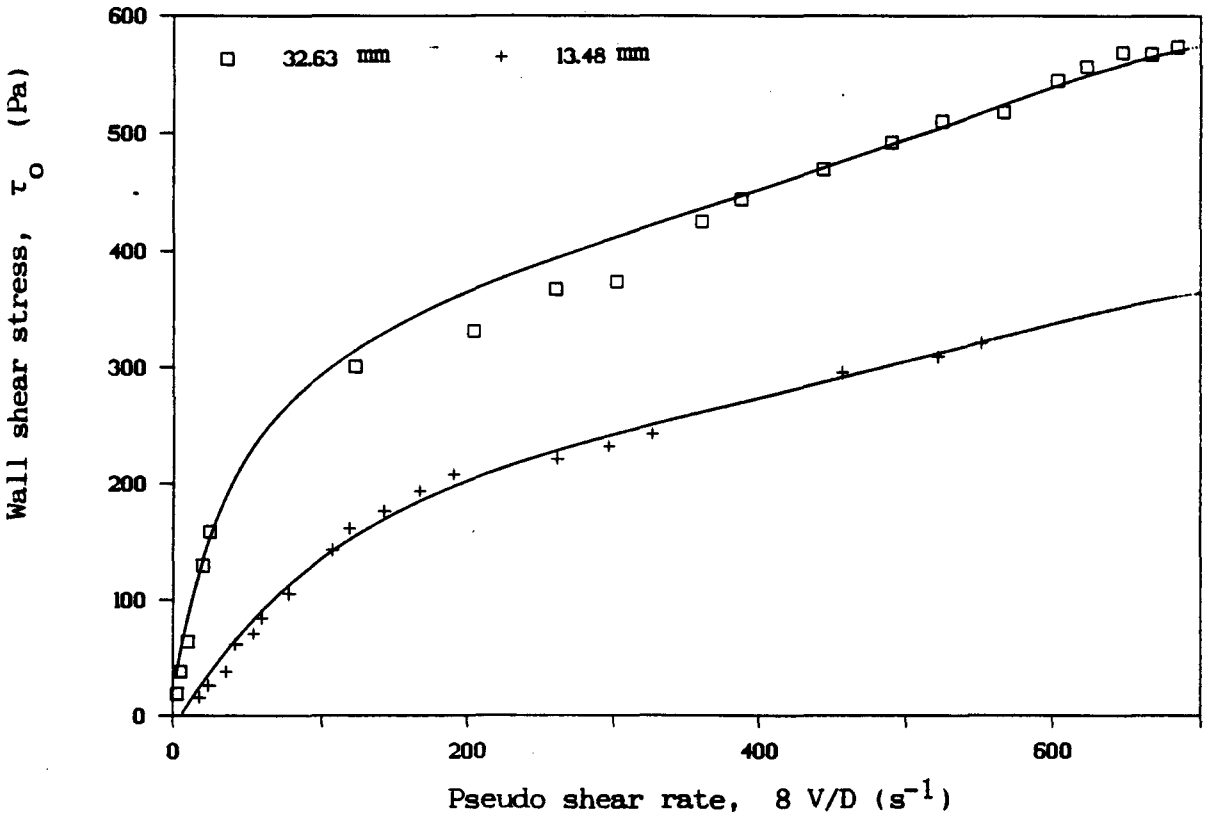

Figure 6.3(a) : Pseudo shear diagram of measured data, S_m = 1,85

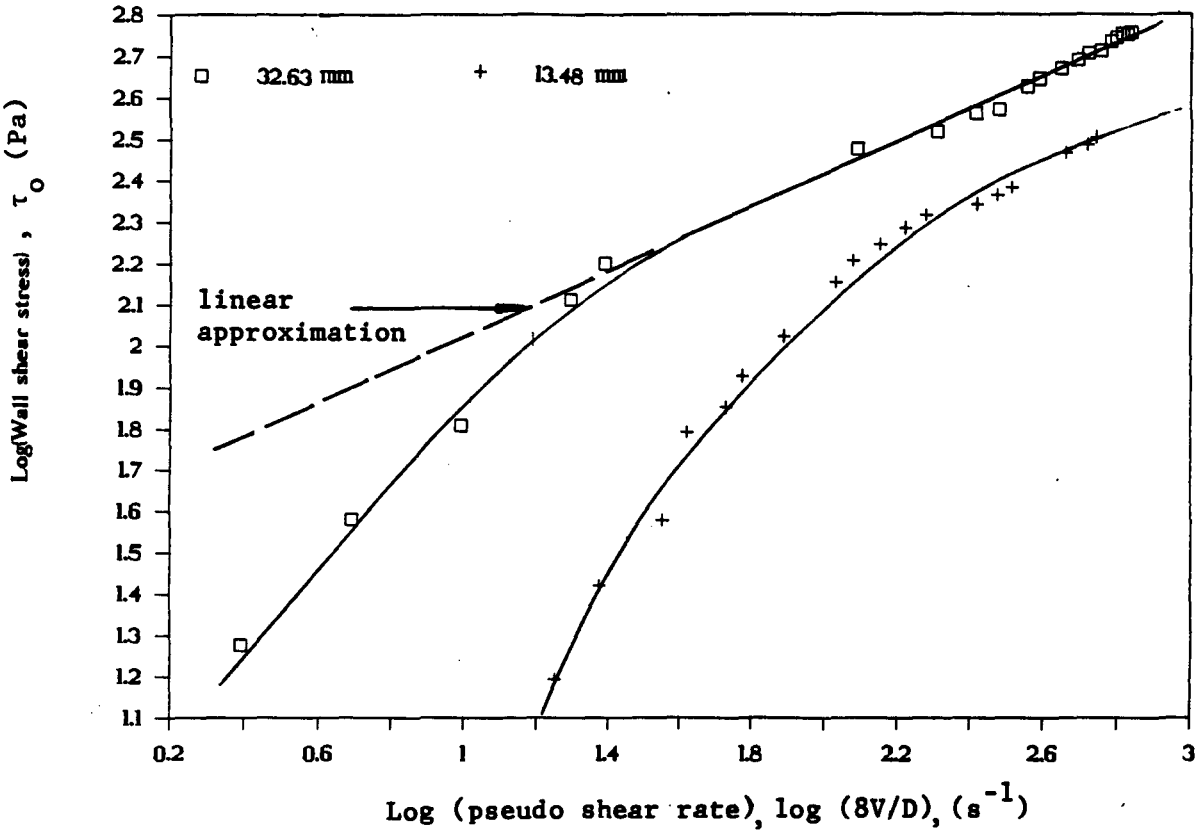

Figure 6.3(b) : Logarithmic plot of τ_o versus pseudo shear rate, $\frac{8V}{D}$

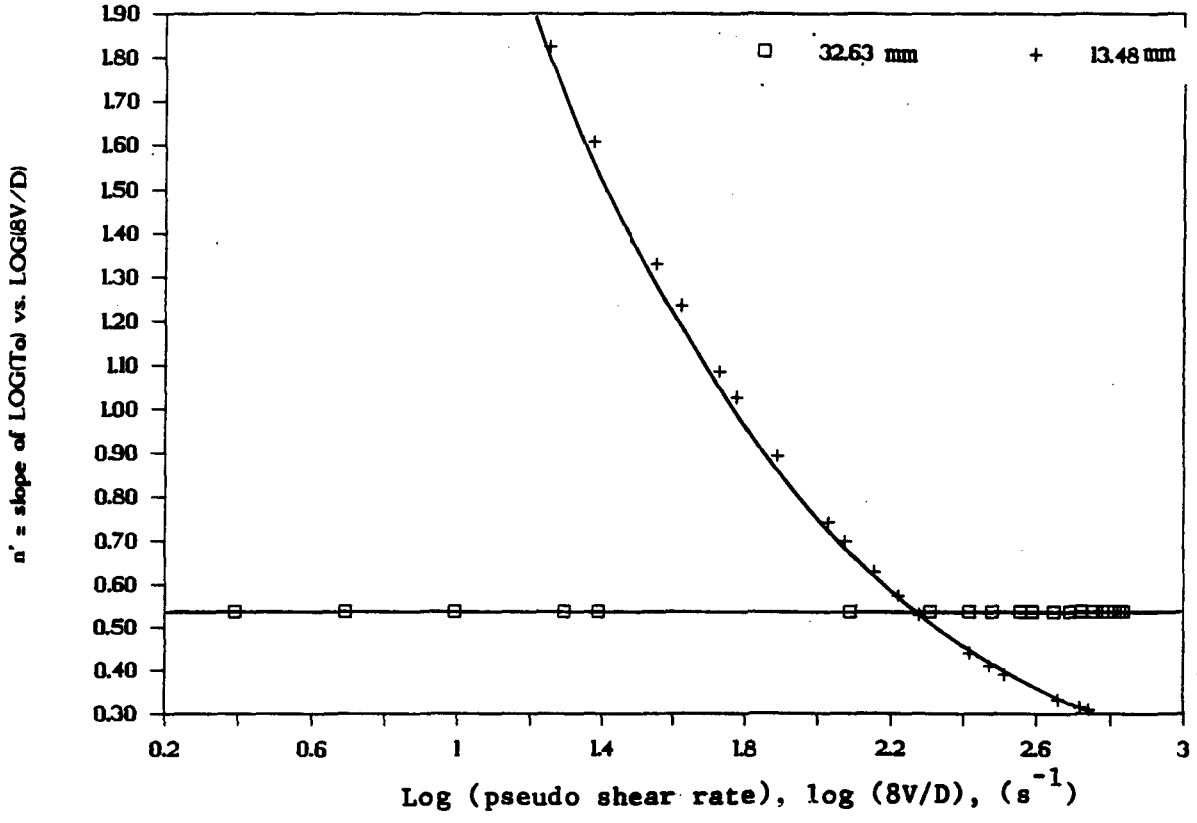

Figure 6.3(c) : Analysis of n' , versus shear rate

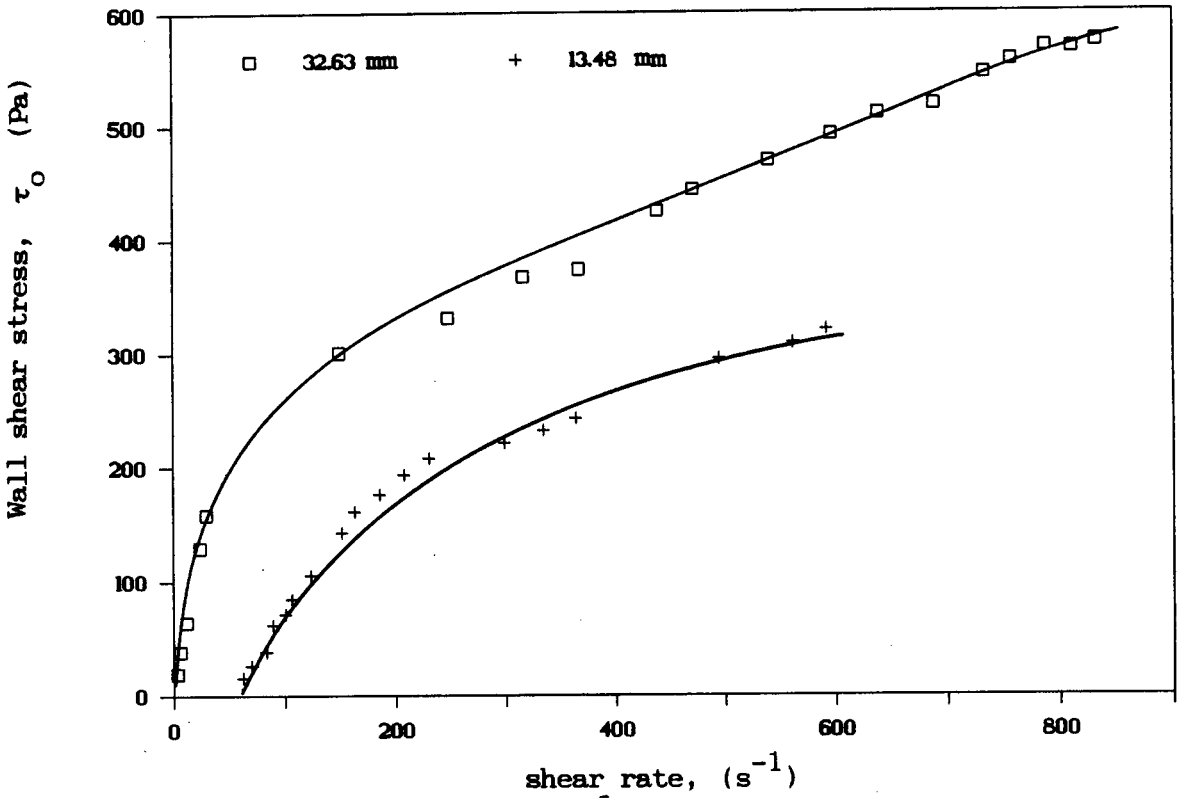

Figure 6.3(d) : Corrected pseudo shear diagram using the Rabinowitsch Mooney transformation

6.5.2 Evaluation of the presence of a slip velocity existing at the pipe wall

The anomalous behaviour can possibly be due to the presence of a slip velocity at the pipe wall. Mooney (1931) first formulated the slip velocity analysis presented below. Windhab and Gleissle (1984) used a variation of the technique to describe rheological data from several types of viscometers and identified a slip shear stress, τ_s , the wall shear stress above which slip occurs. The analysis of Mooney (1931) assumes a slip velocity from the point of incipient motion, and does not include this slip shear stress, τ_s . The difference between the yield stress τ_y and the slip shear stress τ_s is explained by the difference between the point of incipient motion of the particles within the fluid matrix, τ_y (energy required to separate particle flow structure), and the limit of adhesion of the suspension of the fluid to the pipe wall, τ_s .

The generalized flow equation is given by Equation 6.5 and is valid for any rheological constitutive model.

$$Q = \frac{\pi R^3}{\tau_o^3} \int_o^{\tau_o} \tau^2 f(\tau)\, d\tau \tag{6.5}$$

Assuming a slip velocity is presented, denoted u_s and is a function of τ_o, the slip velocity coefficient β, is given by Equation 6.6 in the form of Mooney (1931)

$$u_s = \beta \tau_o \tag{6.6}$$

The modified flow and boundary condition is represented in Figure 6.4 and is given by Equation 6.7

$$Q_{TOTAL} = Q_{SLIP\ FLOW} + Q_{SHEAR\ FLOW} \tag{6.7}$$

$$= \pi u_s R^2 + \frac{\pi R^3}{\tau_o^3} \int_o^{\tau_o} \tau^2 f(\tau)\, d\tau$$

which can be rewritten as

$$\frac{Q}{\pi R^3 \tau_o} = \frac{u_s}{R \tau_o} + \frac{1}{\tau_o^4} \int_o^{\tau_o} \tau^2 f(\tau)\, d\tau \tag{6.8}$$

$$= \frac{\beta}{R} + \frac{1}{\tau_o^4} \int_o^{\tau_o} \tau^2 f(\tau)\, d\tau$$

By determining values of β over a range of measured wall shear stress, the slip velocity can be calculated and the rheogram data corrected using Equation 6.9.

$$Q_{CORRECTED} = Q_{MEASURED} - Q_{SLIP}$$
$$= Q_{MEASURED} - (\beta \tau_o)\, \pi R^2 \qquad (6.9)$$

This correction should reduce the data onto a single rheogram curve. Neill (1988) found that this did not occur for full plant tailings. Analysis of the effective slip could possibly be accounted for using a varying effective slip coefficient β, dependant upon pipe diameter. The analysis for a set of rheogram curves, illustrated in Figure 6.5(a), based on this premise is described below.

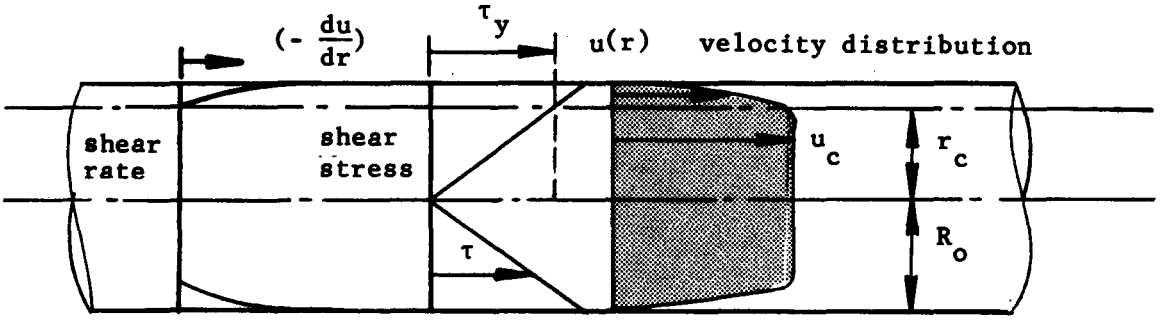

(a) No slip velocity distribution

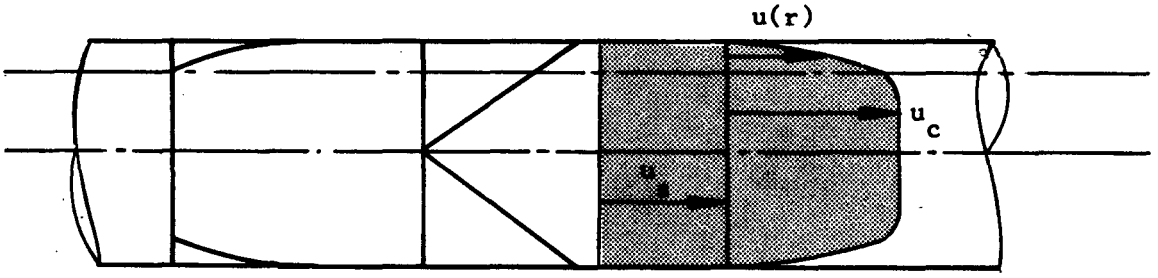

(b) Slip velocity distribution

Figure 6.4 : Modified velocity profile to account for presence of a slip velocity at the pipe wall

Procedure to determine the slip velocity at the pipe wall

1. From the pseudo shear diagram in Figure 6.5(a), a plot of τ_o versus the function $Q/\pi R^3 \tau_o$ is drawn (Figure 6.5(b)).

2. From this graph, a plot of $Q/\pi R^3 \tau_o$ versus $1/R$ is drawn for a range of wall shear stresses (Figure 6.5(c)), representing Equation 6.8 where $Q/\pi R^3 \tau_o = \text{fn}\ (\frac{1}{R})$.

3. Values of Beta, (β), can be obtained from the slope of the curves of constant shear stress in Figure 6.5(c) for each value of τ_o and D .

4. The slip velocity $u_s = \beta \tau_o$ can be calculated for each value of wall shear stress τ_o and diameter, as in Figure 6.5(d).

5. Using the calculated slip velocities from step 4 above, the original pseudo-shear diagram, Figure 6.5(a), can be corrected using Equation 6.9 to account for slip and is given in Figure 6.5(e).

Referring to Figure 6.5(e) it can be seen that the effective slip correction is too high and does not account for the anomalous behaviour. This is because calculated values of Beta in step 3 above result in excessive slip velocities u_s . Using the values of μ_s , the corrected flow in Equation 6.9 becomes negative.

The inclusion of a slip shear stress (Windhab and Gleissle (1984)) could be used to reduce the slip velocity and Equation 6.6 would be rewritten as :

$$\mu_s = \beta (\tau_o - \tau_s) \qquad (6.10)$$

The determination of τ_s would involve the measurement of the velocity of particles at the pipe wall. The yield stress, τ_y , will be dependent only upon the slurry properties, but the slip shear τ_s would be a function of both slurry properties and pipeline properties.

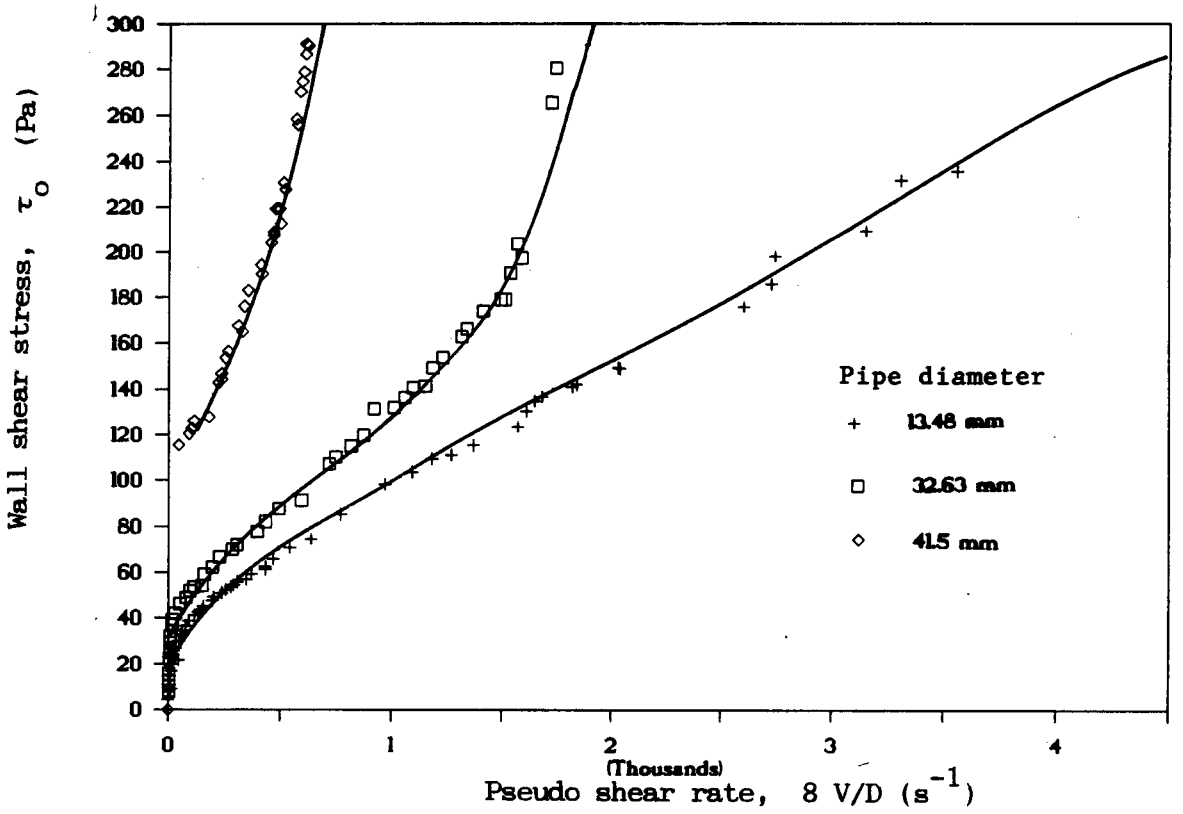

Figure 6.5(a) : Pseudo shear diagram of measured data, S_m = 1,75

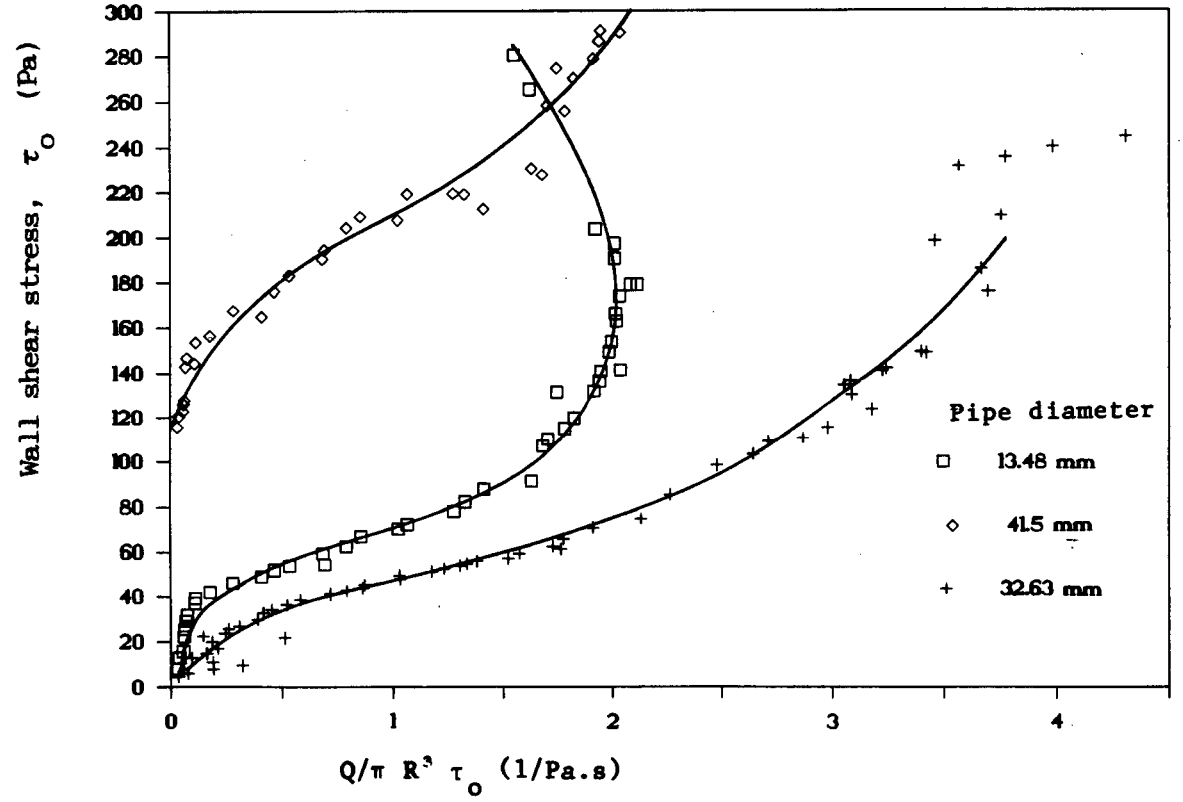

Figure 6.5(b) : Shear stress, τ_o , versus function $Q/\pi R^3 \tau_o$

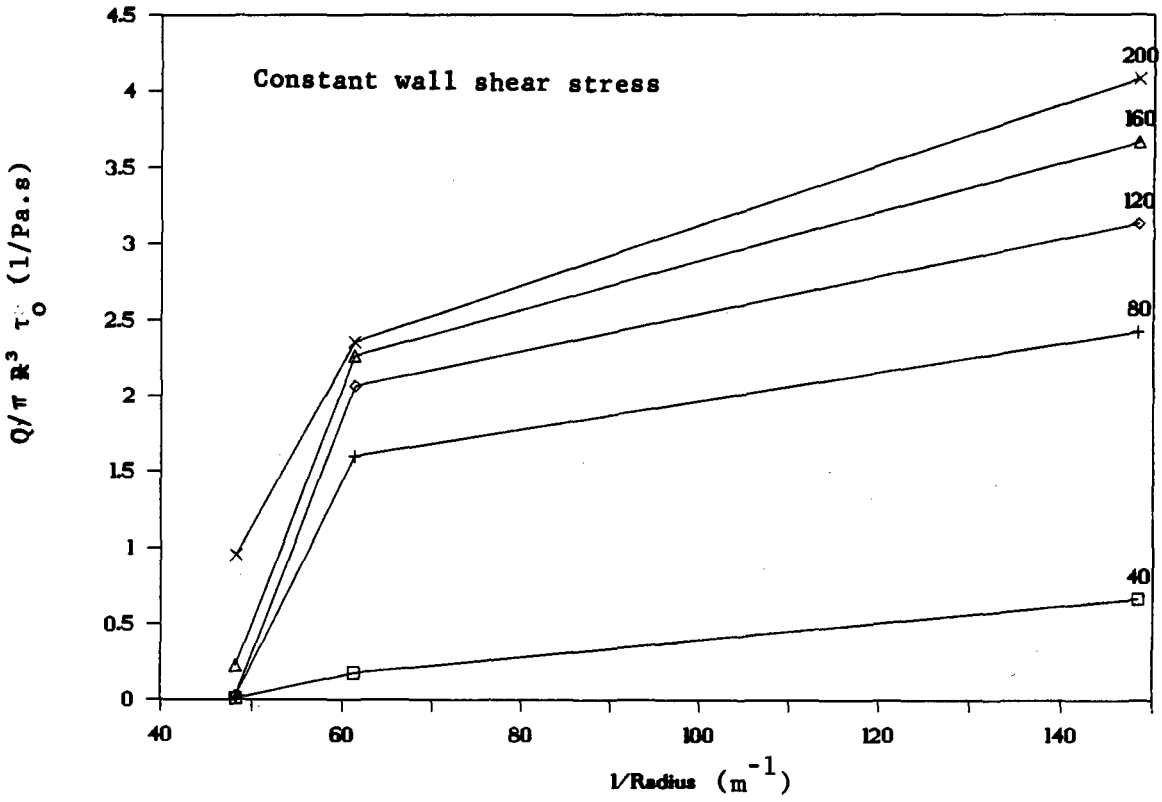

Figure 6.5(c) : Function $Q/\pi R^3 \tau_o$ versus 1/Radius

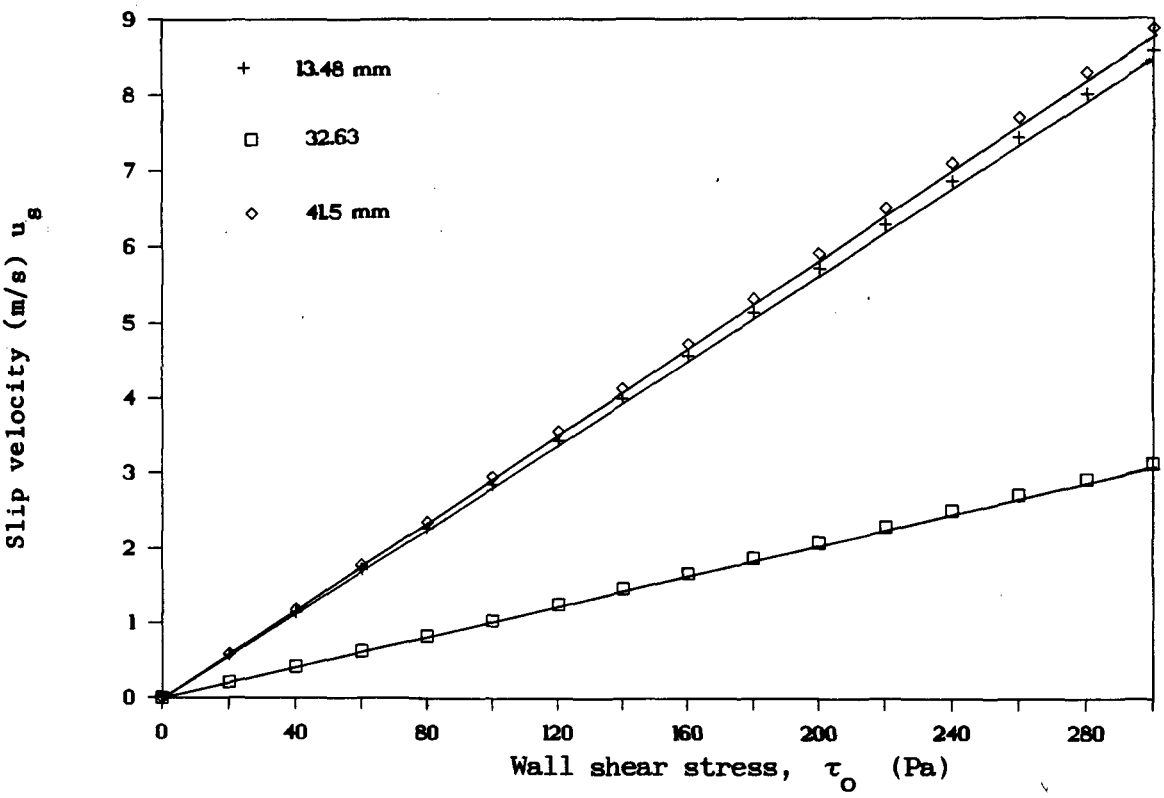

Figure 6.5(d) : Slip velocity, u_s, versus shear stress, τ_o, for each pipe diameter

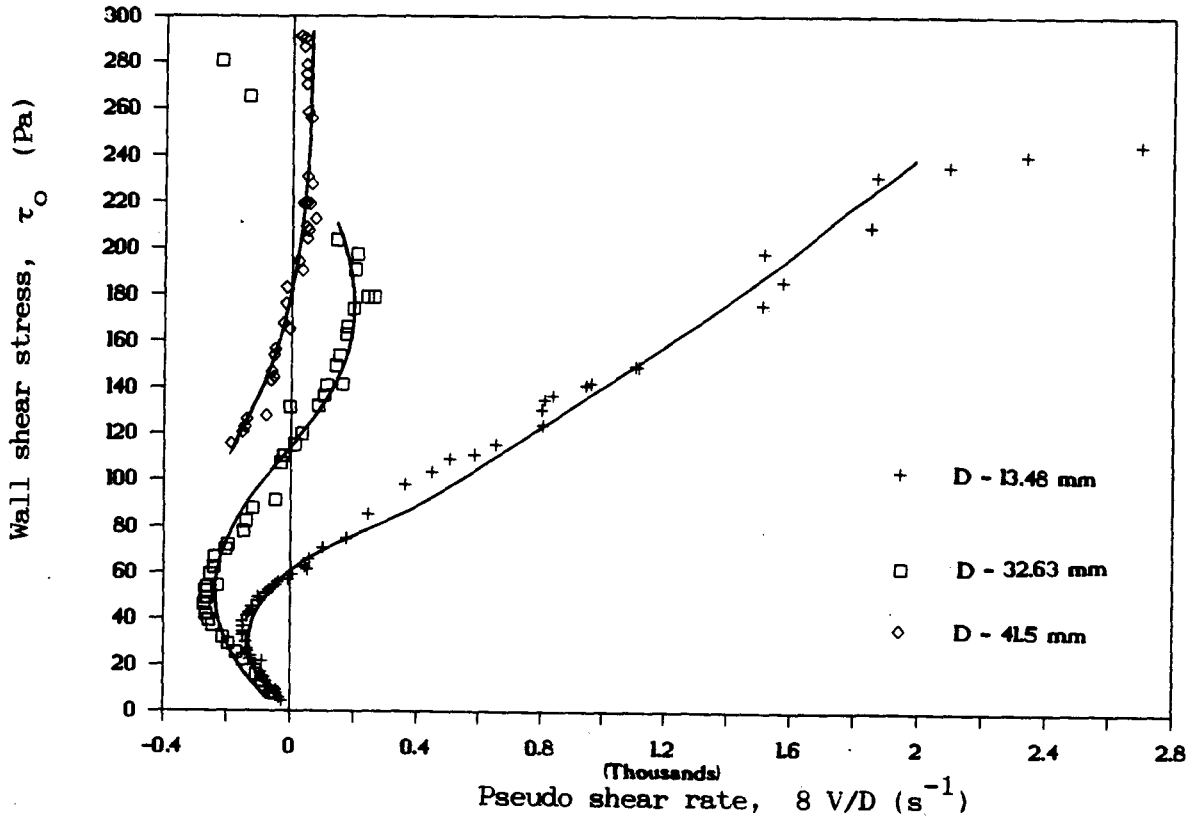

Figure 6.5(e) : Corrected pseudo shear diagram using slip velocities calculated in Figure 6.5(d)

6.5.3 Effect of particle diameter versus pipe diameter to account for anomalous behaviour

Another reason for anomalous behaviour may be the variation in the *in situ* concentration and delivered solids concentration with tube diameter. This phenomenon is normally associated with larger diameter particles when the ratio of particle diameter to tube diameter becomes critical for small diameter tubes. Neill (1988) found that for mineral full plant tailings, no such variation occurred and fully developed stabilised flow existed (i.e. no variation in *in situ* and delivered concentration). For small ratios of d_{50}/D there is a wall effect (Maude and Whitmore (1955)), but for the full plant tailings with $d_{50} \approx 40\ \mu m$, the diameter size ratio is large enough to avoid a decrease in *in situ* concentration due to the pipe wall boundary.

Measurement of both the *in situ* solids concentration and delivered solids concentration in the vertical test facility on full plant tailings showed no significant difference in both the 40 mm NB and the 76 mm NB test loops, confirming the results of Neill (1988).

6.5.4 The existence of a boundary layer to account for anomalous behaviour

Brown (1988) proposes a model for stabilized flow slurries based on solid particle migration towards the pipe axis. This increases the solids concentration towards the centre of the pipe, leaving a sheared annulus at the pipe wall. This is also reported by Smoldyrev (1979) and Rainer (1934). Analysis of the rheograms for full plant tailings indicate that particle migration might occur and a boundary layer could exist.

Assuming a layer of thickness δ and viscosity μ_F exists at the wall, the flow is then given by Equation 6.11

$$Q = \pi (R - \delta)^2 u_{core} + \pi \frac{u_{core}}{2} (2 R \delta - \delta^2) \qquad (6.11)$$

The rate of shear at the wall can be expressed by Equation 6.12 for $\tau_o < \tau_y$

$$(-\frac{du}{dr})_o = \frac{\frac{\tau_o}{\mu}}{\frac{u_{core}}{\delta}} \qquad (6.12)$$

Assuming that δ is small when compared to radius R, then Equation 6.11 can be expressed as

$$Q = \pi R^2 u_{core} \qquad (6.13)$$

and using the continuity equation for tube flow and by substituting 6.11 into 6.13 we get

$$\frac{8V}{D} = \frac{8 \delta \tau_o}{\mu R} \qquad (6.14)$$

For values of $\tau_o < \tau_y$ the less viscous boundary layer does not affect the flow and allows the core to flow at the velocity u_{core}. From the rheogram the initial slope can be determined from Equation 6.15

$$\epsilon = \frac{\tau_o}{(\frac{8V}{D})} \tag{6.15}$$

By using Equations 6.14 and 6.15 the thickness of the boundary layer can be solved to yield Equation 6.16

$$\delta = \frac{\mu R}{8\epsilon} \tag{6.16}$$

Using Equation 6.16 the velocity of the core can be calculated using Equation 6.17 and the raw data can be corrected using Equation 6.18

$$u_{core} = \frac{\tau_o \delta}{\mu} \tag{6.17}$$

$$V_{CORRECT} = V_{MEASURED} - u_{CORE} \ . \tag{6.18}$$

Neill (1988) used this technique to determine whether boundary layer formation was responsible for the anomalous behaviour of full plant tailings. Results indicated that this did not fully explain the behaviour, but led to an increased yield stress and fluid consistency. Possible reasons for the failure of this method is the assumption that the boundary layer thickness δ is small when compared to the pipe radius. Values calculated by Neill (1988) assumed that the annular layer viscosity is equivalent to that of water in Equation 6.16. This is unlikely as the sheared annulus is composed of fine material with a different viscosity to that of the water. This could lead to a significantly greater boundary layer thickness, but would nonetheless not affect the corrected velocity in Equation 6.18 as inspection of Equations 6.16 and 6.17 show that the viscosity, μ, does not affect the core velocity u_c.

6.5.5 Summary of results of the transformation of the pseudo-shear diagram to a rheogram

None of the above methods successfully reduce the measured pseudo-shear diagram onto a single co-incident curve for differing pipe diameters. Each of the analyses assumes a correction of the pseudo-shear rate is required to obtain the corrected or actual shear rate for a viscous fluid. It is proposed herein that the velocity measurements do not need correction because measurements taken for this project are for actual prototype pipeline size and thus represent true pressure gradient versus mean mixture velocity curves for the data.

PART B

6.6 Proposed technique to transform the measured pseudo shear diagrams to true rheograms

It is the aim of this work to formulate a mathematical model to predict $i_m - V_m$ curves for varying pipe diameters and concentrations. To do this successfully it is necessary to quantify precisely what the measured data represents. From the discussion on maximum and freely settled particle packing (C_{bmax} and C_{bfree}), the zone of interest lies between these two parameters. Above the freely settled particle packing concentration (C_{bfree}), the nature of the flow of these slurries clearly changes and the magnitude of deviation from normal viscous flow increases and becomes asymptotic to C_{bmax} as the slurry relative density approaches the maximum attainable packing concentration, C_{bmax}.

It is suggested that the very nature of the flow alters when $C_v > C_{bfree}$. *It is postulated that the total wall shear stress becomes a combination of both a viscous shear stress component and a shear stress component due to the additional solid particles which are present when* $C_v > C_{bmax}$. This is represented by Equation 6.19, where $\tau_{PARTICLE}$ refers to the particle shear stress present at high concentrations.

The measured pressure gradient for the high concentration full plant tailings is comprised of both the pressure gradient due to the viscous shear stress and the pressure gradient due to the presence of the additional solid particles (Equation 6.20).

$$\tau_o = \tau_{VISCOUS} + \tau_{PARTICLE} \qquad (C_v > C_{bfree}) \qquad (6.19)$$

$$\Delta P_{TOTAL} = \Delta P_{VISCOUS} + \Delta P_{PARTICLE} \qquad (C_v > C_{bfree}) \qquad (6.20)$$

This presents two problems.

(1) The viscous portion of the total wall shear stress, τ_o, needs to be determined

(2) The particle contribution to the total wall shear stress, τ_o, needs to be determined.

6.7 Proposed method of analysis for viscous flow component

For viscous flow, the wall shear stress, τ_o, is a function of pipe diameter ($\tau_o = \frac{D\ \Delta P}{4L}$).

As pipe diameter increases so the pressure gradient, $\Delta P/L$ decreases for a constant rate of shear (i.e. as $D \to \infty$, $\Delta P/L \to 0$).

Based on this relationship, the proposed transformation technique to isolate the viscous shear stress and particle shear stress components from the measured shear stress, τ_o, is described below.

In Example 1 the method is presented for a Newtonian rheogram curve for any pipe diameter. In Example 2 the method is presented for a measured set of data for low concentration full plant tailings. In both these cases, the shear stress is entirely viscous and the particle shear stress component will be zero. In Example 3, the method is presented for high concentration full plant tailings in which the shear stress has both viscous and particle shear stress components.

Example 1 - Newtonian rheogram

1. A rheogram for a Newtonian fluid is presented in Figure 6.6 for the laminar flow for any pipe diameter. This is one straight line.

2. Using Figure 6.6, the pressure gradient, $\Delta P/L$, is dermined for a constant shear rate as indicated by a vertical intercept on Figure 6.6 (A to A').

3. For this shear rate (A), there is one value of wall shear stress, (A') i.e. the shear stress is constant and there is a corresponding value of $\Delta P/L$ for any chosen pipe diameter. For each of the chosen diameters, a graph is plotted of $\Delta P/L$ versus $1/D$, as shown in Figure 6.7.

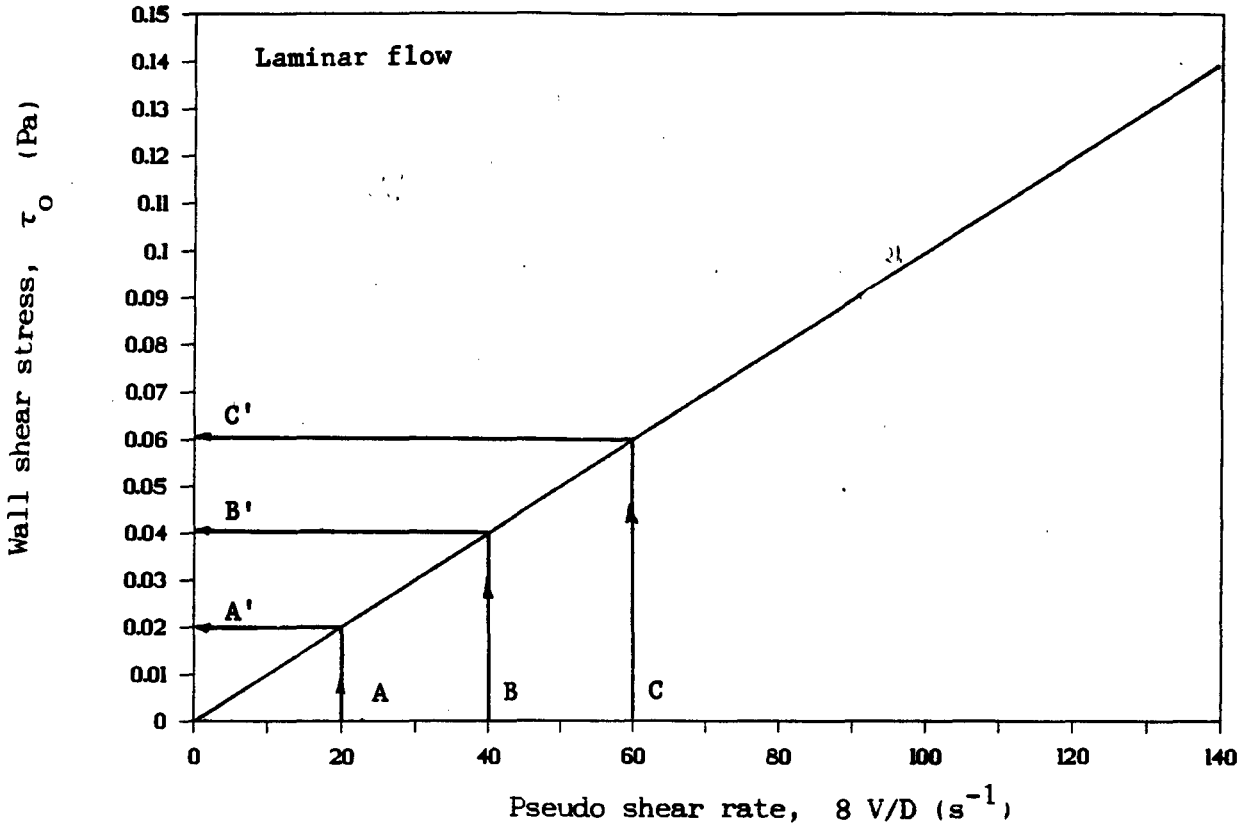

Figure 6.6 : Pseudo shear diagram for Newtonian fluid

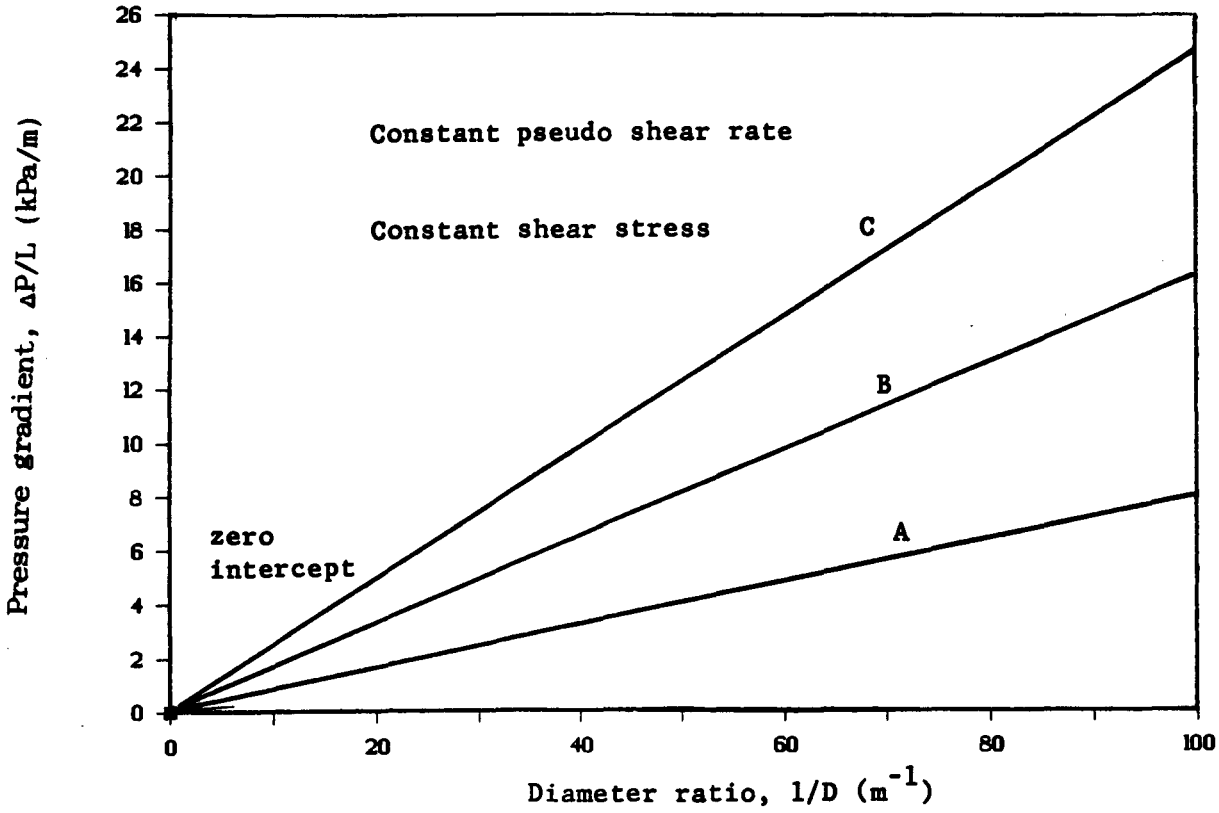

Figure 6.7 : Pressure gradient versus diameter ratio (1/D) for Newtonian fluid in Figure 6.6

4. This procedure (steps 2 and 3) is repeated for several rates of shear as read off the abscissa in Figure 6.6 (B to B', C to C').

5. The intercept on the pressure gradient ordinate of the lines of constant shear at infinite diameter (1/D = 0) on Figure 6.7 is zero.

6. The zero intercept of $\Delta P/L$ at $1/D = 0$ indicates that the flow is entirely viscous in nature.

Example 2 - Low concentration full plant tailings

The procedure outlined above for a Newtonian fluid is demonstrated in Figures 6.8 and 6.9 for low concentration full plant tailings.

Figure 6.8 represents the measured pseudo-shear diagram for the minus 62 micron size fraction of the full plant tailings at a slurry relative density of $S_m = 1,51$. Using the procedure described above, Figure 6.9 is obtained, the graph of $\Delta P/L$ versus $1/D$ for varying shear rates. Extrapolation of the curves in Figure 6.9 intercept the graph at the origin of zero $\Delta P/L$ and $1/D = 0$. Note the linearity of the graph for different pipe diameters.

Using the above technique for viscous slurries the relationship of $1/D$ versus $\Delta P/L$ is seen to be linear for all rates of shear and there is no ordinate intercept and no excess pressure gradient because the curves pass through the zero intercept at $1/D = 0$.

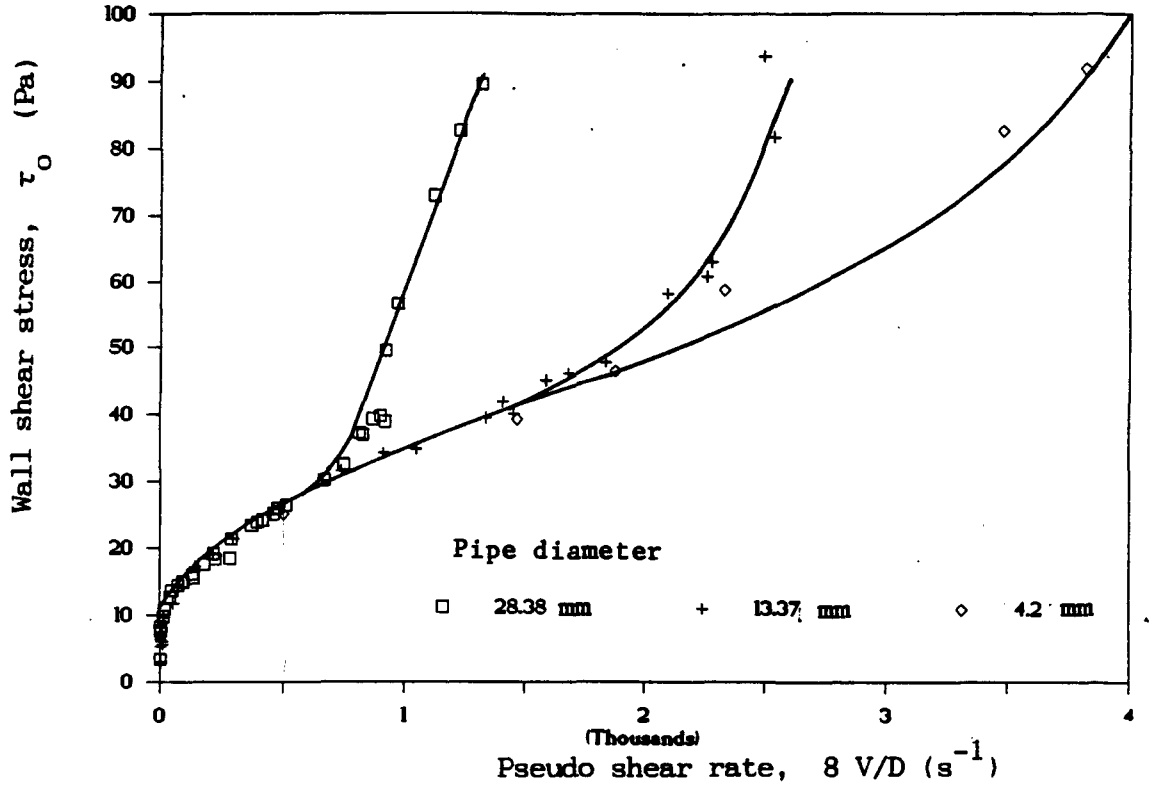

Figure 6.8 : Pseudo shear diagram for low concentration full plant tailings (S_m = 1,51)

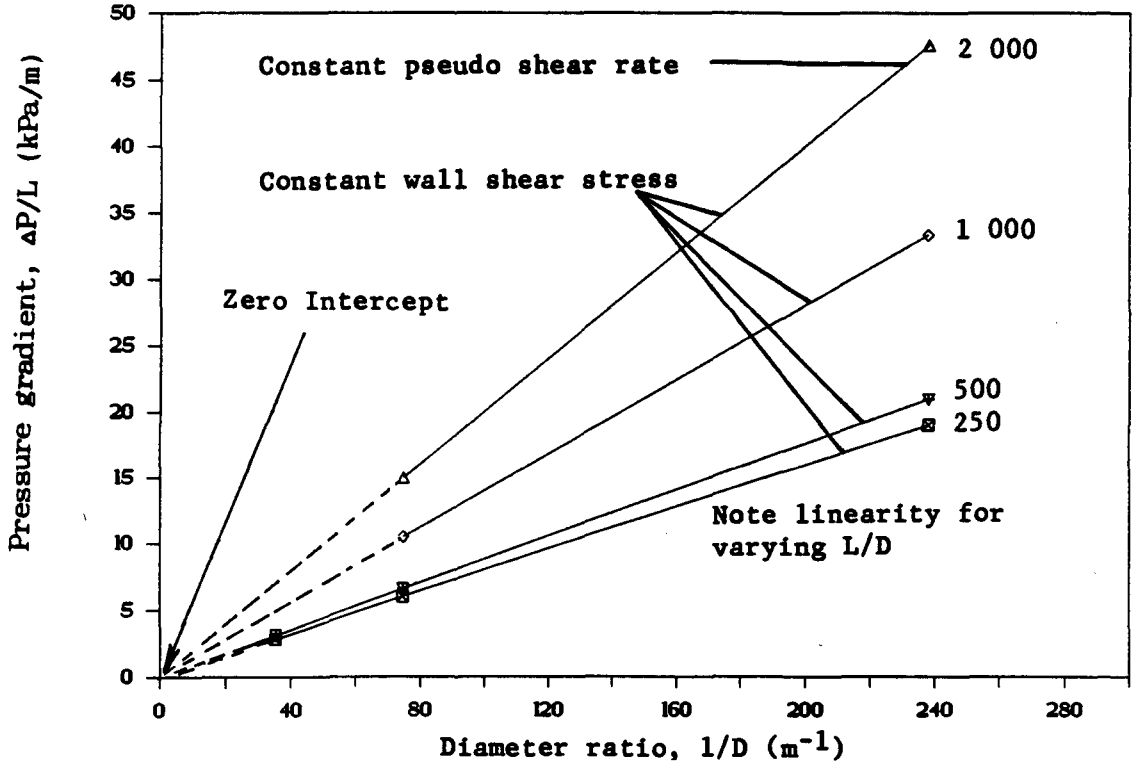

Figure 6.9 : Pressure gradient versus length to diameter ratio (1/D) for low concentration full plant tailings (S_m = 1,51)

Example 3 - Proposed methods of analysis to determine the viscous shear stress component for high concentration full plant tailings

A set of "anomalous" data from the balanced beam tube viscometer is presented in Figure 6.10(a) and the procedure is demonstrated in Figures 6.10(b), 6.10(c) and 6.10(d).

1. For the two diameters selected, a graph of measured pressure gradient versus the diameter ratio (1/D) is plotted for various values of constant shear rate in the laminar flow region of the pseudo-shear diagram (Figure 6.10(b)). When anomalous behaviour occurs, the wall shear stress, τ_o, is not constant for a specified shear rate.

2. ***The intercepts of these lines on Figure 6.10(b) at the ordinate indicates the magnitude of the particle shear stress correction required for that specific pseudo shear rate.*** From the two previous examples (examples 1 and 2), it is shown that the relationship between the pressure gradient and diameter ratio (1/D) is linear. The measured data from the Balanced Beam Tube Viscometer representing the "anomalous" behaviour of full plant tailings is for two pipe diameters only and it is assumed that the variation of measured pressure gradient with increasing diameter ratios is linear. This linearity assumption is later confirmed by the successful scaling of results to larger pipe diameters. Figure 6.10(c) represents the linear relationship of the excess correction of pressure gradient from the ordinate intercepts versus pseudo shear rate for this specific rheogram.

3. Using this linear relationship and Equation 6.19 to correct the wall shear stress to include the viscous component only, i.e.

$$\tau_{\substack{\text{VISCOUS}\\\text{SHEAR}}} = \tau_{\substack{\text{MEASURED}\\\text{SHEAR}}} - \tau_{\substack{\text{PARTICLE}\\\text{SHEAR}}},$$

The rheogram is corrected to include viscous shear only and to exclude particle shear. This corrected rheogram is shown in Figure 6.10(d) and the viscous flow curves are co-incident. This means that the viscous flow component for these slurries can successfully be isolated in this manner.

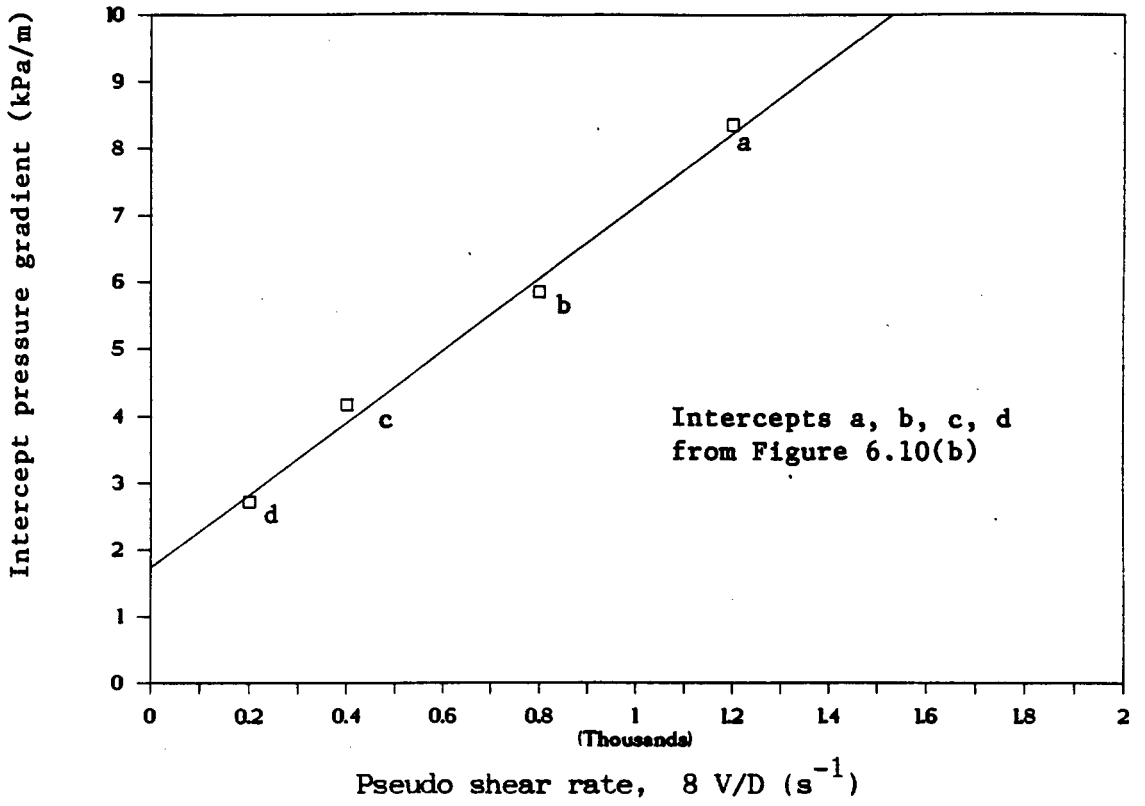

Figure 6.10(c) : Pressure gradient due to particle shear stress versus shear rate for high concentration full plant tailings

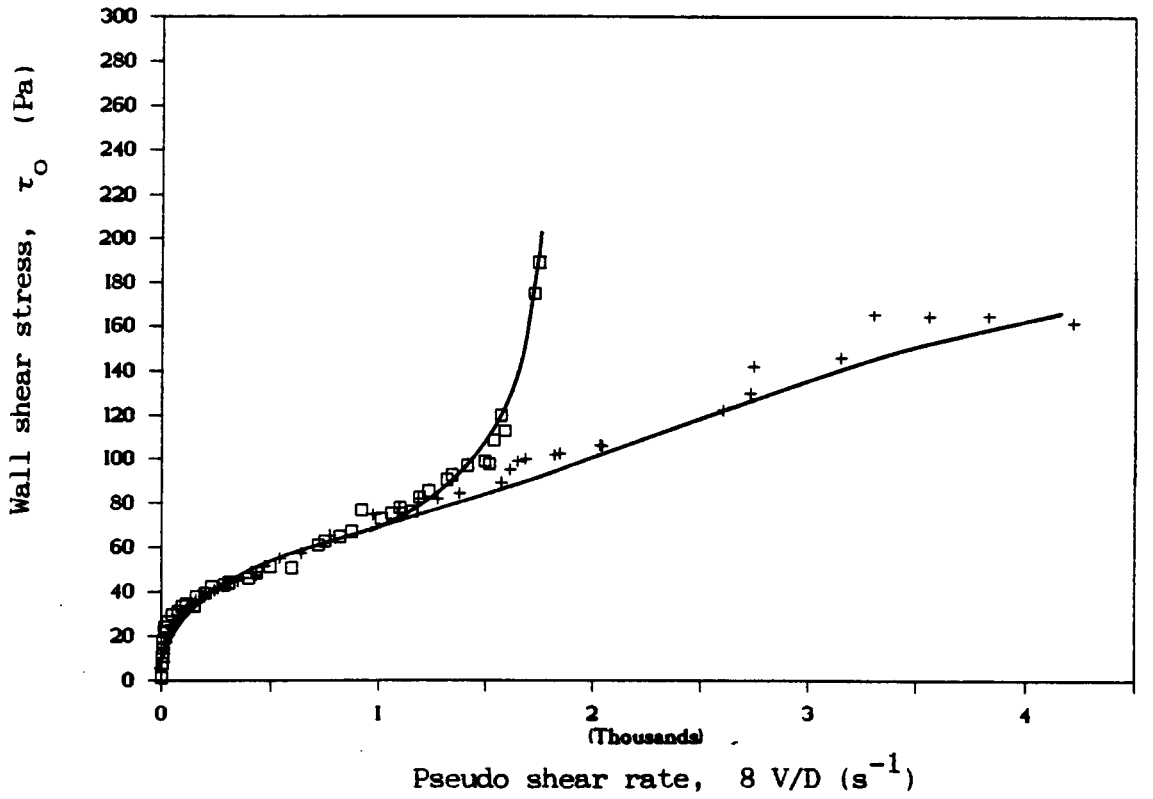

Figure 6.10(d) : Corrected pseudo shear diagram representing the viscous shear stress component of high concentration full plant tailings at S_m = 1,75

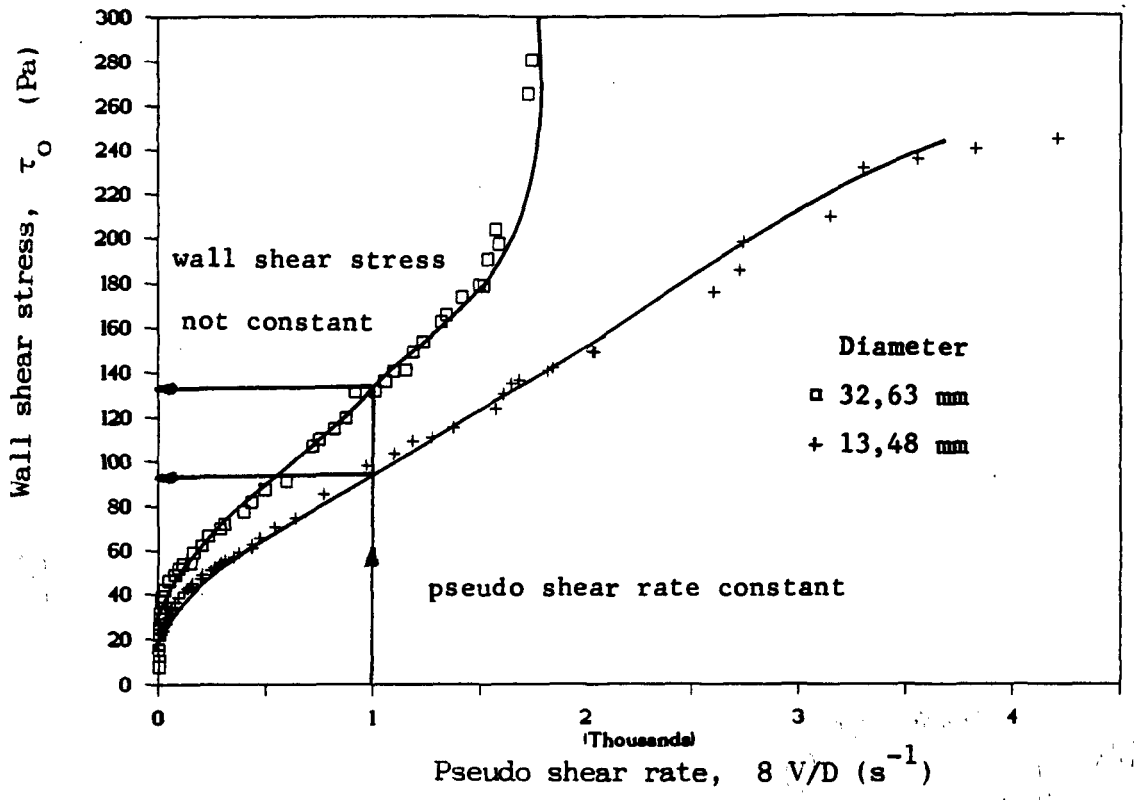

Figure 6.10(a) : Pseudo shear diagram for high concentration full plant tailings (S_m = 1,75)

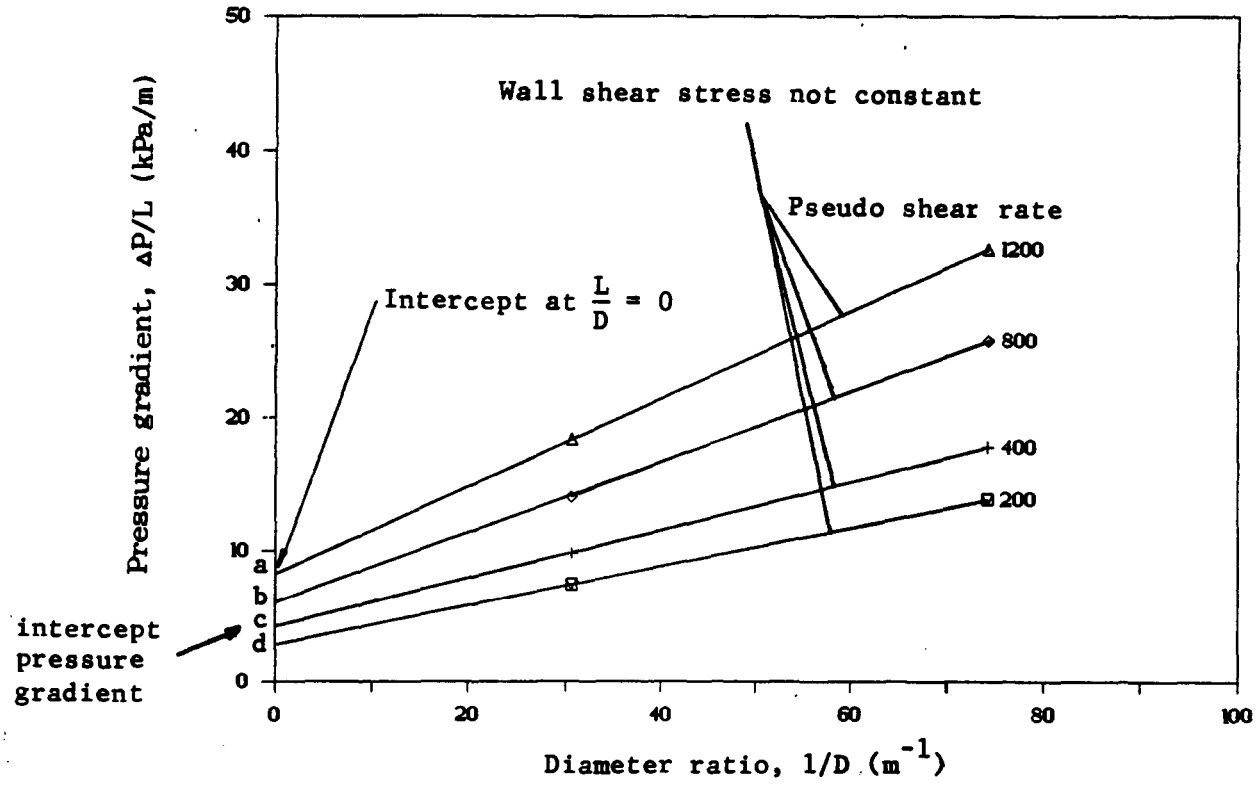

Figure 6.10(b) : Measured pressure gradient versus diameter ratio for constant rates of shear, S_m = 1,75

6.7.1 Illustration of method using the measured data from the Balanced Beam Tube Viscometer

The complete set of BBTV measured data for full plant tailings was transformed to include the viscous shear portion only and exclude the particle shear stress component using this technique. The results are indicated in Figure 6.11(a). Comparison of the raw measured data in Figure 5.2, (reproduced below in Figure 6.11) indicates that the particle portion of the wall shear stress is of a considerable magnitude. Note the values of the wall shear stress in Figure 6.11 compared with the values of the wall shear stress in Figure 5.2.

6.7.2 Determination of rheological parameters (τ_y, K, n) for the viscous component of the full plant tailings

The parameters of the flow can be determined from Figure 6.11 using a yield-pseudoplastic approximation. The values were obtained using an optimization program based on the solution of the minimum error of Equation 6.22 for a yield pseudoplastic slurry for a set of corrected data from the rheograms in Figure 6.11. This technique is described in Appendix B.

$$\frac{8V}{D} = \frac{4n}{K^{1/n}\,\tau^3}(\tau - \tau_y)^{\frac{n+1}{n}}\left[\frac{(\tau-\tau_y)^2}{3n+1} + \frac{2\,\tau_y\,(\tau-\tau_y)}{2n+1} + \frac{\tau_y^2}{n+1}\right] \qquad (6.22)$$

For a given yield stress, τ_y the optimization program selects values of K and n that result in a minimum error in 8V/D for the rheogram. This program is based on work by Slatter (1986) and Neill (1988) who developed the technique for determining τ_y, K and n directly from the pseudo-shear diagram. The results of this analysis using Figure 6.11 are presented in Table 6.1. The values of τ_y, K and n versus slurry relative density are represented by Figures 6.12(a), (b) and (c) respectively for the viscous flow component of full plant tailings only. The data can be fitted to a series of curves for which the equations are given on Figures 6.12(a), (b) and (c).

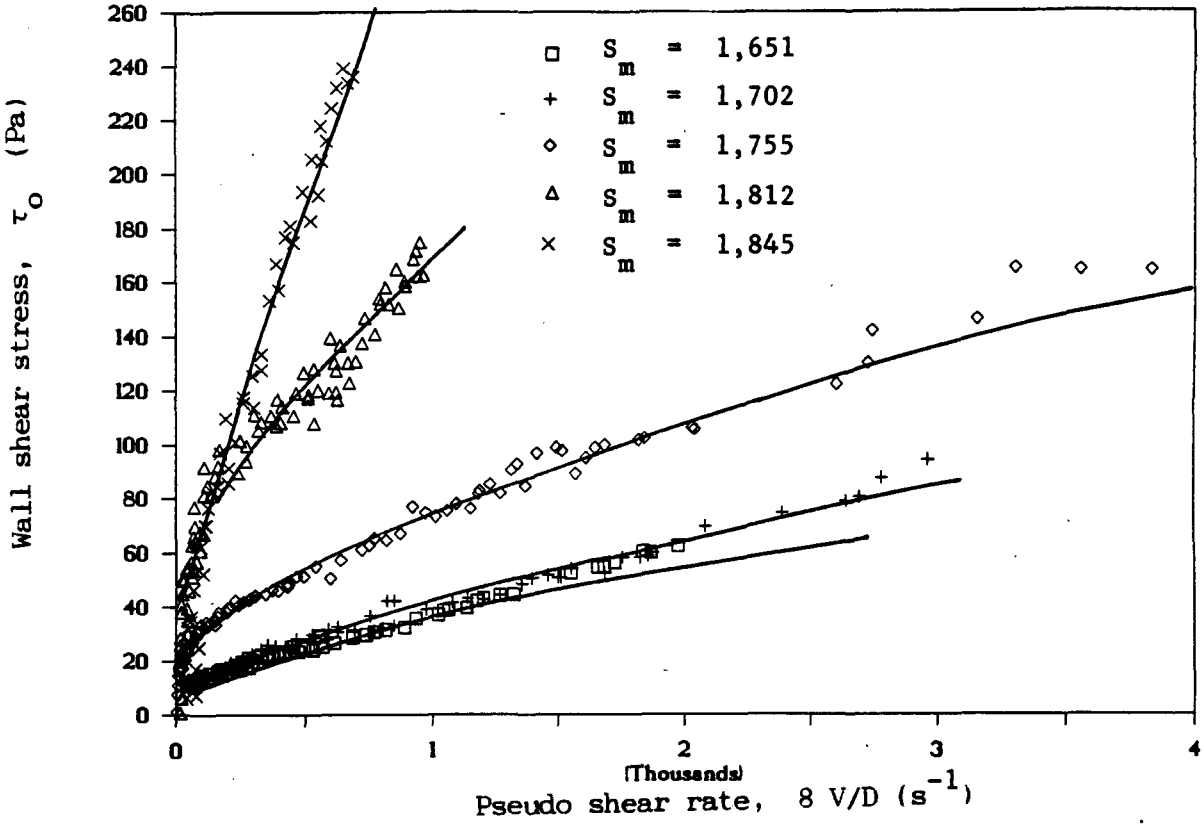

Figure 6.11 : Pseudo shear diagram of viscous shear stress component of the measured total shear stress for full plant tailings

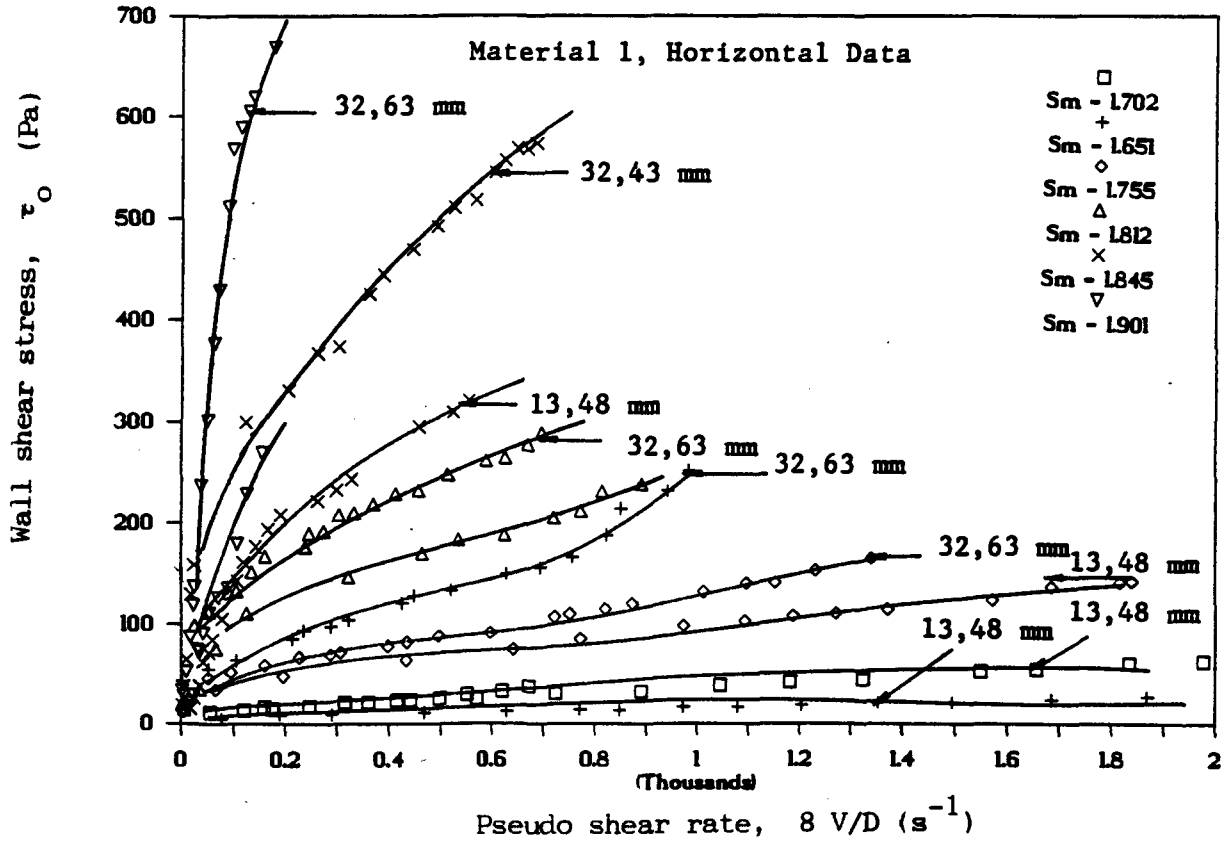

Figure 5.2 : Pseudo shear diagram of measured total shear stress for full plant tailings from the Balanced Beam Tube Viscometer

S_m	Diameter (mm)	V_{crit} (m/s)	$R_{e\ crit}$ **	τ_y (Pa)	K	n
1,650	32,63	2,70	4623	6,00	0,094240	0,83100
1,650	13,48	3,50	3004	6,00	0,094240	0,83100
1,702	32,63	4,00	6130	8,97	0,130264	0,81430
1,702	13,48	5,40	4259	8,97	0,130264	0,81430
1,755	32,63	* 6,00	8699	19,57	0,220896	0,76395
1,755	13,48	* 6,00	4427	19,57	0,220896	0,76395
1,812	32,63	* 6,00	3042	32,61	0,554802	0,78619
1,812	13,48	* 6,00	1518	32,61	0,554802	0,78619
1,846	32,63	* 6,00	2189	35,87	0,511972	0,84482
1,846	13,48	* 6,00	1037	35,87	0,511972	0,84482

* No measured values of laminar to turbulent transition

** generalized Reynolds number

Table 6.1 : Values of τ_y , K and n for the viscous shear stress component

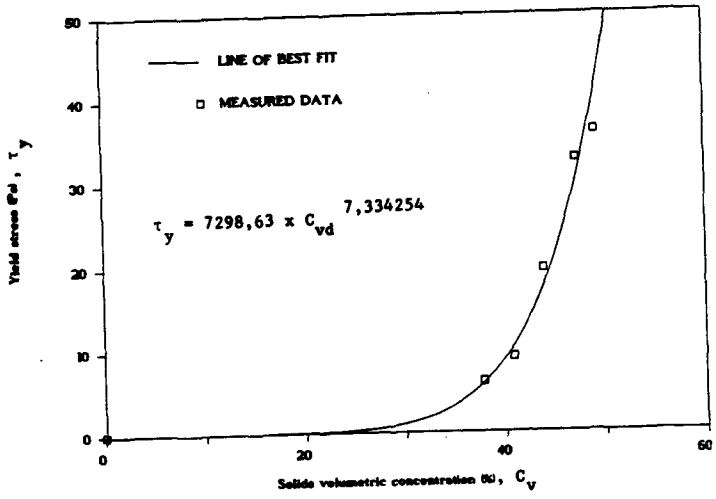

Figure 6.12(a) : Slurry yield stress, τ_y , versus slurry relative density, S_m for full plant tailings

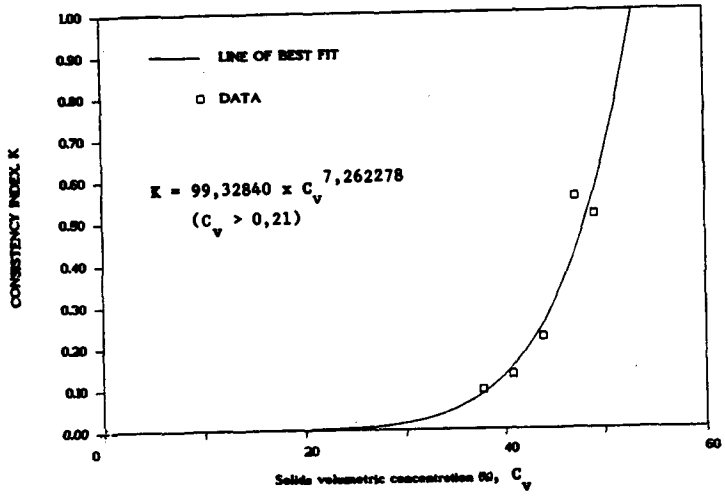

Figure 6.12(b) : Fluid consistency index, K , versus slurry relative density, S_m , for full plant tailings

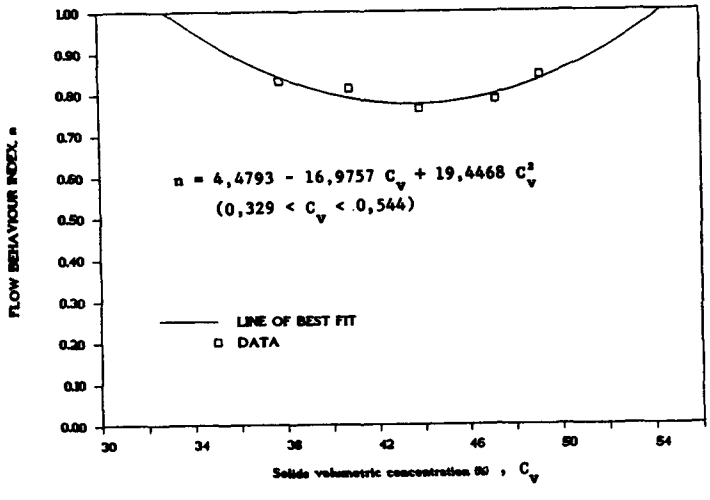

Figure 6.12(c) : Flow behaviour index, n , versus slurry relative density, S_m , for full plant tailings

6.8 Analysis of the particle shear stress component for high concentration full plant tailings

The analysis of the particle shear stress contribution to the total wall shear stress and the modelling of these slurries is discussed below.

The introduction of the concept of separation of the total wall shear stress into two components is used to solve successfully the viscous shear component as demonstrated in Section 6.7. The excess wall shear stress has to be accounted for and several explanations are presented.

6.8.1 Modified velocity profile to include a sheared annular zone and an unsheared central coarse particle plug

The observed anomalous behaviour could be due to a modified velocity distribution, which, when fully developed, contains a significant central unsheared plug and a highly sheared annular region.

Brown (1988) assumed that the coarser particles within the stabilized slurry migrated towards the pipe centre, and left a fine-slurry matrix at the pipe wall in which all the shear takes place. The fluid shear region is confined to the annulus, while the plug moves at a constant velocity. The continuity equation for this proposed flow is as follows :

$$Q_{TOTAL} = Q_{PLUG} + Q_{ANNULUS} \qquad (6.23)$$

$$= \pi r_p^2 u_p + 2\pi \int_{r_p}^{R_o} r\, u(r)\, dr$$

where r_p = radius of plug
u_p = velocity of plug
$u(r)$ = localized velocity in annulus
R_o = pipe diameter.

Figure 6.13 represents the flow model. The localized velocity, u(r) is given by the yield pseudoplastic rheological model (Brown (1988)),

$$\tau(r) = \tau_y + K\left(-\frac{du}{dr}\right)^n \qquad (6.24)$$

where $\tau(r) = \tau_o \frac{r}{R_o}$ proportionality ∝.

For the annular velocity profile, Equation 6.24 yields the following expression (note the lefthand side is equal to the plug velocity, u_p)

$$-\int_{u_p}^{o} du = K^{-1/n} \int_{r_p}^{R_o} \left(\tau_o \frac{r}{R_o} - \tau_y\right)^{1/n} dr \quad . \qquad (6.25)$$

Equation 6.25 is valid for the no-slip boundary condition, (u = 0 when $r = R_o$) and thus Equation 6.23 can be solved. In order to estimate the velocity of the plug for a given flow rate, it is assumed that the plug ✓ moves as a solid unsheared core with no interstitial seepage flow. ✓ From the discharge terms, Q_{PLUG} and $Q_{ANNULUS}$, the relative velocity of the plug can be determined using the method of Govier and Aziz (1972) for capsule transport conditions. This yields :

$$V_{AVERAGE} = \frac{Q_{ANNULUS} + Q_{PLUG}}{\pi R_o^2} \qquad (6.26)$$

$$= \frac{R_o^2 + r_p^2}{2 R_o^2} u_p$$

This can be rearranged to give, R_V, the relative velocity as :

$$R_V = \frac{u_p}{V_{AVERAGE}} = \frac{2}{1 + \left(\frac{r_p}{R}\right)^2} \qquad (6.27)$$

$$= \frac{2}{1 + K^2}$$

where $K = \frac{r_p}{R_o}$.

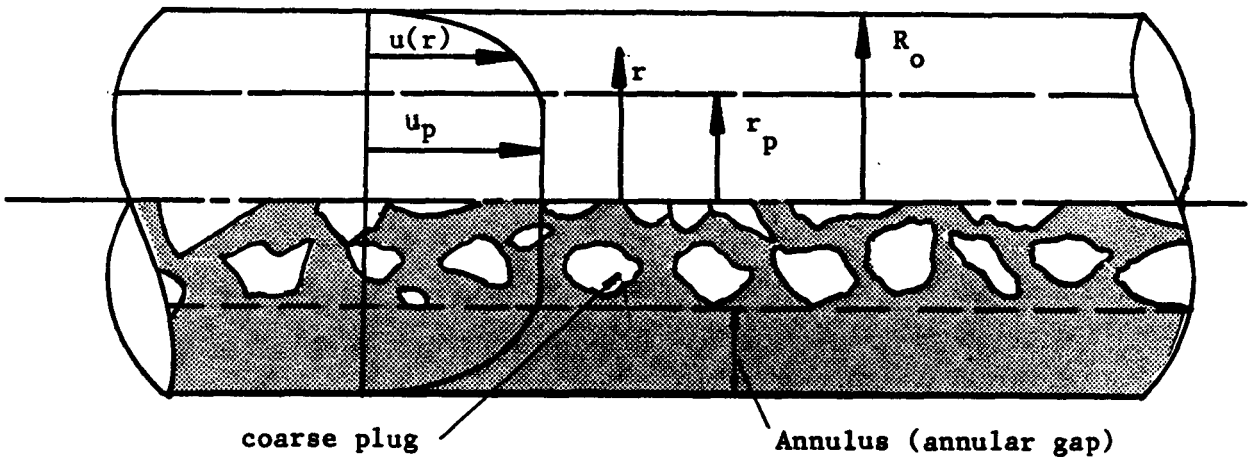

Figure 6.13 : Velocity distribution due to the presence of a coarse plug and sheared annular region (Brown (1988))

Equation 6.28 provides a minimum value of r_p, which is the core radius for a normal yield pseudoplastic velocity distribution.

$$r_p = \frac{\tau_y}{\tau_o} R_o \quad \left\} \text{ minimum value of } r_p \right. \tag{6.28}$$

Brown (1988) does not recommend any values of V_{PLUG} but suggests r_p can be calculated from an estimate of the coarse-coal fraction present. The suggested radius (Brown (1988)), based on the coarse coal fraction is estimated from Equation 6.29, but this requires a knowledge of the fine/coarse particle size ratio.

$$r_p = \left(\frac{\text{Volume of coarse slurry per unit length of pipe}}{\pi}\right)^{0,5} \tag{6.29}$$

Rather than use estimates of coarse particle fractions, the plug radius was calculated for the range of measured data. The iterative solution of Equation 6.25 and 6.26 yielded the core radius ratio, R_c (r_p/R_o), the values of which are presented in Figure 6.14 for a range of pipe diameters and a specific solids concentration. The required plug radius is significantly greater than that given by the yield pseudoplastic ratio (see Equation 6.28). Equation 6.28 yields an exact value of r_p which decreases with increasing shear rate.

Calculated values of r_p became constant at higher velocities, as indicated in Figure 6.14. The plug size initially decreases sharply with increasing velocity and becomes reasonably constant at higher velocities. The rate of decrease of the plug size is dependent upon pipe diameter and is again more pronounced for smaller diameter ranges. The decrease in plug diameter ratio is considerably larger for small pipe diameters, decreasing from full bore plug flow to 93% of the diameter at higher velocities. For the larger pipe diameters, the plug occupies virtually the entire cross-sectional area (R_c = 0,99 at 1 m/s). The effect increases with solids concentration, until at high velocities (6 m/s) the plug occupies the entire cross-sectional area, except for a highly sheared annulus of less than 1 mm in the 100 mm NB pipeline at S_m = 1,90.

The existence of a sheared annulus and increased plug radius due to the coarse solid particles is credible at intermediate solids concentration, but for higher concentrations the required annular gap tends towards the maximum particle size, which would lead to particle contact with the pipe wall as discussed in Section 6.4.1. The core ratio, R_c, needs to be accurately determined and the wall shear stress τ_o, is very sensitive to small variations in the width of the sheared zone in the annulus region. No mechanism is considered in Equation 6.29 to account for the varying size of the annulus illustrated in Figure 6.14.

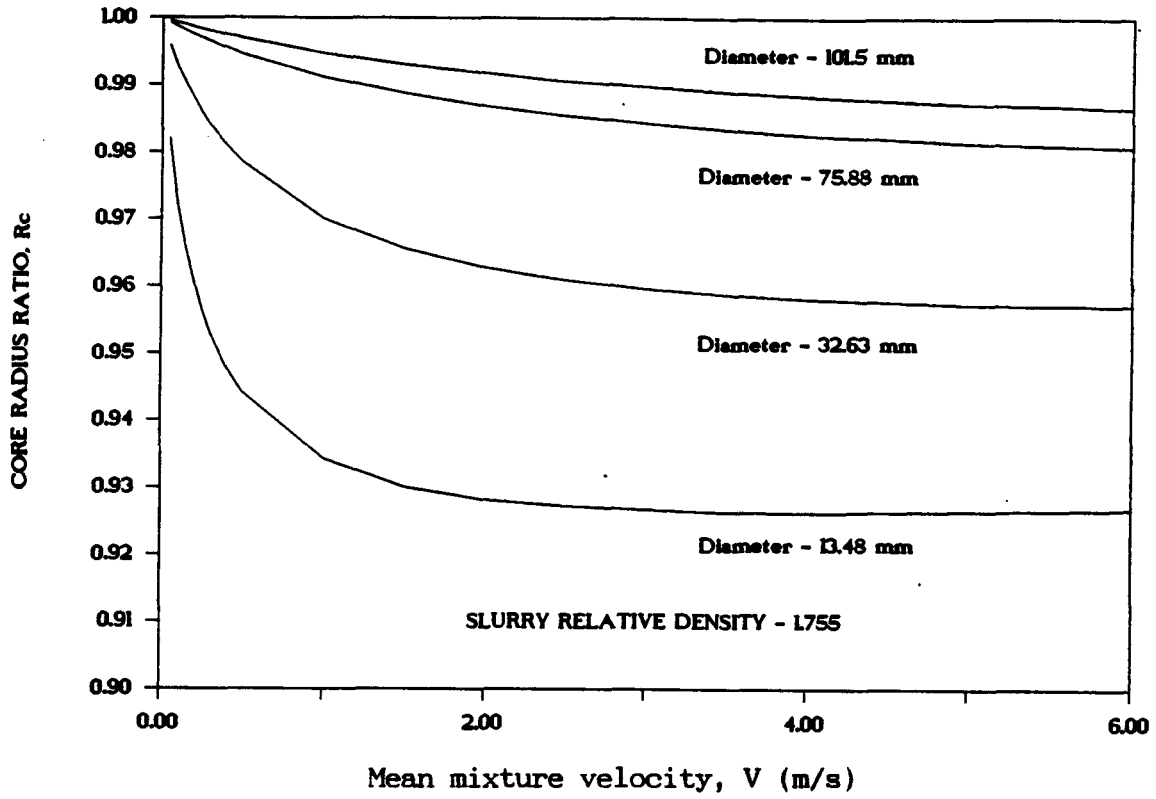

Figure 6.14 : Core ratio, r_p/R_o , versus mixture velocity for full plant tailings at S_m = 1,7545 for differing pipe diameters

Figure 6.15 represents calculated values of the size of the annular layer required for the high concentration slurries. The annular gap varies from 0 mm at low velocities (when $\tau_y = \tau_o$, $r_p = 0$) to a maximum of 2,5 mm at intermediate velocities (see Figure 6.15). This small variation in thickness of the annulus has a significant effect on the calculation of the shear flow and corresponding wall shear stress.

The presence of a coarse plug of these dimensions does not account for the particle shear stress component because at high solids concentrations the width of the annular gap required tends towards zero. It is unlikely that all the shear will take place in an annulus of less than the mean particle size (d_{50}) of 30 μm. The presence of the plug will contribute to an increase in the viscous shear stress component only and does not account for the particle shear stress component.

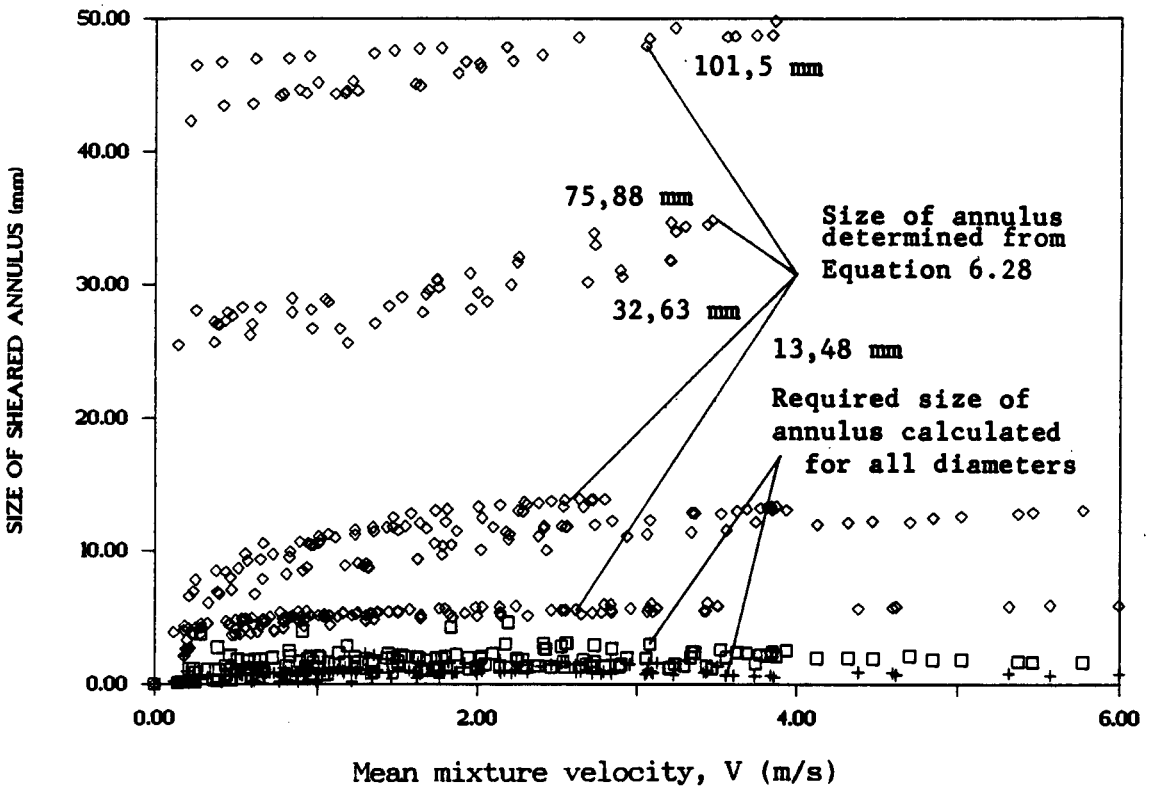

Figure 6.15 : Size of sheared annulus versus mean mixture velocity

6.8.2 Modified velocity profile to include sheared annulus, unsheared plug and a slip velocity

Effective slip was described in Section 6.3.2 and did not adequately describe the anomalous behaviour. Using the parameters of τ_y , K and n for the viscous contribution to the total wall shear stress, a modified slip analysis to include plug flow is presented. From the previous section, Equation 6.23 can be extended to include the slip flow, Q_{SLIP} , as follows :

$$Q_{TOTAL} = Q_{SLIP} + Q_{PLUG} + Q_{ANNULUS} \qquad (6.30)$$

where Q_{TOTAL} = Total volumetric flow rate

Q_{SLIP} = Slip volumetric flow rate

Q_{PLUG} = Coarse plug volumetric flow rate

$Q_{ANNULUS}$ = Annular or shear volumetric flow rate.

Referring to Figure 6.4(b), the slip flow rate is given by

$$Q_{SLIP} = \pi R^2 u_s \tag{6.31}$$

The plug flow rate is given by :

$$Q_{PLUG} = \pi r_p^2 u_p \tag{6.32}$$

and the shear flow rate is expressed by :

$$Q_{ANNULUS} = \frac{\pi R^3}{3} \int_o^{\tau_o} \frac{\tau^3}{\eta(\tau)} d\tau \tag{6.33}$$

where $\eta(\tau)$ = yield pseudoplastic shear stress function.

Assuming the slip velocity, V_s, can be defined according to Mooney (1931) in terms of τ_o and a slip coefficient, beta, we get :

$$Q_{SLIP} = \pi R^2 \tau_o \beta \tag{6.34}$$

From the analysis of Windhab and Gleissle (1984) the shear flow and plug flow can be calculated directly from Equations 6.35 and 6.36 as follows :

$$Q_{ANNULUS} = \frac{\pi R^3}{\tau_o^3} K^{-1/n} \tau_o^{3+1/n} [A + B + C] \tag{6.35}$$

where $A = \dfrac{(1 - \frac{\tau_y}{\tau_o})^{3+1/n}}{3 + 1/n}$

$$B = \frac{2 \frac{\tau_y}{\tau_o} (1 - \frac{\tau_y}{\tau_o})^{2+1/n}}{2 + 1/n}$$

$$C = \frac{(\frac{\tau_y}{\tau_o})^2 (1 - \frac{\tau_y}{\tau_o})^{1+1/n}}{1 + 1/n}$$

The coarse plug flow rate is given by

$$Q_{PLUG} = \frac{\pi R^3}{1+1/n} K^{-1/n} \tau_o^{1/n} \left(\frac{\tau_y}{\tau_o}\right)^2 \left(1 - \frac{\tau_y}{\tau_o}\right)^{1+1/n} \qquad (6.36)$$

Using the measured data, for which the measured flow rate and corrected flow rate are determined according to Equation 6.9, and solving for the slip coefficient, beta (β) from Equations 6.30 and 6.34, the required slip velocity can be calculated. The required slip velocities are of the order of 20 m/s. Results are presented in Figure 6.16 for beta versus slurry relative density over a range of pipe diameters. Most noticeable is the effect of concentration on the magnitude of the slip velocity. Above a slurry relative density of 1,75 there is a marked rapid decrease in the slip velocity for a correspondingly small increase in solids concentration. The slip velocity increases linearly up to this point for increasing pipe diameters and then at the higher concentrations decreases towards zero.

Between the slurry relative densities of 1,75 and 1,81, there is a sudden change in the magnitude of the slip velocity which cannot be ascribed to a growth of the increased plug flow and increased shear in the annular layer. The presence of a modified slip velocity flow, a plug flow and shear flow does not account for the particle shear stress component.

6.8.3 The effect of particle-pipe wall contact at high solids concentrations to account for the particle shear stress

At high solids concentrations, the particles within the slurry are forced together. This particle-particle interaction occurs above the critical relative density, corresponding to the freely settled bed packing concentration, and results in direct particle contact between the solids and the pipe wall. The effect of the solids-pipe wall contact can be described by Figure 6.17. Figure 6.17 represents the pressure distribution within the pipe due to the viscous pressure distribution and the solids-pipe wall pressure distribution. This solids-pipe wall friction is due to the dispersive stress, σ_d, which contributes to the total wall shear stress, τ_o.

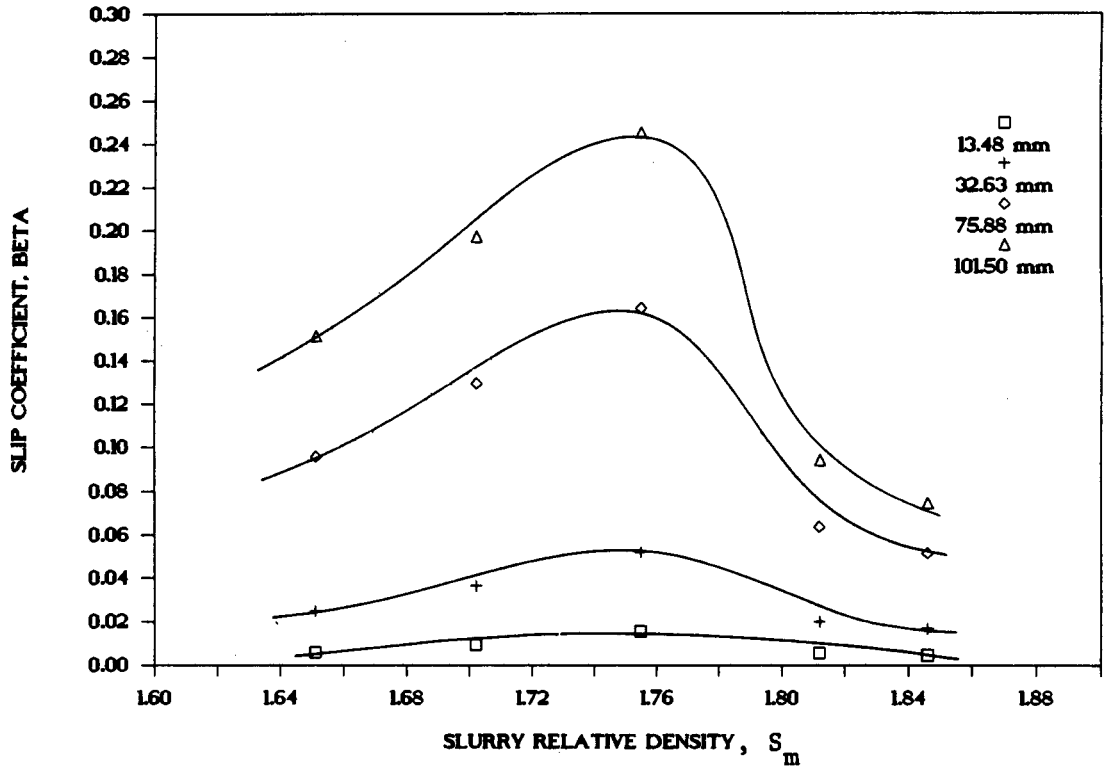

Figure 6.16 : Variation of slip coefficient beta, β , versus slurry relative density S_m

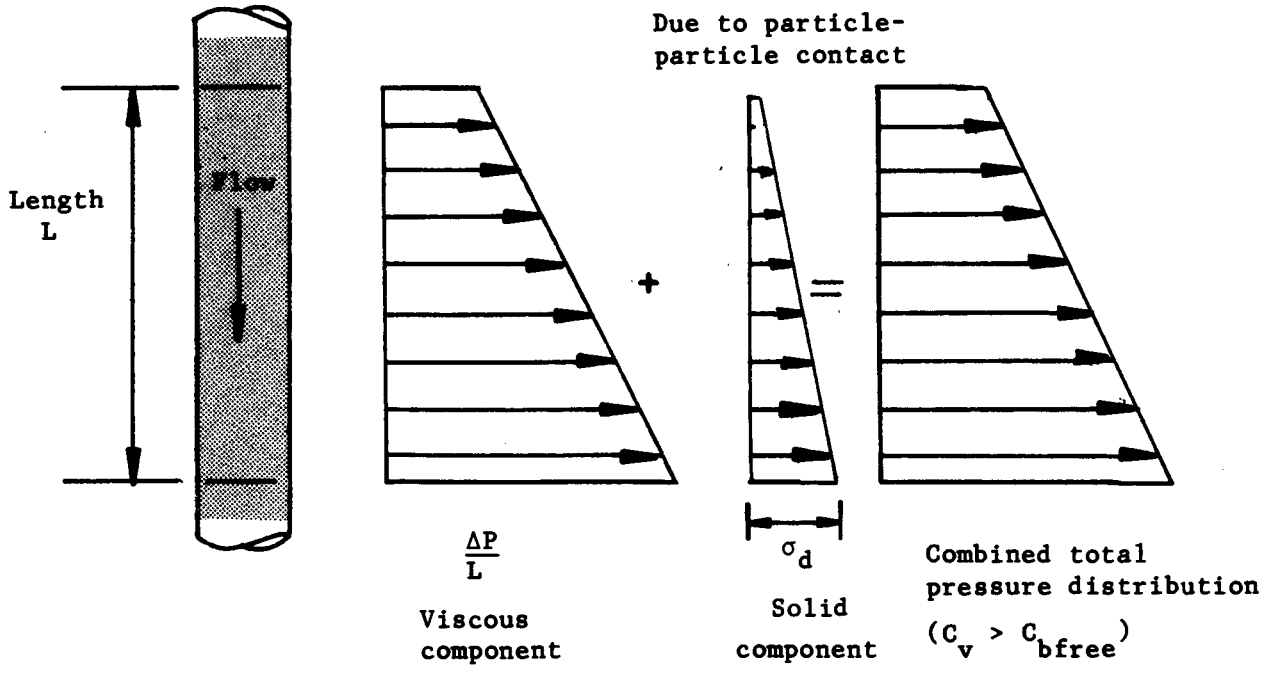

Figure 6.17 : Dispersive stress pressure distribution

The dispersive stress, σ_d , can be represented by Equation 6.37.

$$\sigma_d = K_r \left| \frac{dP}{dx} \right| \tag{6.37}$$

where $\frac{dP}{dx}$ = total pressure gradient due to wall shear stress τ_o
K_r = dispersive stress coefficient.

Using Equation 6.37, the shear stress, τ_p , at the pipe wall due to the solid particle-particle contact is evaluated by :

$$\tau_p = \mu_s \sigma_d \tag{6.38}$$

where μ_s = dynamic coefficient of sliding friction between the slurry particles and the pipe wall.

For this analysis, the static coefficient of sliding friction was measured using the "tilting pipeline" apparatus (Wilson (1972)). This effectively only measures the static coefficient of sliding friction. The dynamic coefficient of sliding friction is slightly less than the static coefficient of sliding friction.

Using the measured values of μ_s ($\mu_s \simeq 0{,}45$) for the full plant tailings, and the measured values of pressure gradient, the dispersive stress coefficient, K_r , was calculated. Results are presented in Figure 6.18. From Figure 6.18 it is seen that the dispersive stress coefficient is a function of both solids concentration and pipe diameter. Combining Equations 6.37 and 6.38, the relationship between the particle pressure gradient and the dispersive stress coefficient, K_r , is shown in Equation 6.39 and 6.40.

The particle shear stress is a function of particle friction and the dispersive stress σ_d . The term particle shear stress is now replaced by the term solid shear stress ($\tau_p = \tau_s$).

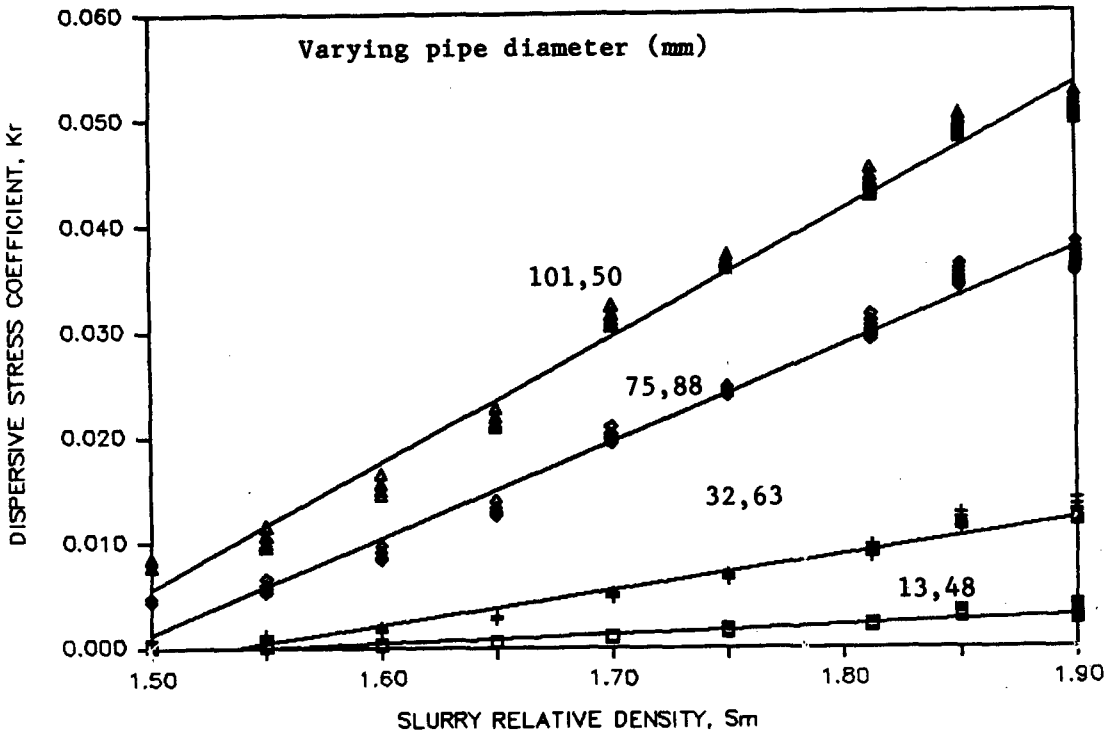

Figure 6.18 : Dispersive stress coefficient, K_r , versus slurry relative density, S_m

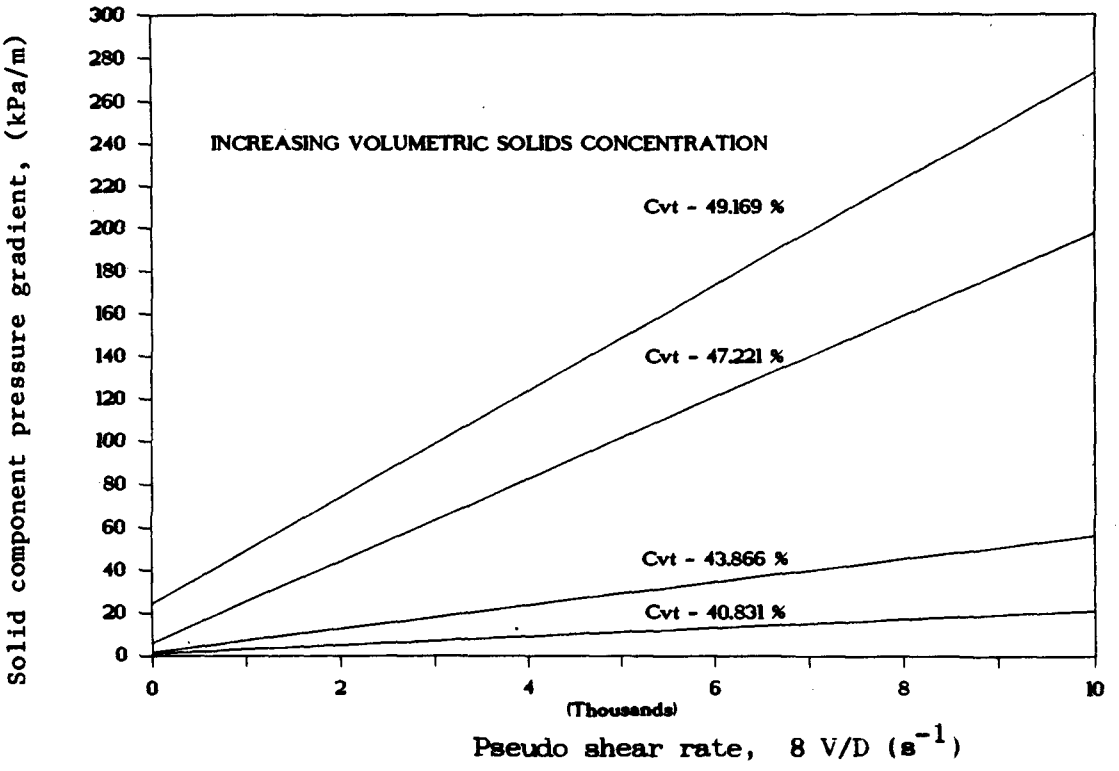

Figure 6.19 : Analysis of the pressure gradient due to the solid shear stress for full plant tailings

$$\tau_s = \mu_s K_r \frac{dP_{TOTAL}}{dx} \qquad (6.39)$$

and $$\frac{dP_{TOTAL}}{dx} = \Delta P = \frac{4 \tau_o}{D}$$

$$\tau_o = \tau_s + \tau_v$$

which yields :

$$\tau_s = \frac{4 \mu_s K_r (\tau_m + \tau_v)}{D}$$

rearranging gives :

$$\tau_s = \frac{4 \mu_s K_r \tau_v}{(D - 4 \mu_s K_r)} \qquad (6.40)$$

where $K_r = fn\ (D\ ,\ C_v)$

For full plant tailings, the dispersive stress coefficient, K_r , can be calculated using the following equation :

$$K_r = a + b S_m \qquad (6.41)$$

where $a = 0{,}0091534042 - 1{,}83476486\ D$

$b = 0{,}0077853195 + 1{,}26903739\ D$

$S_m = C_{vd} (S_s - S_w) + S_w$

Using these results, the pressure gradient due to the solid shear stress versus pseudo shear rate is plotted in Figure 6.19 for high concentration full plant tailings. The increase in the pressure gradient is seen to be linear with increasing pseudo shear rate. For a constant pseudo shear rate, the pressure gradient due to the solid shear stress increases sharply with increasing solids concentration.

6.8.3.1 Scale-up analysis

To verify this technique, the values of the dispersive stress coefficient, K_r , were determined for the data obtained from the Balanced Beam Tube Viscometer.

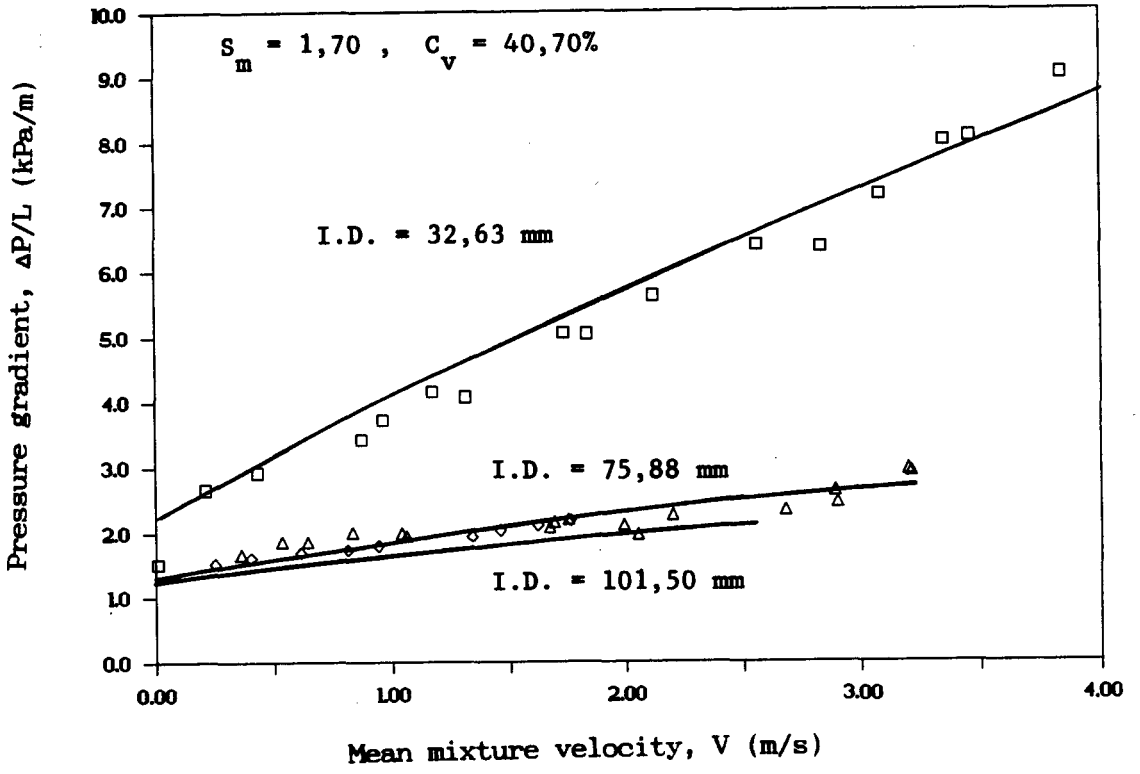

Figure 6.20 : Scale up of results to 75 mm NB and 100 mm NB pipelines

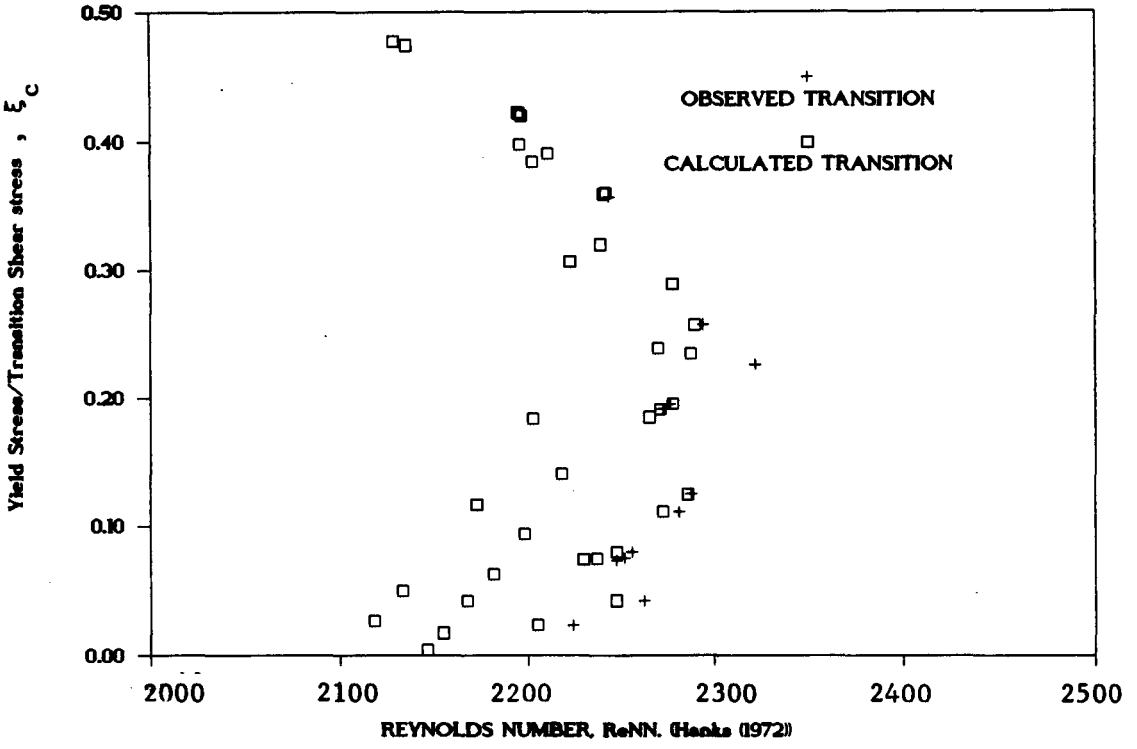

Figure 6.21 : Comparison between observed and measured laminar to turbulent transition (Hanks (1974))

The viscous portion of the total shear stress was determined using the proposed technique in Section 6.7. For these parameters of τ_y , K and n , measured data in the larger pipe diameters is successfully correlated as illustrated in Figure 6.20. The agreement between the predicted and measured curves is reasonable. This means that this method can be used to predict the performance of high concentration full plant tailings for pipes ranging in size from 13,48 mm in diameter to 101,50 mm internal diameter.

6.8.3.2 **Laminar to turbulent transition of full plant tailings**

The measured data indicated a definite laminar to turbulent transition with increasing velocity for the slurries. At low concentrations, up to S_m = 1,651, the flow is largely turbulent. Analysis of various methods for determining the onset of turbulent flow indicated that the method of Hanks (1974) provided the best correlation. These equations were presented in Table 2.3.

Figure 6.21 represents the comparison between the observed and measured transition from laminar to turbulent flow. The observed values are marginally greater than the calculated values. At the high concentrations, this can be attributed to the increased particle-particle contact which will prohibit the onset of turbulent flow.

The critical transition velocity (velocity at which turbulent flow first occurs), was not recorded for all data. For slurry relative densities greater than S_m = 1,70, the flow was always laminar for the range of measured velocities. When turbulent flow was observed it was marked by a rapid increase in pressure gradient.

6.8.3.3 **Turbulent flow of full plant tailings**

Over the range of measured data, the observed turbulent flow can be modelled using the Torrance (1963) relation for smooth wall pipes. The relative roughness ratio, $\frac{\epsilon}{D}$, for the range of pipelines tested indicates smooth wall flow conditions exist. Figure 6.21 represents the comparison of several of the turbulent flow correlations presented in Chapter 2.

The transitional flow which occurs between laminar flow and fully developed turbulent flow is not analysed and is the reason for the discontinuity in the curves at the critical transitional velocity.

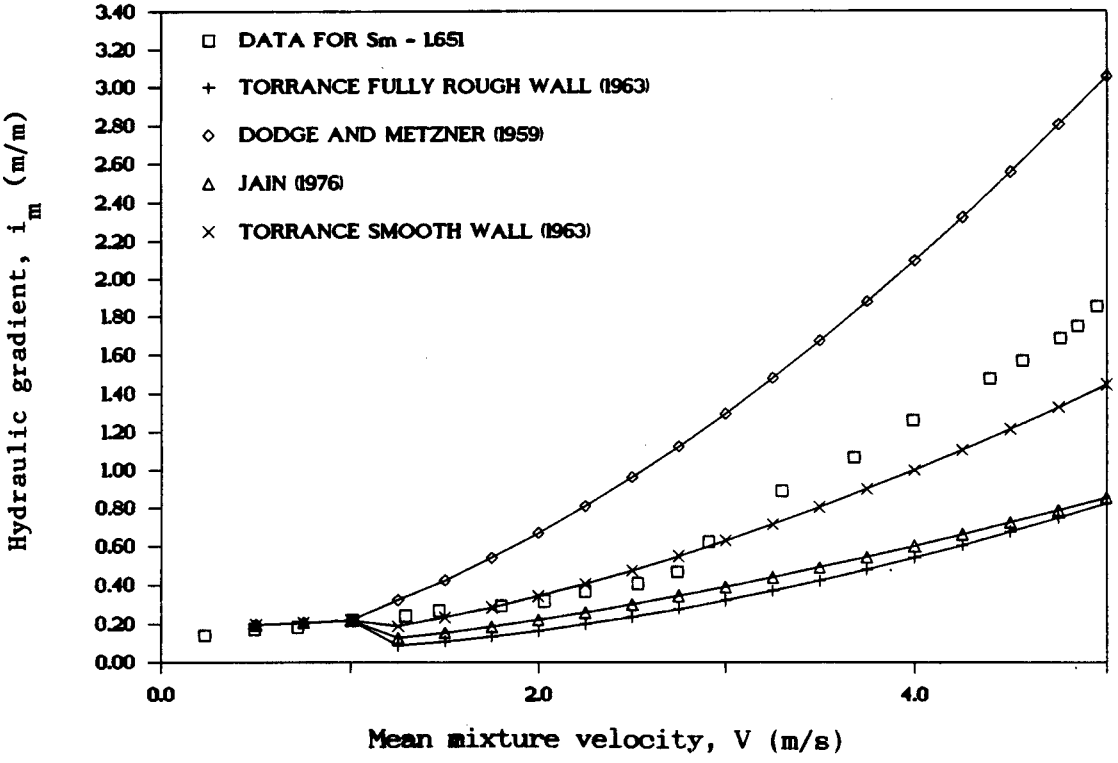

Figure 6.22 : Comparison of turbulent flow models applicable to full plant tailings

6.9 Summary of procedure for analysing the flow behaviour of high concentration full plant tailings

The procedure outlined in the preceeding sections to determine the relationship between pressure gradient versus mean mixture velocity (the ΔP versus V_m curve) for high concentration full plant tailings is summarised below.

6.9.1 Analysis of the viscous shear stress component, τ_{ov}

From a set of tube viscometer data of measured total wall shear stress versus pseudo shear rate for full plant tailings at a solids volumetric concentration greater than the freely settled volumetric concentration, the viscous shear stress contribution to the total measured wall shear stress is obtained. The method is as follows :

1. From the pseudo shear diagram representing the measured data, a graph of measured pressure gradient ($\Delta P/L$) versus diameter ratio (L/D) is plotted.

2. The intercepts of these lines of constant pseudo shear rate at the ordinate is plotted on a graph of the intercept pressure gradient versus pseudo shear rate. This represents the relationship between the correction of wall shear stress required for corresponding pseudo shear rates.

3. Using Equation 6.42, the measured wall shear stress is corrected to include the viscous shear component only.

$$\tau_v = \tau_{measured} - \tau_{solid} \qquad (6.42)$$

4. The rheogram representing the viscous wall shear stress versus shear rate is plotted.

From the corrected rheogram, the rheological parameters of τ_y, K and n can be determined using the yield pseudoplastic constitutive equation. This procedure is outlined in Appendix B.

The viscous wall shear stress, τ_{ov}, is determined from the yield pseudoplastic rheological model.

6.9.2 The determination of the solid wall shear stress, τ_{os}

The solid wall shear stress contribution to the total wall shear stress is only present when the *in situ* solids volumetric (C_{vt}) concentration is greater than the freely settled solids volumetric concentration, C_{bfree}.

The solid wall shear stress, τ_s, is due to both the dispersive stress, σ_d, and the dynamic coefficient of sliding friction, μ_s. This relationship is expressed by Equation 6.43 :

$$\tau_m = \mu_s K_r \left| \frac{dP}{dx} \right| \qquad (6.43)$$

where K_r = dispersive stress coefficient
= fn (C_v , D)

PART FOUR

COMPUTER AIDED ANALYSIS

CHAPTER 7

COMPUTER AIDED DESIGN.
THE COMPUTER PROGRAM FOR THE COMPARISON OF SEVERAL AVAILABLE ANALYTICAL MODELS USED IN THE DESIGN OF BACKFILL RETICULATION PIPELINE SYSTEMS

7.1 Introduction

In order to test the available models and to enable design of backfill piping systems, a computer program was written.

The following functions had to be fulfilled in the compilation of the computer aided design (CAD) program :

1. Present the most commonly used mathematical correlations in the form of a user friendly interactive computer program.

2. Allow for the input of all relevant data in a format that will enable a data base of measured pipeline data to be compiled. The data must include technical input facilities as well as relevant descriptive headings to identify each file and slurry type.

3. To allow for the optimization of the backfill reticulation system design by user selected sensitivity analyses on each of the input variables.

4. To present both on screen graphical and tabular output of calculated results for immediate comparison in the form of the traditional head loss versus mean mixture velocity curve.

5. To compare the selected analytical models on a common basis and to evaluate the limits of applicability of each of the models for full plant backfill slurries.

7.2 Selected analytical models included in computer program

The selection of analytical models includes those correllations that are commonly used by the industry. Additional models were added to include the more recent computer based solutions and mechanistic modelling techniques which represent the more general and widely used slurry types.

The 10 models available for comparison are represented in Table 7.1.

Author/Model	Year	Model Type
Pseudo Fluid	-	$S_m \times i_w$
Durand, R.	1953	Emperical
Newitt *et al*	1955	Emperical
Wasp *et al*	1963-1971	Semi-Emperical
Yield Pseudoplastic	1967-1979	non-Newtonian
Wilson, K.C.	1974-1980	Mechanistic
Streat, M.A.	1986	Mechanistic (Dense Phase)
Lazarus, J. H.	1988-1989	Mechanistic
Sive, A.W.	1988	Mechanistic
Paterson, A.J.C.	1990	non-Newtonian

Table 7.1 : Analytical models included in the computer program

Each of the above analytical models can be classified as either empirical (or semi-empirical), mechanistic or non-Newtonian in formulation. The models in each of these categories will briefly be explained below.

7.2.1 Empirical or semi-empirical models

The empirical models included in the computer program are based on the following publications.

DURAND MODEL

Durand, R. (1953) "Basic relationships of the transportation of solids in pipes - experimental research" Proc. Minnesota Int. Hydraulics Convention Int. Assoc. for Hydraulic Research, p.89-102.

Faddick, R. (1982) "Settling slurries" Course preceding Hydrotransport 8, Johannesburg, B.H.R.A., p.27-42.

NEWITT MODEL

Newitt, D.M., Richardson, J.F., Abbott, M., Turtle, R.B. (1955) "Hydraulic conveying of solids in horizontal pipes" Trans. Inst. Chem. Engrs. v.33, p.93-113.

WASP MODEL

Wasp, E.J., Regan, T.J., Withers, J., Cook, P.A.C., Clancey, J.T. (1963) "Cross country coal pipeline hydraulics" Pipe Line News v.35, p.20-28.

Wasp, E.J., Aude, T.C., Kenny, J.P., Seiter, R.H., Jacques, R.B. (1970) "Deposition velocities, transition velocities, and spatial distribution of solids in slurry pipelines" Hydrotransport 1, B.H.R.A., p.H4-53/76.

Wasp, E.J., Aude, T.C., Seiter, R.H., Thompson, T.L. (1971) "Hetero-Homogeneous solids/liquid flow in the turbulent regime" Advances in solid-liquid flow in pipes and its application (I.Zandi, Ed.) Oxford Pergamon p.199-210.

The traditional approach to determine the pressure gradient for a solid-water mixture is largely empirical, based on the well known Durand type correlation shown below.

$$\phi = K \Psi^{m} \qquad (7.1)$$

where ϕ = head loss parameter

$$= \frac{(i_m - i_w)}{C_v - i_w}$$

Ψ = flow regime parameter

$$= \frac{V_m^2 \sqrt{C_D}}{gD}$$

C_D = drag coefficient of representative particle, normally for the d_{50} particle size.

K,m are experimentally derived constants specific to the slurry type.

This is the essential form of the Durand and Newitt correlations used in the program. The parameters K and n are fixed depending on the model chosen and are those used in the references. The Newitt correlation distinguishes between three types of slurry flow, namely sliding, heterogeneous and pseudo homogeneous and for these three phases the constant K is 66, 1 100 and 1 respectively. The Durand constant K varies from 60 to 180 depending upon slurry type. The Wasp correlation uses the Durand expression to account for the heterogeneous portion of the slurry based on the distinguishing criterion given by Wasp (1971).

The Durand correlation was specifically developed from a series of tests on graded sands and gravels and is strictly only valid for similar material types. Hanks (1982) states that 'uncertainties of the order of ± 40% may be expected from the Durand correlation". As with all empirical solutions, the empirically derived equations describing the behaviour of the data is only valid for the range of measured data from which the empiricism is derived.

To extend the Durand correlation to accommodate a broader range of slurry types, Wasp developed the 'vehicle' concept. The vehicle portion of a slurry is that portion which replaces the carrier fluid as

the support medium and is comprised of the carrier plus those particles below a certain critical size range. The Wasp method was initially derived to calculate the pressure gradient for coal-water slurries and is often used for fully suspended mixed regime flow. Low concentration backfill slurries can be classified as mixed regime or heterogeneous slurries.

7.2.2 Mechanistic models

The mechanistic models included in the computer program are taken from the following references.

WILSON MODEL

Wilson , K.C. (1974) "Co-ordinates for the limit of deposition in pipeline flow", Proc. Hydrotransport 3, B.H.R.A., p.A1-1/16.

Wilson , K.C. (1976) "A unified physically-based analysis of solid liquid pipeline flow" Proc. Hydrotransport 4, B.H.R.A., p.A1-1/12.

Wilson. K.C., Judge, D.G. (1977) "Application of analytic model to stationary-deposit limit in sand-water slurries" 2nd. Int. Symp. on dredging Tech., B.H.R.A., p.J1-1/11.

Wilson, K.C. (1980) "Analysis of slurry flow with a free surface" Proc. Hydrotransport 7, B.H.R.A, p.123-132.

LAZARUS MODEL

Lazarus, J.H. (1989) "Mixed regime slurries in pipelines. I: Mechanistic Model", Journal of Hydraulic Engineering, Vol. 115, No. 11, pp.1496-1509.

SIVE MODEL

Sive, A.W. (1988) "An analytical and experimental investigation of the hydraulic transport of high concentration mixed regime slurries" PhD Dissertation, University of Cape Town, South Africa.

The Wilson model is based on a force balance analysis of a sliding bed flow situation. This approach, known as mechanistic modelling, was later used by Lazarus and Sive to analyse mixed regime slurries. Streat uses a mechanistic approach to model dense phase slurries and for the special case of solids volumetric delivered concentration being equal to the solid packing concentration, a simplified "dense-phase sliding plug" equation is used, represented in Equation 7.2. This equation is entirely dependant upon the correct assessment of μ_s , the coefficient of sliding friction, and needs to be used with care. The equation will generally over-predict the pressure gradient when using typical μ_s values.

$$i_T = 2\,\mu_s\,(S_s - 1)\,C_{vt} + \left(\frac{S_m}{S_w}\right) i_w \qquad (7.2)$$

where i_T = total pressure gradient in metres of water.

The mechanistic Lazarus model consists of 3 primary components - a vehicle portion, a suspended portion and a bed load portion. The vehicle portion is the solids carrier component consisting of the slow non-settling solid particles. The model uses a particle Reynolds number of unity, which corresponds to a particle size of approximately 110 μm for full plant tailings, as the criterion for designating the vehicle portion of the slurry and determining the modified viscosity of the vehicle.

The suspended load portion is determined by dividing the particle size fractions into a suspended portion and a bed load portion using the mean mixture velocity at the threshold of turbulent suspension as the criterion. The remaining solids constitute the bed load portion occupying a fraction of the pipe area. This fraction is determined using Newton's method of approximation to calculate the bed load surface width.

7.2.3 Non-Newtonian models

The yield pseudoplastic rheological model is included in the program. This model is often called the "generalized" yield power law model as it can be used to represent the majority of non-Newtonian fluid types. The full derivation of this model is given in Appendix A and is based on the following references.

YIELD PSEUDOPLASTIC MODEL

Skelland, A.H.P. (1967) "Non-Newtonian flow and heat transfer", John Wiley and Sons Inc., New York.

Govier and Aziz (1972) "The flow of complex mixtures in pipes", Van Nostrand Reinhold, New York 1987 Reprint edition.

Wasp, E.J., Kenny, J.P. and Ghandi, R.L. (1979) "Solid-liquid flow slurry pipeline transportation", Gulf Publishing Co., Houston.

7.3 The computer program

Appendix C contains the program information and operating procedure.

The program is intended to be used as an interactive design tool in the Computer Aided Design of a pipeline system. The major program features are listed below.

1. The mathematical models commonly used by the industry are included in the program.

2. The advantages of the efficient data file format allows for the compilation of an accurate historical data-base of a range of different data, which can be accessed at any time for further analysis.

3. Sophisticated interactive editing of the variables allows for flexibility in the optimization of a pipeline design through rapid sensitivity analyses on any of the input variables.

4. The unique tabular interaction of the selection of mathematical models makes comparisons quick and effective using a log standard error.

5. The analysis of existing pipe systems can be quickly performed to determine limiting operating conditions.

6. Optimization of existing systems to achieve maximum efficiency can be quickly done.

7. The program is entirely user interactive and can be run with a minimum of training.

7.4 Comparison of analytical models

The analytical models are compared on the basis of the log standard error of the variation of calculated and measured pressure gradients. The log standard error is given by Equation 7.4.

$$\text{log standard error} = \sqrt{\frac{\sum_{i=1}^{n}\left[\left(\log_{10}(\text{observed}) - \log_{10}(\text{calculated})\right]^2\right.}{(n-1)}} \qquad (7.4)$$

where n = number of data points.

The computer program optionally calculates the log standard error for each of the chosen correlations compared to a unique set of measured data points. The log standard error gives an indication of which model best approximates the measured data.

7.5 Comparison of empirical and mechanistic analytical models with the measured data using the computer program

The computer program was used to compare the mechanistic and empirical models with the measured data presented in Chapter 5. None of these models are for non-Newtonian fluids and do not have the capability to include non-Newtonian vehicle properties. This analysis demonstrates the range of applicability of the models when using them to predict the flow behaviour of full plant tailings.

Using the data represented in Chapter 5 and plotting the results of the analysis for each set of observed data points on the standard pressure gradient versus mean mixture velocity curve, a set of log standard errors was obtained. A typical pressure gradient versus mean mixture velocity curve for a set of data points for all the models is shown in

Figure 7.1. The bar chart in Figure 7.2 represents the results of the analysis, showing the overall log standard error for each model for each pipe diameter and the overall error for the full range of pipe diameters.

The results are not in close agreement and are summarised in Table 7.1. The models with the smallest overall log standard error are those of Lazarus and Sive, being 0,13 and 0,14 respectively. This corresponds to errors 1,35 times as large as the measured data (antilog of 0,13 = 1,35).

D (mm)	Lazarus	Sive	Wilson	Wasp	Newitt	Streat	Pseudo	Durand
41,5	0,0425	0,0429	0,0580	0,0460	0,0577	0,1150	0,0578	0,1152
101,5	0,2540	0,2534	0,2912	0,2414	0,2394	0,2816	0,2902	0,3174
13,48	0,1030	0,0913	0,1500	0,1310	0,1503	0,0500	0,1503	0,2880
32,63	0,1557	0,1482	0,2100	0,1785	0,2108	0,0865	0,2108	0,2835
Total % Error	0,1365	0,1329	0,1719	0,1439	0,1576	0,1444	0,1717	0,2262

Table 7.2 : Mean log standard error (LSE) for each model

The worst model is that of Streat, with errors of up to 275%, but this is not unexpected as it was derived for a dense phase packed moving bed with a Newtonian carrier. Full plant tailings have a vehicle carrier which is most non-Newtonian in behaviour and this accounts for the large errors in the analysis. The mechanistic models assume Newtonian behaviour for the determination of the vehicle carrier and do not take into account the non-Newtonian yield stress. The definition of the fine vehicle portion as being those particles less than 110 μm (i.e. Rep = 1) does not apply for high concentration full plant tailings behaviour, as a significant percentage (80%) of the particles are below 100 μm and constitute a fully occupied bed load. The mechanism of flow at high concentration is not the same as for mixed-regime flow and the theory is extended beyond its basic formulation.

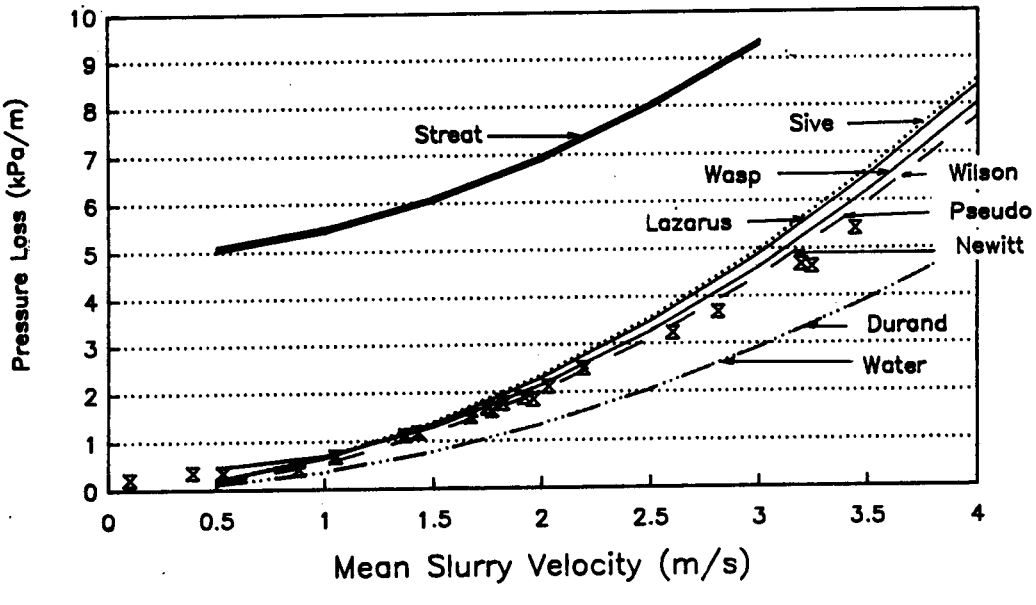

Figure 7.1 : Typical pressure gradient versus mean vertical velocity curve obtained using the models in the computer program

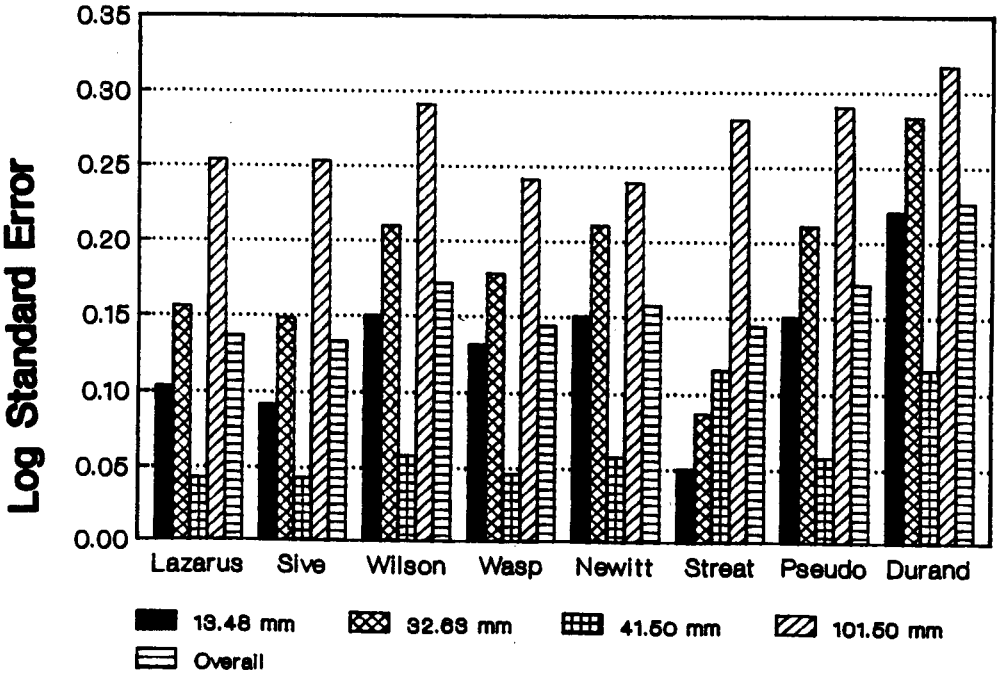

Figure 7.2 : Bar chart representing the overall log standard errors for each of the models used when analysing full plant tailings

The effect of slurry relative density on the accuracy of the model correlations is shown in Figures 7.3 to 7.6. All the analytical models show similar trends. The correlations of Newitt and Wilson approximate the Pseudo fluid correlation and the results are similar. In each instance, the Durand correlation has the highest overall error for these slurry types. This is because an important feature of the empirical correlation is the apparent mean drag coefficient of the settling solids, which for a fine settling slurry is small, and the correlation therefore approaches the clear water friction head loss. The Wasp correlation yields results similar to those of Lazarus and Sive, but the associated error is generally larger. The models of Lazarus and Sive follow the same trend and approximate to a similar solution. It is important to note that all the models under-predict the pressure losses for full plant tailings by the amount given by the log standard error.

For each pipe diameter size, there is a sudden decrease in the accuracy of the models with an increase in slurry density at a specific critical slurry density (S_{mc}). An important feature is that the density at which the increase occurs (S_{mc}) is not consistent with pipe diameter. At two lower diameters of 13,48 mm and 32,63 mm respectively, the increase occurs at S_{mc} = 1,65 for most of the models (at a log standard error of 0,10) and then increases substantially at relative densities greater than 1,65. In the 41,50 mm diameter pipeline, the results indicate that the correlations error increases significantly at $S_{mc} > 1.75$ for a log standard error of 0,05. At the larger pipe diameter of 101,5 mm, the log standard error increases significantly at $S_{mc} > 1,70$.

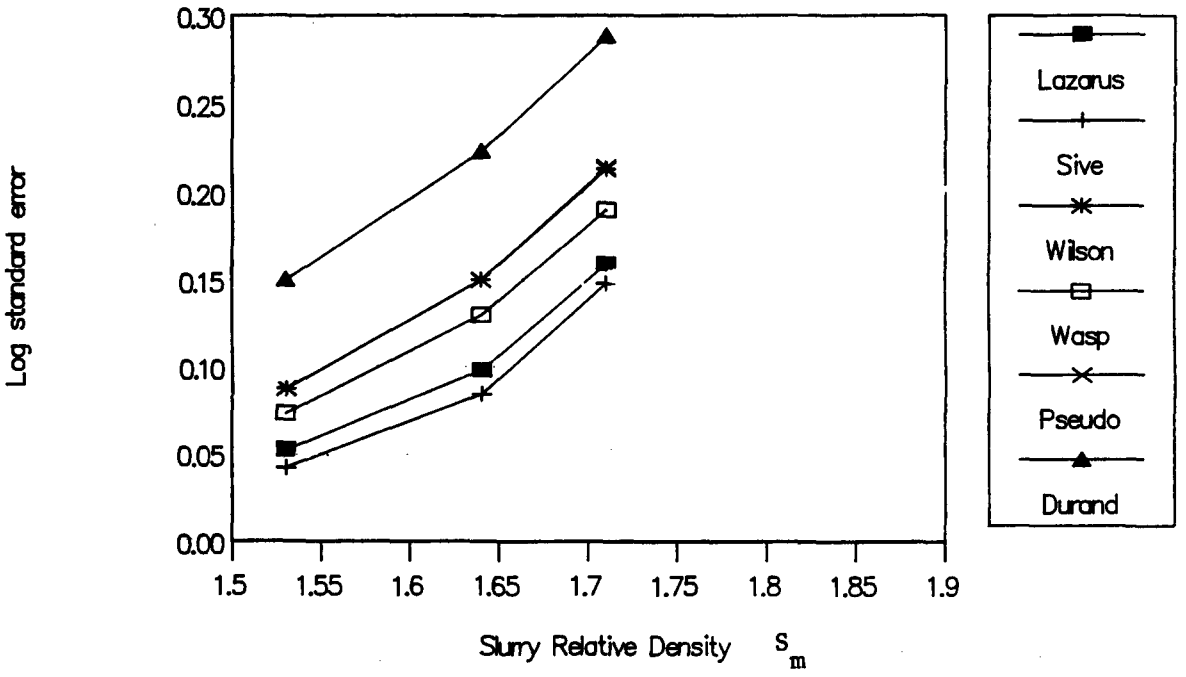

Figure 7.3 : Log standard error versus slurry relative density D = 13,48

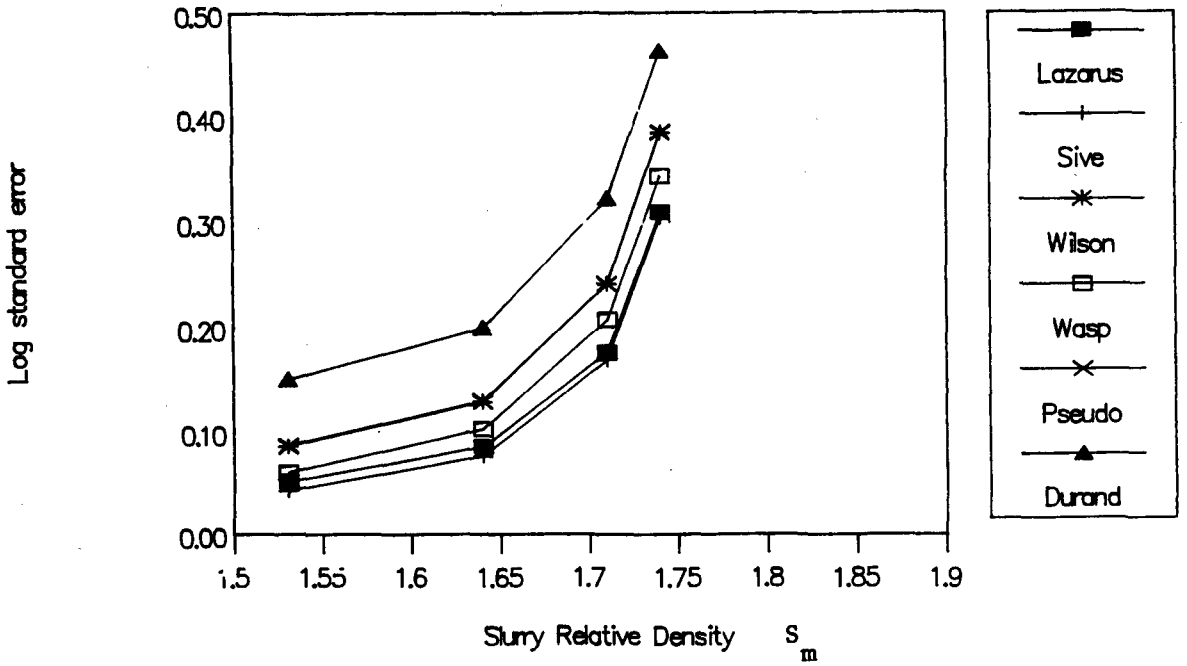

Figure 7.4 : Log standard error versus slurry relative density D = 32,63

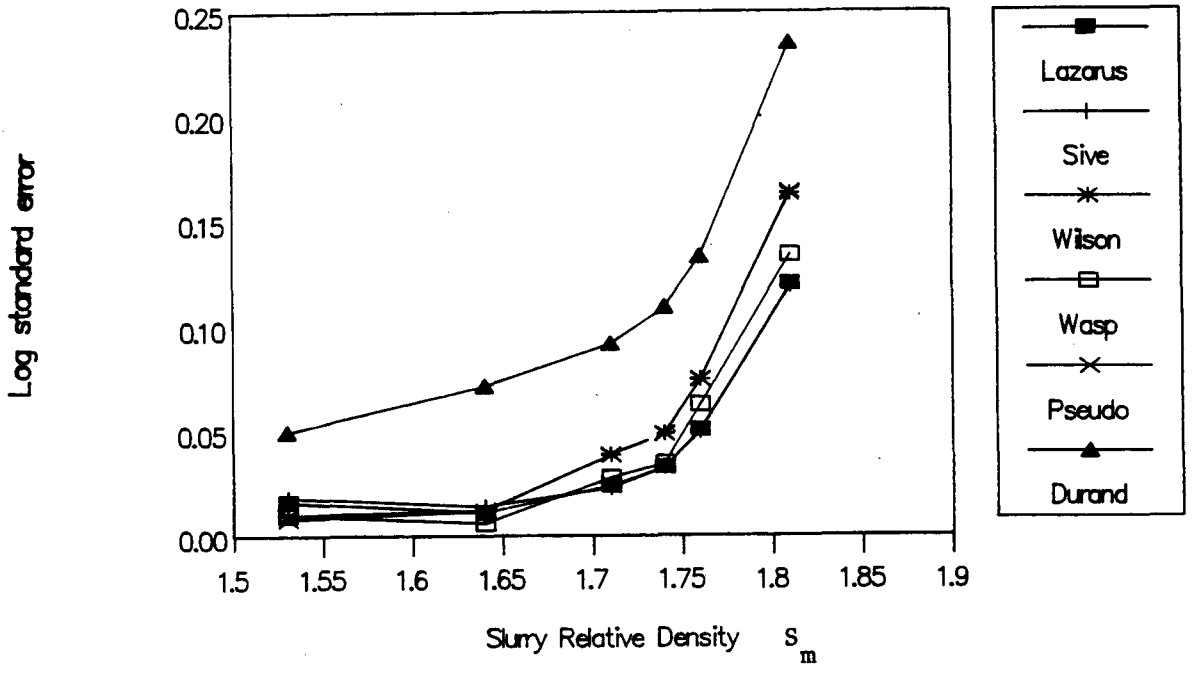

Figure 7.5 : **Log standard error versus slurry relative density D = 41,5**

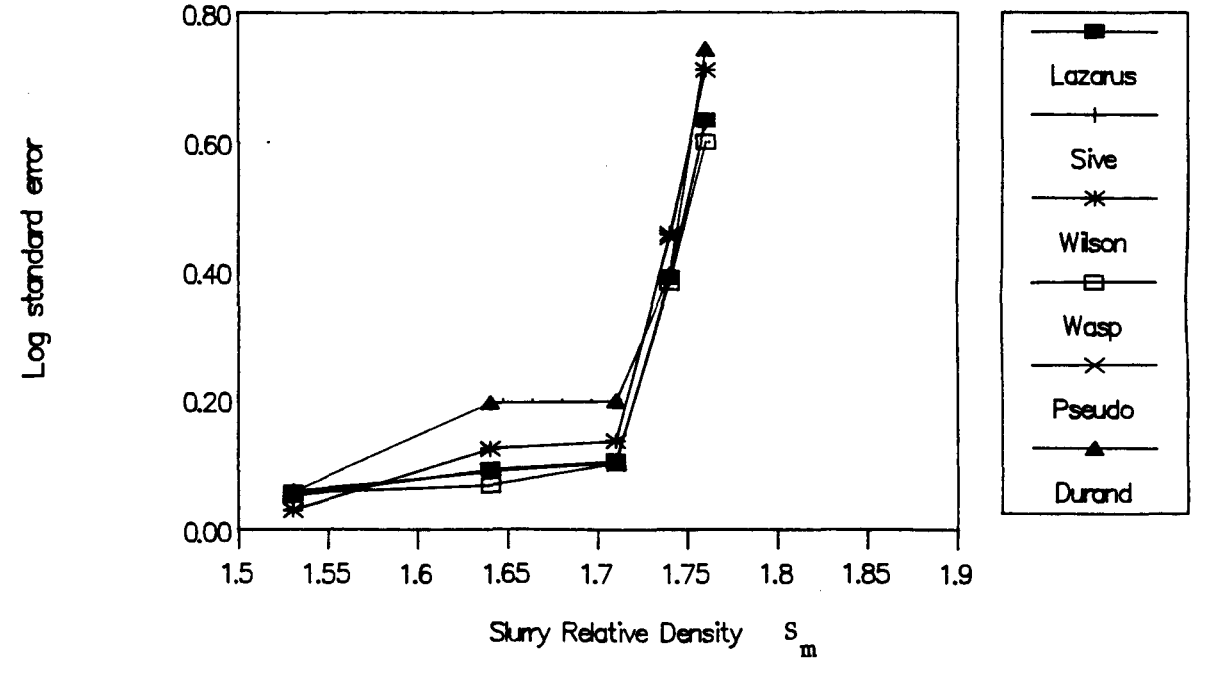

Figure 7.6 : **Log standard error versus slurry relative density D = 101,5**

7.6 Conclusions

1. Based on this computer analysis it is shown that the empirically derived models for heterogeneous flow regimes are not suitable for design use when analysing full plant tailings above a specific value of slurry density S_{mc}.

2. An increase of slurry density above S_{mc} in a specific pipe diameter has a marked effect on the accuracy of the correlations.

3. The slurry density at which the correlations begin to be invalid (S_{mc}) varies with change in pipe diameter.

4. The correlations with the lowest log standard error are the mechanistically based models of Lazarus and Sive. These are valid for the following pipe diameters and relative density range :

D	Maximum S_m	Log Standard Error	
		Sive	Lazarus
13,48	1,65	0,0420	0,0520
32,63	1,65	0,0430	0,0520
41,50	1,75	0,0500	0,0540
101,50	1,50	0,0580	0,0510

CHAPTER 8

COMPARISON OF PROPOSED ANALYTICAL MODEL WITH EXPERIMENTAL DATA

8.1 Introduction

This chapter contains the comparison of the non-Newtonian analytical models in the computer program with the measured data. The models analysed are the current analytical model and the yield pseudoplastic rheological model.

8.2 Comparison of model results with data

The models are compared with the measured data in two ways :

1. Direct comparison between model predicted pressure gradient and measured data at velocities of 1 m/s and 3 m/s.

2. Comparison based on the log standard error analysis discussed in Chapter 7. The models are compared over velocities ranging from 1 m/s to 4 m/s.

Each comparative analysis includes a graph of measured and predicted pressure gradient versus slurry relative density, S_m , and a graph of the log standard error versus slurry relative density, S_m .

8.2.1 Analysis of results

Figure 8.1(a) represents measured and predicted pressure losses for the 13 mm NB pipeline. The data indicates a rapid increase in pressure gradient with increasing slurry relative density, particularly at concentrations greater than S_m = 1,76. The current model follows this trend and predicts values in close agreement with the data. The yield pseudoplastic analysis under-predicts the pressure gradient at the higher solids concentrations. The increase in magnitude of the solid pressure gradient with increasing slurry relative density is indicated by the difference between the current correlation and the yield pseudoplastic model.

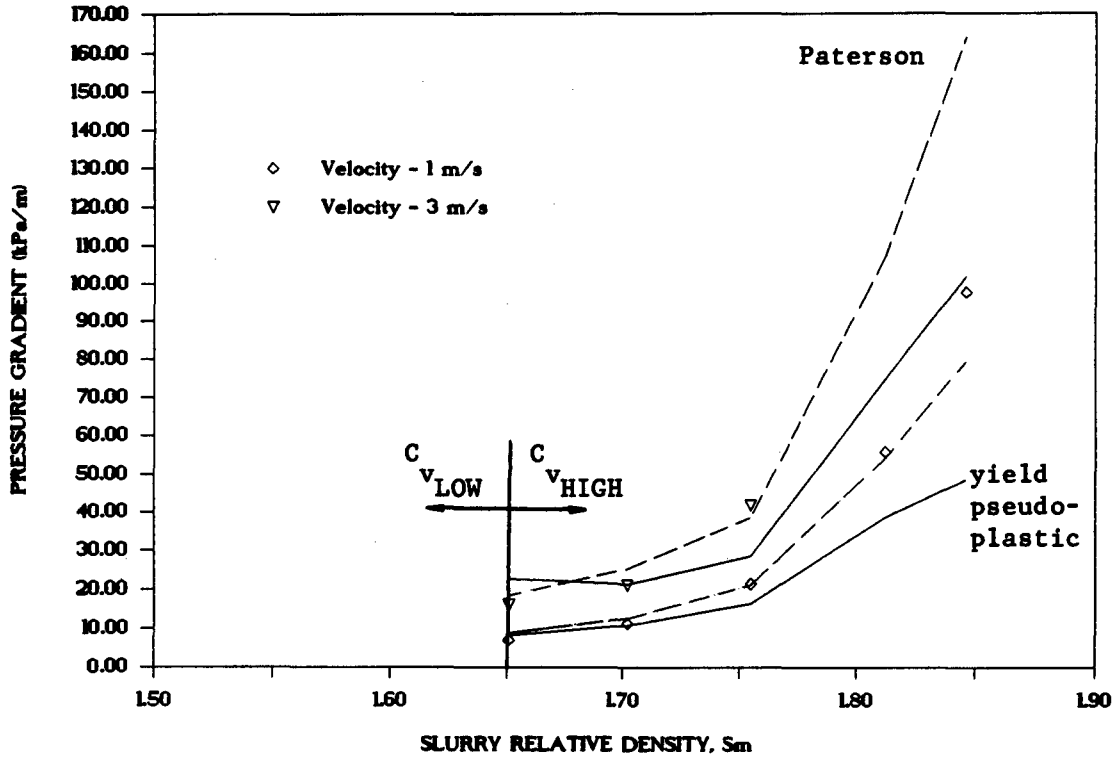

Figure 8.1(a) : Measured and predicted pressure losses : I.D. = 13,48 mm

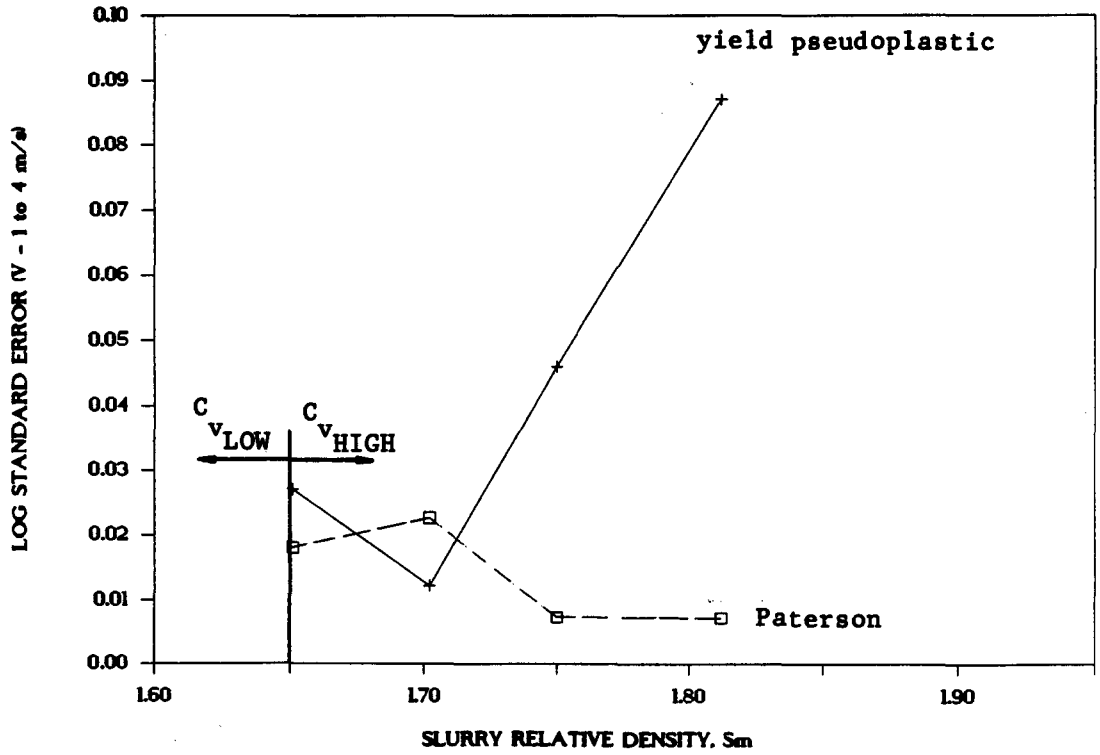

Figure 8.1(b) : Log standard error versus slurry relative density : I.D. = 13,48 mm

The curve of the log standard error versus slurry relative density, Figure 8.1(b), indicates the increase in accuracy of the current model as the solids relative density increases. The yield pseudoplastic model results clearly do not correlate well at the higher solids concentrations.

Results from the 32 mm NB pipeline indicate similar trends to the 13 mm NB test data. Figure 8.2(a) indicates the rapid increase in pressure gradient with increasing slurry relative density and the current model follows this trend. The yield pseudoplastic model consistently under-predicts the pressure gradient and indicates the viscous pressure gradient. The log standard error analysis indicates the relative accuracy of each of the correlations and is shown in Figure 8.2(b).

Figures 8.3(a) and 8.3(b) represent the results of the error analysis for the 75 mm NB test section. At low solids concentrations the flow is predominantly turbulent for velocities of 1 and .3 m/s respectively and the correlations do not accurately represent the measured data. At high solids concentrations, the current model predicts the flow behaviour reasonably well. The log standard error curve, Figure 8.3(b), indicates this and the transition from low to high solids concentration flow is indicated by a corresponding increase in the accuracy of the current model predictions.

This increase in accuracy of the model predictions is clearly seen for the 100 mm NB test data, represented in Figures 8.4(a) and 8.4(b). The current model accuracy increases sharply with increasing solids concentration. At low solids concentration there is a marked difference between the current model and the yield pseudoplastic model. Both models assume smooth wall turbulent flow exists and the Torrance (1963) correlation is used. The difference between the models is that the current model uses the Hanks (1974) criterion to identify the laminar to turbulent transition, and the yield pseudoplastic model uses the Dodge and Metzner (1959) laminar-turbulent transition. At high solids concentrations, the method of Hanks (1974) was shown to predict the laminar to turbulent transition of the full plant tailings (Figure 6.?).

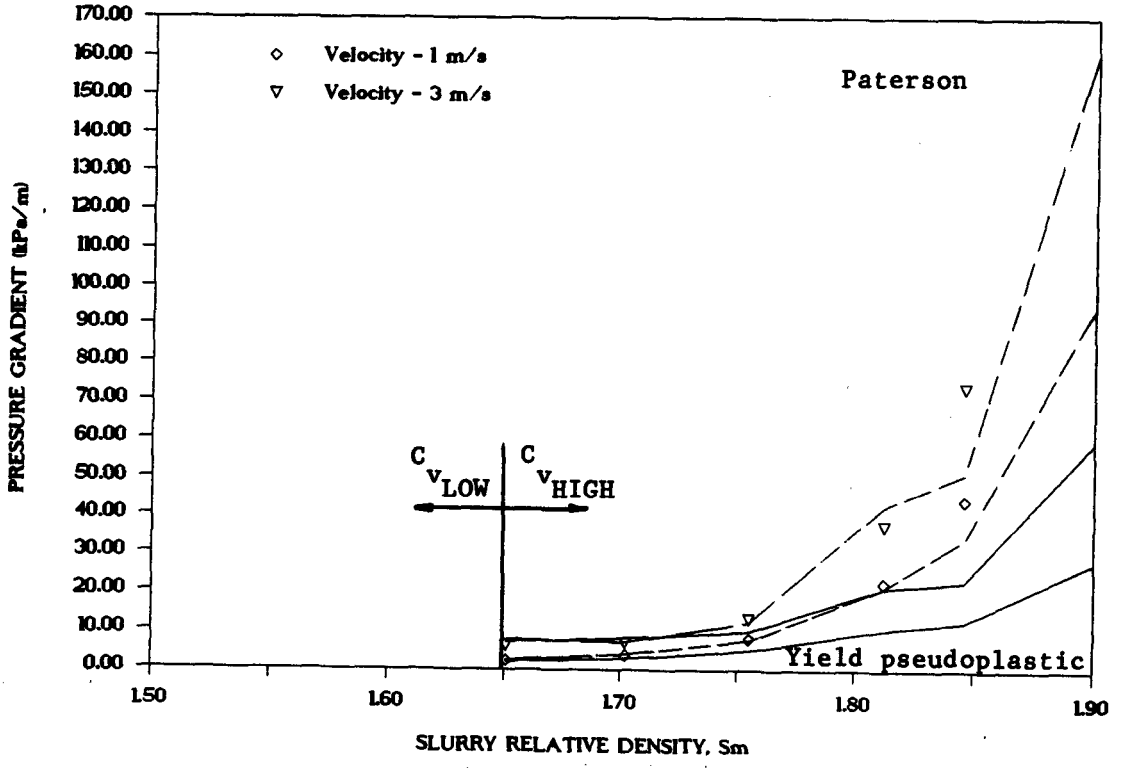

Figure 8.2(a) : Measured and predicted pressure losses : I.D. = 32,63 mm

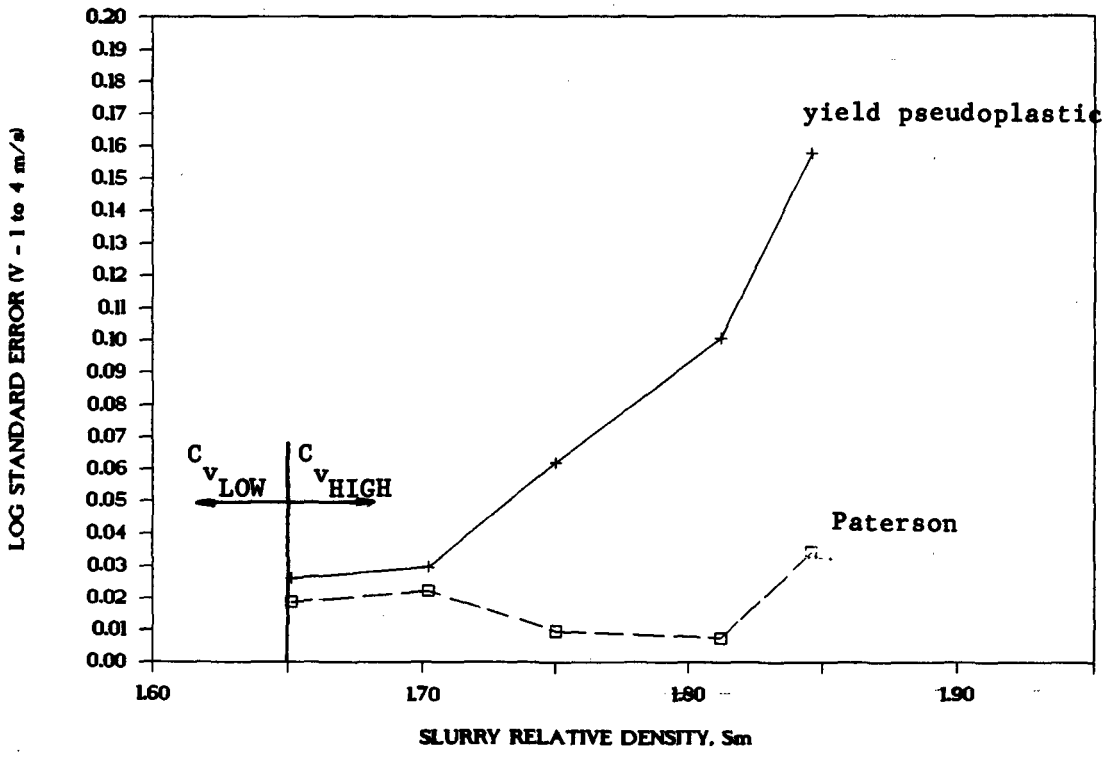

Figure 8.2(b) : Log standard error versus slurry relative density : I.D. = 32,63 mm

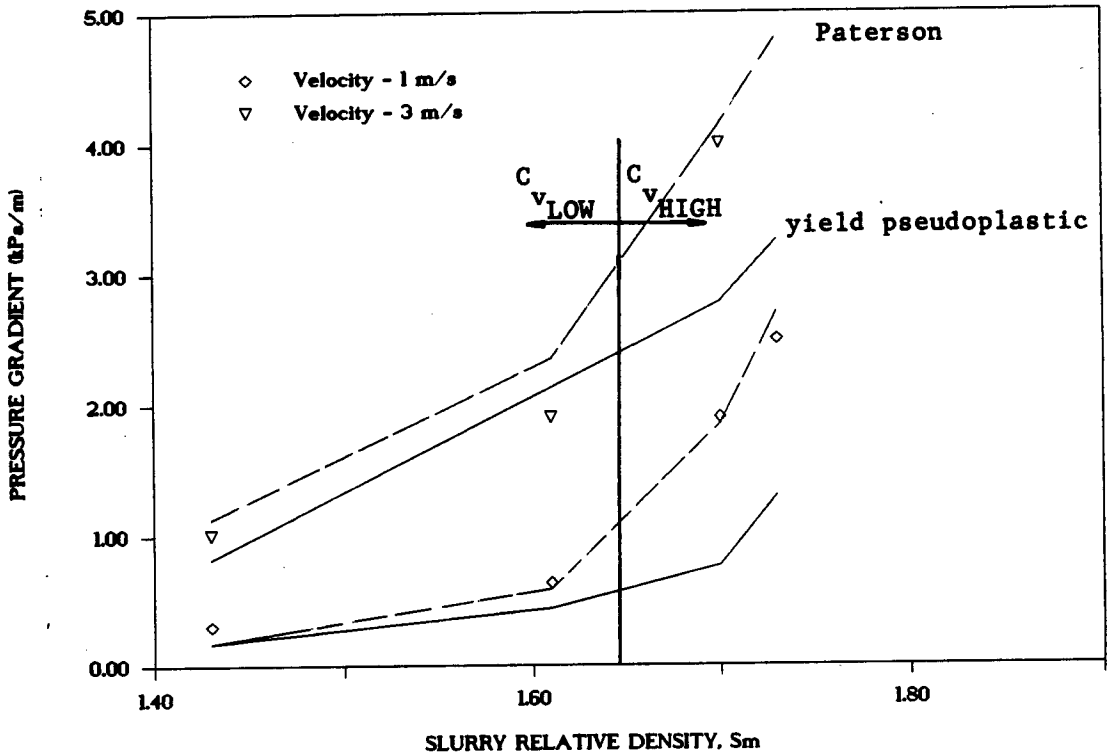

Figure 8.3(a) : Measured and predicted pressure losses : I.D. = 75,88 mm

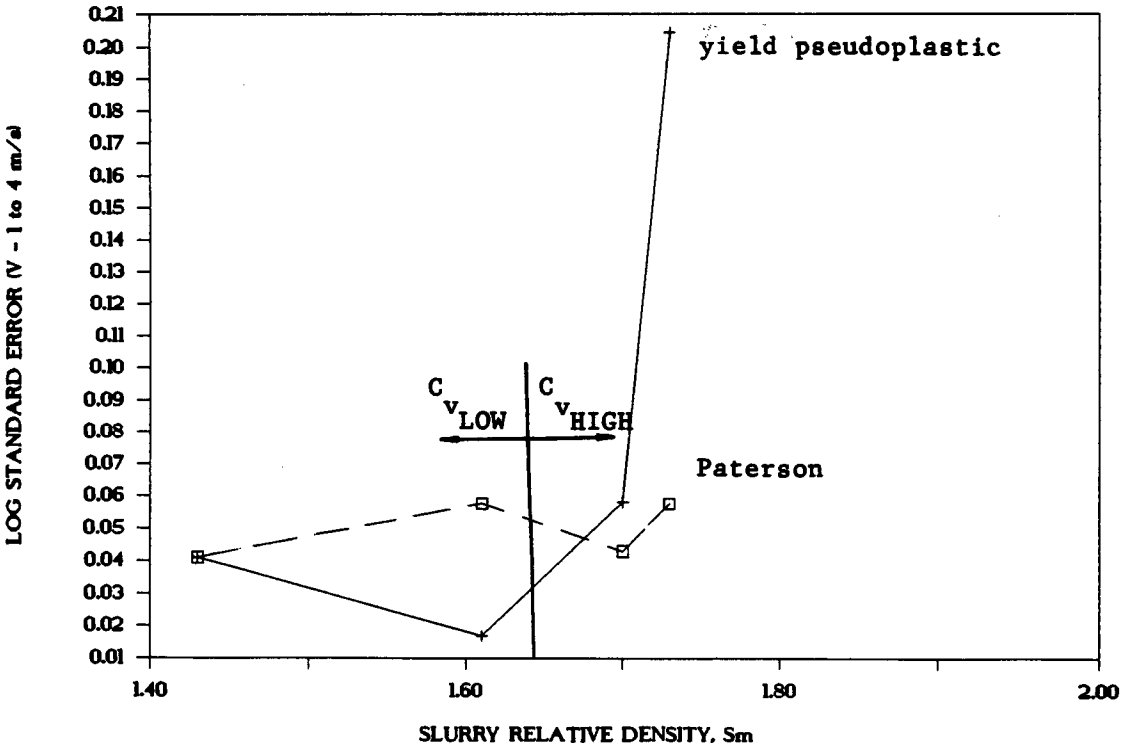

Figure 8.3(b) : Log standard error versus slurry relative density : I.D. = 75,88 mm

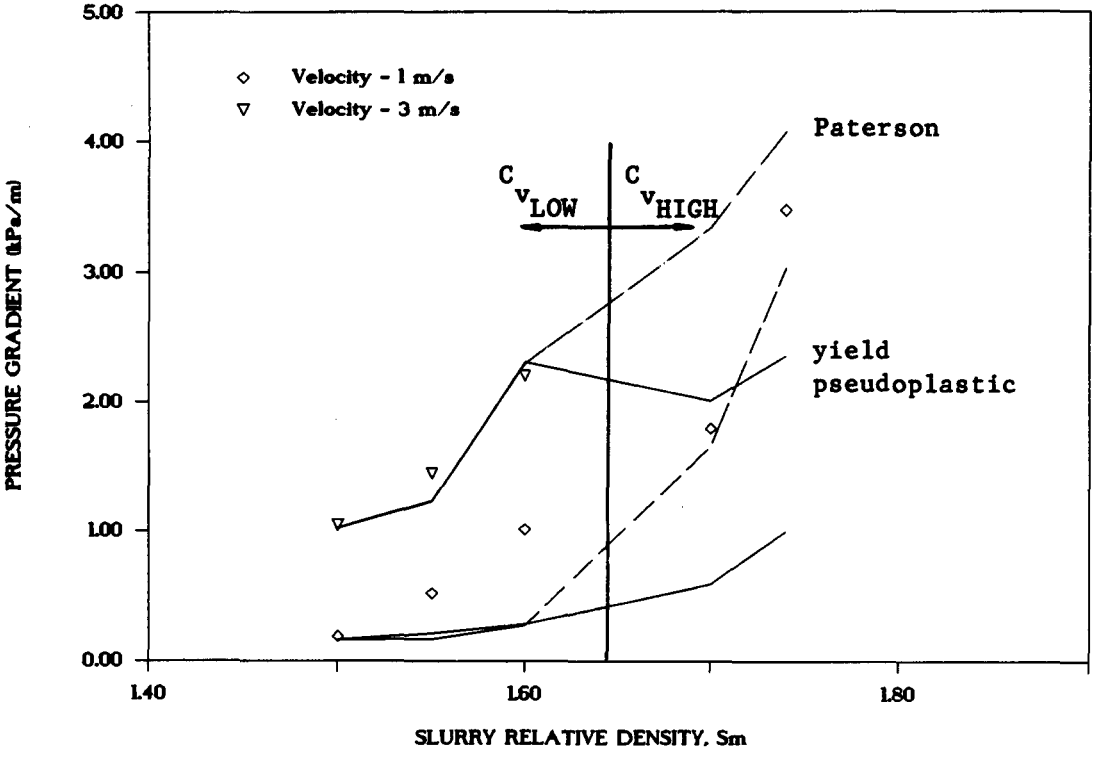

Figure 8.4(a) : Measured and predicted pressure losses : I.D. = 101,50 mm

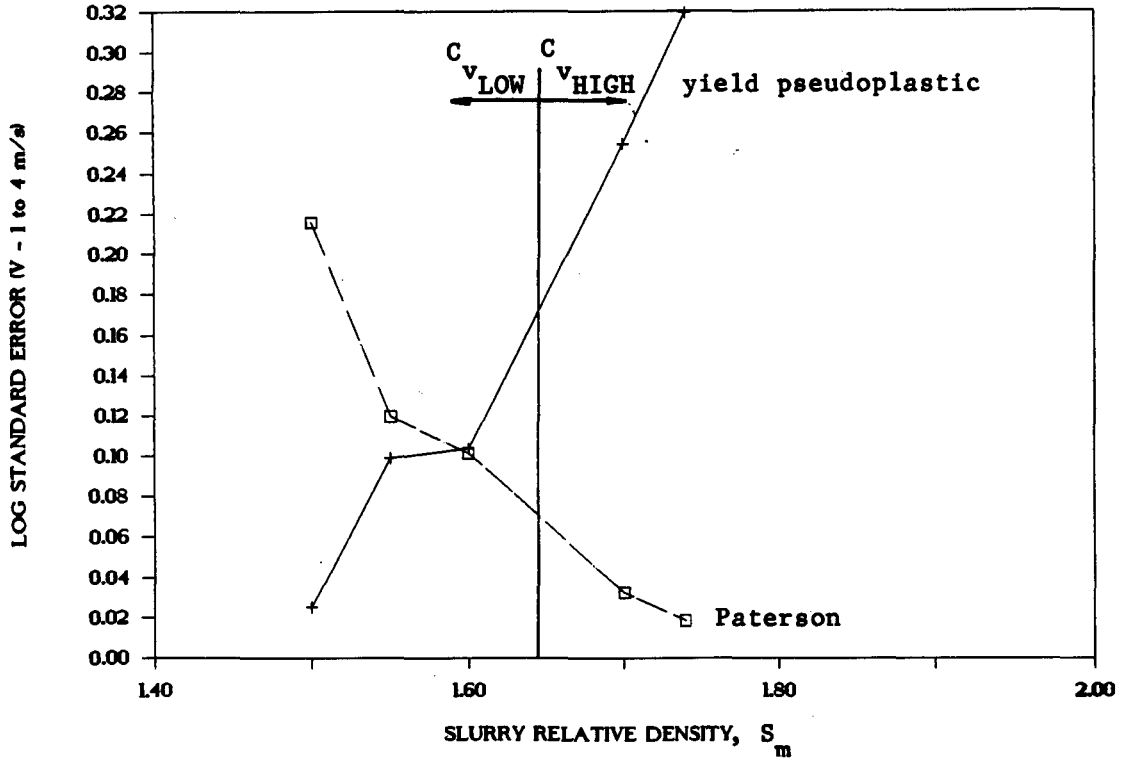

Figure 8.4(b) : Log standard error versus slurry relative density : I.D. = 101,50 mm

The results for these series of error analysis curves are summarised in Table 8.1. The current analytical model has the lowest average log standard error of 0,03977, compared to 0,07956 for the yield pseudoplastic model. Comparison of these results with the results obtained using the mechanistic and empirical model correlations obtained in Chapter 7, indicates that the current model compares favourably to other commonly used correlations. From Table 7.7 (p.7.9) and Table 8.1, it is clear that the current model produces the most consistent results for predicting the flow behaviour of full plant tailings at high concentrations.

Diameter (mm)	S_m	C_v (%)	Log Standard Error Paterson	Yield Pseudoplastic
13,480	1,651	37,414	0,0181	0,0271
	1,702	40,345	0,0227	0,0123
	1,705	43,103	0,0073	0,0460
	1,812	46,667	0,0072	0,0871
32,630	1,651	37,414	0,0186	0,0259
	1,702	40,345	0,0221	0,0300
	1,750	43,103	0,0097	0,0620
	1,812	46,667	0,0074	0,1006
	1,846	48,621	0,0344	0,1578
75,880	1,430	24,713	0,0410	0,0410
	1,610	35,057	0,0576	0,0168
	1,700	40,230	0,0429	0,0581
	1,730	41,954	0,0576	0,2044
101,500	1,500	28,736	0,2159	0,0254
	1,550	31,609	0,1199	0,0990
	1,600	34,483	0,1015	0,1039
	1,700	40,230	0,0327	0,2543
	1,740	42,529	0,0186	0,3194
Average Log Standard Error			0,03977	0,07956

Table 8.1 : Log standard error analysis of pumped data

8.3 Conclusions

1. The proposed model successfully predicts the flow behaviour of pumped high concentration full plant tailings.

2. The model is valid for a diameter range of 13 mm NB to 100 mm NB at solids concentrations greater than the freely settled solids concentration, C_{bfree} .

3. At low solids concentrations, the yield pseudoplastic model adequately describes the flow behaviour of full plant tailings. At high solids concentrations the yield pseudoplastic model is inadequate and the proposed model is required.

4. The correlations developed for the slurry yield stress, τ_y , the fluid consistency index, K , and the flow behaviour index, n , describe the viscous flow of low concentration full plant tailings and the viscous component of high concentration full plant tailings.

5. The current model replaces the commonly used mechanistic and empirical correlations for the hydraulic transport of high concentration full plant tailings.

PART FIVE

CONCLUSIONS

CHAPTER 9

CONCLUSIONS AND RECOMMENDATIONS

This research makes a direct contribution to the understanding of the flow mechanisms of high concentration full plant tailings. Previous research failed to provide an adequate explanation of, and a mathematical model for, the flow behaviour of these types of slurries.

9.1 The major contributions of this thesis are :

9.1.1 High concentration flow

This research identified the need for a distinguishing criterion between low solids volumetric concentration and high solids volumetric concentration. Experimental results showed that the slurry flow changed dramatically at a critical solids concentration. This critical transition is determined from the measurement of the submerged freely settled particle packing concentration. Low concentration slurry flow exists at a solids concentration less than the freely settled solids concentration. High concentration slurry flow occurs for solids concentrations greater than the freely settled concentration and up to the maximum possible solids concentration.

9.1.2 Anomalous behaviour

"Anomalous" behaviour at high concentrations was identified on a rheogram. The behaviour manifested itself as different rheograms for different pipe diameters. The "anomalous" behaviour of high concentration full plant tailings is accounted for in this thesis. It is determined that the "anomalous" behaviour is due to the presence of both a viscous wall shear stress component and a solid wall shear stress component. The solid wall shear stress is due to direct particle-particle contact. This results in a lateral dispersive stress which causes the particles to interact with the pipe wall, resulting in the solid wall shear stress. The solid wall shear stress is significant in altering the rheogram at high solids volumetric concentrations.

9.1.3 Analysis of viscous shear component

A novel method is developed to "subtract" the viscous shear stress component from the total measured wall shear stress. An "anomalous" set of curves on a pseudo shear diagram is transformed to represent the viscous wall shear stress only.

9.1.4 Analysis of solid shear stress component

A method is developed to predict the solid shear stress component for high concentration full plant tailings.

9.1.5 Analytical model

An analytical model is formulated that predicts the pressure gradient required to transport high concentration full plant tailings.

9.1.6 Database

A detailed experimental investigation provided a large database of measured results which was used to evaluate several existing analytical models as well as various models proposed in this thesis to account for "anomalous" behaviour.

9.1.7 Computer program

A unique and sophisticated interactive computer program is developed. The computer program can be used for the design and analysis of slurry pipeline systems. This program fills a direct need in the mining industry and has immediate applications.

9.2 The flow behaviour of full plant tailings

9.2.1 Low concentration full plant tailings are time independent non-Newtonian slurries.

9.2.2 Low concentration full plant tailings can be modelled using the yield pseudoplastic constitutive equation.

9.2.3 Full plant tailings are stabilized slurries. No settling of particles occurs at high solids concentration.

9.2.4 Coarse particles remain uniformly suspended in the full plant tailings slurry. Section 4.5

9.2.5 Full plant tailings exhibit a rapid increase in pressure gradient with increasing slurry relative density beyond the freely settled volumetric concentration. This is an important feature of high concentration flow.

9.2.6 The yield stress, τ_y, and the fluid consistency index, K, of the viscous component increase steeply with increasing slurry relative density. steepness of Diagram

9.2.7 The flow behaviour index, n, of the viscous component decreases with increasing solids concentration (up to C_v = 44%) and then increases at higher concentrations. curvature

9.2.8 Turbulent flow is characterized by a rapid increase in pressure gradient with increasing velocity.

9.3 <u>The analytical model</u>

9.3.1 The analytical model describes the flow behaviour of high concentration full plant tailings.

9.3.2 The total wall shear stress that exists at high concentrations is due to both a viscous wall shear stress and a solid wall shear stress component.

9.3.3 The viscous wall shear stress component is determined from a set of anomalous curves on a psuedo shear diagram.

9.3.4 The parameters of τ_y, K and n analysed for the viscous portion of the slurry are determined using the yield pseudoplastic model. They can also be used to model the low concentration flow behaviour of full plant tailings.

9.3.5 The solid pressure gradient is described by the presence of a radial dispersive stress due to particle-pipe wall contact at concentrations greater than the freely settled bed packing concentration.

9.3.6 The dispersive stress coefficient can be determined from analysis of the measured data and the viscous shear stress parameters.

9.3.7 The laminar to turbulent transition of high concentration full plant tailings can be predicted using the method of Hanks (1974).

9.3.8 Turbulent flow can be modelled using the smooth wall fully turbulent correlation of Torrance (1963).

9.4 Experimental investigation

9.4.1 The test facility constructed was capable of pumping high concentration full plant tailings.

9.4.2 Each data point was measured using a series of time averaged readings.

9.4.3 The measured data was subject to a detailed experimental error analysis.

9.4.4 Instruments were calibrated before each test run to ensure consistent results.

9.4.5 The data obtained from the test facilities is of a high standard.

9.5 Computer program

9.5.1 Mathematical models commonly used by industry are included in the computer program.

9.5.2 The data file handling format allows for the creation of a unified data base.

9.5.3 Interactive editing of the variables allows for flexibility in the optimization of a pipeline design through the rapid sensitivity analysis facility.

9.5.4 Models are compared on a common basis using the log standard error analysis.

9.5.5 The program is entirely user friendly and can be run with a minimum of training.

9.5.6 The program provides a valuable design tool for industry.

9.6 Analysis of the analytical models

9.6.1 All models were compared on the basis of the log standard error.

9.6.2 The existing mechanistic and empirical models presented are not suitable for design use when transporting full plant tailings. These models under-predict the required energy gradients.

9.6.3 The existing mechanistic and empirical models were not intended for use with these slurries, but nonetheless are still used by the industry for pipeline design.

9.6.4 The current model has the lowest overall log standard error when compared with the other models.

9.6.5 The current model is limited in use and is applicable only for pumped high concentration stabilized full plant tailings.

9.6.6 The current model can be used for the design of backfill reticulation systems to transport low and high concentration full plant tailings.

9.7 Future research recommendations

9.7.1 The transitional and turbulent flow of high concentration full plant tailings needs to be evaluated. This will entail an experimental research program.

9.7.2 The proposed technique to account for anomalous behaviour of full plant tailings should be investigated for other mineral tailings.

9.7.3 The definition of high concentration flow is based on the measurement of the particle packing concentration. This criterion should be evaluated for other slurries.

REFERENCES

REFERENCES

Abbas, M.A., Crowe, C.T. (1986), "The effect of particle size and concentration on the flow properties of a homogeneous slurry", Serial No. 76, p.109 - 112.

Ackermann, N.L., Shen, H.T. (1979), "Rheological characteristics of solid-liquid mixtures", *A.I.Ch.E. Journal*, v.25 n.2, p.327 - 332.

Al Taweel, A.M., "The role of aggregate formation in determining the rheology of highly-loaded dispersions", *Chem. Eng. Dept., Tech University of Nova Scotia*, p.417 - 433.

Alessandrini, A., Kikic, I., Lapasin, R., (1983), "Rheology of coal suspensions", *Rheologica Acta.*, v.22, p.500 - 504.

Apelblat, A., Healy, J.C., Joly, M., (1975), "Shear rate in the Couette viscometer with a narrow annular gap between cylinders. A new approximate formula", *Rheological Acta.*, v.14, p.976 - 978.

Ariman, T., Turk, M.A., Sylvester, N.D., (1975), "Suspension rheology - a micro-continuum approach", *Rheological Acta.*, v.14, p.385 - 393.

Ashare, E., Byron Bird, R., Lescarboura, J.A., (1965), "Falling cylinder viscometer for non-Newtonian fluids", *A.I.Ch.E. Journal*, v.11 n.5, p.910 - 916.

Asszonyi, C., Kapolyi, L., Meggyes, T. (1970), "Optimization of particle size in hydraulic pipelining of solids", *Proc. First Int. Conf. on the Hydraulic Transport of Solids in Pipes*, Paper K2, p.K2-21 - K2-37.

Asszonyi, C., Kapolyi, L., Kantas, C., Meggyes, T. (1972), "An experimental method to produce a size distribution ensuring maximum pipeline capacity", *2nd Int. Conf. on the Hydraulic Transport of Solids in Pipes*, Paper D3, p.D3-23 - D3-32.

Aude, T.C., Cowper, N.T., Thompson, T.L., Wasp, E.J. (1971), "Slurry piping systems: trends, design methods, guidelines", *Chemical Engineering*, p.74 - 90.

Aude, T.C., Thompson, T.L., Wasp, E.J. (1974), "Economics of slurry pipeline systems", *3rd Int. Conf. on the Hydraulic Transport of Solids in Pipes*, Paper K2, p.K2-13 - K2-24.

Baker, P.J., Jacobs, B.E.A., Bonnington, S.T. (1979), "A guide to slurry pipeline systems", *publ. BHRA Fluid Engineering*, p.10 - 13.

Bantin, R.A., Streat, M. (1970), "Dense-phase flow of solids-water mixtures in pipelines", *1st Int. Conf. on the Hydraulic Transport of Solids in Pipes*, Paper G1, p.G1-1 - G1-24.

Bantin, R.A., Streat, M. (1972), "Mechanism of hydraulic conveying at high concentration in vertical and horizontal pipes", *2nd Int. Conf. on the Hydraulic Transport of Solids in Pipes*, Paper B2, p.B2-11 - B2-24.

Barnes, H.A., Townsend, P., Walters, K. (1971), "On pulsatile flow of non-Newtonian liquids", *Rheological Acta.*, v.10, p.517 - 527.

Bhattacharyya, A., Imrie, I. (1986), "Development of the Asea mineral slurry transport system for coarse coal", *10th Int. Conf. on the Hydraulic Transport of Solids in Pipes*, Paper C1, p.63 - 67.

Boger, D.V., Nguyen, Q.D., Want, F.M., Colombera, P.M. (1982), "Pipeline design for the transport of high density Bauxite residue slurries", *8th Int. Conf. on the Hydraulic Transport of Solids in Pipes*, Paper E2, p.249 - 263.

Bowen, L.E.R. (1961), "Designing laminar flow systems", *Chem. Engng.*, v.68, p.243 - 248.

Briscoe, B.J., Radwan, H., Streat, M. (1983), "Model experiments on sliding friction for application in hydraulic conveying of solids", *Canadian Journal of Chemical Engineering*, v.61, p.769 - 775.

Brook, N. (1987), "Fluid transport of coarse solids", *Mining Science and Technology*, v.5, p.197 - 217.

Brookes, D.A., Dodwell, C.H. (1984), "The economic and technical evaluation of slurry pipeline transport techniques in the international coal trade", *9th Int. Conf. on the Hydraulic Transport of Solids in Pipes*, Paper A1, p.1 - 31.

Brookes, D.A., Snoek, P.E. (1986), "Stabflow slurry development", *10th Int. Conf. on the Hydraulic Transport of Solids in Pipes*, Paper C3, p.89 - 99.

Brookes, D.A., Snoek, P.E. (1987), "Stabflow slurry development", *Pipes and Pipelines International*, p.11 - 18.

Brown, G.S., (1987), "How to predict pressure drop before designing the piping", *Chemical Engineering*, p.85 - 86.

Brown, N.P. (19-21 October 1988), "Three scale-up techniques for stabilised coal-water slurries", *11th Int. Conf. on Hydraulic Transport of Solids in Pipes*, p.267 - 283.

Burgess, K.E., Reizes, J.A. (1977), "Effect of sizing, specific gravity, and concentration on the performance of centrifugal slurry pumps", *Institute of Mechanical Engineers*, p.12 - 13.

Castillo, C., Williams, M.C. (1979), "Rheology of very concentrated coal suspensions", *Chem. Eng. Commun.*, v.3, p.529 - 547.

Chan, D., Powell, R.L. (1984), "Rheology of suspensions of spherical particles in a Newtonian and a non-Newtonian fluid", *Journal of non-Newtonian Fluid Mechanics*, v.15, p.165 - 179.

Cheng, D.C.H. (1970), "A design procedure for pipeline flow of non-Newtonian dispersed systems", *First Int. Conf. on the Hydraulic Transport of Solids in Pipes*, Paper J5, p.J5-77 - J5-95.

Cheng, D.C.H. (1975), "Pipeline design for non-Newtonian fluids", *The Chemical Engineer*, p.525 - 588.

Chong, Y.O., Teo, C.S., Leung, L.S. (1987), "Recent advances in standpipe flow", *Journal of Pipelines*, v.6, p.121 - 132.

Clarke, B. (1967), "Rheology of coarse settling suspensions", *Trans. Instn. Chem. Engrs.*, v.45, p.T251 - T256.

Cohen, Y., Metzner, A.B. (1981), "Wall effects in laminar flow of fluids through packed beds", *A.I.Ch.E. Journal*, v.27 n.5, p.705 - 715.

Collins, M., Schowalter, W.R. (1963), "Behaviour of non-Newtonian fluids in the entry region of a pipe", *A.I.Ch.E. Journal*, v.9 n.6, p.804 - 809.

Cooke, R., Lazarus, J.H. (1989), Hydrotransport Research Internal Report 89-199, University of Cape Town.

Cooke, R., Lazarus, J.H. (1989), Hydrotransport Research Internal Report 89-203, University of Cape Town.

Cowper, N.T., Thompson, T.L., Aude, T.C., Wasp, E.J. (1972), "Processing steps: keys to successful slurry-pipeline systems", *Chemical Engineering*, p.58 - 67.

Cross, M.M. (1965), "Rheology of non-Newtonian fluids: a new flow equation for pseudoplastic systems", *Journal of Colloid Science*, v.20, p.417 - 437.

Cross, M.M. (1970), "Kinetic interpretation of non-Newtonian flow", *Journal of Colloid and Interface Science*, v.33 n.1, p.30 - 35.

Cruise, W.J. (1985), "Materials for piping systems in gold mines", *Journal of the South African Institute of Mining and Metallurgy*, v.85. 10., p.361 - 365.

Dabak, T., Yucel, O. (1986), "Shear viscosity of high concentration slurries at varying shear rates", *Proc. Int. Symp. on Slurry Flows, A.S.M.E. Winter Annual Meeting*, p.31 - 39.

Dabak, T., Yucel, O. (1987), "Modeling of the concentration and particle size distribution effects on the rheology of highly concentrated suspensions", *Powder Technology*, v.52, p.193 - 206.

Davis, P.K., Shrivastava, P. (1982), "Rheological and pumping characteristics of coal - water suspensions", *Journal of Pipelines*, v.3, p.97 - 107.

De Silva, C.N. (1983), "A theory of concentrated suspensions", *Acta Mechanica*, v.49, p.221 - 239.

Dedegil, M.Y. (1986), "Drag coefficient and settling velocity of particles in non-Newtonian suspensions", *Proc. Int. Symp. on Slurry Flow, A.S.M.E., Winter Annual Meeting*, p.9 - 15.

Dodge, D.W., Metzner, A.B. (1959), "Turbulent flow of non-Newtonian systems", *A.I.Ch.E. Journal*, v.5 n.2, p.189 - 204.

Duckworth, R.A., Pullum, L., Lockyear, C.F. (1983), "The hydraulic transport of coarse coal at high concentration", *CSIRO, Div. of Mineral Engineering*, Australia, p.1 - 25.

Duckworth, R.A., Addie, G.R., Maffet, J.R. (1986), "Mine waste disposal by pipeline using a fine slurry carrier", *11th Int. Conf. on Slurry Technology*, p.187 - 193.

Duckworth, R.A., Pullum, L., Addie, G.R., Lockyear, C.F. (1986), "The pipeline transport of coarse materials in a non-Newtonian carrier fluid", *10th Int. Conf. on the Hydraulic Transport of Solids in Pipes*, Paper C2, p.69 - 87.

Duckworth, R.A. (19-21 October 1988), "Full scale experimental study of the pipeline transport of phosphate matrix slurries", *11th Int. Conf. on the Hydraulic Transport of Solids in Pipes*, p.197 - 213.

Durst, F., Milojevic, D., Schonung, B. (1984), "Eulerian and Langrangian predictions of particulate two-phase flows: a numerical study", *Appl. Math. Modelling*, v.8, p.101 - 115.

Dzuy, N.Q., Boger, D.V. (1983), "Yield stress measurement for concentrated suspensions", *Journal of Rheology*, v.27 n.4, p.321 - 349.

Edwards, M.F., Wilkinson, W.L. (1971), "Review of potential applications of pulsating flow in pipes", *Trans. Instn. Chem. Engrs.*, v.49, p.85 - 94.

Ekmann, J.M., Wildman, D.J., Chen, J.L.S. (1986), "Laminar flow studies of highly loaded suspensions in horizontal pipes", p.85 - 92.

Elfaghi, F.A., Langlinais, J.P., Bourgoyne, A.T., Holden, W.R. (1983), "Frictional pressure losses for single-phase and two-phase flow of drilling muds", *Journal of Energy Resources Technology*, v.10 n.3, p.372 - 379.

Elliott, D.E., Gliddon, B.J. (1970), "Hydraulic transport of coal at high concentrations", *First Int. Conf. on the Hydraulic Trans. of Solids in Pipes*, v.Hydrotransport 1, Paper G2, p.G2-25 - G2-56.

Ercolani, D., Giachetta, G., Pareschi, A. (1987), "Experimental analysis of solid sediment behaviour in sloping pipes for solid-liquid mixtures", *Journal of Pipelines*, v.6., p.205 - 216.

Eyre, D., Brown, N.P., Shook, C.A., Peters, J. (1983), "A probe for point velocities in slurry flows", *Canadian Journal of Chemical Engineering*, v.61, p.597 - 602.

Faddick, R.R. (1974), "Flow properties of coal-water slurries", *3rd Int. Conf. on the Hydraulic Transport of Solids in Pipes*, Paper H1, p.H1-1 - H1-8.

Faddick, R.R., DaBai, G.S. (1977), "Optimization of particle size distribution for coal slurry pipelines", *Slurry Trans. Assoc., 2nd Annual International Tech. Conference*, p.1 - 27.

Faddick, R.R. (1982), "Settling slurries", *Preceeding course notes to Hydrotransport 8*, Johannesburg, R.S.A., B.H.R.A., Section 6.

Fam, D., Scrivener, O., Dodds, J. (1987), "Rheology and flow behaviour of phosphate slurries (mine tailings) in pipes", *Chemical and Engineering Technology*, v.10 n.5, p.305 - 311.

Farris, R.J. (1968), "Prediction of the viscosity of multimodal suspensions from unimodal viscosity data", *Transactions of the Society of Rheology*, v.12 2, p.281 - 301.

Ferrini, F., Battarra, V., Donati, E., Piccinini, C. (1984), "Optimization of particle grading for high concentration coal slurry", *9th Int. Conf. on Hydraulic Transport of Solids in Pipes*, Paper B2, p.63 - 75.

Flint-Petersen, L., Rajaratnam, N. (1987), "A method to measure discharge in pipelines", *Journal of Pipelines*, v.6, p.319 - 323.

Freidel, L. (1985), "Two phase frictional pressure drop correlation for vertical down flow", *German Chemical Engineering*, v.8 n.1, p.32 - 40.

Frith, W.J., Mewis, J., Strivens, T.A. (1987), "Rheology of concentrated suspensions: experimental investigations", *Powder Technology*, v.51, p.27 - 34.

Furness, R.A. (1987), "Developments in pipeline instrumentation", *Measurement and Control*, v.20, p.7 - 17.

Gandhi, R.L. (1982), "An overview of slurry pipelines", *Journal of Pipelines*, v.3, p.1 - 11.

Gandhi, S.L., Cindric, D.T., Williams, R.A. (1987), "Designing piping systems for two-phase flow", *Chemical Engineering Progress*, p.51 - 55.

Gay, E.C., Nelson, P.A., Armstrong, W.P. (1969), "Flow properties of suspensions with high solids concentration", *A.I.Ch.E. Journal*, v.15 n.6, p.815 - 822.

Gilchrist, I.C.R. (1986), "Predicting the values of flow parameters for the design of pipelines conveying backfill slurries", *Chamber of Mines Research Organization*, p.1 - 42.

Goedde, E. (1980), "Hydraulic handling in mining - fully automatic large-scale test unit on a practical scale", *The Australian I.M.M. Conference*, p.105 - 110.

Gopalan, N.P. (1985), "Laminar flow of a suspension in a curved pipe with varying curvature", *International Journal of Engineering Science*, v.23 6, p.621 - 632.

Govier, G.W., Aziz, K. (1972), "The flow of complex mixtures in pipes", *Van Nostrand Reinhold Company*, p.182 - 257.

Graf, W.H., Acaroglu, E.R. (1967), "Homogeneous suspensions in circular conduits", *Journal of the Pipeline Div., American Society of Civil Engineers*, Paper PL2, p.63 - 69.

Hadley, D.W., Weber, J.D. (1975), "Rheological nomenclature", *Rheol. Acta*, v.14, p.1098 - 1109.

Hanks, R.W. (1963), "The laminar-turbulent transition for fluids with a yield stress", *A.I.Ch.E. Journal*, v.9 3, p.306 - 309.

Hanks, R.W. (1968), "On the theoretical calculation of friction factors for laminar, transient and turbulent flow of Newtonian fluids in pipes and between parallel plane walls", *A.I.Ch.E. Journal*, v.14 5, p.691 - 695.

Hanks, R.W., Ricks, B.L. (1974), "Laminar-turbulent transition in flow of pseudoplastic fluids with yield stresses", *J Hydronautics*, v.8 n.4, p.163 - 166.

Hanks, R.W., Dadia, B.H. (1971), "Theoretical analysis of the turbulent flow of non-Newtonian slurries in pipes", *A.I.Ch.E. Journal*, v.17 n.3, p.554 - 556.

Hanks, R.W., Ricks, B.L. (1975), "Transitional and turbulent pipeflow of pseudoplastic fluids", *J. Hydronautics*, v.9 n.1, p.39 - 43.

Hanks, R.W. (1979), "The axial laminar flow of yield-pseudoplastic fluids in a concentric annulus", *Ind. Eng. Chem. Process Des. Dev.*, v.18 n.3, p.488 - 493.

Hanks, R.W. (1981), "Course notes. Hydraulic design for flow of complex fluids", *1981 Richard W. Hanks Associates, Inc. Orem. Utah.*, U.S.A.

Hanks, R.W., Hanks, K.W. (1982), "A new viscometer for determining the effect of particle size distributions and concentration on slurry rheology", p.151 - 161.

Hanks, R.W., Hanks, K.W. (1986), "Accurate pipeflow pressure drop predictions from bench scale tests require correst rheological characterization", Brigham Young University, USA., p.115 - 121.

Hansford, G.S., Levy, C.D., De Kock, J.W. (1976), "Rheological measurements on pulps from S A Gold Mines", *Journal of the S A Institute of Mining and Metallurgy*, p.363 - 369.

Harris, J., Quader, A.K.M.A. (1971), "Design procedures for pipelines transporting non-Newtonian fluids and solid-liquid systems", *Pipes and Pipelines*, v.16 4/5, p.307 - 311.

Harris, J., Quader, A.K.M.A. (1972), "A discussion of design procedures for non-Newtonian solid-liquid systems", *Brit. Chem. Eng.*

Hedstrom, B.O.A. (1952), "Flow of plastics materials in pipes", *Industrial and Engineering Chemistry*, v.44 3, p.651 - 656.

Higashitani, K.O., Lodge, A.S. (1975), "Hole pressure error measurements in pressure-generated shear flow", *Transactions of the Soceity of Rheology*, v.19 2, p.307 - 335.

Hinde, A.L., Kramers, C.P. (1989), "The role of hydrocyclone technology in backfilling operations", *Chamber of Mines of South Africa Research Organization.*

Hoffert, J.R., Poling, G.W. (1985), "The action of lime in promoting pipeline flow of tailing slurries", *Canadian Mineral Processors Division of CIM.*, v.78 880, p.54 - 59.

Hoffman, R.L. (1982), "Discontinuous and dilatant viscosity behaviour in concentrated suspensions. Necessary conditions for their occurrence in viscometer flow", *Advances in Colloidal and Interface Science*, v.17, p.161 - 184.

Horsley, R.R., Reizes, J.A. (1978), "Variation in head loss gradient in laminar slurry pipe flow due to changes in zeta potential", *The South African Mechanical Engineer*, v.28, p.307 - 311.

Horsley, R.R., Reizes, J.A. (1980), "The effect of Zeta potential on the head loss gradient for slurry pipelines with varying slurry concentrations", *7th Int. Conf. on the Hydraulic Transport of Solids in Pipes*, Paper D3, p.163 - 173.

Horsley, R.R. (1982), "Viscometer and pipe loop tests on gold slime slurry at very high concentrations by weight, with and without additives", *Hydrotransport 8*, Paper H1, p.367 - 381.

Hou, H.C. (1988), "On the optimal concentration of fine particles in Hydrotransport", *11th Int. Conf. on the Hydraulic Transport of Solids in Pipes*, p.285 - 294.

Jacobs, B.E.A. (19-21 October 1988), "A review of prediction techniques for the hydraulic transport of coal", *11th Int. Conf. on the Hydraulic Transport of Solids in Pipes*, p.1 - 17.

Jain, A.K. (1976), " Accurate explicit equation for friction factor", *Technical Notes, Journal Hydraulic Div., Proc. A.S.C.E.*, v.102.

Johnson, M. (1982), "Non-Newtonian fluid system design - some problems and their solutions", *8th Int. Conf. on the Hydraulic Transport of Solids in Pipes*, Paper F3, p.291 - 307.

Kakka, R.S., Gandhi, R.L. (1982), "Survey of coarse coal studies", *Proc. 7th Int. Tech. Conf. on Slurry Transportation*, p.65 - 74.

Kearsey, H.A., Cheney, A.G. (1961), "A note on the effect of temperatures on the rheology of Thoria slurries", *Trans. Instn. Chem. Engrs.*, v.39, p.91 - 92.

Kemblowski, Z., Kolodziejski, J. (1973), "Flow resistances of non-Newtonian fluids in transitional and turbulent flow", *International Chemical Engineering*, v.13 n.2, p.265 - 278.

Kenchington, J.M. (1974), "An assessment of methods of pressure drop prediction for slurry transport", *3rd Int. Conf. on the Hydraulic Transport of Solids in Pipes*, Paper F1, p.F1-1 - F1-19.

Keska, J.K. (1984), "Fluctuations of the solid spatial concentration in the stationary 2-phase turbulent flow of heterogeneous mixtures in pipelines", *Journal of Pipelines*, v.4, p.149 - 157.

Khan, A.R., Pirie, R.L., Richardson, J.F. (1987), "Hydraulic transport of solids in horizontal pipelines - predictive methods for pressure gradients", *Chemical Engineering Science*, v.42 n.4, p.767 - 778.

Klose, R.B. (1982), "The hydraulic transport of coal suspensions with coarse particles", *Proc. 7th Int. Tech. Conf. on Slurry Transportation*, p.61 - 64.

Klose, R.B., Mahler, H.W. (1982), "Investigations into the hydraulic transportation behaviour of ore and coal suspensions with coarse particles", *8th Int. Conf. on the Hydraulic Transport of Solids in Pipes*, Paper D2, p.195 - 210.

Klose, R., Navrade, D.H. (1984), "Densecoal pilot transport for production and transportation of highly concentrated coal fuels", *9th Int. Conf. on Hydraulic Transport of Solids in Pipes*, Paper B1, p.47 - 62.

Koren, I. (1978), "Determination of optimal technical solutions of hydraulic conveying systems by means of economic parameters", *5th Int. Conf. on the Hydraulic Transport of Solids in Pipes*, Paper J6, p.J6-75 - J6-86.

Krieger, I.M., Maron, S.H. (1954), "Direct determination of the flow curves of non-Newtonian fluids. III standardization treatment of viscometric data", *Journal of Applied Physics*, v.25 1, p.72 - 75.

Kril, S.I. (1979), "The energy balance for a suspension-bearing flow and its consequences", *Fluid Mechanics - Soviet Research*, v.8 2, p.109 - 117.

Kril, S.I. (1981), "Energy expended by pressure-type slurry flows on generating a concentration distribution in the solids", *Fluid Mechanics - Soviet Research*, v.10 2, p.142 - 147.

Krishna Murthy, V.R., Zandi, M. (1969), "Turbulent flow of non-Newtonian suspensions in pipes", *Journal of the American Society of Civil Engineers*, v.EM1, p.271 - 288.

Lagana, V., Ercolani, E., Prassone, M., Vercellotti, C. (1984), "Snamprogetti's high coal concentration slurry preparation plant", *9th Int. Conf. on the Hydraulic Transport of Solids in Pipes*, Paper B3, p.77 - 88.

Lawler, H.L., Pertuit, P., Tennant, J.D., Cowper, N.T. (1978), "Application of stabilized slurry concepts of pipeline transportation of large particle coal", *3rd Int. Tech Conf. of Slurry Transportation*, p.164 - 178.

Lazarus, J.H., Neilson, I.D. (1978), "A generalised correlation for friction head losses of settling mixtures in horizontal smooth pipelines", *5th Int. Conf. on the Hydraulic Transport of Solids in Pipes*, Paper B1, p.B1-1 - B1-33.

Lazarus, J.H. (1982), "Optimum specific power consumption for transporting settling slurries in pipelines", *8th Int. Conf. on the Hydraulic Transport of Solids in Pipes*, Paper B4, p.123 - 132.

Lazarus, J.H., Sive, A.W. (1984), "A novel balanced beam tube viscometer and the rheological characterization of high concentration fly ash slurries", *9th Int. Conf. on the Hydraulic Transport of Solids in Pipes*, Paper E1, p.207 - 226.

Lazarus, J.H. (1986), "Mechanistic model for mixed regime slurries", Internal Report, Department of Civil Engineering, University of Cape Town.

Lazarus, J.H., Slatter, P.T. (1986), "Comparative rheological characterisation using a balanced beam tube viscometer and rotary viscometer", *10th Int. Conf. on the Hydraulic Transport of Solids in Pipes*, Hydrotransport 10 Paper J2, p.291 - 302.

Lazarus, J.H., Slatter, P.T. (1988), "A method for the rheological characterization of tube viscometer data", *Journal of Pipelines*, v.7, p.165 - 176.

Lazarus, J.H. (1989), "Mixed-regime slurries in pipelines. I: Mechanistic model", Journal of Hydraulic Engineering, v.115, n.11, pp.1496 - 1509.

Lazarus, J.H., Paterson, A.J.C. (1989), "Mechanistic and empirical models for the hydraulic transport of full plant tailings, *Proc. Slurry Transport in the Mining Industry, Hydraulic Conveying Ass. of South Africa*, Paper 3.

Le Fur, B., Martin, M. (1967), "Laminar and transitional flow of drilling muds and various suspensions in circular tubes", *Journal of Fluid Mechanics*, v.30 n.3, p.449 - 464.

Link, J.M., Lavingia, N.J., Faddick, R.R. (1974), "The economic selection of a slurry pipeline", *3rd Int. Conf. on the Hydraulic Transport of Solids in Pipes*, Paper K3, p.K3-25 - K3-41.

Lohrenz, J., Swift, G.W., Kurata, F. (1960), "An experimentally verified theoretical study of the falling cylinder viscometer", *A.I.Ch.E. Journal*, v.6 4, p.547 - 550.

Masuyama, T., Kawashima, T., Noda, K. (1978), "Pressure loss of pseudo-plastic fluid flow containing coarse particles in a pipe", *5th Int. Conf. on the Hydraulic Transport of Solids in Pipes*, Paper D1, p.D1-1 - D1-14.

Mathias, H.J., Kazanskij, I. (1978), "Behaviour of pseudo-plastic slurries in pipe flow", *5th Int. Conf. on the Hydraulic Transport of Solids in Pipes*, Paper C3, p.C3-35 - C3-49.

Maude, A.D., Whitmore, R.L. (1956), "The wall effect and the viscometry of suspensions", *British Journal of Applied Physics*, v.7, p.98 - 102.

McKibben, M., Shook, C.A. (1987), "Experience with radiometric determination of slurry concentration distributions in pipelines", *Journal of Pipelines*, v.6, p.291 - 296.

Metzner, A.B., Reed, J. (1955), "Flow of non-Newtonian fluids - correlation ofthe laminar, transition, and turbulent-flow regions", *A.I.Ch.E. Journal*, v.1 n.4, p.434 - 440.

Michiyoshi, I., Matsumoto, R., Mizuno, K., Nakai, M. (1966), "Flow of slurry through a circular tube. Friction factor for tubes Part III", *International Chemical Engineering*, v.6 2, p.382 - 388.

Miller, J.E. (1984), "Reciprocating pumps for slurry service", *38th Annual Meeting in Chicago*, Illinois, p.1 - 5.

Mooney, M. (1950), "The viscosity of a concentrated suspension of spherical particles", *Annual Meeting of the Society of Rheology*, p.163 - 170.

Mooney, M. (1931), "Explicit formulas for slip and fluidity", *Journal of Rheology*, v.2 n.2, p.210 - 222.

Moshev, V.V. (1979), "Viscosity relationships for heavily filled suspensions", *Fluid Mechanics - Soviet Research*, v.8 n.2, p.88 - 96.

Neill, R.I.G. (1988), "The rheology and flow behaviour of high concentration mineral slurries", Msc Thesis, University of Cape Town.

Newitt, D.M., Richardson, J.F., Abbott, M., Turtle, R.B. (1955), "Hydraulic conveying of solids in horizontal pipes", *Trans. Instn. Chem. Engrs.*, v.33, p.93 - 113.

Newitt, D.M., Richardson, J.F., Gliddon, B.J. (1961), "Hydraulic conveying of solids in vertical pipes", *Trans. Inst. Chem. Engrs.*, v.39, p.93 - 100.

Oba, S., Ota, K., Kawashima, T. (1984), "Analysis on slurry pressure drop by various fluid models", *9th Int. Conf. on Hydraulic Transport of Solids in Pipes*, Paper D2, p.163 - 191.

Oldroyd, J.G. (1948), "The interpretation of observed pressure gradients in laminar flow of non-Newtonian liquids through tubes", *Journal of Colloidal Science*, v.4, p.333 - 342.

Oldroyd, J.G. (1984), "An approach to non-Newtonian fluid mechanics", *Journal of non-Newtonian Fluid Mechanics*, v.14, p.9 - 46.

Paterson, A.J.C., Lazarus, J.H. (1989), "Experimental evaluation of theories for hydraulic transport of slurries in pipelines with special reference to full plant tailings", *Hydrotransport Research Internal Report*, University of Cape Town.

Paterson, A.J.C., Lazarus, J.H. (1989), Hydrotransport research internal reports 89-161, 89-168, 89-174, University of Cape Town.

Paulis, N.J., Silvermetz, D. (1977), "Instrumentation for slurry systems", *Chemical Engineering*, p.107 - 110.

Ponce Campos, C.D., Guntlow, V.P. (1987), "A method of pipe blockage control for nearly horizontal slurry flow", *Journal of Pipelines*, v.6, p.89 - 98.

Quader, A.K.M.A., Wilkinson, W.L. (1980), "Correlation of turbulent flow rate-pressure drop data for non-Newtonian solutions and slurries in pipes", *International Journal of Multiphase Flow*, v.6, p.553 - 561.

Reiner, M. (1934), "The theory of non-Newtonian liquids", *Journal of General and Applied Physcis*, v.5 n.11, p.321 - 341.

Roco, M.C., Shook, C.A. (1982), "Computational approach for coal slurry pipelines", *Proc. 7th Int. Conf. on Slurry Transportation*, p.175 - 192.

Roco, M.C., Shook, C.A. (1983), "Modelling of slurry flow: the effect of particle size", *Canadian Journal of Chemical Engineering*, v.61, p.494 - 503.

Roco, M.C., Mahadevan, S. (1986), "Scale-up technique of slurry pipelines - Part 1: turbulence modelling", *Journal of Energy Resources Technology*, v.108 4, p.269 - 277.

Roco, M.C., Mahavedan, S. (1986), "Scale-up technique of slurry pipelines - Part 2: numerical integration", *Journal of Energy Resources Technology*, v.108 4, p.278 - 285.

Roco, M.C., Shook, C.A. (1987), "New approach to predict concentration distribution in fine particle slurry flows", *PCH Physic Chemical Hydrodynamics*, v.8 n.1, p.43 - 60.

Rose, H.E., Duckworth, R.A. (1969), "Transport of solid particles in liquids and gases", *The Engineer*, p.392 - 483.

Rosen, M.R., Foster, W.W. (1978), "Approximate rheological characterization of Casson fluids", *Journal of Coatings Technology*, v.50 643, p.

Round, G.F., Latto, B. (1976), "Pulsating flows of solid-liquid suspensions", *4th Int. Conf. on the Hydraulic Transport of Solids in Pipes*, Paper D1, p.D1-1 - D1-16.

Round, G.F., El-Sayed, E. (1985), "Pulsating flows of solid/liquid suspensions. Bentonite-clay/water suspensions", *Journal of Pipelines*, v.5, p.95 - 106.

Round, G.F., El-Sayed, E. (1987), "Pulsating flows of solid/liquid suspensions. II coal/water slurries", *Journal of Pipelines*, v.6, p.105 - 116.

Sakamoto, M., Uchida, K., Kamino, Y. (1982), "Transportation of coarse coal with fine particle - water slurry", *8th Int. Conf. on the Hydraulic Transport of Solids in Pipes*, Paper J2, p.433 - 443.

Sanchez-Palencia, E. (1985), "Current problems in high concentration suspensions", *Journal of Theoretical and Applied Mechanics*, v.Special Ed., p.21 - 51.

Satchwell, R.M., Sharma, M.P., Miller, R.L. (1988), "A mathematical model for predicting concentration profiles in liquid-solid fine slurry pipe flows", *Journal of Energy Resources Technology*, v.110 n.3, p.141 - 146.

Sauermann, H.B. (1982), "The influence of particle diameter on the pressure gradients of gold slimes pumping", *8th Int. Conf. on the Hydraulic Transport of Solids in Pipes*, Paper E1, p.241 - 248.

Shaheen, E.I. (1971), "Rheological study of viscosities and pipeline flow of concentrated slurries", *Powder Technology*, v.5, p.245 - 256.

Shook, C.A., Haas, D.B., Husband, W.H.W., Richardson, A.D. and Smith, L.G. (1976), "A vertical tube viscometer for suspensions containing coarse particles", *4th Int. Conf. on the Hydraulic Transport of Solids in Pipes*, Paper F4, p.F4-41 - F4-52.

Shook, C.A. (1985), "Experiments with concentrated slurries of particles with densities near that of the carrier fluid", *Canadian Journal of Chemical Engineering*, v.63, p.861 - 869.

Shook, C.A., Nasr-El-Din, H. (1987), "Effect of a 90 degree bend on slurry velocity and concentration distributions", *Journal of Pipelines*, v.6, p.239 - 252.

Sikdar, S.K. (1979), "Viscosity measurements of non-Newtonian slurry suspensions using rotating viscometers", *Ind. Eng. Chem. Process Des. Dev.*, v.18 n.4, p.722 - 726.

Sikorski, C.F., Lehman, R.L., Sheperd, J.A., "The effects of viscosity reducing chemical additives on slurry rheology pipeline transport performance for various mineral slurries" p.163 - 173.

Sive, A.W., Lazarus, J.H. (1988), "Experimental evaluation of theories for hydraulic transport of mixed regime slurries in pipelines", *Hydrotransport Research Internal Report*, University of Cape Town.

Sive, A.W. (1988), "An analytical and experimental investigation of the hydraulic transport of high concentration mixed regime slurries", **Ph.D.** Dissertation, University of Cape Town.

Skelland, A.H.P. (1967), "Non-Newtonian flow and heat transfer", *Publ. John Wiley & Sons, Inc.*, p.1 - 177.

Slatter, P.T. (1986), "The rheological characterisation of non-Newtonian slurries using a novel balanced beam tube viscometer", Msc dissertation, University of Cape Town.

Slatter, P.T., Lazarus, J.H. (1988), "The application of viscometry to the hydraulic transport of backfill material", *Conf. Backfill in South African Mines (SAIMM)*, p.263 - 285.

Smith, F.L., Fogleman, S.F., Fisher, L.A. (1976), "Slurry system economic parameters", *4th Int. Conf. on the Hydraulic Transport of Solids in Pipes*, Paper G1, p.G1-1 - G1-12.

Smith, J.W., Paradi, J.C. (1982), "Heat transfer to settling slurries in vertical transport", *Journal of Pipelines*, v.3, p.43 - 52.

Smoldyrev, A.Y., Safonov, Y.K. (1979), "Pipeline transport of concentrated slurries", *Publ. Terraspace Inc.*, p.

Snow, R.J., Horsley, R.R. (1987), "The effects of inorganic and organic additives on the pumpability of dense fill slurries", *Journal of Pipelines*, v.6, p.169 - 174.

Soo, S.L. (1987), "Pipe flow of a dense suspension", *Journal of Pipelines*, v.6, p.193 - 203.

Stepanoff, A.J. (1964), "Pumping solid-liquid mixtures", *Mechanical Engineering*, p.29 - 35.

Stepanoff, A.J. (1965), "Pumps and blowers, selected advanced topics. Two-phase flow, flow & pump of solids in suspension & fluid mixtures", *Publ. John Wiley & Sons, Inc.*, p.164 - 293.

Streat, M., Televantos, Y., Carleton, A.J. (1976), "Pilot-plant studies of hydraulic conveying of coarse materials at high concentration in pipelines", *4th Int. Conf. on the Hydraulic Transport of Solids in Pipes*, Paper F2, p.F2-21 - F2-30.

Streat, M. (1982), "A comparison of specific energy consumption in dilute and dense phase conveying of solids-water mixture", *8th Int. Conf. on the Hydraulic Transport of Solids in Pipes*, Hydrotransport 8 B.H.R.A., Paper B3.

Streat, M. (1986), "Dense phase flow of solids-water mixtures in pipelines: A state-of-the-art review", *10th Int. Conf. on the Hydraulic Transport of Solids in Pipes*, Paper B1, p.39 - 41.

Streicher, D.J. (1984), "Optimisation for hydraulic transport of solids in pipes", MSc Thesis, University of Cape Town.

Tadros, T.F. (1985), "Rheology of concentrated suspensions", *Chemistry and Industry*, p.210 - 218.

Tam, K.C., Tiu, C. (1988), "A general correlation for purely viscous non-Newtonian fluids flowing in ducts of arbitrary cross-section", *Canadian Journal of Chemical Engineers*, v.66, p.542 - 549.

Tangsathitkulchai, C., Austin, L.G. (1988), "Rheology of concentrated particles of natural size distribution produced by grinding", *Powder Technology*, v.56, p.293 - 299.

Televantos, Y., Shook, C., Carleton, A., Streat, M. (1979), "Flow of slurries of coarse particles at high solids concentration", *Canadian Journal of Chemical Engineering*, v.57, p.255 - 262.

Thomas, D.G. (1963), "Physical properties and laminar transport characteristics", *Industrial and Engineering Chemistry*, v.55 n.11, p.18 - 29.

Thomas, A.D. (1978), "Coarse particles in a heavy medium - turbulent pressure drop reduction and deposition under laminar flow", *5th Int. Conf. on the Hydraulic Transport of Solids in Pipes*, Paper D5, p.D5-63 - D5-78.

Thompson, T.L., Aude, T.C. (1976), "Slurry pipeline design and operation pitfalls to avoid", *American Society of Mechanical Engineers*, p.1 - 13.

Tomita, Y. (1957), "A study on non-Newtonian flow in pipelines", *Bulletin of JSME*, p.11 - 16.

Torrance, B. McK, (1963), "Friction factors for turbulent non-Newtonian flow in circular pipes", *S.A. Mechanical Engineer*, v.13 , p.89.

Ulusoy, A.G., Miller, D.M., (1979), "Optimal design of pipeline networks carrying homogeneous coal slurry", *Mathematical Programming Study*, v.11., p.85 - 107.

van Diemen, A.J.G., Stein, H.N., (1984), "Energy dissipation during flow of coagulating concentrated suspensions", *Powder Technology*, v.37, p.275 - 287.

Van Wazer, J.R., Lyons, J.W., Kim, K.Y., Colwell, R.E. (1963), "Viscosity and flow measurement - A laboratory handbook of rheology", *Interscience Publishers*, p.1 - 68.

Verkerk, C.G. (1981), "Hydraulic conveying of pastes", *Materials Handling Research Group*, p.1 - 10.

Verkerk, C.G. (1982), "An investigation into the design of slurry pipelines with reference to low and high concentration slurries", MSc Dissertation, p.105 - 247.

Verkerk, C.G. (1986), "Coarse coal high concentration slurry transportation", *10th Int. Conf. on the Hydraulic Transport of Solids in Pipes*, Paper B2, p.55 - 62.

Verkerk, C.G. (1988), "Rheological analysis of JCI slurries", University of Witwatersrand Technology Centre, Research Report.

Wagner, K. (1982), "Consideration of the effect of a wide particle size distribution on calculations for hydraulic conveying", *Bulk Solids Handling*, v.2 2, p.249 - 252.

Want, F.M. (1987), "Pinjarra refinery high density mud disposal system", *12th Slurry Transport Association Conference*, p.483 - 487.

Wasp, E.J., Regan, T.J., Withers, J., Cook, P.A.C. and Clancey, J.T. (1963), "Cross country coal pipeline hydraulics", *Pipeline News*, p.20 - 28.

Wasp, E.J., Thompson, T.L., Aude, T.C. (1970), "Slurry pipeline economics and application", *1st Int. Conf. on the Hydraulic Transport of Solids in Pipes*, Paper K3, p.K3-39 - K3-62.

Wasp, E.J., Kenny, J.P., Gandhi, R.L. (1979), "Solid-liquid flow slurry pipeline transportation", *Trans Tech Publications*, p.46 - 82.

Weltmann, R.N., Green, H. (1943), "Rheological properties of colloidal solutions, pigment suspensions and oil mixtures", *Journal of Applied Physics*, v.14, p.569 - 576.

Wiedenroth, W., Godde, E. (1983), "Hydraulic transport of flotation and other tailings", *Europipe Conference*, Paper 13, p.103 - 108.

Wilson, K.C., Judge, D.G. (1980), "New techniques for the scale-up of pilot-plant results to coal slurry pipelines", *Journal of Powder & Bulk Solids Technology*, v.4, p.15 - 22.

Wilson, K.C., Brown, N.P. (1982), "Analysis of fluid friction in dense-phase pipeline flow", *The Canadian Journal of Chemical Engineering*, v.60, p.83 - 86.

Wilson, K.C., Thomas, A.D. (1985), "A new analysis of the turbulent flow of non-Newtonian fluids", *Canadian Journal of Chemical Engineering*, v.63, p.539 - 546.

Wilson, K.C. (1986), "Effect of solids concentration on deposit velocity", *Journal of Pipelines*, v.5, p.251 - 257.

Wilson, K.C. (1986), "Modelling the effects of non-Newtonian and time-dependant slurry behaviour", *10th Int. Conf. on the Hydraulic Transport of Solids in Pipes*, Paper J1, p.283 - 289.

Windhab, E., Gleissle, W. (1984), "The flow behaviour of highly concentrated suspensions determined with a new shear - and slip flow separating method", *9th Int. Congress on Rheology*, p.

Worster, R.C., Denny, D.F. (1955), "Hydraulic transport of solid material in pipes", *Institution of Mechanical Engineering Proceedings*, v.169, p.565 - 584.

Wright, G.J., Garrett, G.G. (1986), "Wear and performance of materials in pipelines for the hydraulic conveyance of fused ash", *Mintek Report*, Number M242, p.1 - 10.

Yamagata, Y., Kokubo, T., Moro, T. (1980), "Rheological study of viscosities and pipeline flow of coal-oil mixtures", *7th Int. Conf. on the Hydraulic Transport of Solids in Pipes*, Paper G1, p.259 - 275.

Yu, A.B., Standish, N. (1987), "Porosity calculations of multi-component mixtures of spherical particles", *Powder Technology*, v.52, p.233 - 241.

Yu, A.B., Standish, N. (1988), "An analytical-parametric theory of random packing of particles", *Powder Technology*, v.55, p.171 - 186.

APPENDIX D

DATABASE OF MEASURED RESULTS USED FOR THE ANALYSIS OF FULL PLANT TAILINGS

The measured data presented in this appendix was obtained using the following test facilities :

1. Balanced Beam Tube Viscometer (UCT)
2. Vertical Test Facility (UCT)
3. Horizontal pipeline test facility of the Chamber of Mines Research Organization of South Africa.

This data has been discussed in Part 4 of the main thesis document.

The data presented for each test comprises the following :

1. The test facility where the results were obtained.

2. The material characteristics, including the solids relative density and particle size distribution.

3. The slurry parameters, including the slurry relative density and solids concentration by volume and mass.

4. The pipeline characteristics.

5. A table of the measured data including mixture velocity, pressure gradient and temperature.

6. A graph of the measured data representing pressure gradient (kPa/m) versus mixture velocity (m/s).

Table D.1 presents the format of the data test number description.

The data is presented in the following sequence.

Horizontal data

Material 1

I.D. = 13,48 mm

I.D. = 32,63 mm

I.D. = 41,5 mm

I.D. = 75,88 mm

I.D. = 101,5 mm

Material 2

I.D. = 41,5 mm

Material 3

I.D. = 41,5 mm

Vertical data

Material 1

I.D. = 41,5 mm

I.D. = 75,88 mm

Material 2

I.D. = 41,5 mm

Material 3

I.D. = 41,5 mm

TABLE D.1 - DESCRIPTION OF DATABASE FILENAMES

Each Data File has a unique name to easily identify the file contents. The format of the file name is presented below.

NAME OF DATA FILE : FORM = FILENAME.HTR

where FILENAME = Descriptor of form **N N R M C C H Z**
HTR = Filename extension to represent HYDTRANS Data File computer program format

CODE	DESCRIPTION	CODE MEANING
N N	Material Source or Origin	CM : Full Plant 1 C3 : Full Plant 2 DK : Full Plant 3
R	Test Facility where data was measured	V : Vertical Facility C : Chamber of Mines B : Balanced Beam Tube Viscometer
M	Material Type Tested	F : Full Plant Tailings C : Classified Tailings
C C	Mixture Relative Density (Sm)	65 : Refers to Sm = 1.65 73 : Refers to Sm = 1.73
H	Pipeline orientation of test section	H : Horizontal V : Vertical Down
Z	Wildcard used to denote pipe internal diameter according to test facility	S : Small pipe on facility (13.48 on BBTV, 41.5 on Vert.) L : Large Pipe on facility (32.63 on BBTV, 75.88 on Vert.) Blank : Only one size pipe used

DATA FILE : CMBF65HS

Test facility		BBTV University of Cape Town
Test date		Data from RIG NEILL 1988
Material description		Full Plant Tailings
Material relative density		2.740
Slurry relative density		1.651
Solids volumetric concentration	(%)	37.450
Solids mass concentration	(%)	62.150
Pipe internal diameter	(mm)	13.48
Pipe internal roughness	(μm)	5.0
Pipeline gradient		Horizontal

Mixture velocity (m/s)	Pressure gradient (kPa/m)	Slurry temp. (°C)
0.270	4.844	16.0
0.530	6.454	16.0
0.700	6.988	16.0
0.960	7.478	16.0
1.220	8.989	16.0
1.500	9.621	16.0
1.760	11.442	16.0
1.990	12.530	16.0
2.230	13.283	16.0
2.610	15.592	16.0
2.790	16.224	16.0
3.090	17.937	16.0
3.330	18.498	16.0
3.520	20.384	16.0
3.750	27.201	16.0
3.930	28.968	16.0
4.250	31.318	16.0
4.520	44.718	16.0
4.650	49.312	16.0
5.020	57.582	16.0

Particle size distribution
Malvern particle size analyser

Size (μm)	% Passing	% Retained
572.0	100.000	0.000
134.0	90.000	10.000
94.0	80.000	10.000
64.0	70.000	10.000
43.0	60.000	10.000
29.0	50.000	10.000
18.0	40.000	10.000
12.0	30.000	10.000
8.0	20.000	10.000
6.0	10.000	10.000
Pan	0.000	10.000

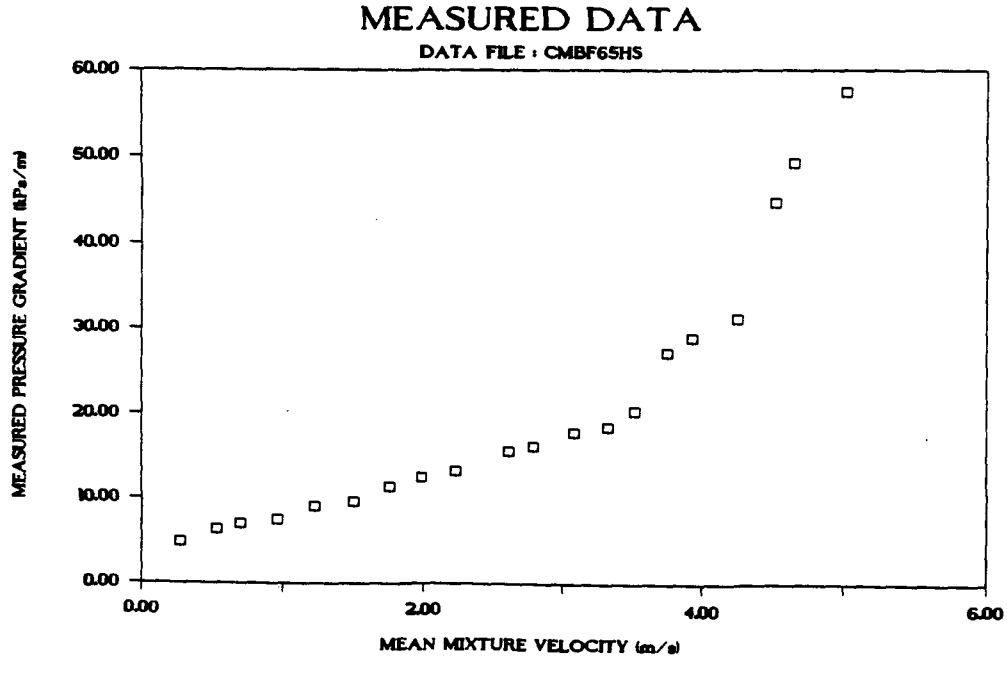

DATA FILE : CMBF70HS

Test facility		BBTV University of Cape Town
Test date		Data from RIG NEILL 1988
Material description		Full Plant Tailings
Material relative density		2.740
Slurry relative density		1.703
Solids volumetric concentration	(%)	40.440
Solids mass concentration	(%)	65.060
Pipe internal diameter	(mm)	13.48
Pipe internal roughness	(μm)	5.0
Pipeline gradient		Horizontal

Mixture velocity (m/s)	Pressure gradient (kPa/m)	Slurry temp. (°C)
0.130	5.238	14.0
0.320	6.700	14.0
0.490	7.802	14.0
0.790	10.450	14.0
1.060	11.486	14.0
1.300	11.936	14.0
1.430	12.719	14.0
1.640	14.806	14.0
1.820	15.719	14.0
2.030	16.327	14.0
2.280	18.389	14.0
2.520	19.077	14.0
2.840	20.349	14.0
3.150	22.982	14.0
3.510	26.233	14.0
4.020	28.453	14.0
4.540	30.921	14.0
4.990	35.650	14.0
5.390	37.999	14.0
5.700	48.807	14.0

Particle size distribution
Malvern particle size analyser

Size (μm)	% Passing	% Retained
572.0	100.000	0.000
134.0	90.000	10.000
94.0	80.000	10.000
64.0	70.000	10.000
43.0	60.000	10.000
29.0	50.000	10.000
18.0	40.000	10.000
12.0	30.000	10.000
8.0	20.000	10.000
6.0	10.000	10.000
Pan	0.000	10.000

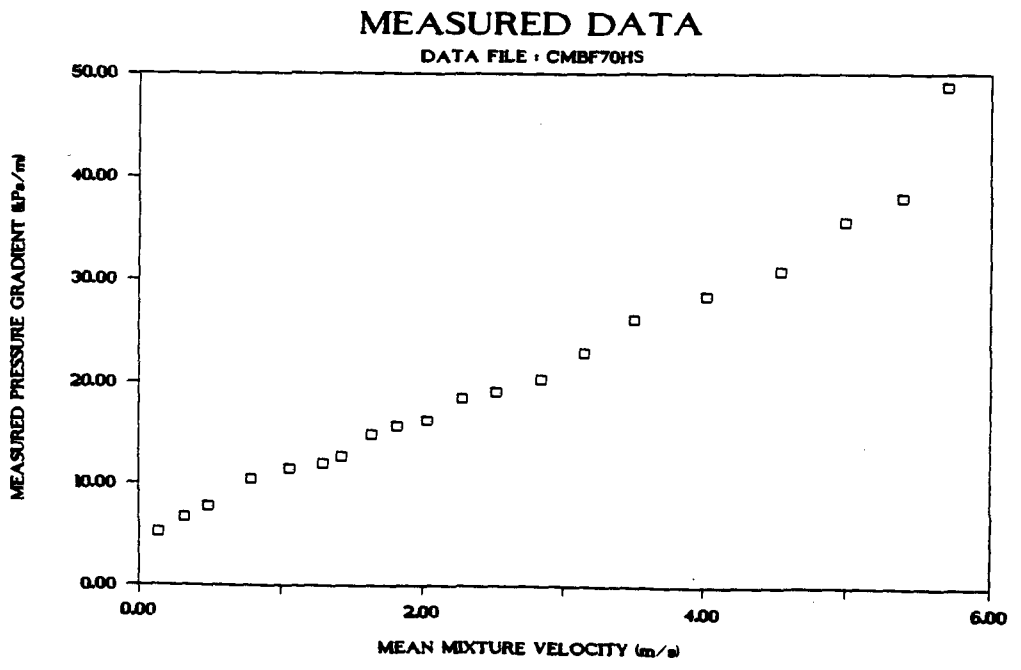

DATA FILE : CMBF75HS

Test facility		BBTV University of Cape Town
Test date		Data from RIG NEILL 1988
Material description		Full Plant Tailings
Material relative density		2.740
Slurry relative density		1.750
Solids volumetric concentration	(%)	43.140
Solids mass concentration	(%)	67.540
Pipe internal diameter	(mm)	13.48
Pipe internal roughness	(μm)	5.0
Pipeline gradient		Horizontal

Mixture velocity (m/s)	Pressure gradient (kPa/m)	Slurry temp. (°C)
0.010	3.736	15.0
0.110	10.149	15.0
0.330	14.107	15.0
0.730	18.852	15.0
1.080	22.221	15.0
1.300	25.289	15.0
1.640	29.180	15.0
1.840	30.720	15.0
2.000	32.243	15.0
2.140	32.933	15.0
2.310	34.230	15.0
2.650	36.712	15.0
2.840	40.558	15.0
3.060	41.828	15.0
3.100	42.139	15.0
3.440	44.211	15.0
4.390	52.231	15.0
4.600	55.172	15.0
5.310	62.257	15.0
5.570	68.765	15.0

Particle size distribution
Malvern particle size analyser

Size (μm)	% Passing	% Retained
572.0	100.000	0.000
134.0	90.000	10.000
94.0	80.000	10.000
64.0	70.000	10.000
43.0	60.000	10.000
29.0	50.000	10.000
18.0	40.000	10.000
12.0	30.000	10.000
8.0	20.000	10.000
6.0	10.000	10.000
Pan	0.000	10.000

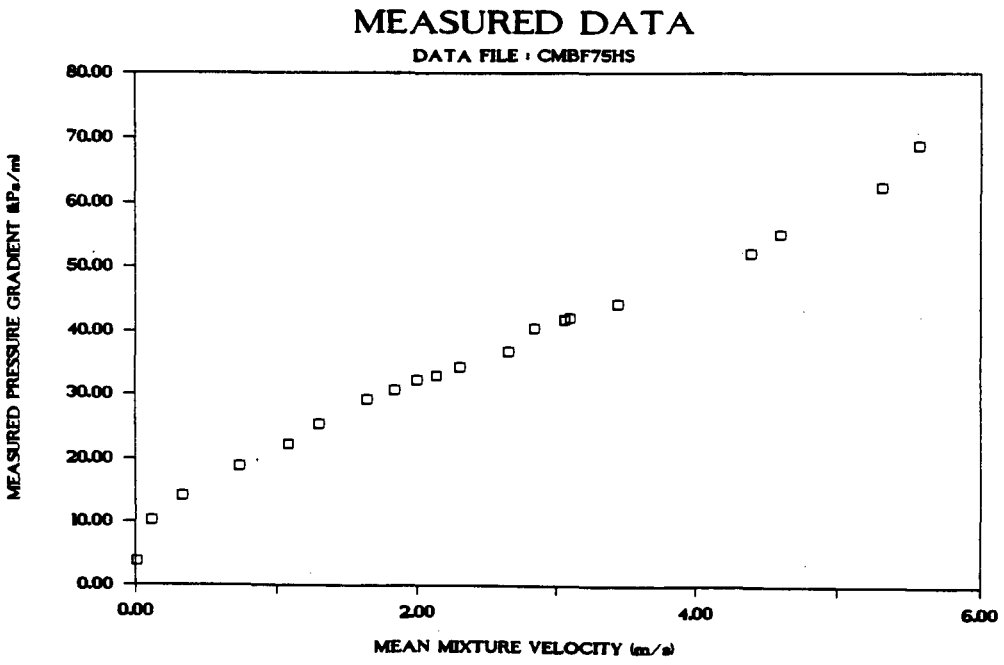

DATA FILE : CMBF81HS

Test facility		BBTV University of Cape Town
Test date		Data from RIG NEILL 1988
Material description		Full Plant Tailings
Material relative density		2.740
Slurry relative density		1.8120
Solids volumetric concentration	(%)	46.667
Solids mass concentration	(%)	70.567
Pipe internal diameter	(mm)	13.48
Pipe internal roughness	(μm)	5.0
Pipeline gradient		Horizontal

Mixture velocity (m/s)	Pressure gradient (kPa/m)	Slurry temp. (°C)
0.010	4.369	20.0
0.060	10.436	20.0
0.110	22.563	20.0
0.210	33.065	20.0
0.540	43.491	20.0
0.780	50.379	20.0
0.900	54.323	20.0
1.050	55.820	20.0
1.210	60.722	20.0
1.300	62.703	20.0
1.370	68.555	20.0
1.500	70.698	20.0

Particle size distribution
Malvern particle size analyser

Size (μm)	% Passing	% Retained
572.0	100.000	0.000
134.0	90.000	10.000
94.0	80.000	10.000
64.0	70.000	10.000
43.0	60.000	10.000
29.0	50.000	10.000
18.0	40.000	10.000
12.0	30.000	10.000
8.0	20.000	10.000
6.0	10.000	10.000
Pan	0.000	10.000

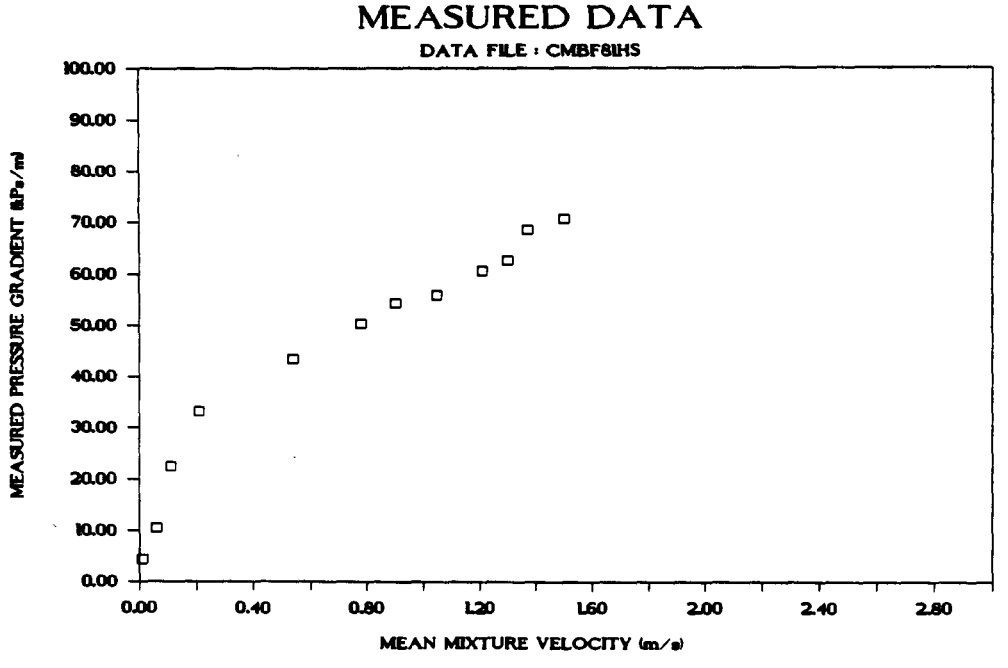

DATA FILE : CMBF85HS

Test facility		BBTV University of Cape Town
Test date		Data from RIG NEILL 1988
Material description		Full Plant Tailings
Material relative density		2.740
Slurry relative density		1.846
Solids volumetric concentration	(%)	48.650
Solids mass concentration	(%)	72.210
Pipe internal diameter	(mm)	13.48
Pipe internal roughness	(μm)	5.0
Pipeline gradient		Horizontal

Mixture velocity (m/s)	Pressure gradient (kPa/m)	Slurry temp. (°C)
0.030	4.642	20.0
0.040	7.839	20.0
0.060	11.265	20.0
0.070	18.447	20.0
0.090	21.177	20.0
0.100	25.120	20.0
0.130	31.317	20.0
0.180	42.501	20.0
0.200	48.010	20.0
0.240	52.441	20.0
0.280	57.396	20.0
0.320	61.682	20.0
0.440	65.673	20.0
0.500	68.947	20.0
0.550	72.161	20.0
0.770	87.646	20.0
0.880	91.681	20.0
0.930	95.251	20.0

Particle size distribution
Malvern particle size analyser

Size (μm)	% Passing	% Retained
572.0	100.000	0.000
134.0	90.000	10.000
94.0	80.000	10.000
64.0	70.000	10.000
43.0	60.000	10.000
29.0	50.000	10.000
18.0	40.000	10.000
12.0	30.000	10.000
8.0	20.000	10.000
6.0	10.000	10.000
Pan	0.000	10.000

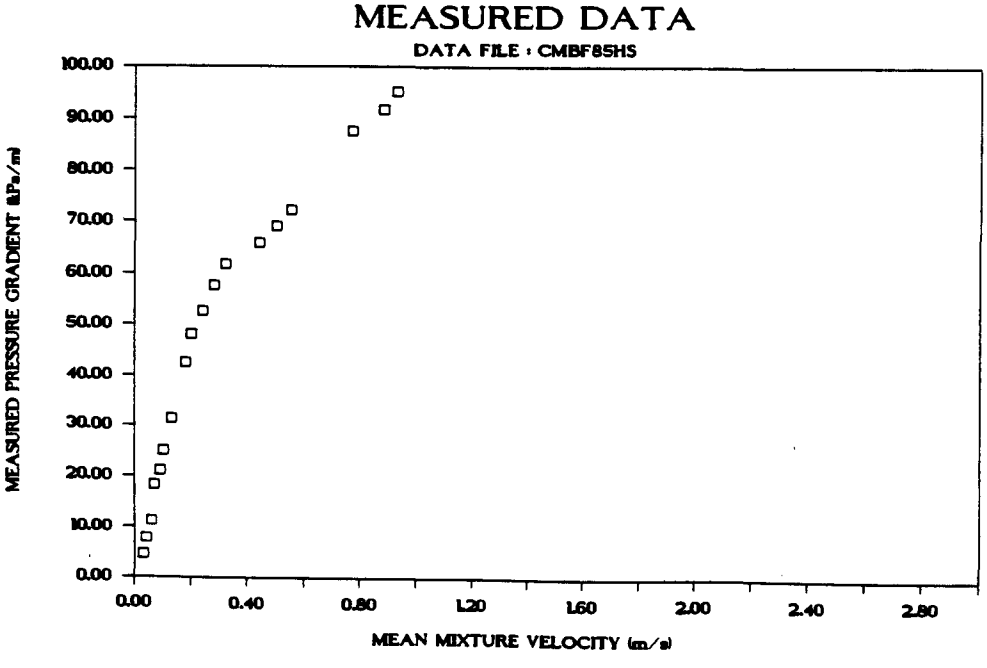

DATA FILE : CMBF90HS

Test facility		BBTV University of Cape Town
Test date		Data from RIG NEILL 1988
Material description		Full Plant Tailings
Material relative density		2.740
Slurry relative density		1.902
Solids volumetric concentration	(%)	52.470
Solids mass concentration	(%)	75.040
Pipe internal diameter	(mm)	13.48
Pipe internal roughness	(μm)	5.0
Pipeline gradient		Horizontal

Mixture velocity (m/s)	Pressure gradient (kPa/m)	Slurry temp. (°C)
0.010	4.096	20.0
0.020	5.288	20.0
0.030	6.365	20.0
0.040	8.693	20.0
0.050	22.119	20.0
0.060	21.751	20.0
0.070	27.068	20.0
0.090	32.946	20.0
0.120	37.624	20.0
0.150	40.451	20.0
0.180	53.172	20.0
0.210	67.790	20.0
0.260	80.061	20.0

Particle size distribution
Malvern particle size analyser

Size (μm)	% Passing	% Retained
572.0	100.000	0.000
134.0	90.000	10.000
94.0	80.000	10.000
64.0	70.000	10.000
43.0	60.000	10.000
29.0	50.000	10.000
18.0	40.000	10.000
12.0	30.000	10.000
8.0	20.000	10.000
6.0	10.000	10.000
Pan	0.000	10.000

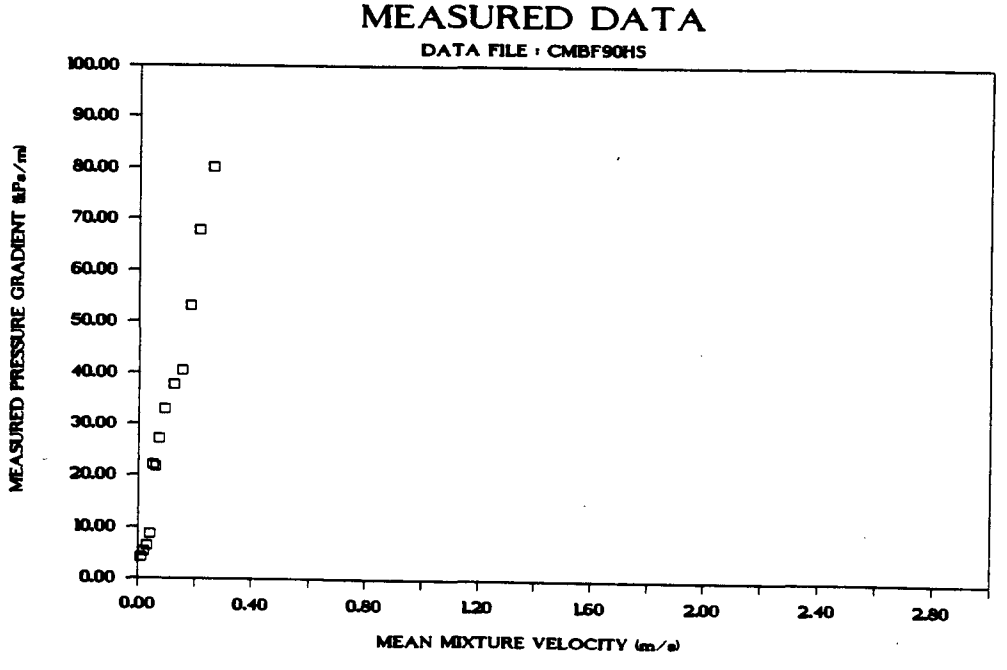

DATA FILE : CMBF65HL

Test facility		BBTV University of Cape Town
Test date		Data from RIG NEILL 1988
Material description		Full Plant Tailings from COM
Material relative density		2.740
Slurry relative density		1.6510
Solids volumetric concentration	(%)	37.414
Solids mass concentration	(%)	62.092
Pipe internal diameter	(mm)	32.63
Pipe internal roughness	(μm)	5.0
Pipeline gradient		Horizontal

Mixture velocity (m/s)	Pressure gradient (kPa/m)	Slurry temp. (°C)
0.230	1.413	16.0
0.490	1.710	16.0
0.720	1.808	16.0
1.010	2.156	16.0
1.290	2.389	16.0
1.470	2.639	16.0
1.800	2.892	16.0
2.030	3.128	16.0
2.250	3.613	16.0
2.530	4.005	16.0
2.740	4.605	16.0
2.910	6.125	16.0
3.300	8.713	16.0
3.680	10.452	16.0
3.990	12.383	16.0
4.390	14.504	16.0
4.560	15.389	16.0
4.760	16.549	16.0
4.850	17.137	16.0
4.950	18.169	16.0

Particle size distribution
Malvern particle size analyser

Size (μm)	% Passing	% Retained
572.0	100.000	0.00
134.0	90.000	10.00
94.0	80.000	10.00
64.0	70.000	10.00
43.0	60.000	10.00
29.0	50.000	10.00
18.0	40.000	10.00
12.0	30.000	10.00
8.0	20.000	10.00
6.0	10.000	10.00
Pan	0.000	10.00

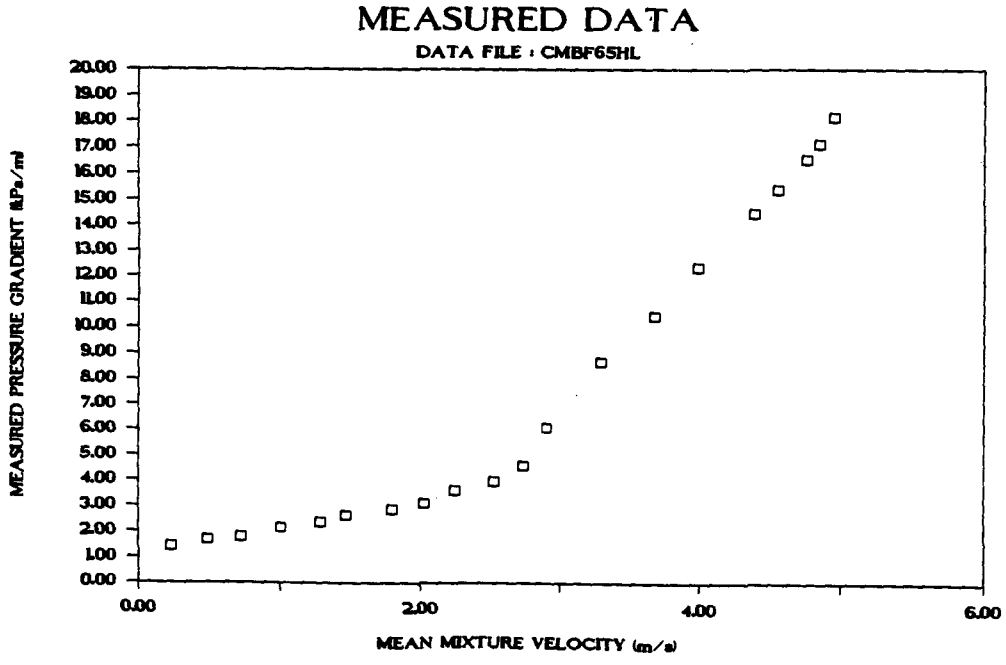

DATA FILE : CMBF70HL

Test facility		BBTV University of Cape Town
Test date		Data from RIG NEILL 1988
Material description		Full Plant Tailings
Material relative density		2.740
Slurry relative density		1.703
Solids volumetric concentration	(%)	40.440
Solids mass concentration	(%)	65.060
Pipe internal diameter	(mm)	32.63
Pipe internal roughness	(μm)	5.0
Pipeline gradient		Horizontal

Mixture velocity (m/s)	Pressure gradient (kPa/m)	Slurry temp. (°C)
0.010	1.517	14.0
0.210	2.658	14.0
0.430	2.923	14.0
0.870	3.414	14.0
0.960	3.727	14.0
1.170	4.150	14.0
1.310	4.073	14.0
1.730	5.050	14.0
1.830	5.040	14.0
2.120	5.622	14.0
2.560	6.382	14.0
2.830	6.359	14.0
3.080	7.171	14.0
3.350	8.001	14.0
3.460	8.061	14.0
3.840	9.020	14.0
4.010	10.387	14.0
4.460	14.034	14.0
4.890	18.488	14.0
5.200	21.872	14.0

Particle size distribution
Malvern particle size analyser

Size (μm)	% Passing	% Retained
572.0	100.000	0.000
134.0	90.000	10.000
94.0	80.000	10.000
64.0	70.000	10.000
43.0	60.000	10.000
29.0	50.000	10.000
18.0	40.000	10.000
12.0	30.000	10.000
8.0	20.000	10.000
6.0	10.000	10.000
Pan	0.000	10.000

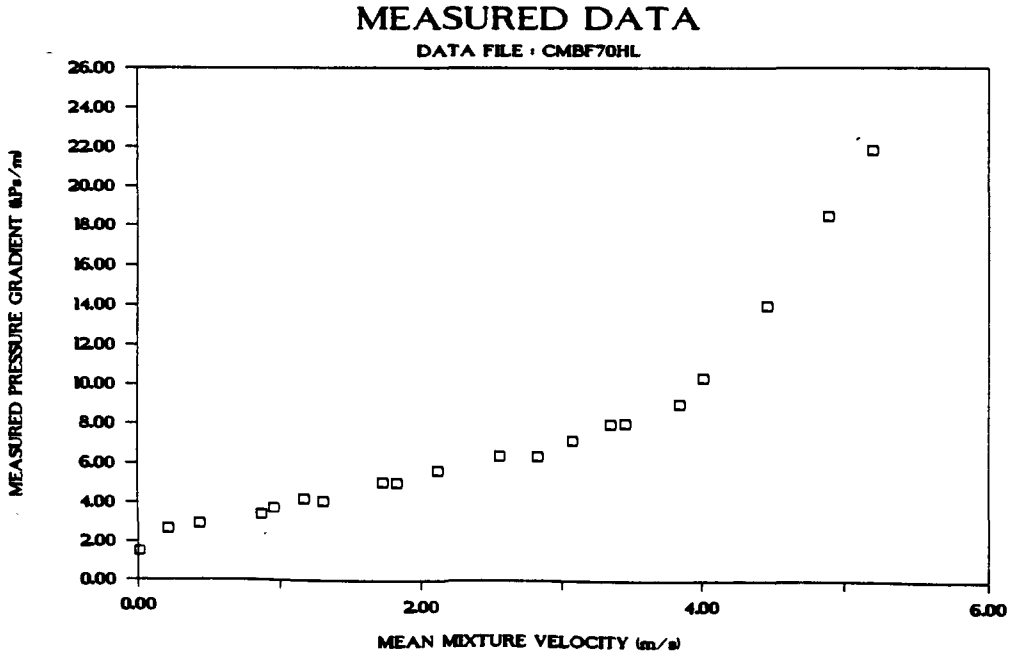

DATA FILE : CMBF75HL

Test facility		BBTV University of Cape Town
Test date		Data from RIG NEILL 1988
Material description		Full Plant Tailings
Material relative density		2.740
Slurry relative density		1.754
Solids volumetric concentration	(%)	43.370
Solids mass concentration	(%)	67.740
Pipe internal diameter	(mm)	32.63
Pipe internal roughness	(μm)	5.0
Pipeline gradient		Horizontal

Mixture velocity (m/s)	Pressure gradient (kPa/m)	Slurry temp. (°C)
0.010	1.569	15.0
0.210	5.654	15.0
0.390	6.361	15.0
0.660	7.248	15.0
0.930	8.172	15.0
1.170	8.579	15.0
1.250	8.816	15.0
1.620	9.525	15.0
1.770	10.048	15.0
2.020	10.737	15.0
2.430	11.192	15.0
2.940	13.132	15.0
3.060	13.500	15.0
3.340	14.100	15.0
3.560	14.682	15.0
4.130	16.187	15.0
4.470	17.254	15.0
4.700	17.341	15.0
5.020	18.871	15.0
5.460	20.360	15.0

Particle size distribution
Malvern particle size analyser

Size (μm)	% Passing	% Retained
572.0	100.000	0.000
134.0	90.000	10.000
94.0	80.000	10.000
64.0	70.000	10.000
43.0	60.000	10.000
29.0	50.000	10.000
18.0	40.000	10.000
12.0	30.000	10.000
8.0	20.000	10.000
6.0	10.000	10.000
Pan	0.000	10.000

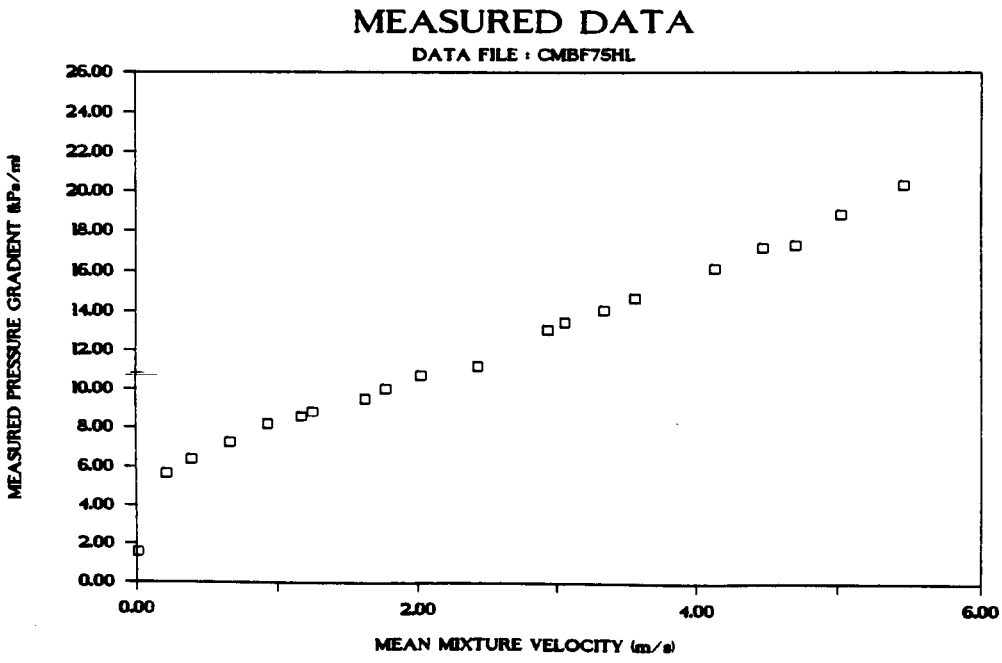

DATA FILE : CMBF81HL

Test facility		BBTV University of Cape Town
Test date		Data from RIG NEILL 1988
Material description		Full Plant Tailings
Material relative density		2.740
Slurry relative density		1.812
Solids volumetric concentration	(%)	46.710
Solids mass concentration	(%)	70.620
Pipe internal diameter	(mm)	32.63
Pipe internal roughness	(μm)	5.0
Pipeline gradient		Horizontal

Mixture velocity (m/s)	Pressure gradient (kPa/m)	Slurry temp. (°C)
0.010	2.530	20.0
0.100	12.094	20.0
0.210	13.779	20.0
0.370	16.170	20.0
0.430	16.351	20.0
0.550	18.611	20.0
0.660	20.488	20.0
0.970	21.639	20.0
1.000	23.254	20.0
1.110	23.514	20.0
1.230	25.515	20.0
1.350	25.736	20.0
1.500	26.735	20.0
1.680	27.989	20.0
1.860	28.456	20.0
2.090	30.304	20.0
2.400	32.058	20.0
2.550	32.378	20.0
2.730	33.973	20.0
2.840	35.450	20.0

Particle size distribution
Malvern particle size analyser

Size (μm)	% Passing	% Retained
572.0	100.000	0.000
134.0	90.000	10.000
94.0	80.000	10.000
64.0	70.000	10.000
43.0	60.000	10.000
29.0	50.000	10.000
18.0	40.000	10.000
12.0	30.000	10.000
8.0	20.000	10.000
6.0	10.000	10.000
Pan	0.000	10.000

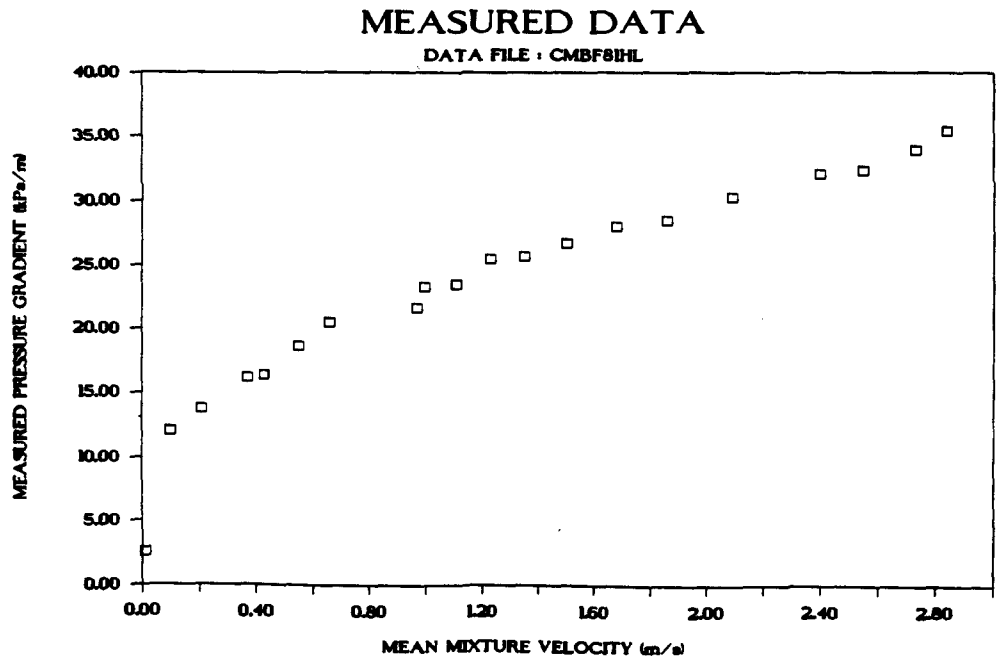

DATA FILE : CMBF85HL

Test facility		BBTV University of Cape Town
Test date		Data from RIG NEILL 1988
Material description		Full Plant Tailings
Material relative density		2.740
Slurry relative density		1.846
Solids volumetric concentration	(%)	48.650
Solids mass concentration	(%)	72.210
Pipe internal diameter	(mm)	32.63
Pipe internal roughness	(μm)	5.0
Pipeline gradient		Horizontal

Mixture velocity (m/s)	Pressure gradient (kPa/m)	Slurry temp. (°C)
0.010	2.323	18.0
0.020	4.654	18.0
0.040	7.890	18.0
0.080	15.894	18.0
0.100	19.463	18.0
0.500	36.844	18.0
0.830	40.608	18.0
1.060	45.008	18.0
1.230	45.830	18.0
1.470	52.143	18.0
1.580	54.478	18.0
1.810	57.599	18.0
2.000	60.350	18.0
2.140	62.609	18.0
2.310	63.562	18.0
2.460	66.850	18.0
2.540	68.304	18.0
2.640	69.772	18.0
2.720	69.628	18.0
2.790	70.357	18.0

Particle size distribution
Malvern particle size analyser

Size (μm)	% Passing	% Retained
572.0	100.000	0.000
134.0	90.000	10.000
94.0	80.000	10.000
64.0	70.000	10.000
43.0	60.000	10.000
29.0	50.000	10.000
18.0	40.000	10.000
12.0	30.000	10.000
8.0	20.000	10.000
6.0	10.000	10.000
Pan	0.000	10.000

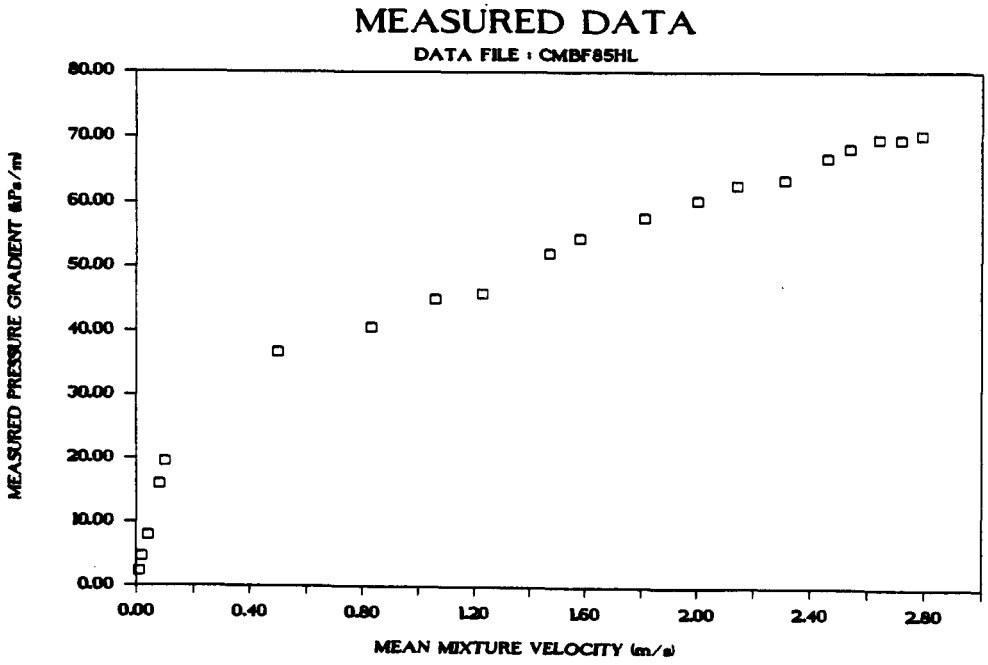

DATA FILE : CMBF90HL

Test facility		BBTV University of Cape Town
Test date		Data from RIG NEILL 1988
Material description		Full Plant Tailings
Material relative density		2.740
Slurry relative density		1.902
Solids volumetric concentration	(%)	51.870
Solids mass concentration	(%)	74.720
Pipe internal diameter	(mm)	32.63
Pipe internal roughness	(μm)	5.0
Pipeline gradient		Horizontal

Mixture velocity (m/s)	Pressure gradient (kPa/m)	Slurry temp. (°C)
0.010	4.113	20.0
0.020	3.486	20.0
0.040	6.416	20.0
0.070	10.723	20.0
0.090	14.603	20.0
0.100	16.818	20.0
0.150	29.067	20.0
0.200	36.980	20.0
0.250	46.239	20.0
0.290	52.663	20.0
0.360	62.698	20.0
0.400	69.596	20.0
0.460	72.203	20.0
0.520	74.258	20.0
0.560	75.929	20.0
0.720	82.036	20.0

Particle size distribution
Malvern particle size analyser

Size (μm)	% Passing	% Retained
572.0	100.000	0.000
134.0	90.000	10.000
94.0	80.000	10.000
64.0	70.000	10.000
43.0	60.000	10.000
29.0	50.000	10.000
18.0	40.000	10.000
12.0	30.000	10.000
8.0	20.000	10.000
6.0	10.000	10.000
Pan	0.000	10.000

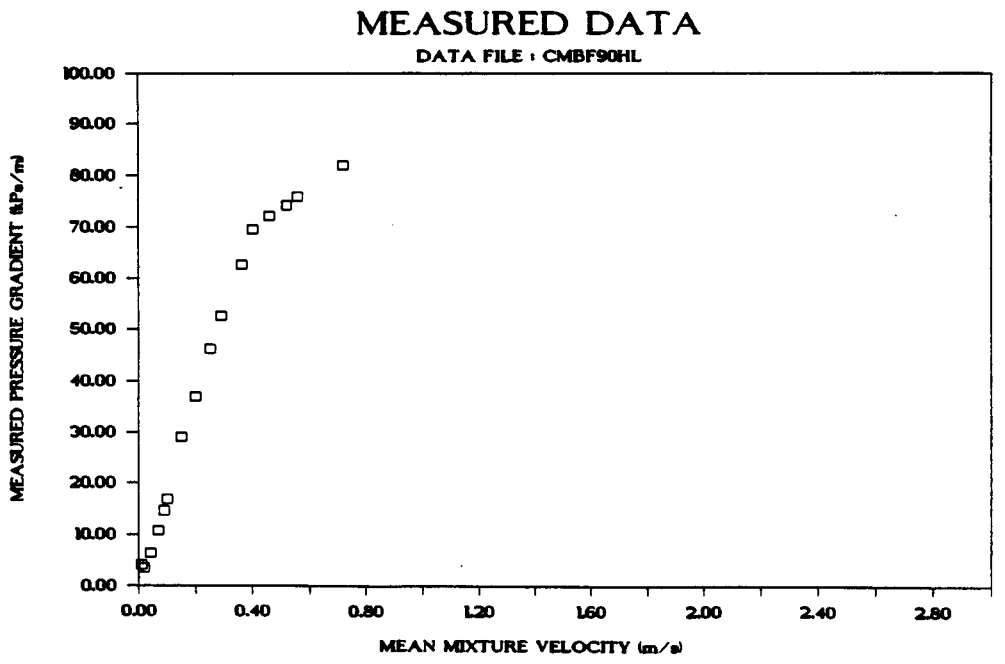

DATA FILE : CMVF53H.

Test facility		Vertical Test Facility
Test date		1989
Material description		Chamber of Mines Full Plant
Material relative density		2.720
Slurry relative density		1.530
Solids volumetric concentration	(%)	30.850
Solids mass concentration	(%)	54.850
Pipe internal diameter	(mm)	41.50
Pipe internal roughness	(μm)	103.0
Pipeline gradient		Horizontal

Mixture velocity (m/s)	Pressure gradient (kPa/m)	Slurry temp. (°C)
3.440	5.411	28.5
3.240	4.620	28.5
3.190	4.665	28.5
2.810	3.666	28.5
2.600	3.228	28.5
2.190	2.494	28.5
2.030	2.115	28.5
1.960	1.850	28.5
1.920	1.889	29.5
1.820	1.766	29.5
1.770	1.621	29.5
1.750	1.678	29.5
1.670	1.504	29.5
1.430	1.169	29.5
1.370	1.105	30.0
1.050	0.682	30.0
0.880	0.421	30.0
0.530	0.351	30.0
0.390	0.358	30.0
0.100	0.220	30.0

Particle size distribution
Malvern particle size analyser

Size (μm)	% Passing	% Retained
564.0	100.000	0.000
262.0	100.000	0.000
168.0	95.500	4.500
113.0	86.200	9.300
84.0	77.400	8.800
65.0	70.500	6.900
50.0	64.800	5.700
39.0	59.000	5.800
30.0	54.500	4.500
21.0	49.600	4.900
11.0	33.900	15.700
6.0	18.800	15.100
Pan	000.000	18.800

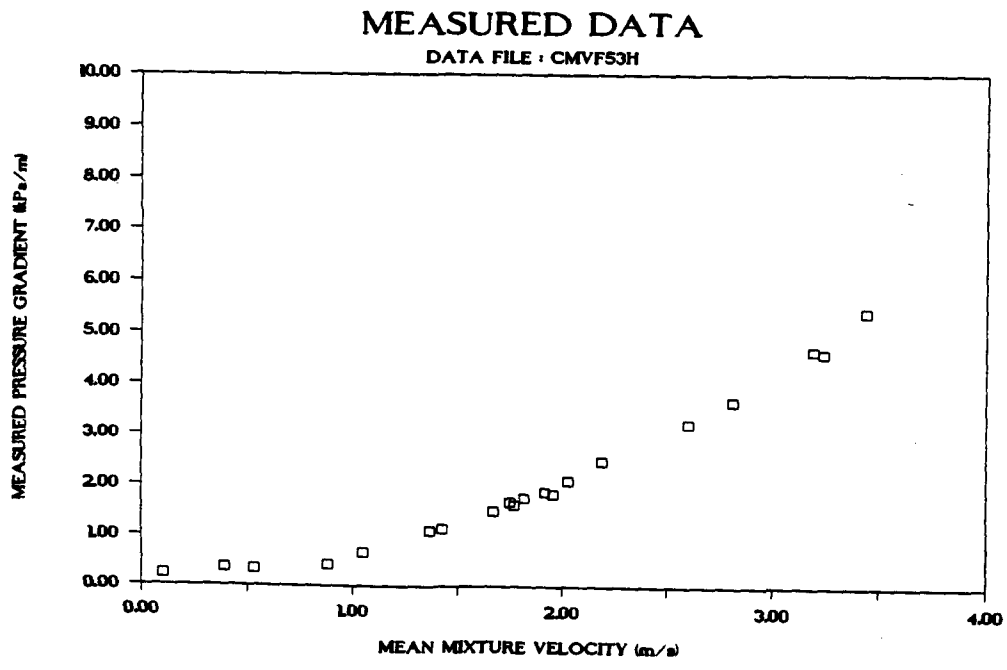

DATA FILE : CMVF65H.

Test facility		Vertical Test Facility UCT.
Test date		1989
Material description		Chamber of Mines Full Plant
Material relative density		2.720
Slurry relative density		1.620
Solids volumetric concentration	(%)	36.080
Solids mass concentration	(%)	60.580
Pipe internal diameter	(mm)	41.50
Pipe internal roughness	(μm)	103.0
Pipeline gradient		Horizontal

Mixture velocity (m/s)	Pressure gradient (kPa/m)	Slurry temp. (°C)
3.290	5.838	26.0
3.130	5.092	26.0
2.990	4.739	26.0
2.690	4.029	26.0
2.580	3.432	27.0
2.290	3.064	27.0
2.150	2.740	27.0
2.050	2.275	27.0
1.820	1.878	27.0
1.780	1.750	27.0
1.640	1.568	27.0
1.370	1.143	28.5
1.220	0.988	28.5
1.160	0.890	28.5
0.930	0.780	28.5
0.870	0.730	28.5
0.670	0.680	28.5
0.410	0.582	28.5
0.110	0.442	28.5
0.030	0.417	28.5

Particle size distribution
Malvern particle size analyser

Size (μm)	% Passing	% Retained
564.0	100.000	0.000
262.0	100.000	0.000
168.0	95.500	4.500
113.0	86.200	9.300
84.0	77.400	8.800
65.0	70.500	6.900
50.0	64.800	5.700
39.0	59.000	5.800
30.0	54.500	4.500
21.0	49.600	4.900
11.0	33.900	15.700
6.0	18.800	15.100
Pan	000.000	18.800

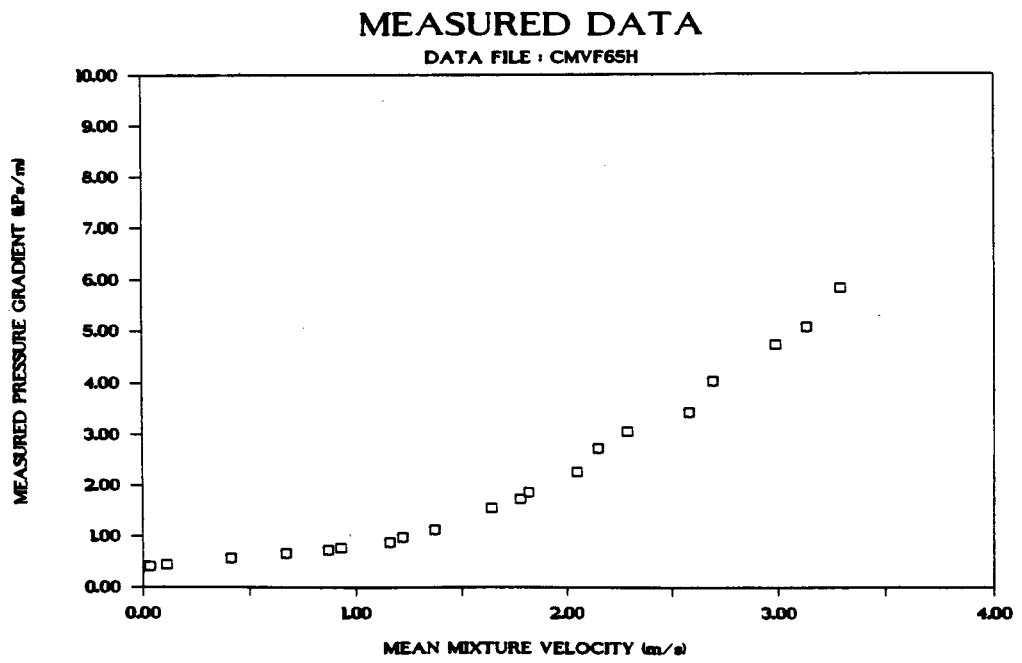

DATA FILE : CMVF71H.

Test facility		Vertical Test Facility
Test date		1989
Material description		Chamber of Mines Full Plant
Material relative density		2.720
Slurry relative density		1.710
Solids volumetric concentration	(%)	41.310
Solids mass concentration	(%)	65.710
Pipe internal diameter	(mm)	41.50
Pipe internal roughness	(μm)	103.0
Pipeline gradient		Horizontal

Mixture velocity (m/s)	Pressure gradient (kPa/m)	Slurry temp. (°C)
3.300	6.024	27.0
3.210	6.167	27.0
3.170	5.748	27.0
3.110	5.844	27.0
3.060	5.449	27.5
2.930	5.120	27.5
2.800	4.793	27.5
2.700	4.531	27.5
2.410	3.470	27.5
2.300	3.594	27.5
2.120	2.939	27.5
2.000	2.639	27.5
1.830	2.492	27.5
1.650	2.303	27.5
1.510	2.162	27.5
1.380	2.058	27.5
1.160	1.933	28.0
0.850	1.738	28.0
0.540	1.854	28.0
0.240	1.507	28.0

Particle size distribution
Malvern particle size analyser

Size (μm)	% Passing	% Retained
564.0	100.000	0.000
262.0	100.000	0.000
168.0	95.500	4.500
113.0	86.200	9.300
84.0	77.400	8.800
65.0	70.500	6.900
50.0	64.800	5.700
39.0	59.000	5.800
30.0	54.500	4.500
21.0	49.600	4.900
11.0	33.900	15.700
6.0	18.800	15.100
Pan	000.000	18.800

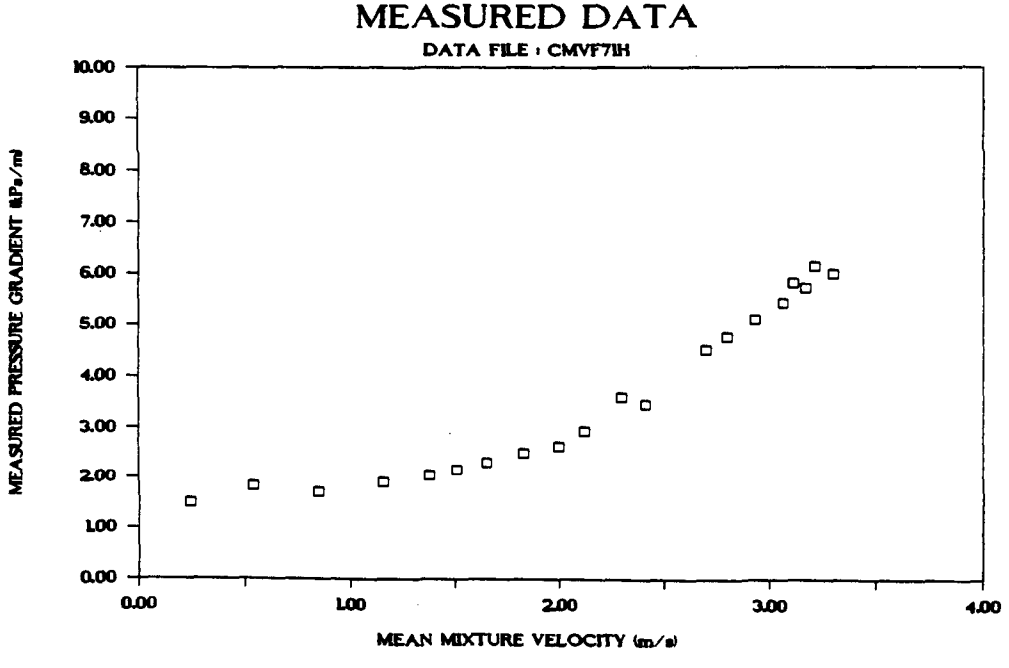

C.5.4 Program utilities

Several utility applications are available. These include both graphic and advanced user interface options.

1. The particle size distribution curve for the currently selected data files in option 4.1 can be viewed on a linear-log set of axes representing the cumulative percentage passing versus particle size.

2. The pseudo shear diagrams for the currently chosen data files can be viewed on a set of common axes. The term "pseudo shear" is used, since this option does not use the Rabinowitsch-Mooney transformation to determine the rheogram, but uses the raw data entered into the data file table.

3. The analytical models require the input of several experimentally measured constants. The methods for the determination of these constants and the necessary calculations are available as an additional option.

4. The results of a series of calculations performed in option 4 can be exported from the current program to an ASCII data file. This data file can be imported into a commercially available spreadsheet program for further plotting and presentation. Both comparative data files (option 4.1) and theoretical data files (option 4.2) can be exported in this manner.

5. The user-interface to manage data files can be selected and customized to individual prompts using a separate utility program. This program will access and create the required directory structure used for the storage of data files within the data base.

APPENDICES

APPENDIX A

DERIVATION OF THE YIELD PSEUDOPLASTIC CONSTITUTIVE EQUATION

We start with the completely general constitutive equation for circular tube flow:-

$$-\frac{du}{dr} = f(\tau) \tag{A.1}$$

A force balance on a cylindrical element of radius r and length dL yields

$$\pi r^2 \, dP = 2\pi r \tau \, dL$$

$$\therefore \quad \frac{dP}{dL} = \frac{2\tau}{r}$$

and $$\frac{dP}{dL} = \frac{2\tau_o}{R}$$

$$\therefore \quad r = \frac{R\tau}{\tau_o}, \quad r^2 = \frac{R^2\tau^2}{\tau_o^2} \text{ and } dr = \frac{R}{\tau_o} d\tau \tag{A.2}$$

also $$\tau_o = \frac{D\Delta P}{4L}.$$

The flow rate can be obtained by integrating the velocity profile :

$$Q = 2\pi \int_o^R u.r.dr \tag{A.3}$$

Integrating by parts :

$$Q = \pi \left[u r^2 - \int r^2 \frac{du}{dr} dr \right]_o^R \tag{A.4}$$

Assuming that $u_o = 0$ (no slip at the tube wall)

$$Q = -\pi \int_o^R r^2 \frac{du}{dr}\, dr$$

$$= \pi \int_o^{\tau_o} \frac{R^2\tau^2}{\tau_o^2} \cdot \left(-\frac{du}{dr}\right) \cdot \frac{R}{\tau_o} \cdot d\tau \qquad \text{(substituting A4)}$$

$$= \frac{\pi R^3}{\tau_o^3} \int_o^{\tau_o} \tau^2 \cdot f(\tau) \cdot d\tau \qquad \text{(A.5)}$$

Applying the continuity equation $Q = \pi R^2 V$ gives

$$\frac{8V}{D} = \frac{4}{\tau_o^3} \int_o^{\tau_o} \tau^2 f(\tau)\, d\tau \qquad \text{(A.6)}$$

In the plug region :

$0 \leq r \leq r_{plug}$

$0 \leq \tau \leq \tau_y$

and $f(\tau) = 0$ (A.7)

In the sheared region :

$r_{plug} \leq r \leq R$

$\tau_y \leq \tau \leq \tau_o$

$$\text{and } f(\tau) = \left(\frac{1}{K}\right)^{1/n} (\tau - \tau_y)^{1/n} \qquad \text{(A.8)}$$

For fluids with a yield stress Equation A.6 becomes

$$\frac{8V}{D} = \frac{4}{\tau_o^3} \left[\int_o^{\tau_y} \tau^2 f(\tau)\, d\tau + \int_{\tau_y}^{\tau_o} \tau^2 f(\tau)\, d\tau \right] \qquad \text{(A.9)}$$

Applying the conditions A.7 and A.8 gives

$$\frac{8V}{D} = \frac{4}{\tau_o^3}\left(\frac{1}{K}\right)^{1/n} \int_{\tau_y}^{\tau_o} \tau^2 \, (\tau - \tau_y)^{1/n} \, d\tau \qquad (A.10)$$

set $x = \tau - \tau_y$

then $dx = d\tau$

and $\tau = x + \tau_y$

Equation A.10 becomes

$$\frac{8V}{D} = \frac{4}{\tau_o^3}\left(\frac{1}{K}\right)^{1/n} \int_{\tau_y}^{\tau_o} \tau^2 \, (x - \tau_y)^2 \, x^{1/n} \, dx$$

$$= \frac{4}{\tau_o^3}\left(\frac{1}{K}\right)^{1/n} \int_{\tau_y}^{\tau_o} \left(x^{\frac{2n+1}{n}} + 2\tau_y \, x^{\frac{n+1}{n}} + \tau_y^2 \, x^{\frac{1}{n}}\right) dx$$

$$= \frac{4n}{\tau_o^3}\left(\frac{1}{K}\right)^{1/n} \left[\frac{x^{\frac{3n+1}{n}}}{\frac{3n+1}{n}} + 2\tau_y \frac{x^{\frac{2n+1}{n}}}{\frac{2n+1}{n}} + \tau_y^2 \frac{x^{\frac{n+1}{n}}}{\frac{n+1}{n}}\right]_{\tau_y}^{\tau_o}$$

$$= \frac{4n}{\tau_o^3}\left(\frac{1}{K}\right)^{1/n} \left[\frac{(\tau-\tau_y)^{\frac{3n+1}{n}}}{3n+1} + 2\tau_y \frac{(\tau-\tau_y)^{\frac{2n+1}{n}}}{2n+1} + \tau_y^2 \frac{(\tau-\tau_y)^{\frac{n+1}{n}}}{n+1}\right]_{\tau_y}^{\tau_o}$$

$$= \frac{4n}{\tau_o^3}\left(\frac{1}{K}\right)^{1/n} \left[\frac{(\tau_o-\tau_y)^{\frac{3n+1}{n}}}{3n+1} + 2\tau_y \frac{(\tau_o-\tau_y)^{\frac{2n+1}{n}}}{2n+1} + \tau_y^2 \frac{(\tau_o-\tau_y)^{\frac{n+1}{n}}}{n+1}\right]$$

$$\frac{8V}{D} = \frac{4n}{\tau_o^3}\left(\frac{1}{K}\right)^{1/n} (\tau_o - \tau_y)^{\frac{n+1}{n}} \left[\frac{(\tau_o-\tau_y)^2}{3n+1} + 2\tau_y \frac{(\tau_o-\tau_y)}{2n+1} + \frac{\tau_y^2}{n+1}\right] \qquad (A.11)$$

BINGHAM PLASTIC (n = 1)

Applying the condition n = 1 to Equation A.11 gives

$$\frac{8V}{D} = \frac{4}{K\tau_y^3}(\tau_o - \tau_y)^2\left[\frac{(\tau_o-\tau_y)^2}{4} + 2\tau_y\frac{(\tau_o-\tau_y)}{3} + \frac{\tau_y^2}{2}\right]$$

$$= \frac{4}{K\tau_y^3}(\tau_o - \tau_y)^2\left[\frac{\tau_o^2}{4} + \frac{(\tau_o\,\tau_y)}{6} + \frac{\tau_y^2}{12}\right]$$

$$= \frac{4}{K}\left[1 - \frac{4}{3}\left(\frac{\tau_y}{\tau_o}\right) + \frac{1}{3}\left(\frac{\tau_y}{\tau_o}\right)^4\right]$$

Setting $\alpha = \frac{\tau_y}{\tau_o}$, $\eta_p = K$ and making τ_o the subject of the equation yields the Buckingham equation given by

$$\tau_o = \frac{8V}{D}\eta_p \frac{1}{(1 - 4/3\alpha + \alpha^4/3)} \qquad (A.12)$$

POWER LAW ($\tau_y = 0$)

Applying the condition of $\tau_o = 0$ to Equation A.11 gives

$$\frac{8V}{D} = \frac{4n}{\tau_o^3}\left(\frac{1}{K}\right)^{1/n}\tau_o^{\frac{n+1}{n}}\frac{\tau_o^3}{1+3n}$$

$$= \frac{4n\,\tau_o^{1/n}}{K^{1/n}(1+3n)} \qquad (A.13)$$

NEWTONIAN ($\tau_y = 0$, n = 1)

Applying the conditions of $\tau_y = 0$ and n = 1 to Equation A.11 gives

$$\frac{8V}{D} = \frac{\tau_o}{K}$$

Setting $\mu = K$ and making τ_o the subject of the equation gives

$$\tau_o = \mu\frac{8V}{D} \qquad (A.14)$$

Substituting in the continuity equation yields the Hagen-Poiseuille equation given by

$$Q = \frac{\pi R^3}{4 \mu} \tau_o \qquad (A.15)$$

APPENDIX B

THE DETERMINATION OF THE RHEOLOGICAL PARAMETERS τ_y , K and n FOR THE MEASURED DATA USING THE YIELD PSEUDOPLASTIC EQUATION

B.1 Introduction

This program fits the yield pseudoplastic equation given by

$$\frac{8V}{D} = \frac{4n}{K^{1/n}\tau^3} (\tau - \tau_y)^{\frac{n+1}{n}} \left[\frac{(\tau-\tau_y)^2}{3n+1} + \frac{2\tau_y (\tau-\tau_y)}{2n+1} + \frac{\tau_y^2}{n+1} \right] \qquad (B.1)$$

to a set of data on pseudo-shear diagram.

B.2 Description

The value of the yield stress (τ_y) is read off the pseudo-shear diagram directly. Using this value the program selects the values of K and n that give the minimum error in 8V/D on a graph of 8V/D versus τ_o . The error for fixed value of τ_y , K and n is given by

$$\text{Error} = \sqrt{\sum_{i=1}^{N} \left(\left(\frac{8V_i}{D} \right)_{obs} - \left(\frac{8V_i}{D} \right)_{calc} \right)^2 / N-1}$$

$$= \sqrt{\sum_{i=1}^{N} \left(\left(\frac{8V_i}{D} \right)_{obs} - \left(\frac{4n}{K^{1/n}\tau_i^3} (\tau_i - \tau_y)^{\frac{n+1}{n}} \right.\right.}$$

$$\left.\left. \left[\frac{(\tau_i-\tau_y)^2}{3\ n+1} + \frac{2\tau_y (\tau_i-\tau_y)}{2n+1} + \frac{\tau_y^2}{n+1} \right] \right) \right)^2 / N-1 \qquad (B.2)$$

where N = Number of measured data points.

At a fixed value of n the minimum value for K is obtained by setting dError/dK = 0. This gives

$$K_{min} = 1/\left[\frac{2\sum_{i=1}^{N}\left(V_i/D\right)}{N\sum_{i=1}^{N}\left(\left(\frac{(\tau_i-\tau_y)^2}{3n+1}+\frac{2\tau_y(\tau_i-\tau_y)}{2n+1}+\frac{\tau_y^2}{n+1}\right)/\tau_o^3\right)}\right]^N \qquad (B.3)$$

The program calculates the error over a range of n values at the minimum K value. The value of n with the lowest error yields the best fit values of K and n. The error in the fit is calculated as error in $8V/D$ per point using Equation B.2.

APPENDIX C

COMPUTER PROGRAM

USERS MANUAL

C.1 Computer program technical information

The computer program requires the following hardware configuration :

1. an IBM PC/XT/AT compatible personal computer with a minimum of 512 Kb of memory.

2. The computer should preferably have a hard disk drive. The program is designed for use on a hard disk, but can be run from an external diskette drive.

3. An 8086 or 80286AT math co-processor is not essential, but recommended for speed of processing.

4. An Epson compatible printer connected to the computer parallel port.

5. Preferably MS.DOS 3.2 or later.
   Note : The program does not run on UNIX based systems.

C.2 Program contents

The program is provided on two separate 360 Kb diskettes.

Disk 1 contains the following files :

INSTALL.EXE - Used to install HYDTRANS onto hard drive.
HYDTRANS.EXE - Main program
HYDTRANS.HLP - Help file
GRAPH.DEF - Graphic setup file
FILETREE.DEF - File directory information
README.DOC - Additional information

Disk 2 contains the following utility programs :

CONVERT.EXE - Program to export data files
SETUP.EXE - Program to specify database path and directory structure.

C.3 Installation

To install the program on the hard disk

1. At the A:> prompt, insert disk # 1 into drive, type INSTALL and press <ENTER>.

2. Proceed with screen instructions until the program has been installed on the hard disk.

3. Once the program has been successfully installed, remove the diskettes and store in a safe place to be used as a backup.

4. To run the program, change to the selected sub-directory on the hard drive, type HYDTRANS and press <ENTER>.

5. When using the program, the left, right, up and down cursor keys are used to select an option.

Running from a 360 Kb diskette

1. The program will run from a 360 Kb diskette, but access to data files will be slower than for a fixed drive.

C.4 General use of program

When using the program, observe the following basic rules :

1. Use the screen prompts for information.

2. Use the HELP facility until familiar with the program.

3. When an error message occurs, the program waits for the user to press a key to continue.

4. Check that all data file input parameters are given for each data file. This means :

   a) All the tables have data for the selected pipe range.

   b) The slurry table has been calculated.

   c) The solids particle size distribution has been correctly entered and both the percentage passing and percentage retained have been calculated.

C.5 Computer program format

The format of the program allows for the input of all the relevant data in tabular form. The specific format developed for data input is unique and allows for fast and easy manipulation of the input variables.

The program is divided into four main modules, illustrated in Figure C.1, which are accessed from the main program menu. The main program menu has the format illustrated in Figure C.2. Individual topics are highlighted as the user selects the current module. At any stage of the program a context sensitive help facility can be viewed containing information relevant to the current screen. There are a total of 12 help topics available, shown in Figure C.3, which can be referred to at any time.

Each of the main modules is further divided into sub-sections which perform specific functions, and are described below.

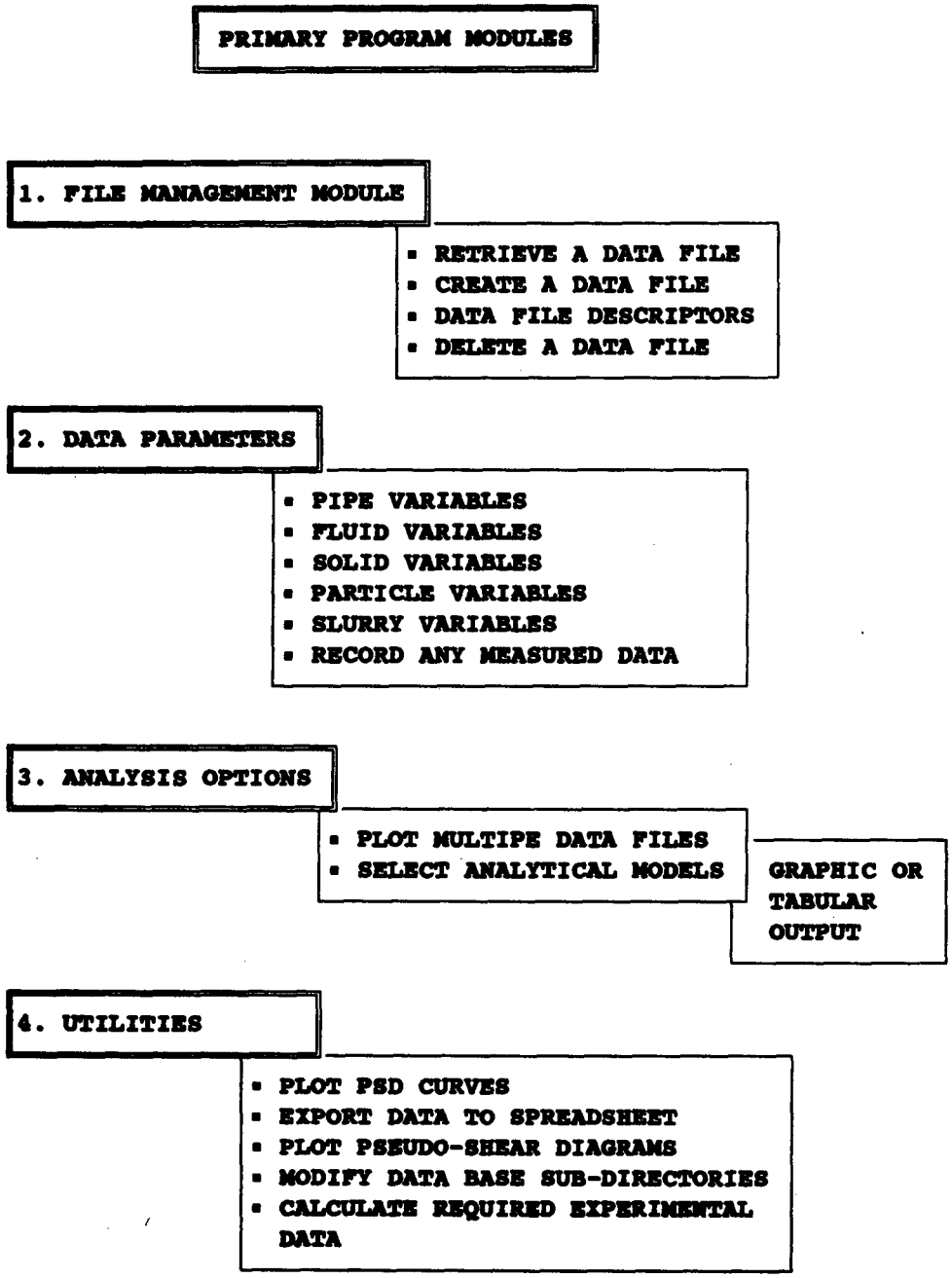

Figure C.1 : The computer program primary modules

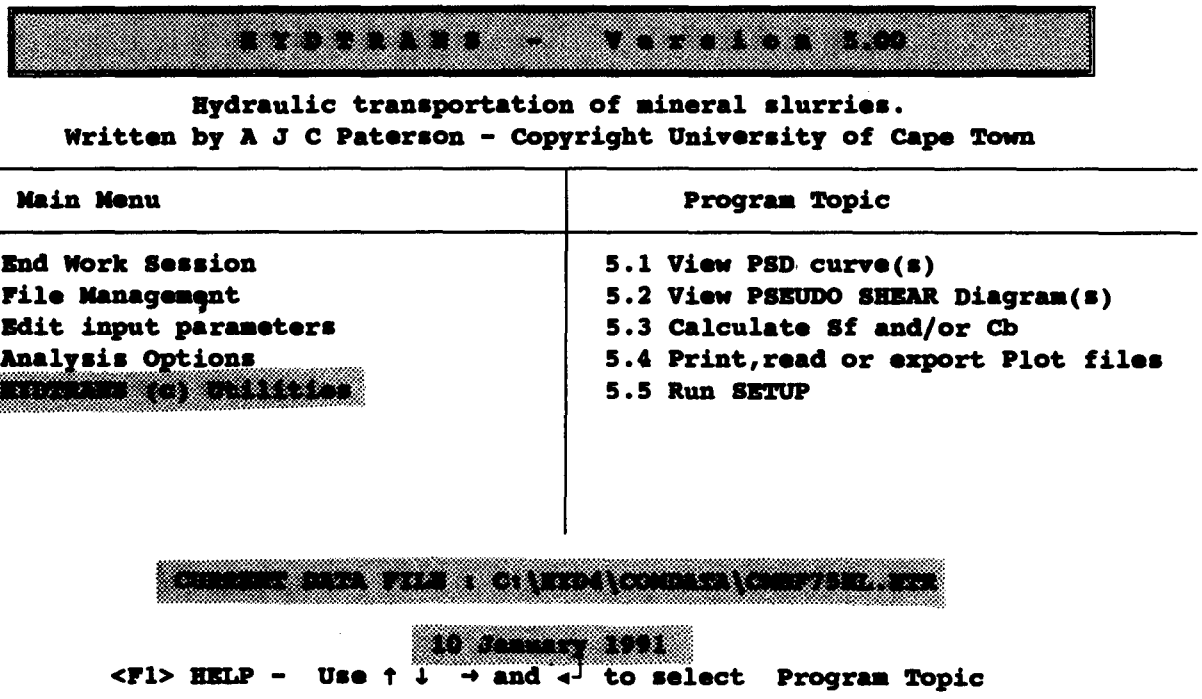

Figure C.2 : Main program menu

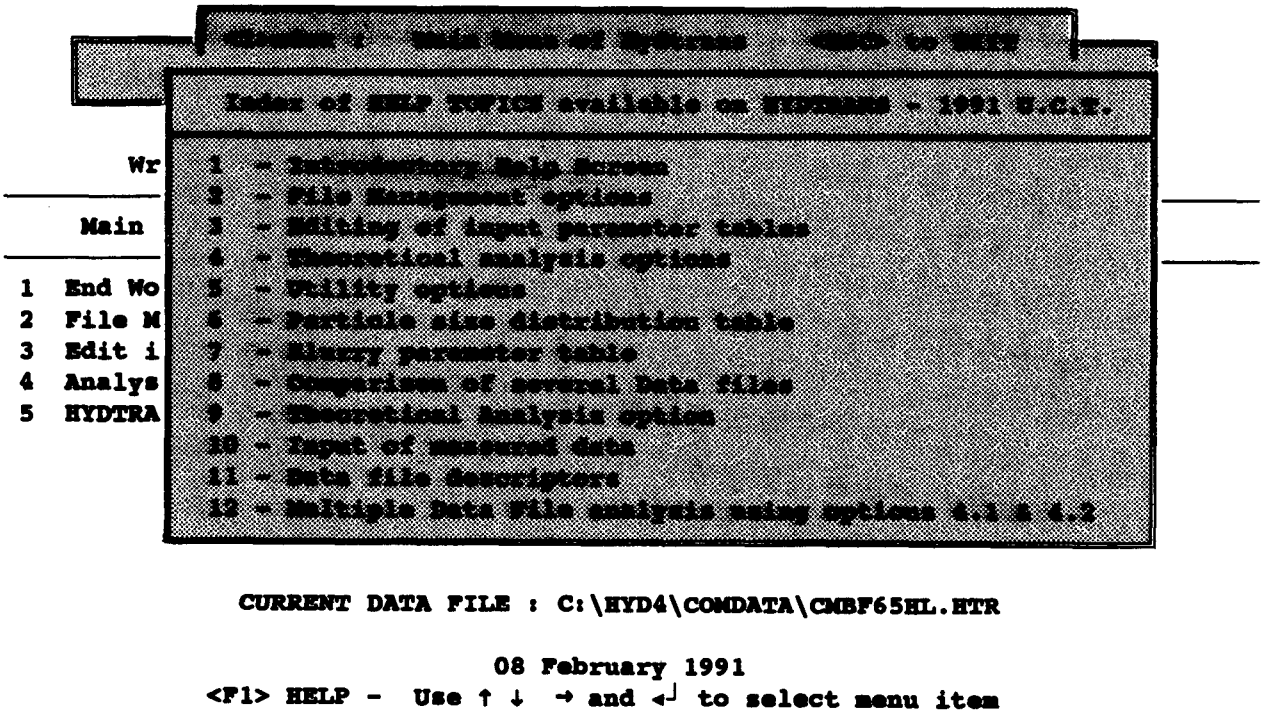

Figure C.3 : Index of program help topics

C.5.1 File management module

In order to create a uniform data base, a specifically tailored data file format is used. The file management module allows for the creation, retrieval and deletion of data files from within the main program structure. The data files can be stored or accessed in any number of separate sub-directories on the computer hard disk. These sub-directories are created by a utility program and can be customized by the user.

Each data file can be described by a unique set of historical and factual descriptions containing the following information :

1. Material description
2. Nominal pipe diameter
3. Average slurry density
4. Average slurry temperature
5. Nominal solids concentration
6. Test location/site of any measured data
7. Test date and duration
8. Pipeline material
9. Pump description
10. Additional information, e.g. inclined pipe measurements, problems encountered.

These labels are not used for mathematical analysis, but serve to identify the data file when printing results and input data.

C.5.2 Data file parameters

The variables used in the analytical models are input and accessed in the data parameters module and are given in Table C.1. Each set or group of variables is broken down into five divisions relating to :

- pipeline variables, illustrated in Figure C.4
- fluid variables, illustrated in Figure C.5
- solids variables, illustrated in Figure C.6
- particle variables, illustrated in Figure C.7
- slurry variables, illustrated in Figure C.8.

INPUT VARIABLES

Pipe Variables	Pipe Diameter (D), Pipe Roughness (k)
Fluid Variables	Fluid Relative Density (S_w), Plastic Viscosity (K), Flow Behaviour Index (n), Yield Stress (τ_y), Temperature (T)
Solids Table	Solids Relative Density (S_s), Loose Packing Density (C_{bfree}), Maximum Packing Density (C_{bmax}), Solids Friction (μ_s)
Particle Variables	Solids Particle Size Distribution (PSD), Solids Shape Factor (S_f)
Slurry Variables	Solids Concentration by Volume (C_v), Solids Concentration by Weight (C_w), Slurry Relative Density (S_m), Slurry Mean Mixture Velocity (V_m)

OUTPUT VARIABLES

Friction Loss	Head Loss per Unit Length ($\Delta H/L_m$) Pressure Loss per Unit Length ($\Delta P/L$)

Table C.1 : Computer program input and output variables

INPUT PIPE TABLE

Current File : C:\HYD4\COMDATA\CMBF65HL.HTR

Pipe variables	Diameter D(mm)	Roughness k(μm)	Length L(m)	Level1 Z1(m)	Level2 Z2(m)
1	32.63	5.0	1.00	000.00	000.00
2	0.00	5.0	1.00	000.00	000.00
3	32.63	5.0	1.00	000.00	000.00
4	32.63	5.0	1.00	000.00	000.00
5	32.63	5.0	1.00	000.00	000.00
6	32.63	5.0	1.00	000.00	000.00
7	32.63	5.0	1.00	000.00	000.00
8	32.63	5.0	1.00	000.00	000.00
9	32.63	5.0	1.00	000.00	000.00
10	32.63	5.0	1.00	000.00	000.00

Use ↑ ↓ → to select cell [Type new value and press RETURN]
< F1> - HELP - R - to repeat column entry - [Esc] to return to main menu

Figure C.4 : Pipeline variables table

INPUT FLUID TABLE

Current File : C:\HYD4\COMDATA\CMBF65HL.HTR

Fluid variables	Relative density (Sw)	Plastic viscosity K (Pas^n)	Flow index n	Yield stress τy (Pa)	Temp degrees (°C)
1	1.0000	0.094240	0.831	6.000	20.00
2	1.0000	0.094240	0.831	6.000	20.00
3	1.0000	0.094240	0.831	6.000	20.00
4	1.0000	0.094240	0.831	6.000	20.00
5	1.0000	0.094240	0.831	6.000	20.00
6	1.0000	0.094240	0.831	6.000	20.00
7	1.0000	0.094240	0.831	6.000	20.00
8	1.0000	0.094240	0.831	6.000	20.00
9	1.0000	0.094240	0.831	6.000	20.00
10	1.0000	0.094240	0.831	6.000	20.00

Use ↑ ↓ → to select cell [Type new value and press RETURN]
<F1> - HELP - R - to repeat column entry - [Esc] to return to main menu

Figure C.5 : Fluid variables table

INPUT SOLIDS TABLE

Current File : C:\HYD4\COMDATA\CMBF65HL.HTR

Solids variables	Solids Rel. density (Ss)	Free Solids Packing (Cb free)	Max. Solids Packing (Cb max)	Solids Friction coeff. (μs)
1	2.740	0.350	0.501	0.480
2	2.740	0.350	0.501	0.480
3	2.740	0.350	0.501	0.480
4	2.740	0.350	0.501	0.480
5	2.740	0.350	0.501	0.480
6	2.740	0.350	0.501	0.480
7	2.740	0.350	0.501	0.480
8	2.740	0.350	0.501	0.480
9	2.740	0.350	0.501	0.480
10	2.740	0.350	0.501	0.480

Use ↑ ↓ → to select cell [Type new value and press RETURN]
<F1> - HELP - R - to repeat column entry - [Esc] to return to main menu

Figure C.6 : Solids variables table

INPUT PARTICLE TABLE

Current File : C:\HYD4\COMDATA\CMBF65HL.HTR

Particle variables	Particle sizes (μm)	Percent pass. (%)	Percent ret. (%)	Shape factor
1	273.0	100.000	0.00	0.550
2	134.0	90.000	10.00	0.550
3	94.0	80.000	10.00	0.550
4	64.0	70.000	10.00	0.550
5	43.0	60.000	10.00	0.550
6	29.0	50.000	10.00	0.550
7	18.0	40.000	10.00	0.550
8	12.0	30.000	10.00	0.550
9	8.0	20.000	10.00	0.550
10	6.0	10.000	10.00	0.550
Pan	0.0	0.000	10.00	0.550
12	0.0	0.000	0.00	0.550
**	0.0	0.000	0.00	0.550

<F1> HELP - Use ↑ ↓ → to select cell [Type new value and press RETURN]
[C] Calculate - [R] Repeat column entry - [Esc] Return to main menu

Figure C.7 : Particle variables table

Current File :C:\HYD4\COMDATA\CMBF65HL.HTR
- Set variables to zero before changes - Use [Alt R] Keys

Slurry variables	Solid mass flow rate Ms(kg/s)	Slurry flow rate (l/s)	Concentration by volume Cvd(%)	Concentration by mass Cwd(%)	Relative density Sm	Mean mixture velocity Vm(m/s)
1	0.80	0.420	37.410	62.090	1.651	0.500
2	0.00	0.000	37.410	62.090	1.651	1.000
3	1.30	1.250	37.410	62.090	1.651	1.500
4	1.70	1.670	37.410	62.090	1.651	2.000
5	2.10	2.090	37.410	62.090	1.651	2.500
6	2.60	2.510	37.410	62.090	1.651	3.000
7	3.00	2.930	37.410	62.090	1.651	3.500
8	3.40	3.340	37.410	62.090	1.651	4.000
9	3.90	3.760	37.410	62.090	1.651	4.500
10	4.30	4.180	37.410	62.090	1.651	5.000

<F1> HELP - Use ↑ ↓ → to select cell [Type new value and press RETURN]
[C] Calculate - [R] Repeat column entry - [Esc] Return to main menu

Figure C.8 : Slurry variables table

Each of the variables is entered into each sub-section using a spreadsheet format. For example, the pipe variable table is used to enter pipe internal diameter (mm), pipe roughness (μm), pipe length (m) and pipe elevations (m) at the end points. Each table is comprised of both columns and rows, each cell or block denoted by its row and column number. There are always 10 rows per table. Each row in each table comprises a set of data corresponding to all other rows of the same set for all remaining tables. Thus data in row 1 of the pipe table corresponds to data in row 1 of the solids table. The inter-relationship of the data file tables is shown in Figure C.9. This facility means that for a given particle size distribution of a particular slurry, the varying of a particular quantity can easily be performed. This is best explained as follows. A fundamental assumption is that the particle size distribution of the particles remains the same and is characterised by a solid particle relative density, S_s , which is constant for all size fractions.

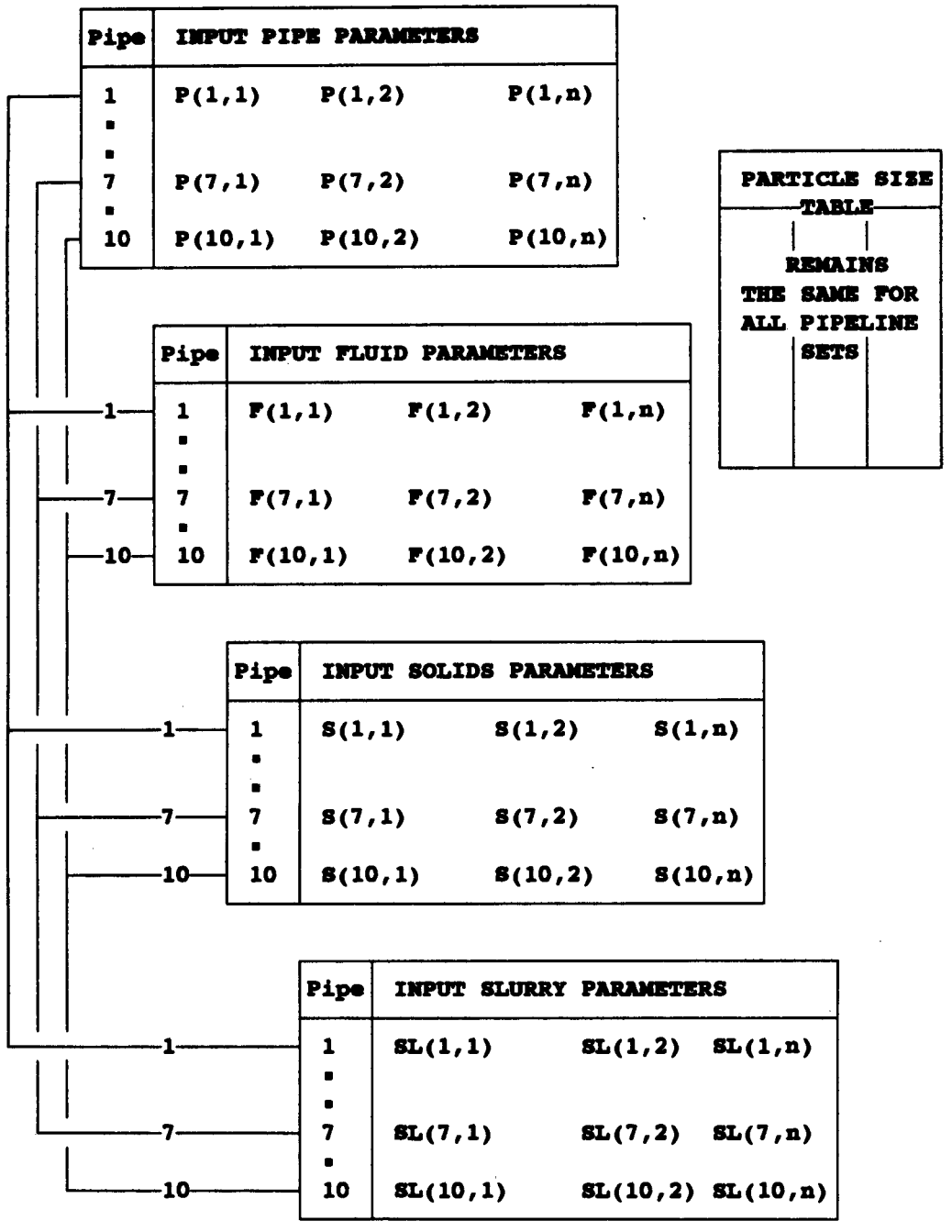

Note: Data for PIPE 1 is in line 1 of all tables
Data for PIPE 2 is in line 2 of all tables etc.

Figure C.9 : Row and column inter-relationship of data file tables

To quantify the effect of slurry relative density on calculated pipeline pressure gradient and keeping other conditions constant for a particular chosen model, the following steps are performed, bearing in mind Figure C.9 and the table relationships.

1. Set all the rows in the pipe table, the fluid table and the solids table to constant values.

2. Move to the slurry parameter table, option 3.5, and reset all the column values to zero. This is done using a hotkey combination, explained in the help facility. Once all values, S_m , have been reset to zero, move to the relative density column, and for each row enter the chosen relative density value. When all the rows have been completed, an automatic recalculation procedure determines the remaining parameters in the slurry table.

3. All 10 rows in each of the tables now contain the same data, except the slurry table which contains the variations of slurry density.

When these tables are correctly used in conjunction with the several models available, it is a powerful and quick method of performing a variety of optimization and sensitivity analyses on any of the variables contained within the data parameter tables.

If measured data is available, up to 30 data points containing the following information can be entered and stored in the data file using the data file table, option 3.6, shown in Figure C.10.

1. Measured velocity (m/s)
2. Measured pressure gradient (kPa/m)
3. Measured slurry relative density (S_m)
4. Measured solids volumetric concentration (C_{vd})
5. Measured slurry temperature (°C)
6. Observed bed conditions.

DATA TABLE

Current File : C:\HYD4\COMDATA\CMBF65HL.HTR

<Pg 1 of 3>

No	Measured Velocity (m/s)	Measured Pressure Loss (kPa/m)	Measured Delivered Conc. (%)	Measured Slurry Density (Sm)	Measured Slurry Temp. (°C)	Observed Bed Cond.
1	0.330	1.413	37.450	1.650	16.00	Sliding
2	0.490	1.710	37.450	1.650	16.00	Sliding
3	0.720	1.808	37.450	1.650	16.00	Sliding
4	1.010	2.156	37.450	1.650	16.00	Sliding
5	1.290	2.389	37.450	1.650	16.00	Sliding
6	1.470	2.639	37.450	1.650	16.00	Sliding
7	1.800	2.892	37.450	1.650	16.00	Sliding
8	2.030	3.128	37.450	1.650	16.00	Sliding
9	2.250	3.613	37.450	1.650	16.00	Sliding
10	2.530	4.005	37.450	1.650	16.00	Sliding

<Page Down>

Use ↑ ↓ → to select cell [Type new value and press RETURN]
<F1> HELP - [R] to repeat column entry - [Esc] to return to main menu

Figure C.10 : Table to store measured data - the data file table

These data points are used for the analysis of the log standard error when comparing the results of the model calculations against the measured data. The data in these tables is not used in conjunction with the remaining tables.

C.5.3 Analysis options module

The third module contains the routines to view or print the data file and to perform the numeric processing of the data. There are two options within this module :

Option 4.1 This option is used to graphically compare up to 10 sets of measured data on one set of axes using the pressure gradient versus mean mixture velocity curve. This measured dataand the file descriptors can be printed to obtain a hard copy for further reference. Figure C.11 represents the layout for selecting data files.

PLOT MULTIPLE DATA FILES

Current File : C:\HYD4\COMDATA\CMBF65HL.HTR

Edit Keys	File No.	Data File	Yes/No	Options	Options
	1	CMBF65HL	Yes	Max. Vel.	5.0
F2 Edit	2	CMBF65HS	No	Max. P	10.0
Table	3	CMBF70HS	No	UNITS	(kPa/m)
	4	CMBF70HL	Yes		
F3 Edit	5	CMBF81HL	Yes	Vel. min.	0.0
Titles	6	CMBF85HS	No	Vel. Inc.	.50
	7		No		
F4 File	8		No	Graph +	Yes
Select	9		No		
	10		No		
<Enter> Selects Yes/No	1st. Title	HYDTRANS SOFTWARE U.C.T 1990			
	2nd. Title	Hydraulic transport of Solids			
	X Title	Mean mixture velocity			
	Y Title	Pressure Gradient			

Use ↑ ↓ → to select cell [Type new value and press RETURN]
<F1> HELP - [G] - to begin plot - [Esc] to return to main menu

Figure C.11 : Option 4.1 - plot multiple data files. The table is used to select which data files are to be viewed on the screen or analysed in option 4.2

[illegible] Current File : C:\HYD4\COMDATA\CMBF65HL.HTR

Edit Keys	Model No.	Model Name	Yes/No	Options	Options	View Keys
	1	Paterson	Yes			Alt F1-F10
F2 Edit	2	Sive	No	Max. Vel.	5.0	To quick
Table	3	Lazarus	No	Max. P	10.0	view pipe
	4	Wilson	No	UNITS	(kPa/m)	data
F3 Edit	5	Yield_PP	Yes			
Titles	6	Wasp	No	Min. Vel.	0.0	
	7	Newitt	No	Vel. inc.	.50	Alt G
<Enter>	8	Streat	Yes	Durand K	180	to quick
Selects	9	Pseudo	No	Graph +	Yes	view
Yes/No	10	Durand	No	Auto Mode	No	current
	11	Cl. Water	Yes	Log Error	Yes	Graph
	* File *	Plot Data	Yes			
	1st. Title	HYDTRANS SOFTWARE U.C.T 1990				
	2nd. Title	Hydraulic transport of Solids				
	X Title	Mean mixture velocity				
	Y Title	Pressure Gradient				

Use ↑ ↓ → to select cell [Type new value and press RETURN]
<F1> HELP - [G] - to begin plot - [Esc] to return to main menu

Figure C.12 : Option 4.2 - table used to select which of the available analytical models are to be selected for analysis of the data

Option 4.2 The analytical model choice option is used to compare both graphically and on the basis of the log standard error the results of any of the selected mathematical models on the same set of axes. The model selection is done using Figure C.12 which provides maximum flexibility for selecting analysis options.

Both these two options are interlinked, as shown in Figure C.13. The analysis and file comparison procedure is as follows :

1. From option 4.1, "Select Multiple Data files", the first file name is chosen if the option to plot is 'Yes". (This is normally the current file).

2. The data tables for this file are read for the first pipe range.

3. Each of the models in option 4.2 for which the selection is "Yes" are used to calculate a series of results on the $i_m - V_m$ curve for the current pipe range.

4. Step 2 and 3 are repeated for each pipe range until all the selected ranges are plotted.

IMPORTANT NOTE : The number of pipe ranges to calculate a series of results is determined by setting the proceeding pipe diameter to zero. To calculate results for pipe row 1 only, set pipe row 2 diameter to zero. To calculate results for pipe ranges 1 to 5, the pipe diameter in option 3.1 for pipe row 6 must be set to zero.

5. The next data file from option 4.1 is selected and steps 2-5 are repeated.

The above routine can be used to compare a variety of measured data files to any of the analytical models and demonstrates the powerful program applications. At each stage of the sequence, a hard copy of the results can be obtained.

INTERACTION OF ANALYSIS OPTION TABLES

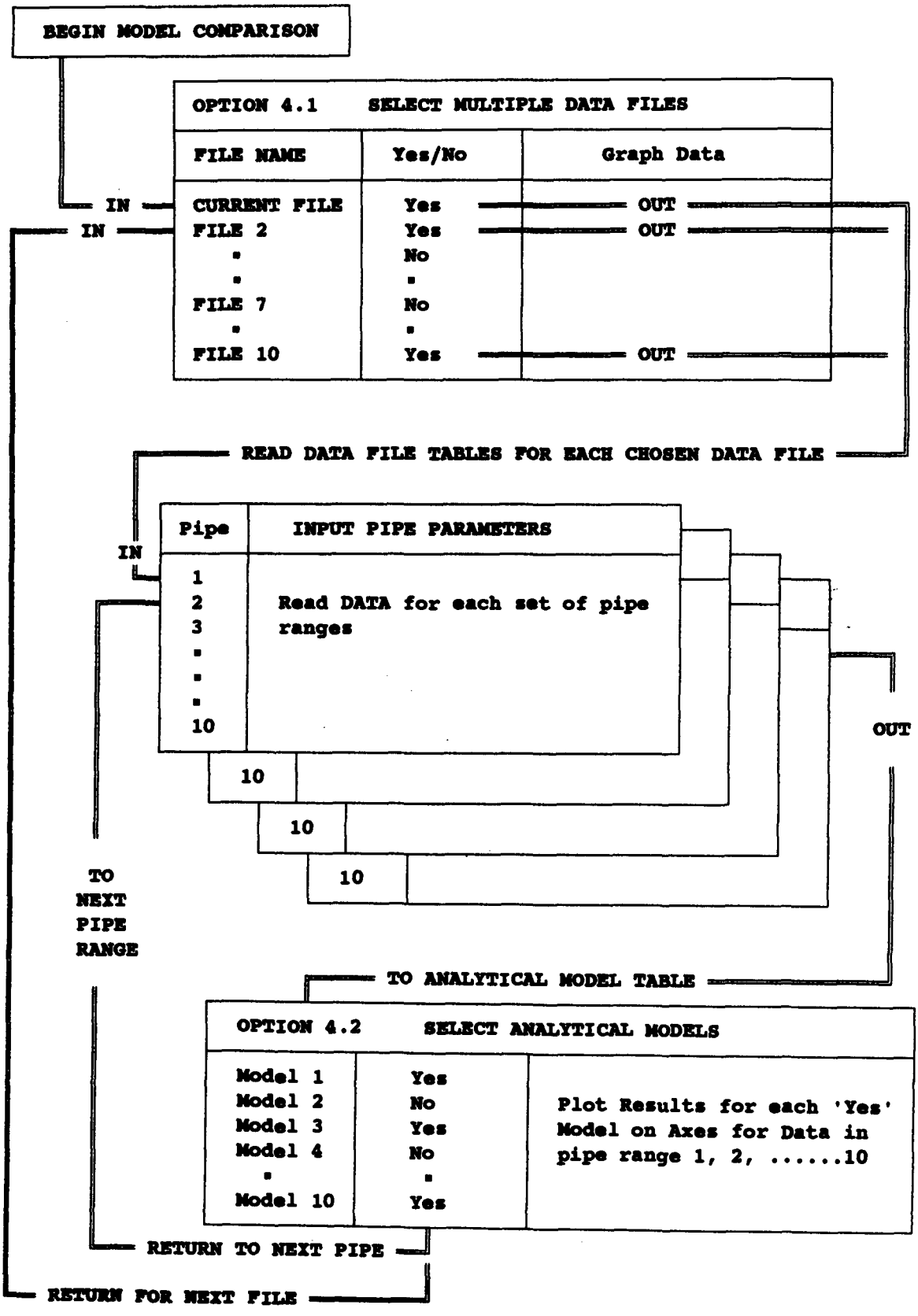

Figure C.13 : Interaction between option 4.1 and 4.2 to plot and analyse multiple sets of data

DATA FILE : CMVF74H.

Test facility		Vertical Test Facility
Test date		1989
Material description		Chamber of Mines Full Plant
Material relative density		2.720
Slurry relative density		1.730
Solids volumetric concentration	(%)	42.480
Solids mass concentration	(%)	66.780
Pipe internal diameter	(mm)	41.22
Pipe internal roughness	(μm)	103.0
Pipeline gradient		Horizontal

Mixture velocity (m/s)	Pressure gradient (kPa/m)	Slurry temp. (°C)
3.320	5.935	28.0
3.310	6.287	28.0
3.170	5.718	28.0
3.100	5.493	28.0
2.970	5.055	28.0
2.840	4.734	28.0
2.690	4.299	28.0
2.590	4.100	28.0
2.090	3.025	28.0
2.030	2.899	28.0
1.760	2.699	28.0
1.260	2.084	28.0
1.220	2.096	28.0
0.960	1.885	28.0
0.860	1.848	28.0
0.440	1.547	28.0
0.400	1.563	28.0
0.320	1.473	28.0
0.230	1.471	28.0
0.090	1.311	28.0

Particle size distribution
Malvern particle size analyser

Size (μm)	% Passing	% Retained
564.0	100.000	0.000
262.0	100.000	0.000
168.0	95.500	4.500
113.0	86.200	9.300
84.0	77.400	8.800
65.0	70.500	6.900
50.0	64.800	5.700
39.0	59.000	5.800
30.0	54.500	4.500
21.0	49.600	4.900
11.0	33.900	15.700
6.0	18.800	15.100
Pan	000.000	18.800

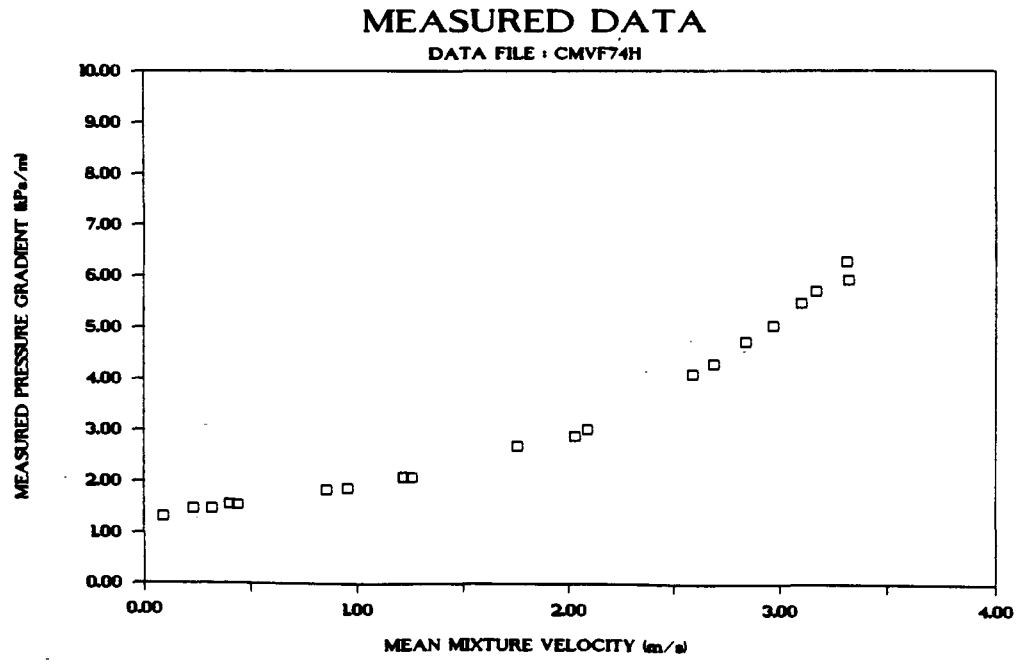

DATA FILE : CMVF76H.

Test facility		Vertical Test Facility
Test date		1989
Material description		Chamber of Mines Full Plant
Material relative density		2.720
Slurry relative density		1.760
Solids volumetric concentration	(%)	44.220
Solids mass concentration	(%)	68.340
Pipe internal diameter	(mm)	41.50
Pipe internal roughness	(μm)	103.0
Pipeline gradient		Horizontal

Mixture velocity (m/s)	Pressure gradient (kPa/m)	Slurry temp. (°C)
3.230	6.997	27.0
3.170	6.880	27.0
3.140	6.721	27.0
3.060	6.360	27.0
2.970	6.164	27.0
2.700	5.554	27.0
2.590	5.370	27.0
2.530	5.291	27.0
2.430	5.017	27.0
2.420	5.040	27.0
2.370	4.906	28.5
2.130	4.684	28.5
1.780	4.297	28.5
1.690	3.981	28.5
1.370	3.772	28.5
1.200	3.508	28.5
0.930	3.082	28.5
0.550	3.039	28.5
0.470	2.905	28.5
0.220	2.724	28.5

Particle size distribution
Malvern particle size analyser

Size (μm)	% Passing	% Retained
564.0	100.000	0.000
262.0	100.000	0.000
168.0	95.500	4.500
113.0	86.200	9.300
84.0	77.400	8.800
65.0	70.500	6.900
50.0	64.800	5.700
39.0	59.000	5.800
30.0	54.500	4.500
21.0	49.600	4.900
11.0	33.900	15.700
6.0	18.800	15.100
Pan	000.000	18.800

MEASURED DATA

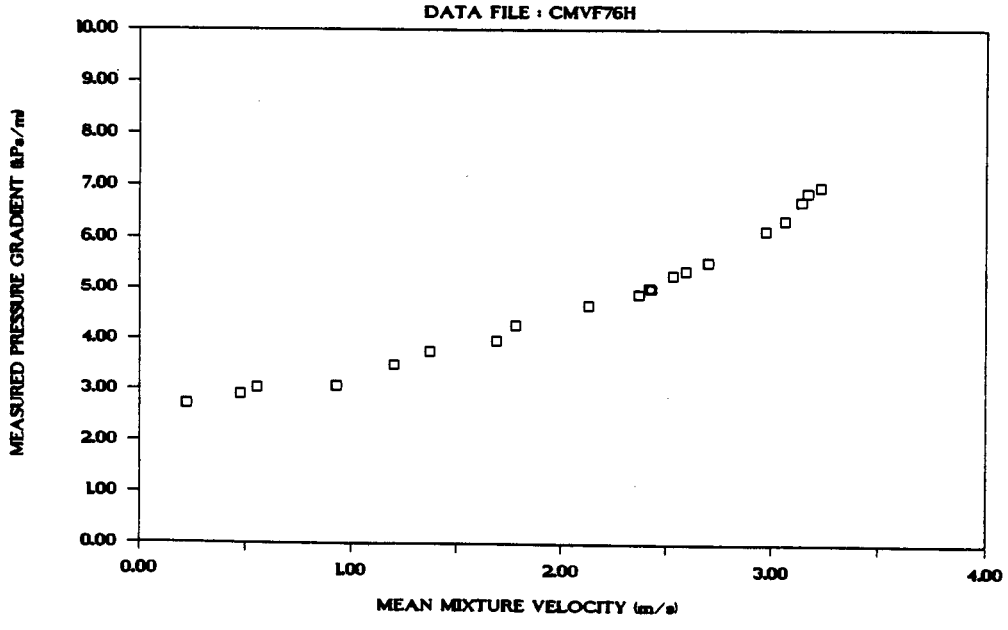

DATA FILE : CMVF81H.

Test facility		Vertical Test Facility
Test date		1989
Material description		Chamber of Mines Full Plant
Material relative density		2.720
Slurry relative density		1.810
Solids volumetric concentration	(%)	47.120
Solids mass concentration	(%)	70.820
Pipe internal diameter	(mm)	41.50
Pipe internal roughness	(μm)	103.0
Pipeline gradient		Horizontal

Mixture velocity (m/s)	Pressure gradient (kPa/m)	Slurry temp. (°C)
2.650	7.503	28.0
2.470	8.179	28.0
2.270	7.754	28.0
2.080	7.689	28.0
2.020	7.416	28.0
1.940	7.019	28.0
1.860	7.124	28.0
1.790	7.073	28.0
1.770	6.971	28.0
1.710	6.848	28.0
1.550	6.511	28.5
1.520	6.616	28.5
1.500	6.588	28.5
1.010	6.204	28.5
0.670	6.139	28.5
0.430	5.606	28.5
0.370	5.535	28.5
0.190	4.557	28.5
0.120	2.985	28.5
0.020	3.593	28.5

Particle size distribution
Malvern particle size analyser

Size (μm)	% Passing	% Retained
564.0	100.000	0.000
262.0	100.000	0.000
168.0	95.500	4.500
113.0	86.200	9.300
84.0	77.400	8.800
65.0	70.500	6.900
50.0	64.800	5.700
39.0	59.000	5.800
30.0	54.500	4.500
21.0	49.600	4.900
11.0	33.900	15.700
6.0	18.800	15.100
Pan	000.000	18.800

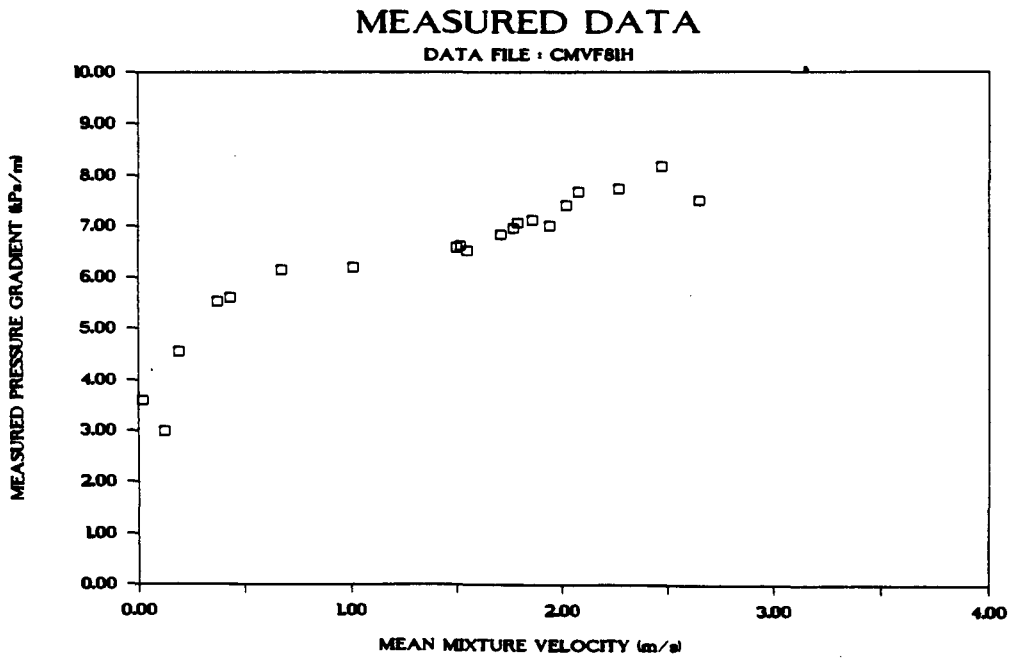

DATA FILE : CMVF85H.

Test facility		Vertical Test Facility
Test date		1989
Material description		Chamber of Mines Full Plant
Material relative density		2.720
Slurry relative density		1.850
Solids volumetric concentration	(%)	49.450
Solids mass concentration	(%)	72.700
Pipe internal diameter	(mm)	41.50
Pipe internal roughness	(μm)	103.0
Pipeline gradient		Horizontal

Mixture velocity (m/s)	Pressure gradient (kPa/m)	Slurry temp. (°C)
1.440	10.314	28.0
1.430	10.246	28.0
1.370	10.116	28.0
1.310	10.640	28.0
1.300	10.575	28.0
1.290	9.805	28.5
1.280	10.038	28.5
1.230	10.703	28.5
1.180	9.632	28.5
1.070	10.097	28.5
1.050	11.132	29.5
1.040	9.849	29.5
1.000	9.510	29.5
0.790	9.778	29.5
0.760	9.932	29.5
0.710	9.660	30.5
0.570	9.280	30.5
0.560	9.250	30.5
0.120	7.448	30.5
0.100	7.588	30.5

Particle size distribution
Malvern particle size analyser

Size (μm)	% Passing	% Retained
564.0	100.000	0.000
262.0	100.000	0.000
168.0	95.500	4.500
113.0	86.200	9.300
84.0	77.400	8.800
65.0	70.500	6.900
50.0	64.800	5.700
39.0	59.000	5.800
30.0	54.500	4.500
21.0	49.600	4.900
11.0	33.900	15.700
6.0	18.800	15.100
Pan	000.000	18.800

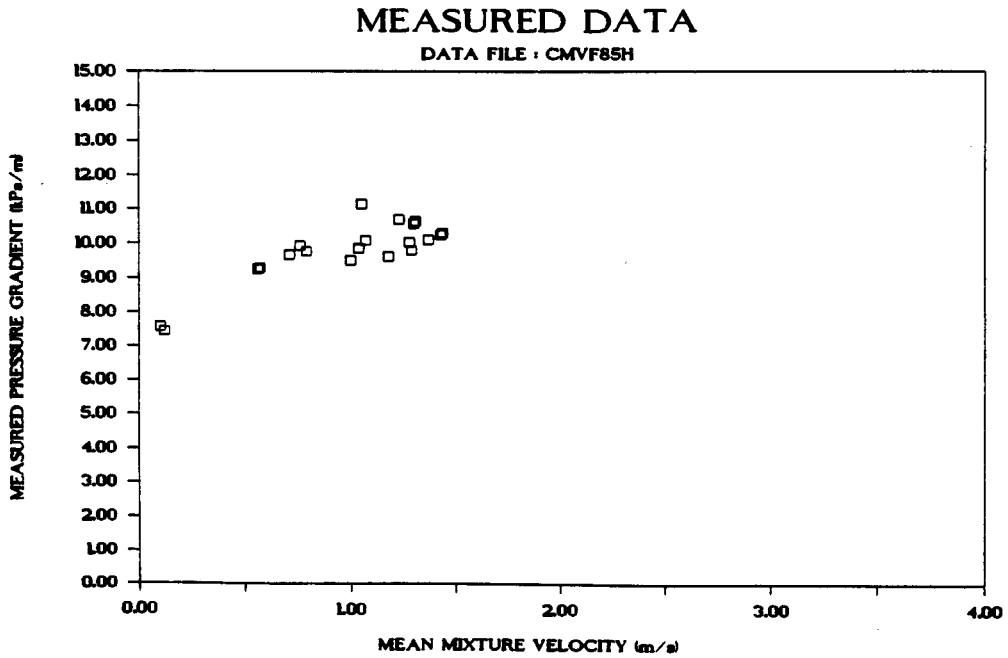

DATA FILE : CMVF43HL

Test facility		Vertical test facility at UCT
Test date		November 1979 Thesis student
Material description		Chamber of Mines Full Plant
Material relative density		2.720
Slurry relative density		1.430
Solids volumetric concentration	(%)	25.040
Solids mass concentration	(%)	47.640
Pipe internal diameter	(mm)	75.88
Pipe internal roughness	(μm)	10.0
Pipeline gradient		Horizontal

Mixture velocity (m/s)	Pressure gradient (kPa/m)	Slurry temp. (°C)
0.280	0.168	25.0
0.420	0.231	25.0
0.720	0.403	25.0
0.990	0.446	25.0
1.190	0.367	25.0
1.190	0.394	25.0
1.510	0.531	25.0
1.550	0.651	25.0
1.850	0.669	25.0
2.140	0.671	25.0
2.500	0.802	25.0
3.000	1.114	25.0
3.030	0.999	25.0
3.070	1.093	25.0
3.350	1.182	25.0
3.730	1.528	25.0
3.990	1.705	25.0
4.250	1.592	25.0
4.630	2.025	25.0
4.650	2.007	25.0

Particle size distribution
Malvern particle size analyser

Size (μm)	% Passing	% Retained
564.0	100.000	0.000
262.0	100.000	0.000
160.0	95.500	4.500
113.0	86.200	9.300
84.0	77.400	8.800
65.0	70.500	6.900
50.0	64.800	5.700
39.0	59.000	5.800
30.0	54.500	4.500
21.0	49.600	4.900
11.0	33.900	15.700
6.0	18.000	15.900
Pan	0.000	18.000

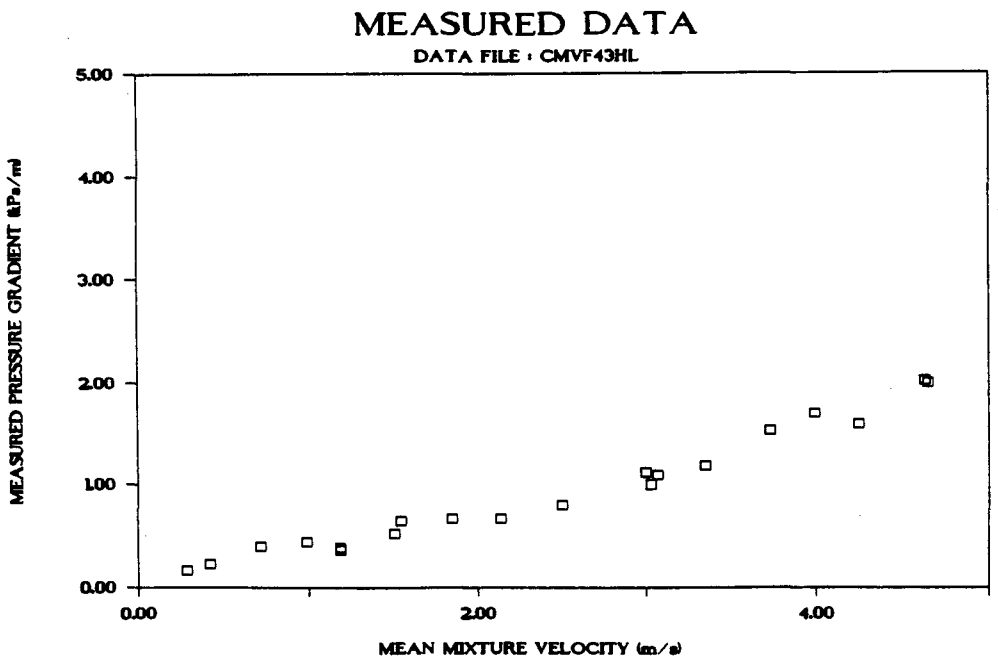

DATA FILE : CMVF61HL

Test facility		Vertical test facility at UCT
Test date		November 1989 Thesis student
Material description		Chamber of Mines Full Plant
Material relative density		2.720
Slurry relative density		1.610
Solids volumetric concentration	(%)	35.500
Solids mass concentration	(%)	59.980
Pipe internal diameter	(mm)	75.88
Pipe internal roughness	(μm)	10.0
Pipeline gradient		Horizontal

Mixture velocity (m/s)	Pressure gradient (kPa/m)	Slurry temp. (°C)
3.470	2.394	25.0
3.440	2.153	25.0
3.300	2.057	25.0
3.240	1.855	25.0
3.210	2.257	25.0
2.730	1.485	25.0
2.720	1.812	25.0
2.250	1.249	25.0
2.240	1.163	25.0
1.940	1.031	25.0
1.740	0.966	25.0
1.740	0.954	25.0
1.520	0.821	25.0
1.440	0.763	25.0
1.180	0.593	25.0
1.130	0.648	25.0
0.580	0.621	25.0
0.440	0.724	25.0

Particle size distribution
Malvern particle size analyser

Size (μm)	% Passing	% Retained
564.0	100.000	0.000
262.0	100.000	0.000
160.0	95.500	4.500
113.0	86.200	9.300
84.0	77.400	8.800
65.0	70.500	6.900
50.0	64.800	5.700
39.0	59.000	5.800
30.0	54.500	4.500
21.0	49.600	4.900
11.0	33.900	15.700
6.0	18.000	15.900
Pan	0.000	18.000

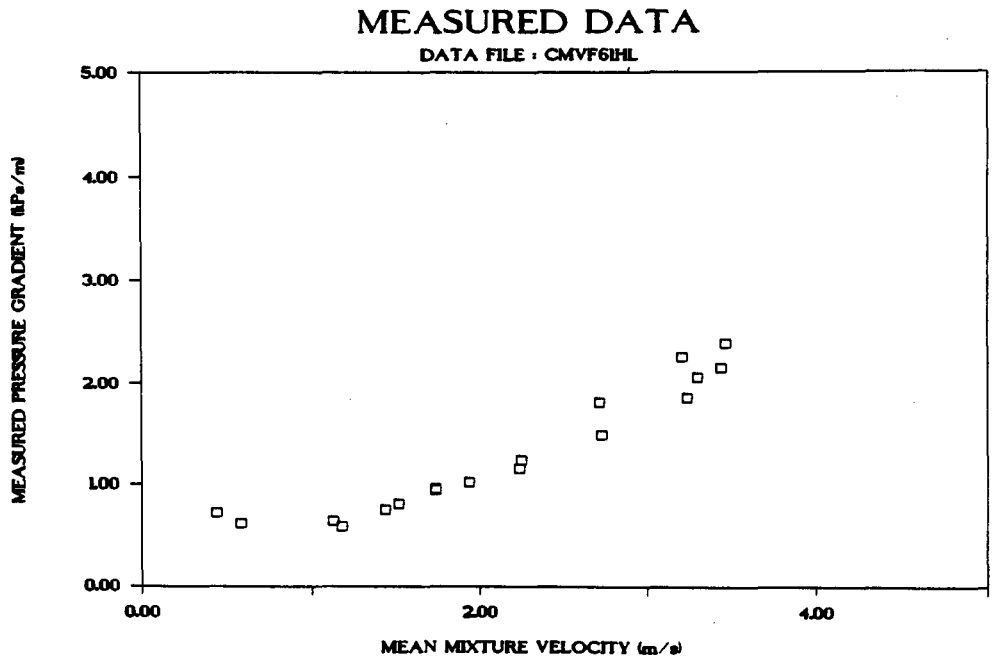

DATA FILE : CMVF70HL

Test facility		Vertical test facility at UCT
Test date		November 1989
Material description		Chamber of Mines Full Plant
Material relative density		2.720
Slurry relative density		1.700
Solids volumetric concentration	(%)	40.730
Solids mass concentration	(%)	65.170
Pipe internal diameter	(mm)	75.88
Pipe internal roughness	(μm)	10.0
Pipeline gradient		Horizontal

Mixture velocity (m/s)	Pressure gradient (kPa/m)	Slurry temp. (°C)
3.210	2.929	25.0
3.200	2.961	25.0
2.900	2.451	25.0
2.890	2.627	25.0
2.680	2.334	25.0
2.200	2.261	25.0
2.050	1.964	25.0
1.990	2.105	25.0
1.750	2.196	25.0
1.690	2.149	25.0
1.670	2.067	25.0
1.060	1.944	25.0
1.040	1.987	25.0
0.830	2.004	25.0
0.640	1.860	25.0
0.530	1.858	25.0
0.360	1.670	25.0

Particle size distribution
Malvern particle size analyser

Size (μm)	% Passing	% Retained
564.0	100.000	0.000
262.0	100.000	0.000
160.0	95.500	4.500
113.0	86.200	9.300
84.0	77.400	8.800
65.0	70.500	6.900
50.0	64.800	5.700
39.0	59.000	5.800
30.0	54.500	4.500
21.0	49.600	4.900
11.0	33.900	15.700
6.0	18.000	15.900
Pan	0.000	18.000

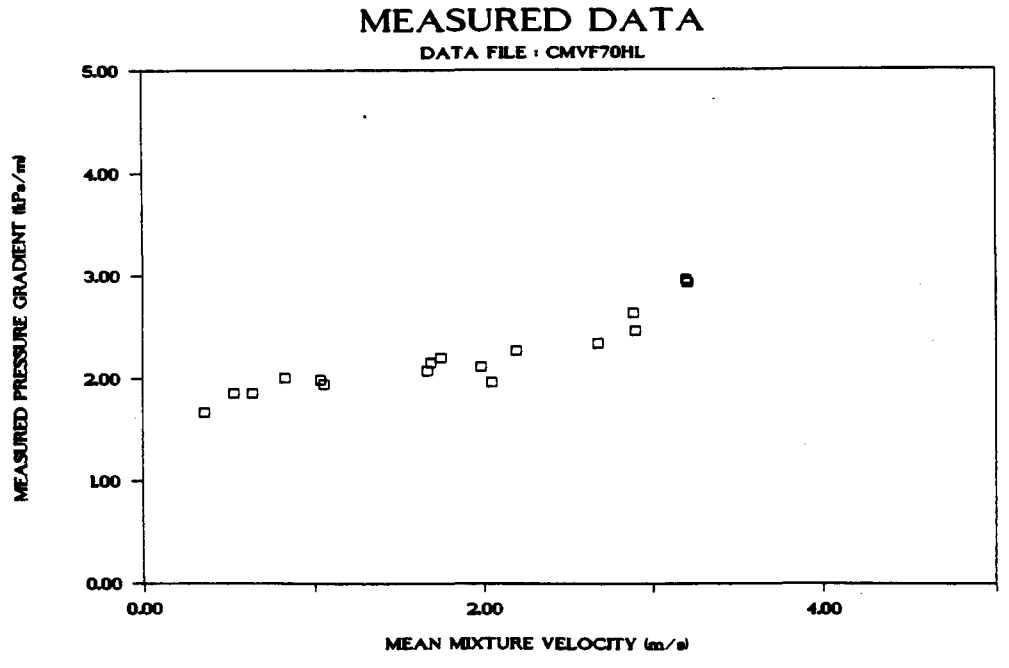

DATA FILE : CMVF73HL

Test facility		Vertical test facility at UCT
Test date		November 1989
Material description		Chamber of Mines Full Plant
Material relative density		2.720
Slurry relative density		1.730
Solids volumetric concentration	(%)	42.480
Solids mass concentration	(%)	66.780
Pipe internal diameter	(mm)	75.88
Pipe internal roughness	(μm)	10.0
Pipeline gradient		Horizontal

Mixture velocity (m/s)	Pressure gradient (kPa/m)	Slurry temp. (°C)
1.950	2.796	25.0
1.650	2.711	25.0
1.350	2.516	25.0
0.960	2.426	25.0
0.950	2.761	25.0
0.830	2.712	25.0
0.590	2.488	25.0
0.470	2.637	25.0
0.430	2.549	25.0
0.390	2.480	25.0
0.380	2.488	25.0
0.360	2.213	25.0
0.250	2.755	25.0
0.140	2.182	25.0

Particle size distribution
Malvern particle size analyser

Size (μm)	% Passing	% Retained
564.0	100.000	0.000
262.0	100.000	0.000
160.0	95.500	4.500
113.0	86.200	9.300
84.0	77.400	8.800
65.0	70.500	6.900
50.0	64.800	5.700
39.0	59.000	5.800
30.0	54.500	4.500
21.0	49.600	4.900
11.0	33.900	15.700
6.0	18.000	15.900
Pan	0.000	18.000

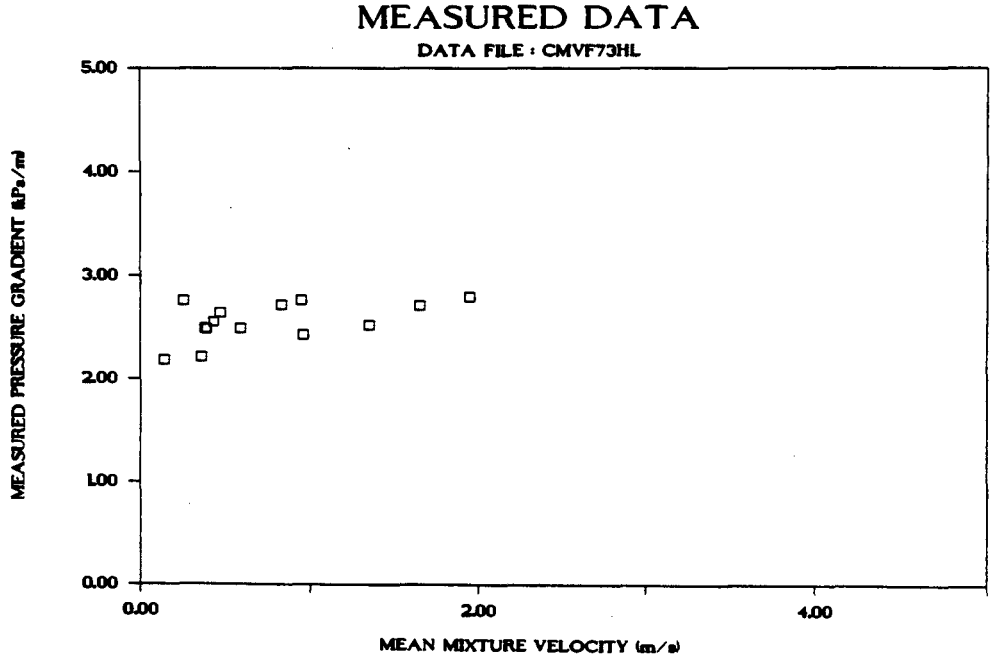

DATA FILE : CMCF50H.

Test facility		Chamber of Mines
Test date		
Material description		Full Plant Tailings
Material relative density		2.720
Slurry relative density		1.500
Solids volumetric concentration	(%)	29.110
Solids mass concentration	(%)	52.790
Pipe internal diameter	(mm)	101.50
Pipe internal roughness	(μm)	40.0
Pipeline gradient		Horizontal

Mixture velocity (m/s)	Pressure gradient (kPa/m)	Slurry temp. (°C)
3.860	1.830	21.0
3.230	1.200	21.0
2.620	0.800	21.0
2.170	0.580	21.0
1.910	0.420	21.0
1.630	0.290	21.0

Particle size distribution
Malvern particle size analyser

Size (μm)	% Passing	% Retained
425.0	100.000	0.000
300.0	100.000	0.000
212.0	100.000	0.000
150.0	99.400	0.600
106.0	93.200	6.200
38.0	58.900	34.300

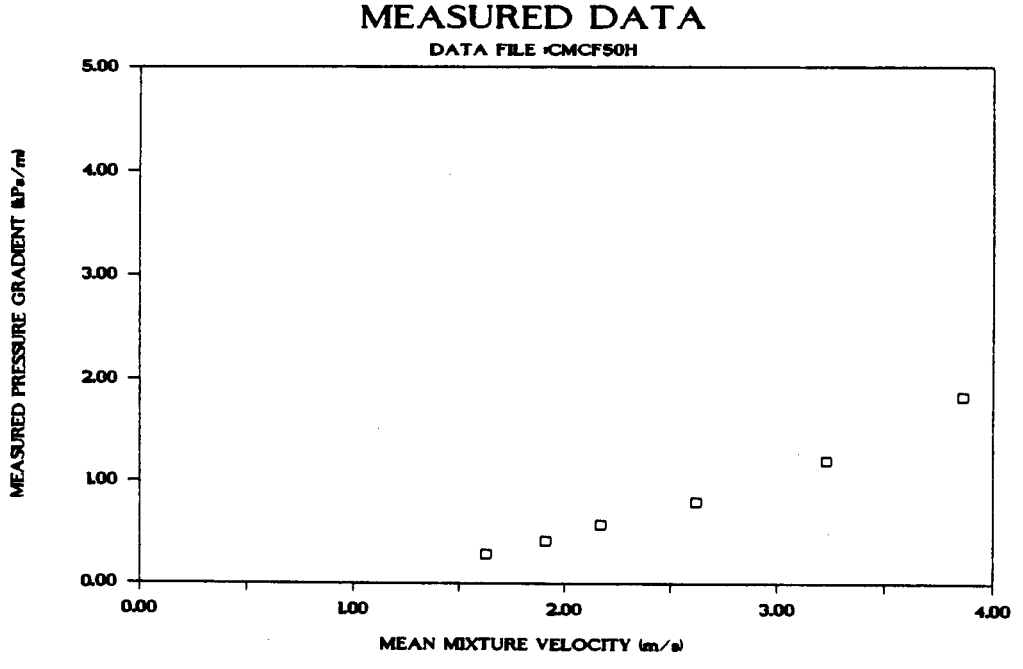

DATA FILE : CMCF55H.

Test facility		Chamber of Mines
Test date		1987
Material description		Full Plant Tailings
Material relative density		2.720
Slurry relative density		1.550
Solids volumetric concentration	(%)	32.020
Solids mass concentration	(%)	56.180
Pipe internal diameter	(mm)	101.50
Pipe internal roughness	(μm)	40.0
Pipeline gradient		Horizontal

Mixture velocity (m/s)	Pressure gradient (kPa/m)	Slurry temp. (°C)
2.390	0.980	32.0
2.010	0.770	32.0
3.070	1.530	32.0
1.100	0.530	32.0
1.170	0.550	32.0
2.000	0.820	32.0

Particle size distribution
Malvern particle size analyser

Size (μm)	% Passing	% Retained
425.0	100.000	0.000
300.0	100.000	0.000
212.0	100.000	0.000
150.0	99.400	0.600
106.0	93.200	6.200
38.0	58.900	34.300

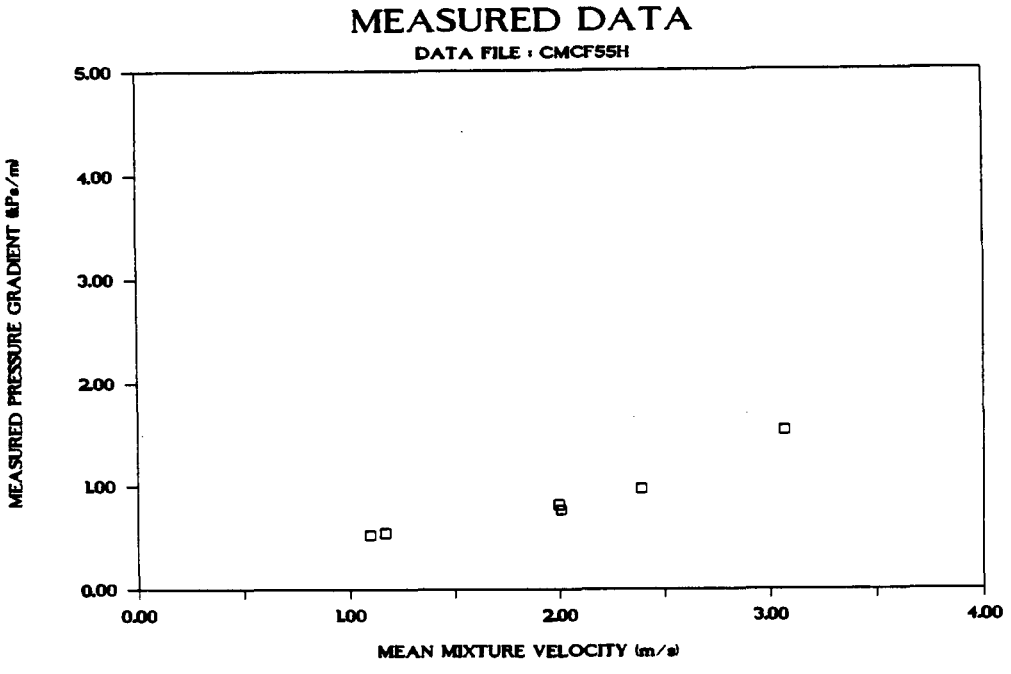

DATA FILE : CMCF60H.

Test facility		Chamber of Mines
Test date		
Material description		Full Plant Tailings
Material relative density		2.720
Slurry relative density		1.600
Solids volumetric concentration	(%)	34.920
Solids mass concentration	(%)	59.370
Pipe internal diameter	(mm)	101.50
Pipe internal roughness	(μm)	40.0
Pipeline gradient		Horizontal

Mixture velocity (m/s)	Pressure gradient (kPa/m)	Slurry temp. (°C)
3.740	3.270	00.0
3.610	3.110	00.0
2.210	1.630	00.0
1.870	1.320	00.0
1.600	1.130	00.0
3.840	3.270	00.0
3.560	3.050	00.0
3.050	2.300	00.0
1.240	1.040	00.0
1.160	1.010	00.0
0.920	1.010	00.0
0.780	1.000	00.0

Particle size distribution
Malvern particle size analyser

Size (μm)	% Passing	% Retained
425.0	100.000	0.000
300.0	100.000	0.000
212.0	99.900	0.100
150.0	99.400	0.500
106.0	93.500	5.900
38.0	57.000	36.500
Pan	000.000	57.000

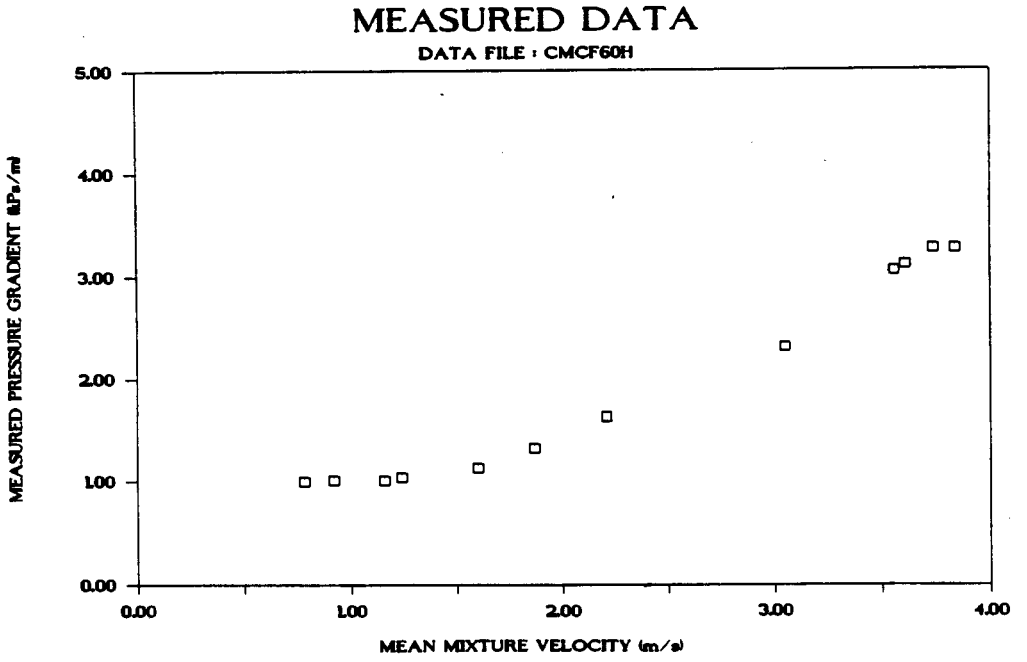

DATA FILE : CMCF70H.

Test facility		Chamber of Mines
Test date		
Material description		Full Plant Tailings
Material relative density		2.720
Slurry relative density		1.700
Solids volumetric concentration	(%)	40.730
Solids mass concentration	(%)	65.170
Pipe internal diameter	(mm)	101.50
Pipe internal roughness	(μm)	40.0
Pipeline gradient		Horizontal

Mixture velocity (m/s)	Pressure gradient (kPa/m)	Slurry temp. (°C)
1.760	2.180	32.0
1.620	2.100	32.0
1.460	2.030	32.0
1.340	1.930	32.0
0.940	1.790	32.0
0.610	1.690	32.0
0.810	1.730	32.0
0.400	1.610	32.0
0.250	1.520	32.0

Particle size distribution
Malvern particle size analyser

Size (μm)	% Passing	% Retained
425.0	100.000	0.000
300.0	100.000	0.000
212.0	99.900	0.100
150.0	99.800	0.100
106.0	93.800	6.000
38.0	65.900	27.900
10.0	30.000	35.900
Pan	000.000	30.000

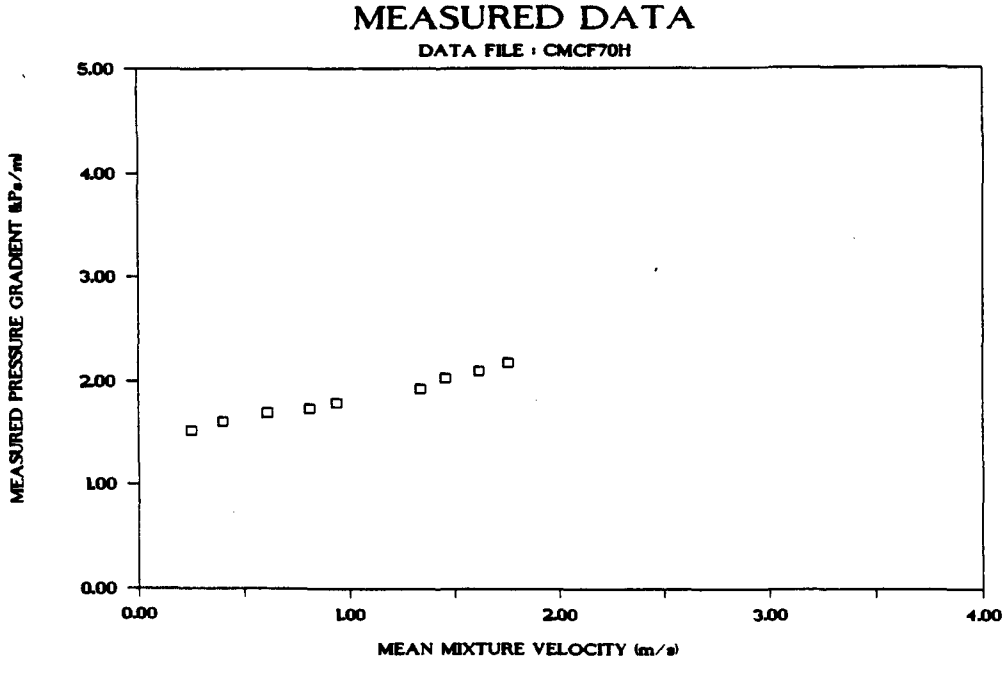

DATA FILE : CMCF74H.

Test facility		Chamber of Mines
Test date		
Material description		Full Plant Tailings
Material relative density		2.720
Slurry relative density		1.740
Solids volumetric concentration	(%)	43.060
Solids mass concentration	(%)	67.310
Pipe internal diameter	(mm)	101.50
Pipe internal roughness	(μm)	40.0
Pipeline gradient		Horizontal

Mixture velocity (m/s)	Pressure gradient (kPa/m)	Slurry temp. (°C)
0.410	2.750	00.0
0.210	2.370	00.0
0.590	2.800	00.0
0.760	3.030	00.0
0.880	3.260	00.0
0.990	3.580	00.0
1.210	3.650	00.0

Particle size distribution
Malvern particle size analyser

Size (μm)	% Passing	% Retained
425.0	100.000	0.000
300.0	100.000	0.000
212.0	99.900	0.100
150.0	99.800	0.100
106.0	94.100	5.700
38.0	64.300	29.800
10.0	20.000	44.300

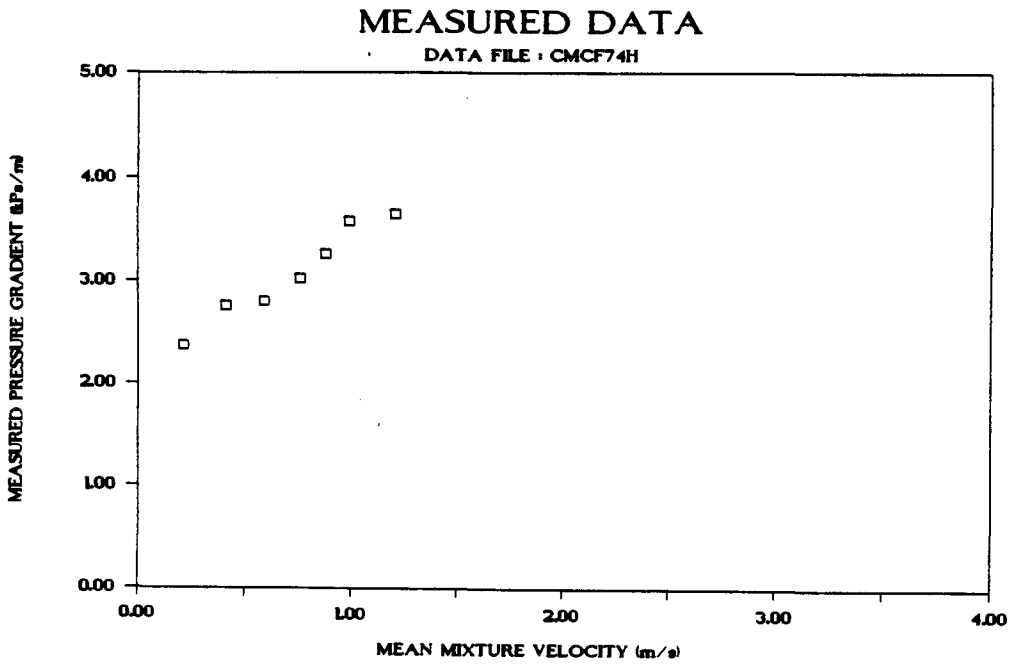

DATA FILE : C3VF75H.

Test facility		Vertical Test Facility
Test date		February 1989
Material description		Full plant Tailings
Material relative density		2.680
Slurry relative density		1.750
Solids volumetric concentration	(%)	44.680
Solids mass concentration	(%)	68.420
Pipe internal diameter	(mm)	41.20
Pipe internal roughness	(μm)	170.0
Pipeline gradient		Horizontal

Mixture velocity (m/s)	Pressure gradient (kPa/m)	Slurry temp. (°C)
1.050	10.460	27.5
1.110	11.620	27.5
0.950	10.800	27.5
0.800	9.030	27.5
0.610	8.800	28.5
0.610	9.240	28.5
0.410	9.010	28.5
0.070	8.220	28.5
0.390	7.840	28.5
0.320	7.890	28.5
0.210	7.740	29.0
0.180	7.720	29.0
0.180	7.730	29.0
0.120	7.720	29.0

Particle size distribution
Malvern particle size analyser

Size (μm)	% Passing	% Retained
262.0	97.500	2.500
160.0	90.300	7.200
113.0	82.100	8.200
84.0	73.800	8.300
65.0	66.100	7.700
50.0	59.600	6.500
39.0	54.600	5.000
30.0	49.400	5.200
24.0	43.500	5.900
19.0	38.000	5.500
15.0	33.100	4.900
11.0	27.900	5.200
Pan	0.000	27.900

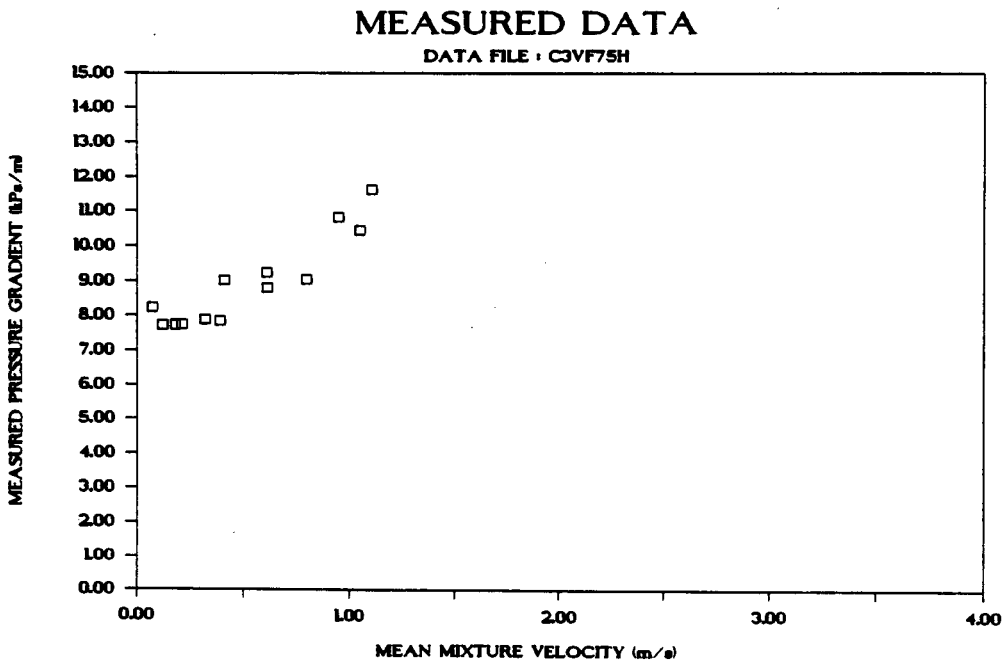

DATA FILE : C3VF74H.

Test facility		University of Cape town
Test date		December 1988
Material description		Full Plant tailings
Material relative density		2.680
Slurry relative density		1.740
Solids volumetric concentration	(%)	44.110
Solids mass concentration	(%)	67.950
Pipe internal diameter	(mm)	41.20
Pipe internal roughness	(μm)	106.0
Pipeline gradient		Horizontal

Mixture velocity (m/s)	Pressure gradient (kPa/m)	Slurry temp. (°C)
1.450	9.470	26.5
1.260	9.150	26.5
1.110	8.340	26.5
0.590	7.630	26.5
0.720	8.130	26.5
0.930	8.590	26.5
0.720	8.230	26.5
0.560	8.000	26.5
0.310	7.650	26.5
0.260	7.460	26.5
0.250	7.410	00.0

Particle size distribution
Malvern particle size analyser

Size (μm)	% Passing	% Retained
262.0	100.000	0.000
160.0	98.900	1.100
113.0	93.000	5.900
84.0	86.000	7.000
65.0	79.300	6.700
50.0	73.100	6.200
39.0	67.300	5.800
30.0	60.800	6.500
24.0	53.800	7.000
19.0	47.300	6.500
15.0	41.600	5.700
11.0	35.200	6.400

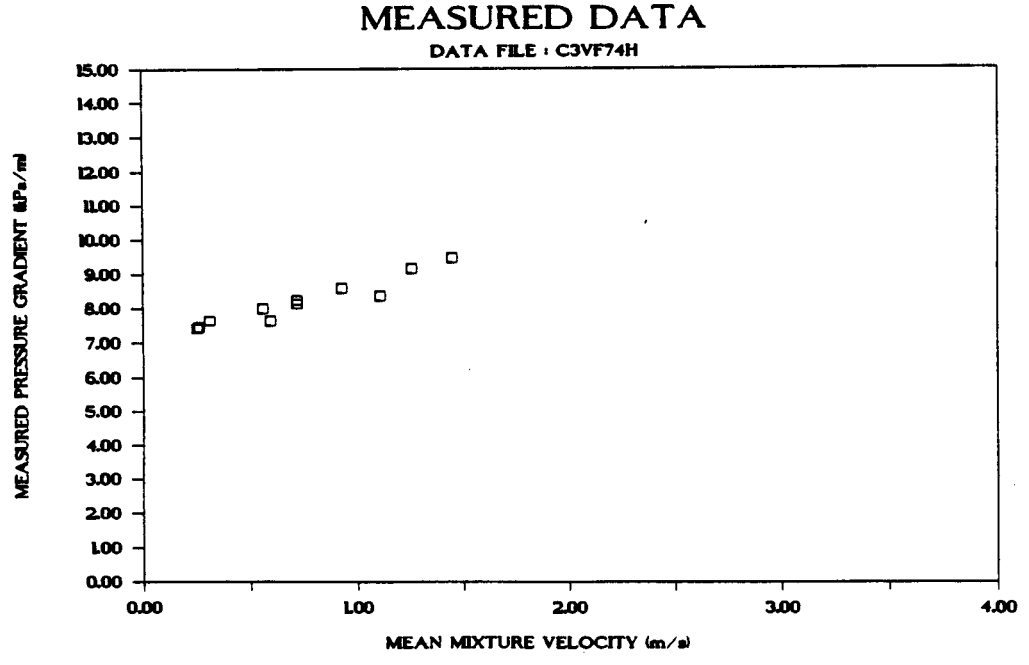

DATA FILE : C3VF64H.

Test facility		Vertical Test facility at UCT.
Test date		February 1989
Material description		Full Plant Tailings
Material relative density		2.680
Slurry relative density		1.6400
Solids volumetric concentration	(%)	38.132
Solids mass concentration	(%)	62.313
Pipe internal diameter	(mm)	41.22
Pipe internal roughness	(μm)	103.0
Pipeline gradient		Horizontal

Mixture velocity (m/s)	Pressure gradient (kPa/m)	Slurry temp. (°C)
2.970	4.551	26.5
2.860	4.193	26.5
2.780	3.893	26.5
2.540	3.297	26.5
2.410	2.859	26.5
2.000	1.994	27.0
1.650	1.619	27.0
1.630	1.558	27.0
1.350	1.773	27.0
1.070	1.523	27.0
1.030	1.484	27.5
0.720	1.331	27.5
0.650	1.315	27.5
0.580	1.211	27.5
0.460	1.162	27.5
0.240	1.075	27.5

Particle size distribution
Malvern particle size analyser

Size (μm)	% Passing	% Retained
564.0	100.000	0.000
262.0	97.500	2.500
160.0	90.300	7.200
113.0	82.100	8.200
84.0	73.800	8.300
65.0	66.100	7.700
50.0	59.500	6.600
39.0	54.500	5.000
30.0	49.300	5.200
24.0	43.400	5.900
19.0	37.900	5.500
15.0	33.100	4.800
Pan	000.000	33.100

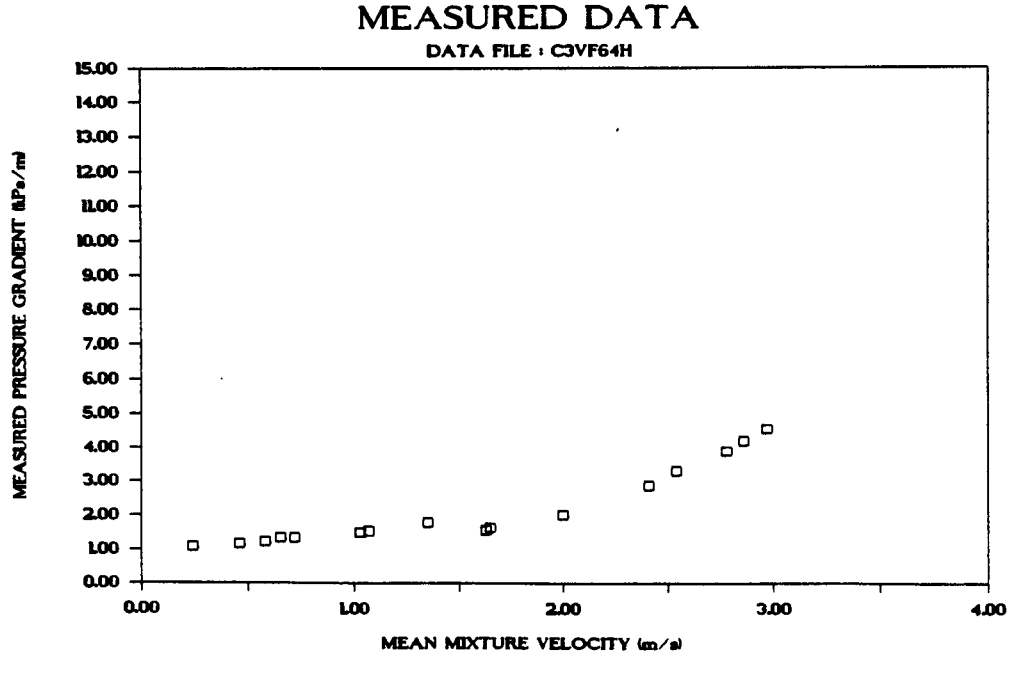

DATA FILE : C3VF72H.

Test facility		University of Cape Town
Test date		December 1988
Material description		Full Plant Tailings
Material relative density		2.680
Slurry relative density		1.7200
Solids volumetric concentration	(%)	42.891
Solids mass concentration	(%)	66.830
Pipe internal diameter	(mm)	41.22
Pipe internal roughness	(μm)	106.0
Pipeline gradient		Horizontal

Mixture velocity (m/s)	Pressure gradient (kPa/m)	Slurry temp. (°C)
2.410	5.700	28.5
2.250	5.230	28.5
1.920	5.300	29.0
2.030	5.740	28.5
1.910	5.450	29.0
1.800	5.320	29.0
1.640	5.240	29.0
1.550	5.070	29.0
1.410	4.810	29.0
1.320	4.660	29.5
1.170	4.320	29.5
0.930	4.160	29.5
0.810	3.920	29.5
0.720	3.850	29.5
0.420	3.730	29.5
0.130	2.380	29.5

Particle size distribution
Malvern particle size analyser

Size (μm)	% Passing	% Retained
262.0	97.500	2.500
160.0	90.300	7.200
113.0	82.100	8.200
84.0	73.800	8.300
65.0	66.100	7.700
50.0	59.600	6.500
39.0	54.600	5.000
30.0	49.400	5.200
24.0	43.500	5.900
19.0	38.000	5.500
15.0	33.100	4.900
11.0	27.900	5.200
Pan	0.000	27.900

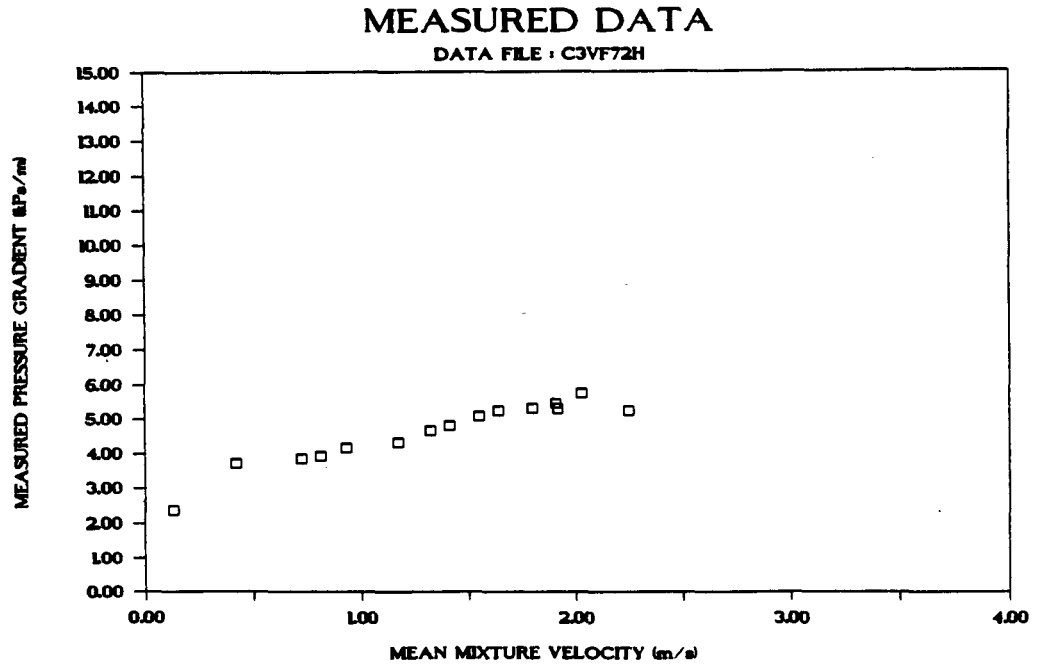

DATA FILE : DKVF84H.

Test facility		Vertical Test Facility at UCT
Test date		
Material description		Full plant tailings
Material relative density		2.800
Slurry relative density		1.835
Solids volumetric concentration	(%)	46.420
Solids mass concentration	(%)	70.830
Pipe internal diameter	(mm)	41.22
Pipe internal roughness	(μm)	170.0
Pipeline gradient		Horizontal

Mixture velocity (m/s)	Pressure gradient (kPa/m)	Slurry temp. (°C)
0.820	10.814	29.0
0.810	10.955	29.0
0.800	11.697	29.0
0.800	10.971	29.0
0.790	10.820	29.0
0.780	10.764	29.0
0.770	10.712	29.0
0.760	10.588	29.0
0.720	10.581	29.0
0.640	10.196	29.0
0.490	8.864	29.5
0.410	8.870	29.5
0.370	8.847	29.5
0.340	8.707	29.5
0.300	7.461	29.5
0.180	7.751	29.5
0.160	7.533	29.5
0.140	6.910	29.5
0.040	5.810	29.5

Particle size distribution
Malvern particle size analyser

Size (μm)	% Passing	% Retained
564.0	100.000	0.000
262.0	99.100	0.900
160.0	91.600	7.500
113.0	81.300	10.300
84.0	72.600	8.700
65.0	64.900	7.700
50.0	57.500	7.400
39.0	50.700	6.800
30.0	44.500	6.200
24.0	38.300	6.200
19.0	32.700	5.600
15.0	27.800	4.900
Pan	0.000	27.800

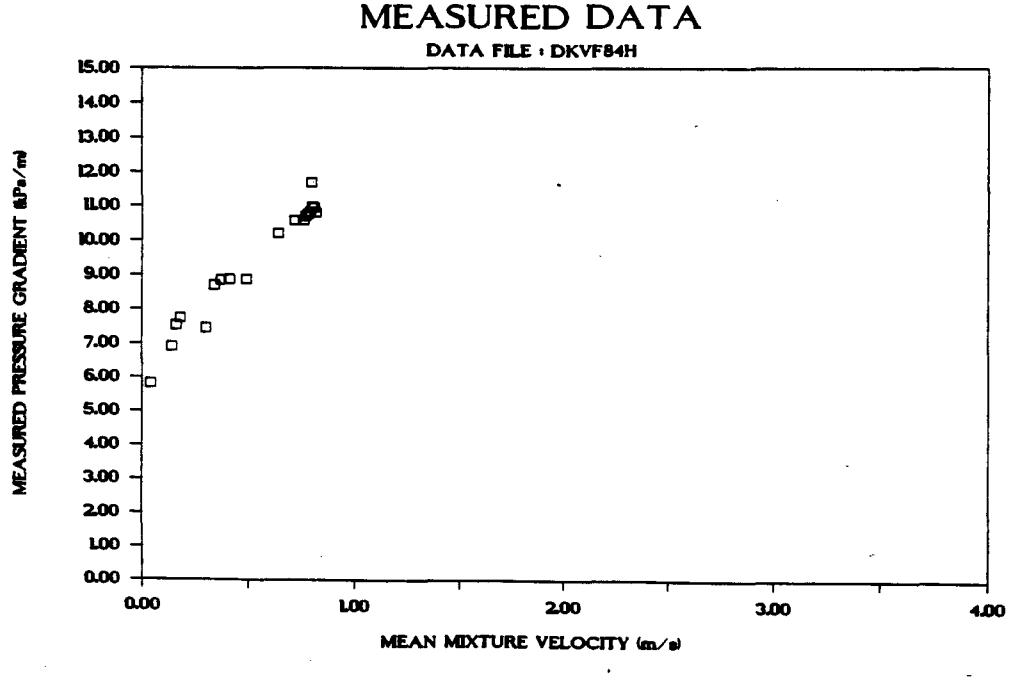

DATA FILE : DKVF80H.

Test facility		Vertical Test Facility at UCT
Test date		
Material description		Full plant tailings
Material relative density		2.800
Slurry relative density		1.800
Solids volumetric concentration	(%)	44.480
Solids mass concentration	(%)	69.180
Pipe internal diameter	(mm)	41.22
Pipe internal roughness	(μm)	170.0
Pipeline gradient		Horizontal

Mixture velocity (m/s)	Pressure gradient (kPa/m)	Slurry temp. (°C)	Particle size distribution Malvern particle size analyser Size (μm)	% Passing	% Retained
1.870	8.941	28.5	564.0	100.000	0.000
1.850	9.133	28.5	262.0	99.100	0.900
1.670	8.887	29.0	160.0	91.600	7.500
1.530	8.090	29.0	113.0	81.300	10.300
1.460	8.462	29.0	84.0	72.600	8.700
1.340	8.491	29.5	65.0	64.900	7.700
1.080	8.012	29.5	50.0	57.500	7.400
0.930	5.584	29.5	39.0	50.700	6.800
0.860	6.300	29.5	30.0	44.500	6.200
0.560	5.567	29.5	24.0	38.300	6.200
0.370	5.368	30.5	19.0	32.700	5.600
0.010	3.544	30.5	15.0	27.800	4.900

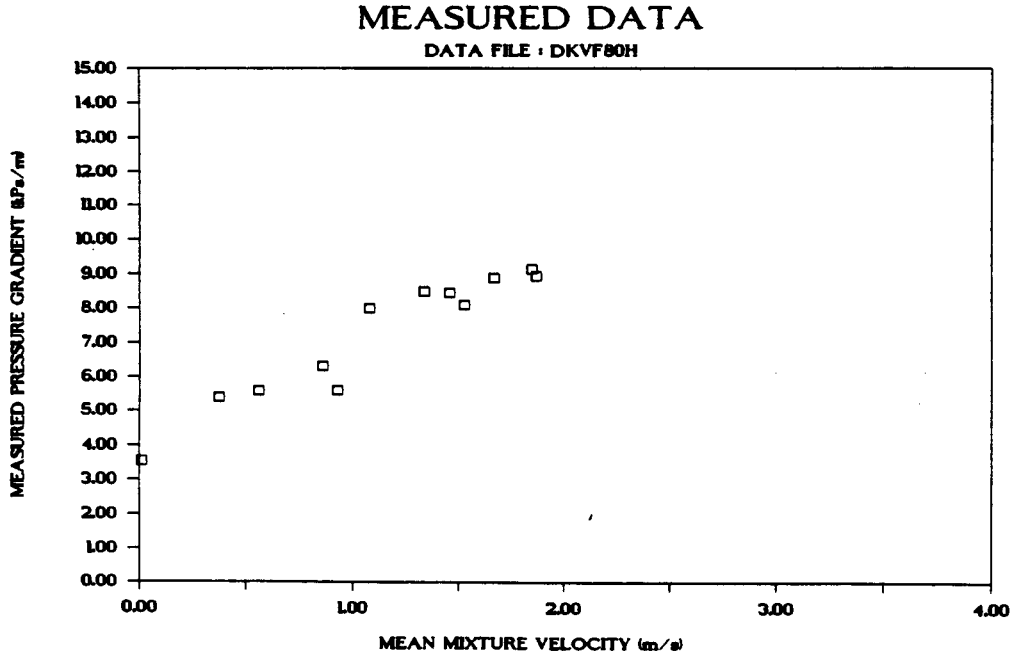

DATA FILE : DKVF76H.

Test facility		Vertical Test Facility at UCT
Test date		
Material description		Full plant tailings
Material relative density		2.800
Slurry relative density		1.760
Solids volumetric concentration	(%)	42.250
Solids mass concentration	(%)	67.220
Pipe internal diameter	(mm)	41.22
Pipe internal roughness	(μm)	170.0
Pipeline gradient		Horizontal

Mixture velocity (m/s)	Pressure gradient (kPa/m)	Slurry temp. (°C)
2.920	7.723	28.0
2.910	7.769	28.0
2.850	7.621	28.0
2.770	7.470	28.0
2.660	7.112	28.0
2.340	6.202	28.0
2.190	6.104	29.5
2.060	5.719	29.5
1.510	4.881	29.5
1.330	4.553	29.5
0.680	3.260	29.5
0.640	3.689	29.5
0.480	3.149	29.5
0.230	2.661	29.5

Particle size distribution
Malvern particle size analyser

Size (μm)	% Passing	% Retained
564.0	100.000	0.000
262.0	99.100	0.900
160.0	91.600	7.500
113.0	81.300	10.300
84.0	72.600	8.700
65.0	64.900	7.700
50.0	57.500	7.400
39.0	50.700	6.800
30.0	44.500	6.200
24.0	38.300	6.200
19.0	32.700	5.600
15.0	27.800	4.900
Pan	0.000	27.800

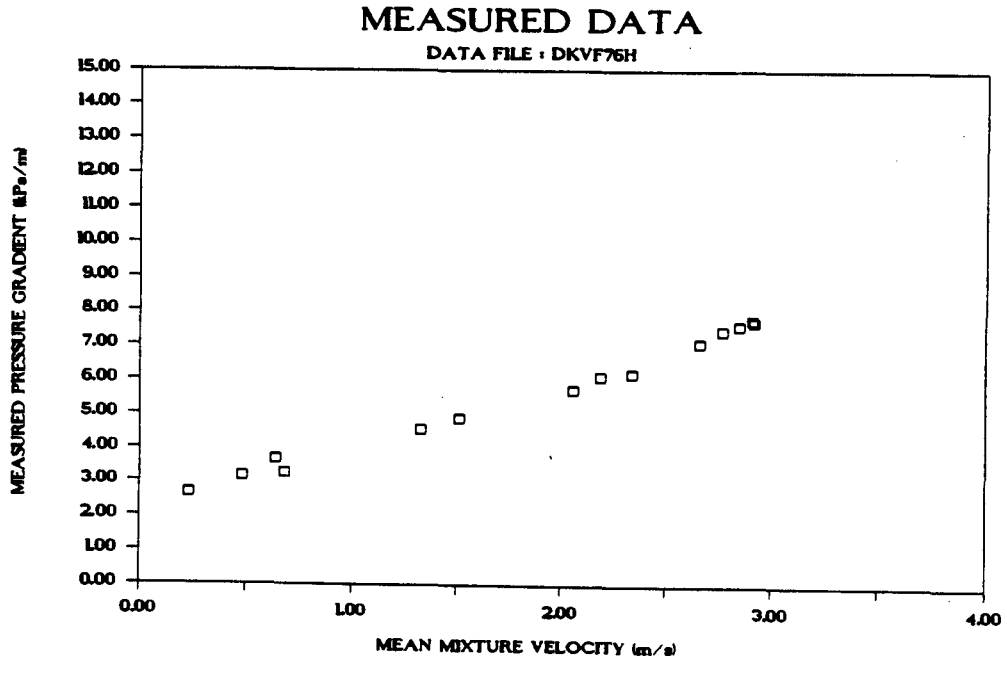

DATA FILE : DKVF69H.

Test facility		Vertical Test Facility at UCT
Test date		April, 1989
Material description		Full plant tailings
Material relative density		2.800
Slurry relative density		1.690
Solids volumetric concentration	(%)	38.370
Solids mass concentration	(%)	63.570
Pipe internal diameter	(mm)	41.22
Pipe internal roughness	(μm)	170.0
Pipeline gradient		Horizontal

Mixture velocity (m/s)	Pressure gradient (kPa/m)	Slurry temp. (°C)
3.290	7.031	28.5
3.270	6.795	28.5
3.270	6.828	28.5
3.150	6.560	28.5
3.080	6.192	28.5
2.900	5.595	28.5
2.540	5.137	29.5
2.140	3.179	29.5
2.000	2.633	29.5
1.730	2.317	29.5
1.550	2.050	29.5
1.150	1.510	30.0
0.470	1.211	30.0
0.030	0.710	30.0

Particle size distribution
Malvern particle size analyser

Size (μm)	% Passing	% Retained
564.0	100.000	0.000
262.0	99.100	0.900
160.0	91.600	7.500
113.0	81.300	10.300
84.0	72.600	8.700
65.0	64.900	7.700
50.0	57.500	7.400
39.0	50.700	6.800
30.0	44.500	6.200
24.0	38.300	6.200
19.0	32.700	5.600
15.0	27.800	4.900
Pan	0.000	27.800

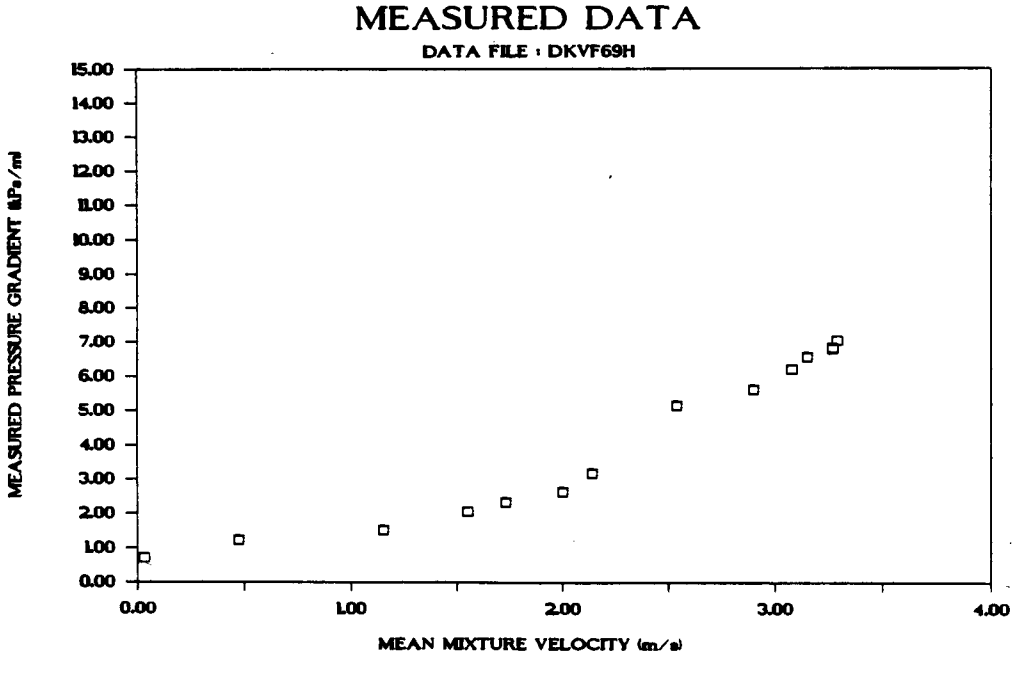

DATA FILE : CMVF53VS

Test facility		Vertical Test Facility
Test date		1989
Material description		Chamber of Mines Full Plant
Material relative density		2.72
Slurry relative density		1.5100
Solids volumetric concentration	(%)	29.69
Solids mass concentration	(%)	53.49
Pipe internal diameter	(mm)	41.50
Pipe internal roughness	(μm)	207.0
Pipeline gradient		Vertical

Mixture velocity (m/s)	Pressure gradient (kPa/m)	Slurry temp. (°C)
3.44	6.413	28.5
3.24	5.963	28.5
3.19	5.697	28.5
2.81	4.461	28.5
2.60	3.963	28.5
2.19	3.003	28.5
2.03	2.563	28.5
1.96	2.458	28.5
1.92	2.407	29.5
1.82	2.129	29.5
1.77	2.135	29.5
1.75	2.055	29.5
1.67	1.870	29.5
1.43	1.692	29.5
1.37	1.641	30.0
1.05	1.082	30.0
0.88	0.999	30.0
0.53	0.683	30.0
0.39	0.678	30.0
0.10	0.543	30.0

Particle size distribution
Malvern particle size analyser

Size (μm)	% Passing	% Retained
564	100.00	0.00
262	100.00	0.00
168	95.50	4.50
113	86.20	9.30
84	77.40	8.80
65	70.50	6.90
50	64.80	5.70
39	59.00	5.80
30	54.50	4.50
21	49.60	4.90
11	33.90	15.70
6	18.80	15.10
Pan	0.00	18.80

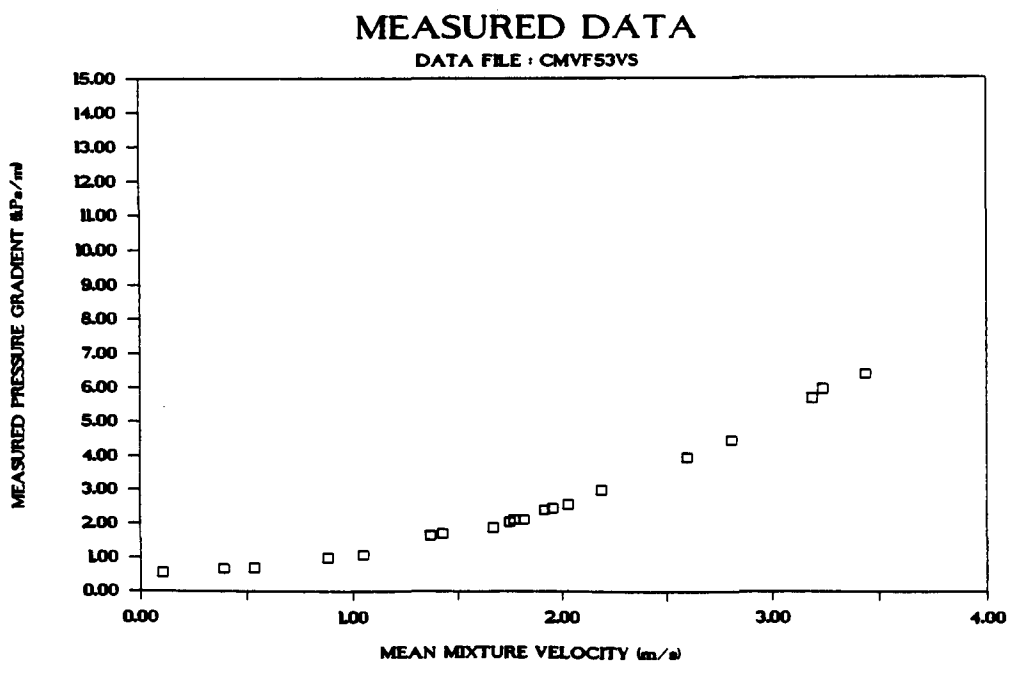

DATA FILE : CMVF65VS

Test facility		Vertical Test Facility U.C.T.
Test date		1989
Material description		Chamber of Mines Full Plant
Material relative density		2.72
Slurry relative density		1.6300
Solids volumetric concentration	(%)	36.66
Solids mass concentration	(%)	61.18
Pipe internal diameter	(mm)	41.50
Pipe internal roughness	(μm)	207.0
Pipeline gradient		Vertical

Mixture velocity (m/s)	Pressure gradient (kPa/m)	Slurry temp. (°C)
3.29	6.313	26.0
3.13	5.825	26.0
2.99	5.459	26.0
2.69	4.484	26.0
2.58	4.118	27.0
2.29	3.330	27.0
2.15	3.083	27.0
2.05	2.598	27.0
1.82	2.266	27.0
1.78	2.101	27.0
1.64	1.579	27.0
1.37	1.183	28.5
1.22	1.188	28.5
1.16	1.104	28.5
0.93	1.016	28.5
0.87	0.973	28.5
0.67	1.018	28.5
0.41	0.870	28.5
0.11	0.756	28.5
0.03	0.726	28.5

Particle size distribution
Malvern particle size analyser

Size (μm)	% Passing	% Retained
564	100.00	0.00
262	100.00	0.00
168	95.50	4.50
113	86.20	9.30
84	77.40	8.80
65	70.50	6.90
50	64.80	5.70
39	59.00	5.80
30	54.50	4.50
21	49.60	4.90
11	33.90	15.70
6	18.80	15.10
Pan	0.00	18.80

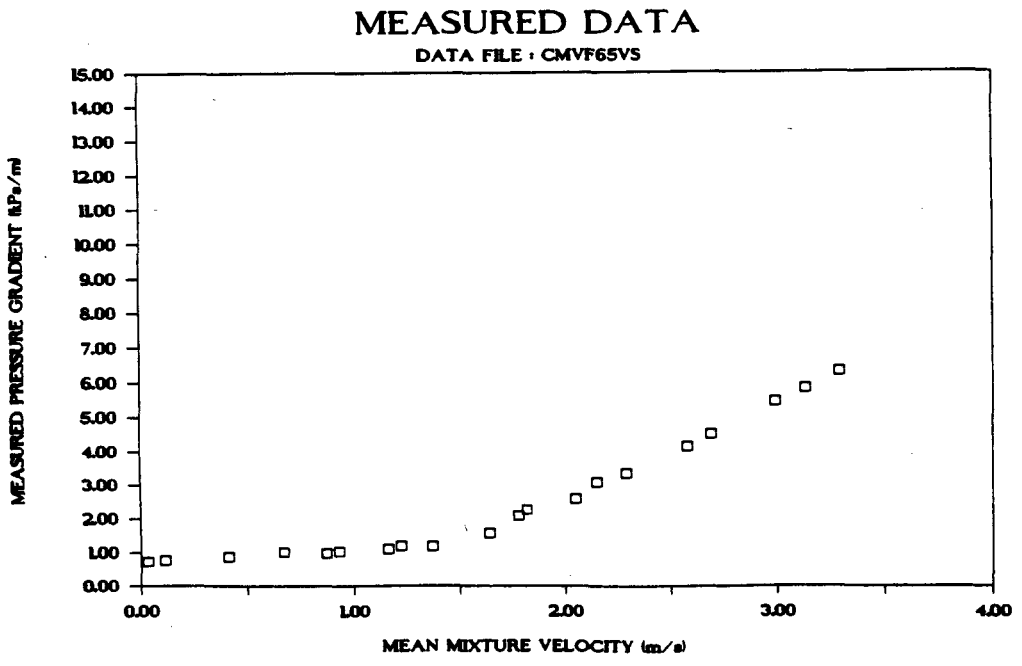

DATA FILE : CMVF71VS

Test facility		Vertical Test Facility
Test date		1989
Material description		Chamber of Mines Full Plant
Material relative density		2.72
Slurry relative density		1.7100
Solids volumetric concentration	(%)	41.31
Solids mass concentration	(%)	65.71
Pipe internal diameter	(mm)	41.50
Pipe internal roughness	(μm)	103.0
Pipeline gradient		Vertical

Mixture velocity (m/s)	Pressure gradient (kPa/m)	Slurry temp. (°C)
3.30	7.151	27.0
3.21	6.867	27.0
3.17	6.526	27.0
3.11	6.057	27.0
3.06	6.221	27.5
2.93	5.741	27.5
2.80	4.981	27.5
2.70	3.375	27.5
2.41	3.241	27.5
2.30	2.740	27.5
2.12	2.891	27.5
2.00	3.055	27.5
1.83	2.890	27.5
1.65	2.698	27.5
1.51	2.762	27.5
1.38	2.577	27.5
1.16	2.618	28.0
0.85	2.090	28.0
0.54	1.854	28.0
0.24	1.575	28.0

Particle size distribution
Malvern particle size analyser

Size (μm)	% Passing	% Retained
564	100.00	0.00
262	100.00	0.00
168	95.50	4.50
113	86.20	9.30
84	77.40	8.80
65	70.50	6.90
50	64.80	5.70
39	59.00	5.80
30	54.50	4.50
21	49.60	4.90
11	33.90	15.70
6	18.80	15.10
Pan	0.00	18.80

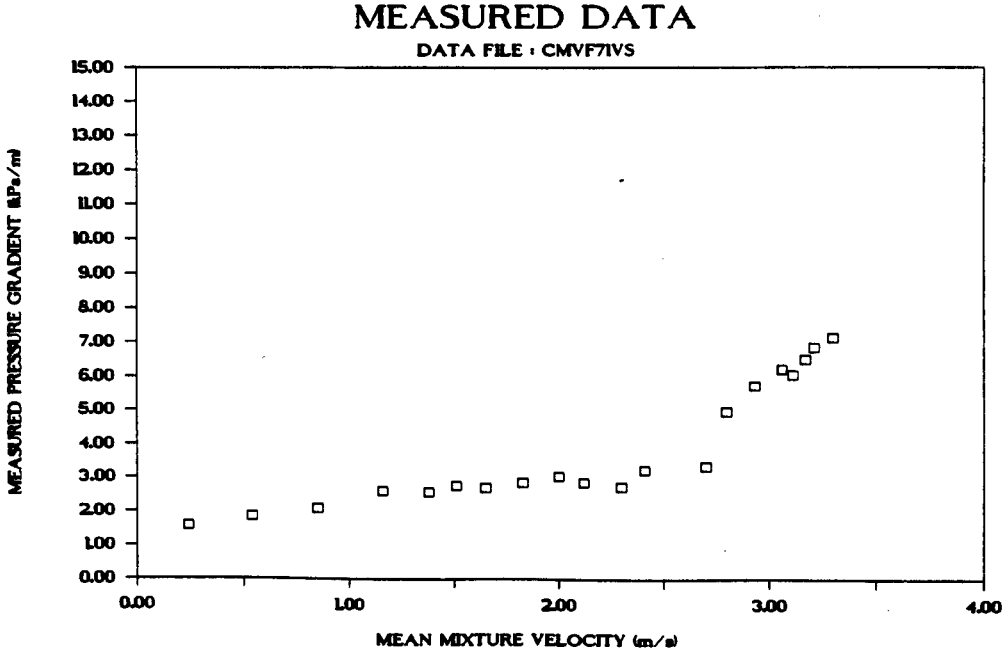

DATA FILE : CMVF74VS

Test facility		Vertical Test Facility
Test date		1989
Material description		Chamber of Mines Full Plant
Material relative density		2.72
Slurry relative density		1.7300
Solids volumetric concentration	(%)	42.48
Solids mass concentration	(%)	66.78
Pipe internal diameter	(mm)	41.50
Pipe internal roughness	(μm)	103.0
Pipeline gradient		Vertical

Mixture velocity (m/s)	Pressure gradient (kPa/m)	Slurry temp. (°C)
3.32	6.955	28.0
3.31	6.717	28.0
3.17	6.640	28.0
3.10	6.377	28.0
2.97	5.398	28.0
2.84	3.988	28.0
2.69	3.314	28.0
2.59	3.423	28.0
2.09	3.078	28.0
2.03	3.076	28.0
1.76	2.739	28.0
1.26	2.757	28.0
1.22	2.733	28.0
0.96	2.520	28.0
0.86	2.464	28.0
0.44	2.091	28.0
0.40	2.153	28.0
0.32	1.858	28.0
0.23	1.787	28.0
0.09	1.817	28.0

Particle size distribution
Malvern particle size analyser

Size (μm)	% Passing	% Retained
564	100.00	0.00
262	100.00	0.00
168	95.50	4.50
113	86.20	9.30
84	77.40	8.80
65	70.50	6.90
50	64.80	5.70
39	59.00	5.80
30	54.50	4.50
21	49.60	4.90
11	33.90	15.70
6	18.80	15.10
Pan	0.00	18.80

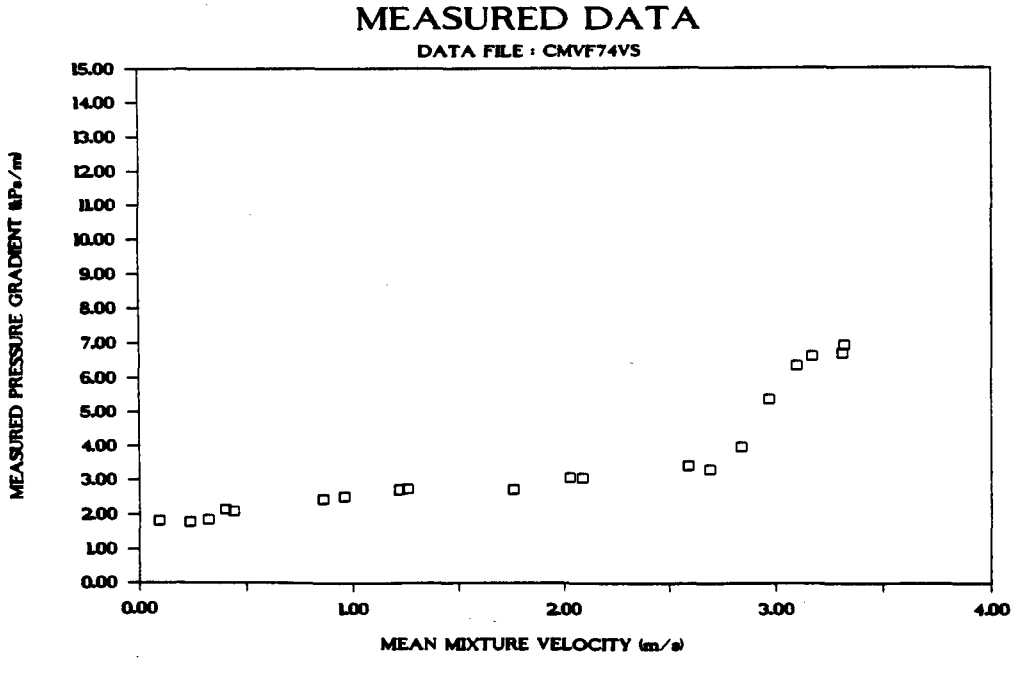

DATA FILE : CMVF76VS

Test facility		Vertical Test Facility
Test date		1989
Material description		Chamber of Mines Full Plant
Material relative density		2.72
Slurry relative density		1.7600
Solids volumetric concentration	(%)	44.22
Solids mass concentration	(%)	68.34
Pipe internal diameter	(mm)	41.50
Pipe internal roughness	(μm)	103.0
Pipeline gradient		Vertical

Mixture velocity (m/s)	Pressure gradient (kPa/m)	Slurry temp. (°C)
3.23	6.411	27.0
3.17	6.321	27.0
3.14	6.591	27.0
3.06	5.982	27.0
2.97	5.832	27.0
2.70	5.441	27.0
2.59	5.255	27.0
2.53	5.236	27.0
2.43	5.089	27.0
2.42	5.108	27.0
2.37	5.154	28.5
2.13	4.846	28.5
1.78	4.079	28.5
1.69	4.259	28.5
1.37	4.088	28.5
1.20	4.050	28.5
0.93	3.415	28.5
0.55	3.436	28.5
0.47	3.439	28.5
0.22	3.267	28.5

Particle size distribution
Malvern particle size analyser

Size (μm)	% Passing	% Retained
564	100.00	0.00
262	100.00	0.00
168	95.50	4.50
113	86.20	9.30
84	77.40	8.80
65	70.50	6.90
50	64.80	5.70
39	59.00	5.80
30	54.50	4.50
21	49.60	4.90
11	33.90	15.70
6	18.80	15.10
Pan	0.00	18.80

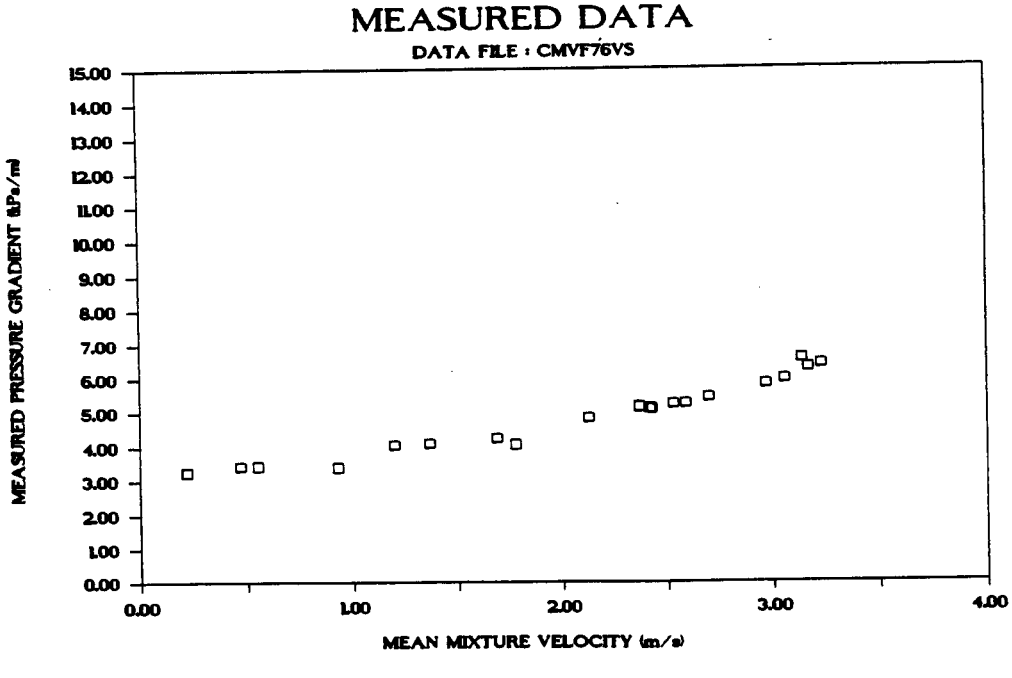

DATA FILE : CMVF81VS

Test facility		Vertical Test Facility
Test date		1989
Material description		Chamber of Mines Full Plant
Material relative density		2.72
Slurry relative density		1.8100
Solids volumetric concentration	(%)	47.12
Solids mass concentration	(%)	70.82
Pipe internal diameter	(mm)	41.50
Pipe internal roughness	(μm)	103.0
Pipeline gradient		Vertical

Mixture velocity (m/s)	Pressure gradient (kPa/m)	Slurry temp. (°C)
2.65	8.648	28.0
2.47	8.290	28.0
2.27	8.155	28.0
2.08	8.029	28.0
2.02	8.000	28.0
1.94	7.770	28.0
1.86	7.644	28.0
1.79	7.595	28.0
1.77	7.594	28.0
1.71	7.312	28.0
1.55	7.100	28.5
1.52	7.220	28.5
1.50	7.121	28.5
1.01	6.462	28.5
0.67	5.869	28.5
0.43	5.552	28.5
0.37	5.401	28.5
0.19	4.975	28.5
0.12	5.496	28.5
0.02	5.093	28.5

Particle size distribution
Malvern particle size analyser

Size (μm)	% Passing	% Retained
564	100.00	0.00
262	100.00	0.00
168	95.50	4.50
113	86.20	9.30
84	77.40	8.80
65	70.50	6.90
50	64.80	5.70
39	59.00	5.80
30	54.50	4.50
21	49.60	4.90
11	33.90	15.70
6	18.80	15.10
Pan	0.00	18.80

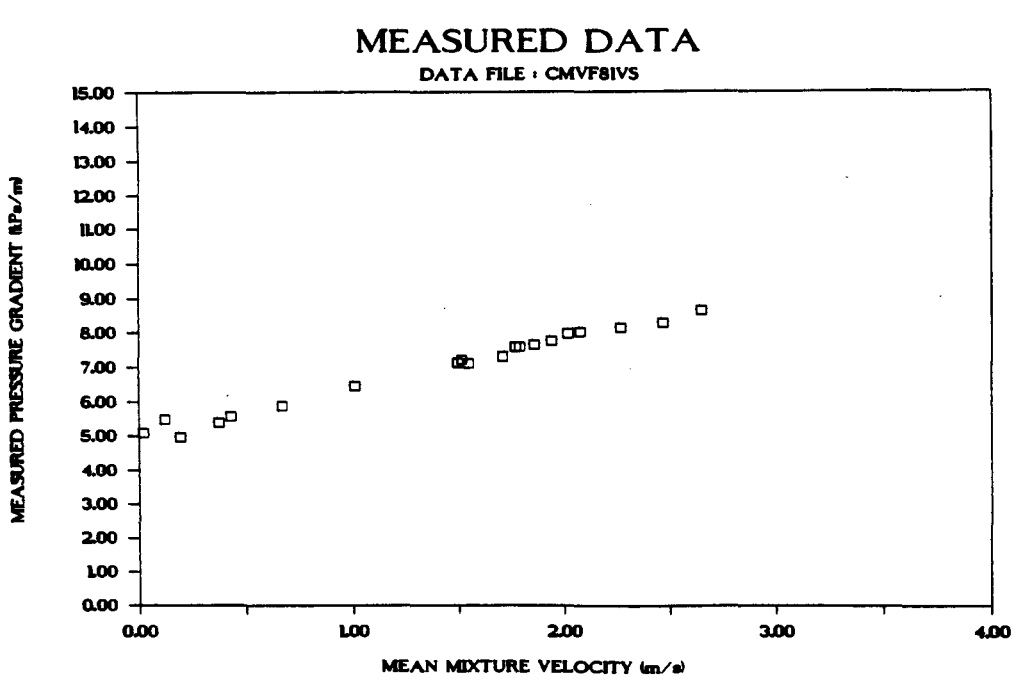

DATA FILE : CMVF85VS

Test facility		Vertical Test Facility
Test date		1989
Material description		Chamber of Mines Full Plant
Material relative density		2.72
Slurry relative density		1.8500
Solids volumetric concentration	(%)	49.45
Solids mass concentration	(%)	72.70
Pipe internal diameter	(mm)	41.50
Pipe internal roughness	(μm)	103.0
Pipeline gradient		Vertical

Mixture velocity (m/s)	Pressure gradient (kPa/m)	Slurry temp. (°C)
1.44	11.317	28.0
1.43	11.385	28.0
1.37	11.040	28.0
1.31	11.222	28.0
1.30	11.162	28.0
1.29	10.946	28.5
1.28	10.817	28.5
1.23	11.132	28.5
1.18	10.894	28.5
1.07	10.708	28.5
1.05	10.127	29.5
1.04	10.925	29.5
1.00	10.925	29.5
0.79	10.739	29.5
0.76	10.249	29.5
0.71	9.646	30.5
0.57	9.897	30.5
0.56	9.901	30.5
0.12	8.475	30.5
0.10	8.265	30.5

Particle size distribution
Malvern particle size analyser

Size (μm)	% Passing	% Retained
564	100.00	0.00
262	100.00	0.00
168	95.50	4.50
113	86.20	9.30
84	77.40	8.80
65	70.50	6.90
50	64.80	5.70
39	59.00	5.80
30	54.50	4.50
21	49.60	4.90
11	33.90	15.70
6	18.80	15.10
Pan	0.00	18.80

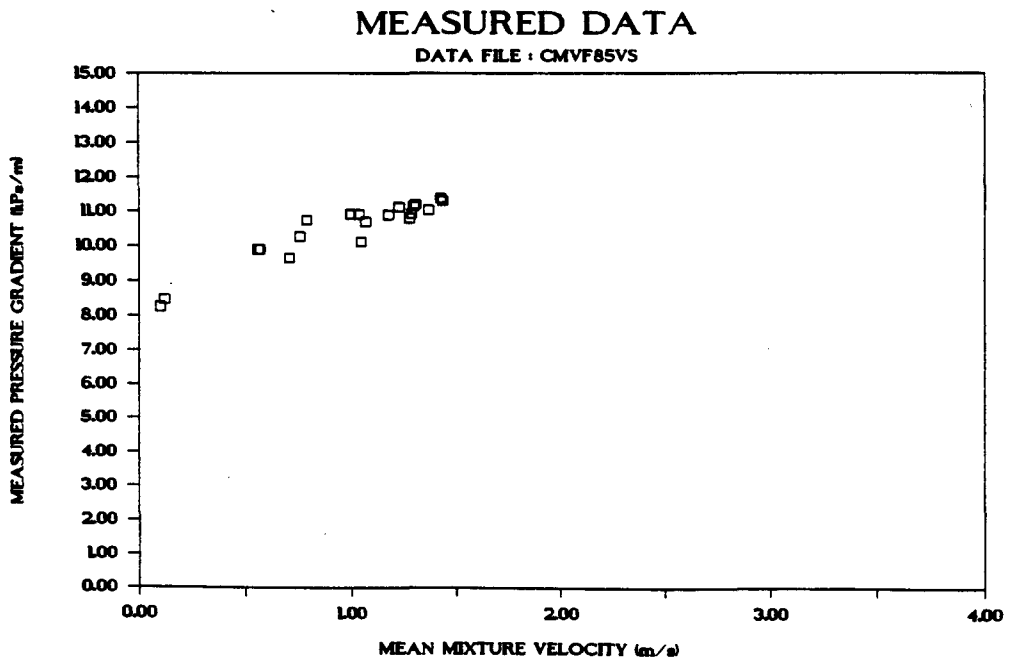

DATA FILE : C3VF64VS

Test facility		Vertical Test facility at UCT.
Test date		February 1989
Material description		Full Plant Tailings
Material relative density		2.680
Slurry relative density		1.6400
Solids volumetric concentration	(%)	38.132
Solids mass concentration	(%)	62.313
Pipe internal diameter	(mm)	41.22
Pipe internal roughness	(μm)	103.0
Pipeline gradient		Vertical

Mixture velocity (m/s)	Pressure gradient (kPa/m)	Slurry temp. (°C)
2.969	5.044	26.5
2.860	4.658	26.5
2.776	4.211	26.5
2.541	3.567	26.5
2.407	2.842	26.5
2.000	2.135	27.0
1.646	2.008	27.0
1.633	1.777	27.0
1.345	1.658	27.0
1.069	1.701	27.0
1.026	1.671	27.5
0.720	1.510	27.5
0.645	1.473	27.5
0.584	1.420	27.5
0.458	1.371	27.5
0.243	1.418	27.5

Particle size distribution
Malvern particle size analyser

Size (μm)	% Passing	% Retained
564.0	100.000	0.000
262.0	97.500	2.500
160.0	90.300	7.200
113.0	82.100	8.200
84.0	73.800	8.300
65.0	66.100	7.700
50.0	59.500	6.600
39.0	54.500	5.000
30.0	49.300	5.200
24.0	43.400	5.900
19.0	37.900	5.500
15.0	33.100	4.800
Pan	000.000	33.100

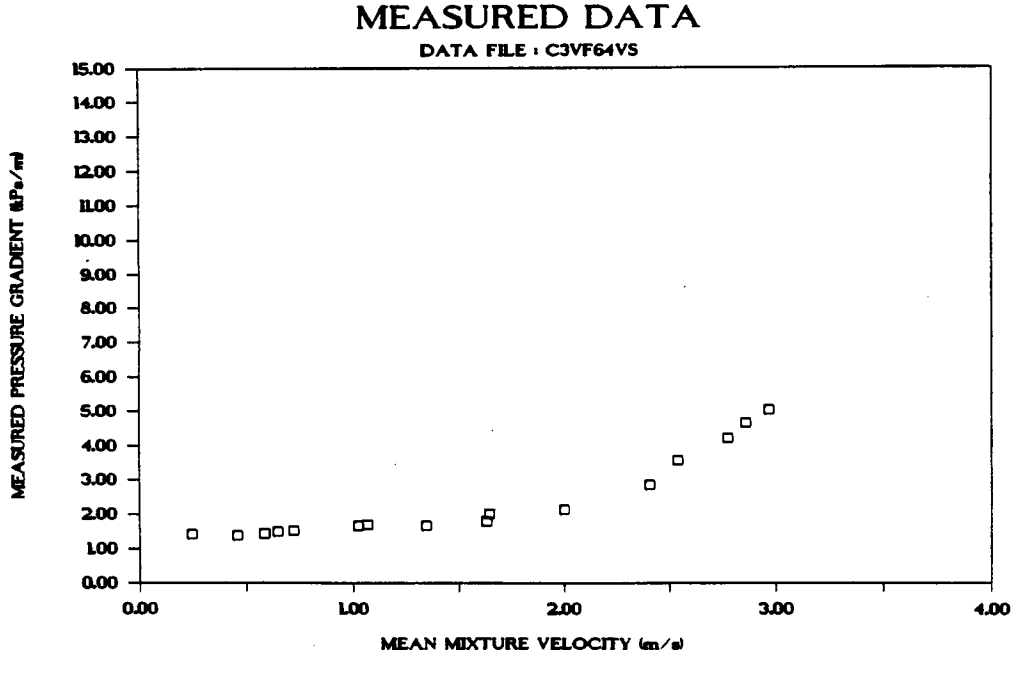

DATA FILE : C3VF72VS

Test facility		University of Cape Town
Test date		December 1988
Material description		Full Plant Tailings
Material relative density		2.680
Slurry relative density		1.7200
Solids volumetric concentration	(%)	42.891
Solids mass concentration	(%)	66.830
Pipe internal diameter	(mm)	41.22
Pipe internal roughness	(μm)	106.0
Pipeline gradient		Vertical

Mixture velocity (m/s)	Pressure gradient (kPa/m)	Slurry temp. (°C)
2.414	5.631	28.5
2.246	6.860	28.5
2.033	5.907	29.0
1.916	6.351	28.5
1.909	5.745	29.0
1.803	5.973	29.0
1.637	5.614	29.0
1.551	5.709	29.0
1.405	5.674	29.0
1.318	4.958	29.5
1.174	4.482	29.5
0.934	4.471	29.5
0.807	4.289	29.5
0.715	4.113	29.5
0.420	3.886	29.5
0.125	4.123	29.5

Particle size distribution
Malvern particle size analyser

Size (μm)	% Passing	% Retained
262.0	97.500	2.500
160.0	90.300	7.200
113.0	82.100	8.200
84.0	73.800	8.300
65.0	66.100	7.700
50.0	59.600	6.500
39.0	54.600	5.000
30.0	49.400	5.200
24.0	43.500	5.900
19.0	38.000	5.500
15.0	33.100	4.900
11.0	27.900	5.200
Pan	0.000	27.900

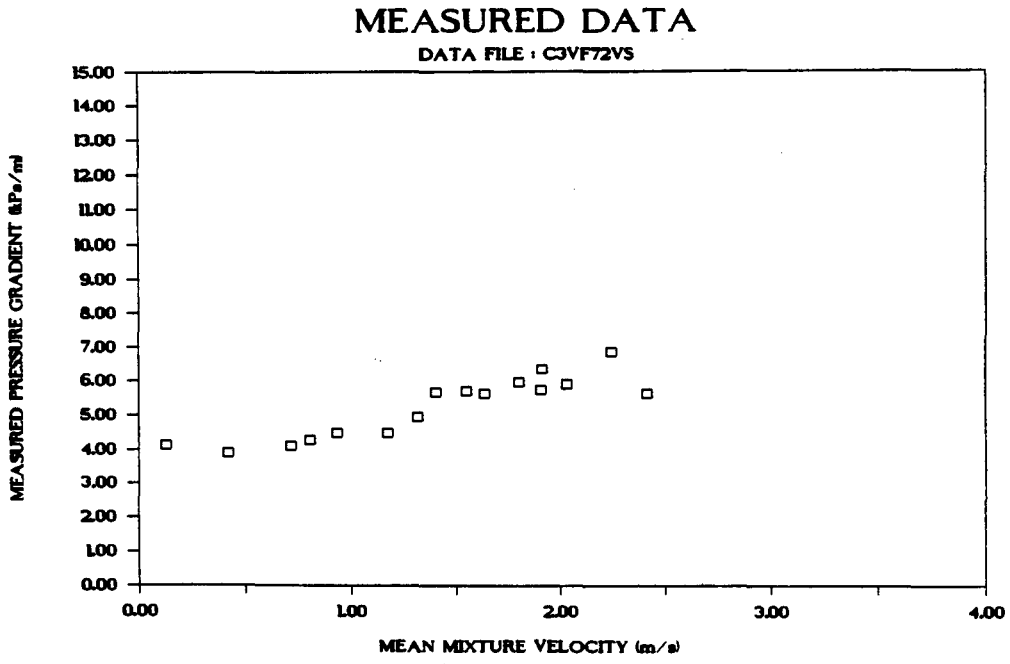

DATA FILE : C3VF74VS

Test facility		University of Cape town
Test date		December 1988
Material description		Full Plant tailings
Material relative density		2.680
Slurry relative density		1.740
Solids volumetric concentration	(%)	44.110
Solids mass concentration	(%)	67.950
Pipe internal diameter	(mm)	41.20
Pipe internal roughness	(μm)	106.0
Pipeline gradient		Vertical

Mixture velocity (m/s)	Pressure gradient (kPa/m)	Slurry temp. (°C)
1.449	10.484	26.5
1.265	9.100	26.5
1.114	9.368	27.0
0.951	8.970	27.0
0.717	8.419	28.0
0.691	7.892	28.0
0.591	8.700	28.0
0.560	8.452	29.0
0.305	8.309	29.0
0.260	8.241	29.0
0.252	8.167	29.0

Particle size distribution
Malvern particle size analyser

Size (μm)	% Passing	% Retained
262.0	100.000	0.000
160.0	98.900	1.100
113.0	93.000	5.900
84.0	86.000	7.000
65.0	79.300	6.700
50.0	73.100	6.200
39.0	67.300	5.800
30.0	60.800	6.500
24.0	53.800	7.000
19.0	47.300	6.500
15.0	41.600	5.700
11.0	35.200	6.400

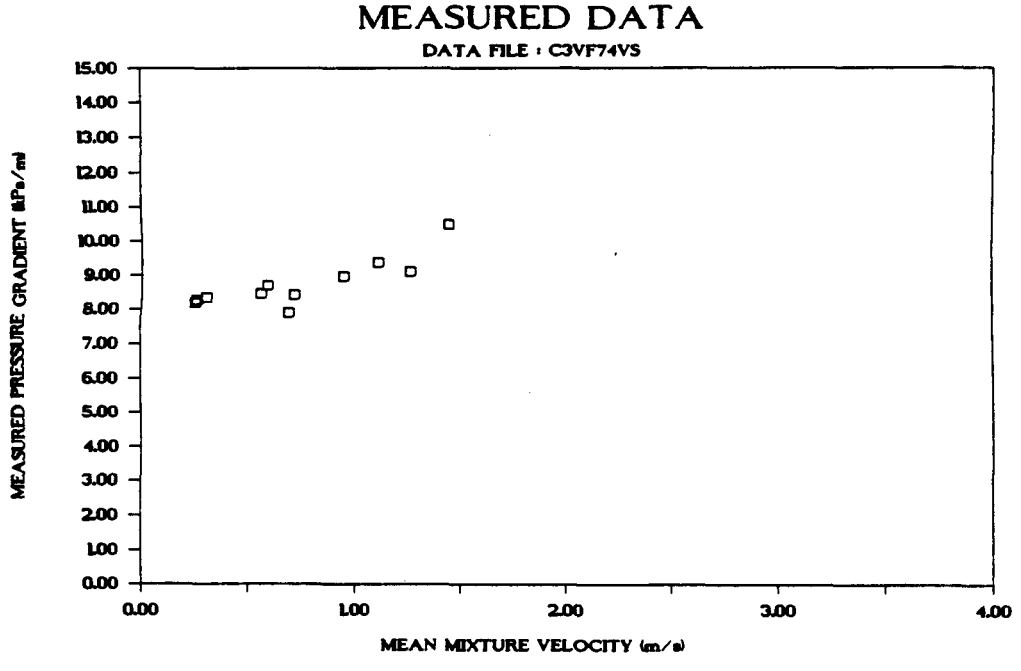

DATA FILE : C3VF75VS

Test facility		Vertical Test Facility
Test date		February 1989
Material description		Full plant Tailings
Material relative density		2.680
Slurry relative density		1.750
Solids volumetric concentration	(%)	44.680
Solids mass concentration	(%)	68.420
Pipe internal diameter	(mm)	41.20
Pipe internal roughness	(μm)	170.0
Pipeline gradient		Vertical

Mixture velocity (m/s)	Pressure gradient (kPa/m)	Slurry temp. (°C)
1.113	11.019	27.5
1.053	11.109	27.5
0.949	10.583	27.5
0.796	10.334	27.5
0.610	9.855	28.5
0.605	9.845	28.5
0.406	9.666	28.5
0.389	8.967	28.5
0.323	9.006	28.5
0.209	8.904	28.5
0.180	8.815	29.0
0.175	8.756	29.0
0.117	8.688	29.0
0.073	9.137	29.0

Particle size distribution
Malvern particle size analyser

Size (μm)	% Passing	% Retained
262.0	97.500	2.500
160.0	90.300	7.200
113.0	82.100	8.200
84.0	73.800	8.300
65.0	66.100	7.700
50.0	59.600	6.500
39.0	54.600	5.000
30.0	49.400	5.200
24.0	43.500	5.900
19.0	38.000	5.500
15.0	33.100	4.900
11.0	27.900	5.200
Pan	0.000	27.900

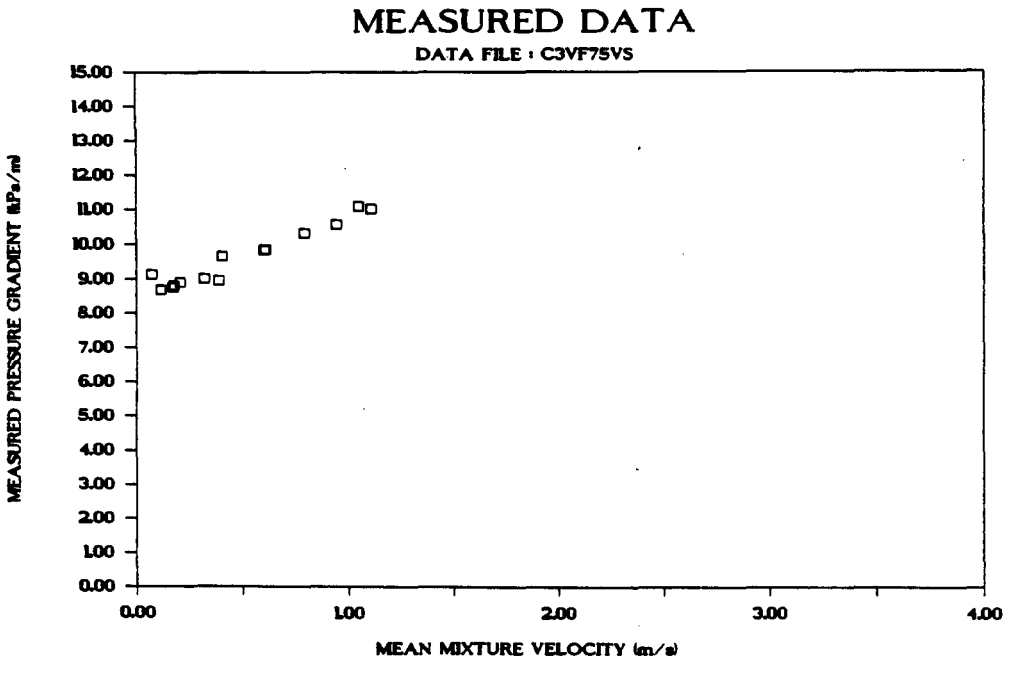

DATA FILE : DKVF69VS

Test facility		Vertical Test Facility at UCT
Test date		April, 1989
Material description		Full plant tailings
Material relative density		2.800
Slurry relative density		1.690
Solids volumetric concentration	(%)	38.370
Solids mass concentration	(%)	63.570
Pipe internal diameter	(mm)	41.22
Pipe internal roughness	(μm)	170.0
Pipeline gradient		Vertical

Mixture velocity (m/s)	Pressure gradient (kPa/m)	Slurry temp. (°C)
3.285	6.442	28.5
3.273	6.254	28.5
3.272	6.294	28.5
3.153	6.777	28.5
3.075	6.493	28.5
2.900	5.749	28.5
2.539	3.093	29.5
2.141	2.471	29.5
1.996	2.303	29.5
1.727	2.317	29.5
1.552	1.867	29.5
1.148	1.685	30.0
0.473	1.406	30.0
0.029	1.072	30.0

Particle size distribution
Malvern particle size analyser

Size (μm)	% Passing	% Retained
564.0	100.000	0.000
262.0	99.100	0.900
160.0	91.600	7.500
113.0	81.300	10.300
84.0	72.600	8.700
65.0	64.900	7.700
50.0	57.500	7.400
39.0	50.700	6.800
30.0	44.500	6.200
24.0	38.300	6.200
19.0	32.700	5.600
15.0	27.800	4.900
Pan	0.000	27.800

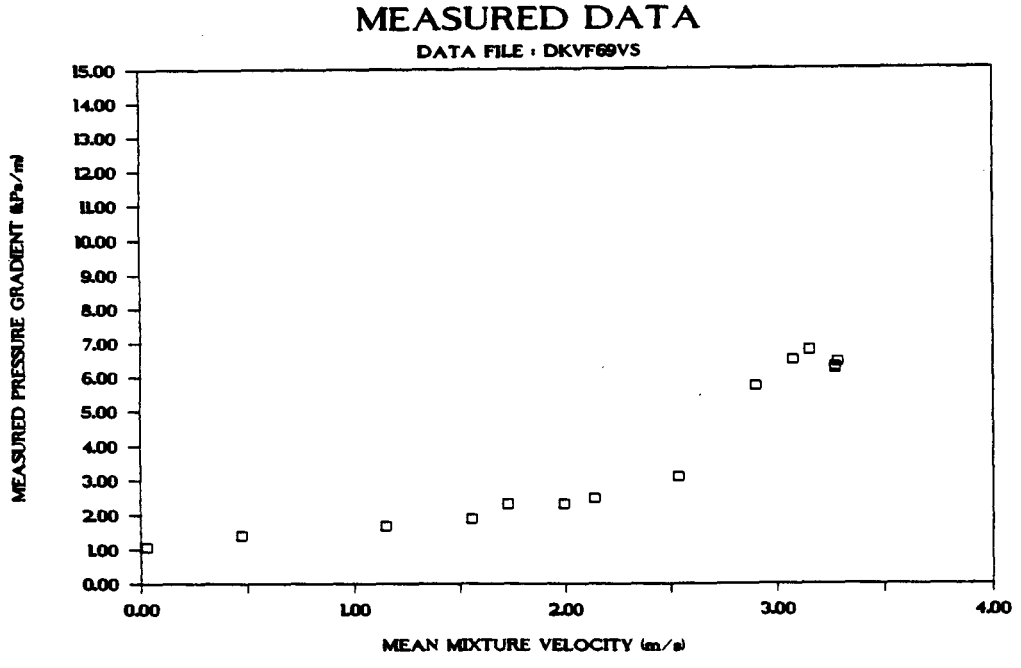

DATA FILE : DKVF76VS

Test facility		Vertical Test Facility at UCT
Test date		
Material description		Full plant tailings
Material relative density		2.800
Slurry relative density		1.760
Solids volumetric concentration	(%)	42.250
Solids mass concentration	(%)	67.220
Pipe internal diameter	(mm)	41.22
Pipe internal roughness	(μm)	170.0
Pipeline gradient		Vertical

Mixture velocity (m/s)	Pressure gradient (kPa/m)	Slurry temp. (°C)
2.924	7.015	28.0
2.913	6.799	28.0
2.849	6.865	28.0
2.769	6.856	28.0
2.656	6.772	28.0
2.341	5.953	28.0
2.190	5.835	29.5
2.062	5.741	29.5
1.514	4.589	29.5
1.326	4.264	29.5
0.678	3.695	29.5
0.644	3.549	29.5
0.482	3.529	29.5
0.233	3.580	29.5

Particle size distribution
Malvern particle size analyser

Size (μm)	% Passing	% Retained
564.0	100.000	0.000
262.0	99.100	0.900
160.0	91.600	7.500
113.0	81.300	10.300
84.0	72.600	8.700
65.0	64.900	7.700
50.0	57.500	7.400
39.0	50.700	6.800
30.0	44.500	6.200
24.0	38.300	6.200
19.0	32.700	5.600
15.0	27.800	4.900
Pan	0.000	27.800

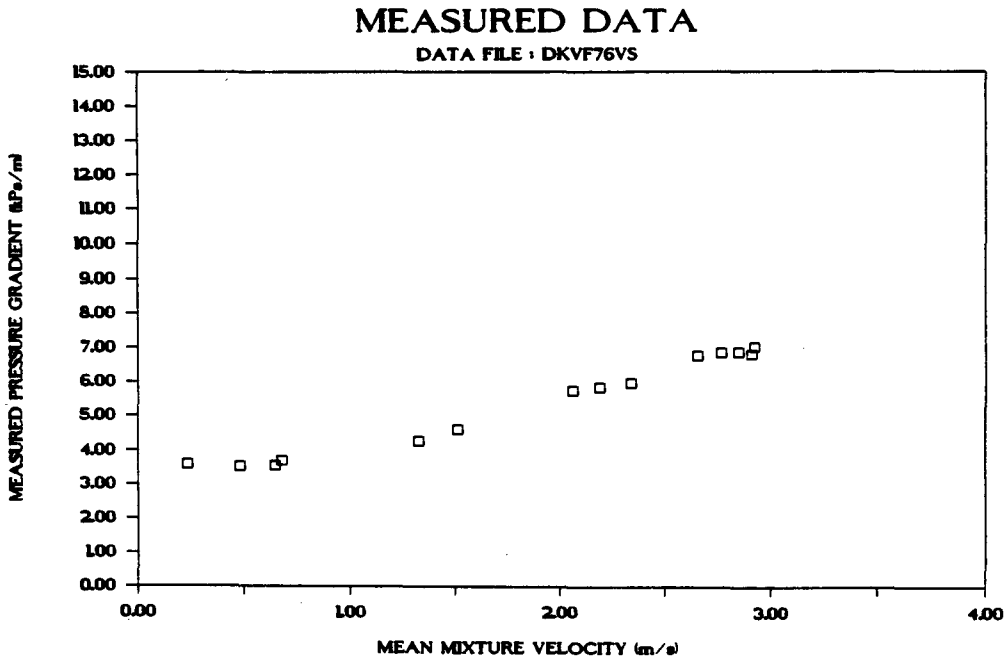

DATA FILE : DKVF80VS

Test facility		Vertical Test Facility at UCT
Test date		
Material description		Full plant tailings
Material relative density		2.800
Slurry relative density		1.800
Solids volumetric concentration	(%)	44.480
Solids mass concentration	(%)	69.180
Pipe internal diameter	(mm)	41.22
Pipe internal roughness	(μm)	170.0
Pipeline gradient		Vertical

Mixture velocity (m/s)	Pressure gradient (kPa/m)	Slurry temp. (°C)	Particle size distribution Malvern particle size analyser Size (μm)	% Passing	% Retained
1.867	10.013	28.5	564.0	100.000	0.000
1.853	10.231	28.5	262.0	99.100	0.900
1.672	10.178	29.0	160.0	91.600	7.500
1.526	10.042	29.0	113.0	81.300	10.300
1.459	10.064	29.0	84.0	72.600	8.700
1.336	10.064	29.5	65.0	64.900	7.700
1.077	10.092	29.5	50.0	57.500	7.400
0.927	9.767	29.5	39.0	50.700	6.800
0.859	9.759	29.5	30.0	44.500	6.200
0.562	9.771	29.5	24.0	38.300	6.200
0.366	9.745	30.5	19.0	32.700	5.600
0.007	9.786	30.5	15.0	27.800	4.900

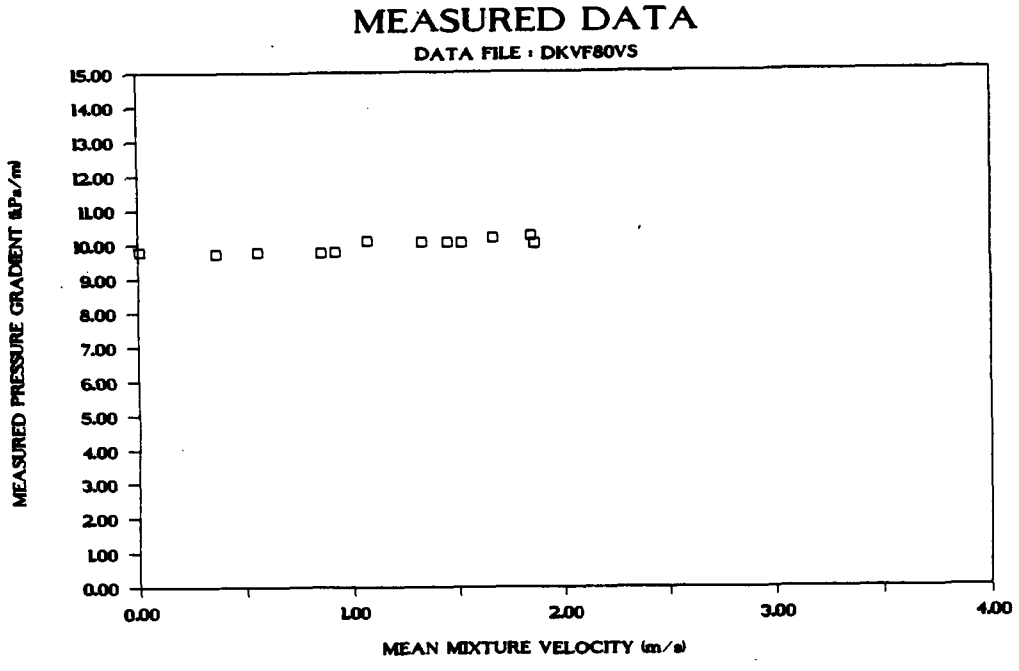

DATA FILE : DKVF84VS

Test facility		Vertical Test Facility at UCT
Test date		April 1989
Material description		Full plant tailings
Material relative density		2.800
Slurry relative density		1.835
Solids volumetric concentration	(%)	46.420
Solids mass concentration	(%)	70.830
Pipe internal diameter	(mm)	41.22
Pipe internal roughness	(μm)	170.0
Pipeline gradient		Vertical

Mixture velocity (m/s)	Pressure gradient (kPa/m)	Slurry temp. (°C)
0.816	10.862	29.0
0.808	10.970	29.0
0.804	10.947	29.0
0.797	10.945	29.0
0.790	10.935	29.0
0.784	11.008	29.0
0.771	11.023	29.0
0.755	10.925	29.0
0.723	10.947	29.0
0.491	9.221	29.0
0.408	9.140	29.5
0.370	8.469	29.5
0.339	8.957	29.5
0.303	8.898	29.5
0.179	8.340	29.5
0.162	8.592	29.5
0.139	8.917	29.5
0.038	8.435	29.5

Particle size distribution
Malvern particle size analyser

Size (μm)	% Passing	% Retained
564.0	100.000	0.000
262.0	99.100	0.900
160.0	91.600	7.500
113.0	81.300	10.300
84.0	72.600	8.700
65.0	64.900	7.700
50.0	57.500	7.400
39.0	50.700	6.800
30.0	44.500	6.200
24.0	38.300	6.200
19.0	32.700	5.600
15.0	27.800	4.900
Pan	0.000	27.800

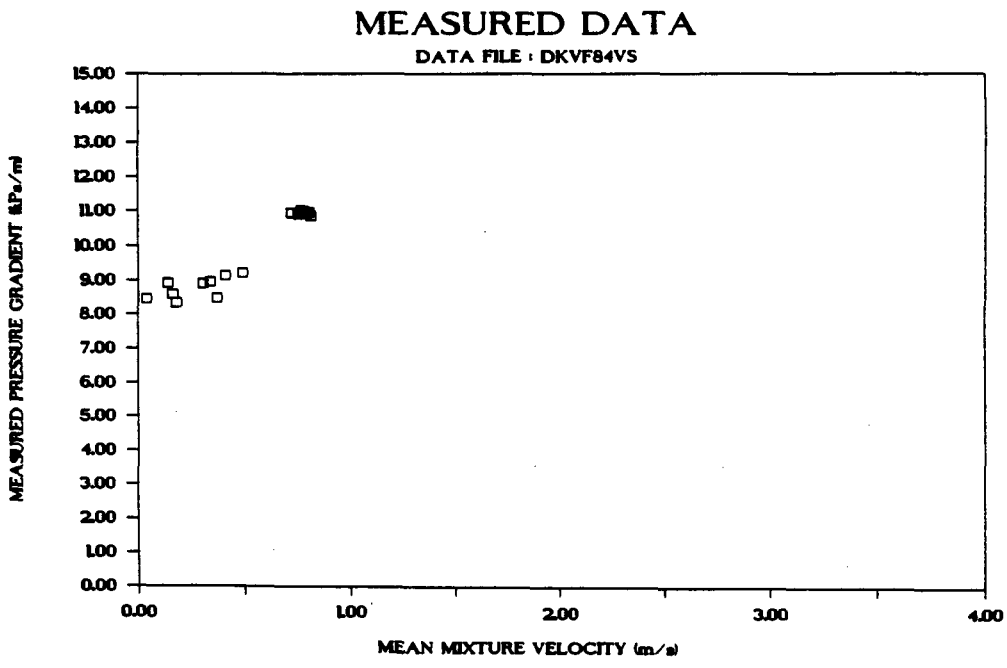

DATA FILE : CMVF43VL

Test facility		Vertical test facility at UCT
Test date		November 1979
Material description		Chamber of Mines Full Plant
Material relative density		2.720
Slurry relative density		1.430
Solids volumetric concentration	(%)	25.040
Solids mass concentration	(%)	47.640
Pipe internal diameter	(mm)	75.88
Pipe internal roughness	(μm)	10.0
Pipeline gradient		Vertical

Mixture velocity (m/s)	Pressure gradient (kPa/m)	Slurry temp. (°C)	Particle size distribution Malvern particle size analyser		
			Size (μm)	% Passing	% Retained
4.651	2.910	25.0	564.0	100.000	0.000
4.631	2.411	25.0	262.0	100.000	0.000
4.252	2.266	25.0	160.0	95.500	4.500
3.999	2.385	25.0	113.0	86.200	9.300
3.731	1.753	25.0	84.0	77.400	8.800
3.345	1.245	25.0	65.0	70.500	6.900
3.070	1.170	25.0	50.0	64.800	5.700
3.032	1.658	25.0	39.0	59.000	5.800
3.000	1.013	25.0	30.0	54.500	4.500
2.496	0.766	25.0	21.0	49.600	4.900
2.139	0.293	25.0	11.0	33.900	15.700
1.854	0.141	25.0	6.0	18.000	15.900

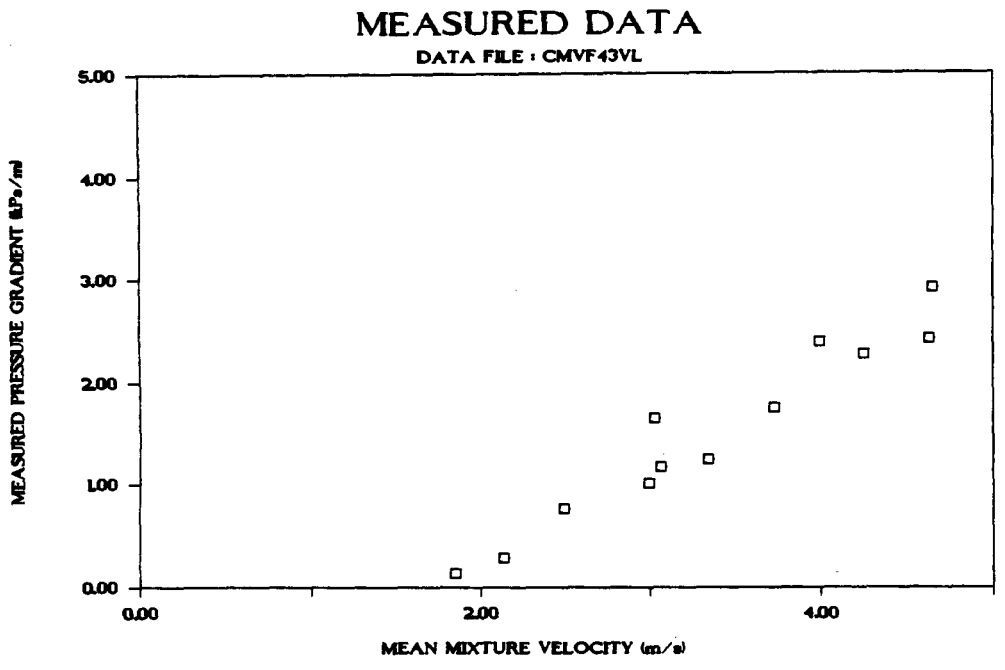

DATA FILE : CMVF61VL

Test facility		Vertical test facility at UCT
Test date		November 1989
Material description		Chamber of Mines Full Plant
Material relative density		2.720
Slurry relative density		1.610
Solids volumetric concentration	(%)	35.500
Solids mass concentration	(%)	59.980
Pipe internal diameter	(mm)	75.88
Pipe internal roughness	(μm)	10.0
Pipeline gradient		Vertical

Mixture velocity (m/s)	Pressure gradient (kPa/m)	Slurry temp. (°C)
3.468	2.978	25.0
3.440	2.695	25.0
3.298	2.141	25.0
3.241	1.739	25.0
3.207	2.138	25.0
2.734	1.384	25.0
2.715	1.422	25.0
2.245	0.682	25.0
2.236	0.802	25.0
1.940	0.526	25.0
1.738	0.426	25.0
1.736	0.439	25.0
1.523	0.469	25.0
1.439	0.338	25.0
1.179	0.522	25.0
1.127	0.258	25.0
0.579	0.420	25.0
0.442	0.504	25.0

Particle size distribution
Malvern particle size analyser

Size (μm)	% Passing	% Retained
564.0	100.000	0.000
262.0	100.000	0.000
160.0	95.500	4.500
113.0	86.200	9.300
84.0	77.400	8.800
65.0	70.500	6.900
50.0	64.800	5.700
39.0	59.000	5.800
30.0	54.500	4.500
21.0	49.600	4.900
11.0	33.900	15.700
6.0	18.000	15.900
Pan	0.000	18.000

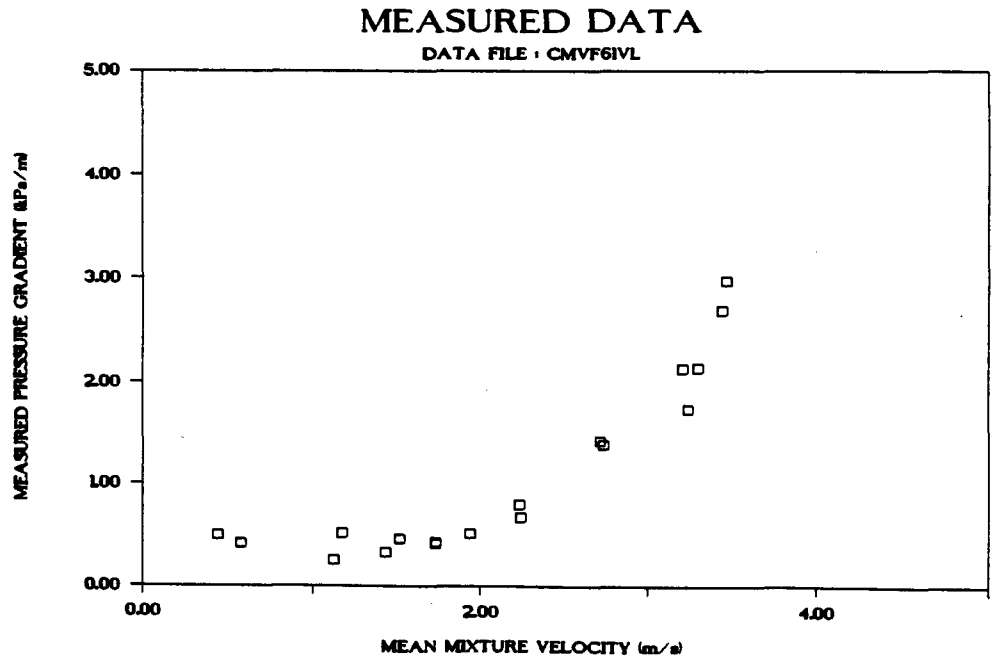

DATA FILE : CMVF70VL

Test facility		Vertical test facility at UCT
Test date		November 1989
Material description		Chamber of Mines Full Plant
Material relative density		2.720
Slurry relative density		1.700
Solids volumetric concentration	(%)	40.730
Solids mass concentration	(%)	65.170
Pipe internal diameter	(mm)	75.88
Pipe internal roughness	(μm)	10.0
Pipeline gradient		Vertical

Mixture velocity (m/s)	Pressure gradient (kPa/m)	Slurry temp. (°C)
3.206	3.710	25.0
3.197	4.137	25.0
2.899	2.338	25.0
2.897	2.194	25.0
2.675	2.150	25.0
2.200	1.969	25.0
2.050	1.781	25.0
1.988	1.737	25.0
1.754	1.822	25.0
1.687	1.712	25.0
1.674	1.821	25.0
1.056	1.643	25.0
1.040	1.754	25.0
0.831	1.582	25.0
0.644	1.604	25.0
0.529	1.382	25.0
0.362	1.329	25.0

Particle size distribution
Malvern particle size analyser

Size (μm)	% Passing	% Retained
564.0	100.000	0.000
262.0	100.000	0.000
160.0	95.500	4.500
113.0	86.200	9.300
84.0	77.400	8.800
65.0	70.500	6.900
50.0	64.800	5.700
39.0	59.000	5.800
30.0	54.500	4.500
21.0	49.600	4.900
11.0	33.900	15.700
6.0	18.000	15.900
Pan	0.000	18.000